

**University *Mediterranea* of Reggio Calabria**  
**Department of Agriculture**

**PhD Thesis**

**SPATIO-TEMPORAL EXPRESSIONS  
OF THE PLANT MORPHO-  
PHYSIOLOGICAL AND MOLECULAR  
RESPONSES TO MULTIPLE  
STRESSES**

Candidate

Rosa Vescio

Tutor

Prof. Agostino Sorgonà

## Table of contents

ABSTRACT.....	5
RIASSUNTO.....	6
GENERAL INTRODUCTION.....	7
Climate change.....	7
What is a plant stress? .....	9
How do plants respond to stress? .....	10
Morphological responses.....	12
Physiological responses.....	14
Metabolic and Molecular responses.....	16
Combined stresses and plant responses to multiple stresses.....	18
Spatio-temporal components of plant responses to stress. ....	21
AIMS AND ORGANISATION OF THESIS.....	24
<b>CHAPTER 1: THE WITHIN-PLANT VARIATION IN THE MORPHO-PHYSIOLOGICAL TRAITS AND VOCS PROFILE OF THE ENDEMIC RARE <i>Salvia ceratophylloides</i> ARD. (LAMIACEAE).</b>	26
<b>1.1. Introduction.....</b>	27
<b>1.2. Materials and Methods.....</b>	29
1.2.1. <i>Species and sites</i> .....	29
1.2.2. <i>Measurements and samplings</i> .....	30
1.2.3. <i>Physiological analysis</i> .....	30
1.2.4. <i>Morphological analysis</i> .....	31
1.2.5. <i>VOC analysis: Headspace/Solid-Phase Micro-Extraction (HS/SPME) GC-MS analysis</i> .....	32
1.2.6. <i>Statistical analysis</i> .....	33
<b>1.3. Results.....</b>	35
1.3.1. <i>Physiological performances and morphological traits of <i>S. ceratophylloides</i></i>	35
1.3.2. <i>VOCs analysis of <i>Salvia ceratophylloides</i> in its habitat</i> .....	41
<b>1.4. Discussion.....</b>	46
1.4.1. <i>The assessment of the morpho-physiological traits of rare <i>Salvia ceratophylloides</i> Ard</i> .....	46
1.4.2. <i>Do the within-plant patterns of the photosynthetic performance, morphological traits and metabolic profiles occur?</i> .....	47
<b>1.5. Conclusions.....</b>	50
<b>CHAPTER 2: ABIOTIC AND BIOTIC COMBINED STRESS IN TOMATO: ADDITIVE, SYNERGIC AND ANTAGONISTIC EFFECTS AND WITHIN-PLANT PHENOTYPIC PLASTICITY.....</b>	59
<b>2.1. Introduction.....</b>	59
<b>2.2. Materials and Methods.....</b>	61
2.2.1. <i>Experimental procedure and Plant material</i> .....	61

2.2.2.	<i>Growth condition</i> .....	63
2.2.3.	<i>Insect Rearing</i> .....	65
2.2.4.	<i>Abiotic stress and Herbivory treatment</i> .....	66
2.2.5.	<i>First experimental set: synergic, antagonistic and additive effects</i> .....	68
2.2.6.	<i>Second experiment: within-plant phenotypic plasticity</i> .....	72
<b>2.3.</b>	<b>Results and Discussion</b> .....	74
2.3.1.	<i>Are the morpho-physiological responses to individual stresses different from the combined ones in tomato plants? Are additive, synergistic or antagonistic effects in the combined stress?</i> .....	74
2.3.2.	<i>Do the tomato responses to the single and combined stress occurred at between- or within-plant levels?</i> .....	98
<b>2.4.</b>	<b>Conclusions</b> .....	111
	<b>CHAPTER 3: SINGLE AND COMBINED ABIOTIC STRESS IN MAIZE ROOT MORPHOLOGY</b> .....	113
<b>3.1.</b>	<b>Introduction</b> .....	114
<b>3.2.</b>	<b>Materials and Methods</b> .....	116
3.2.1.	<i>Plant material and growth condition and treatments</i> .....	116
3.2.2.	<i>Treatments</i> .....	117
3.2.3.	<i>Morphological Root Analysis</i> .....	117
3.2.4.	<i>Statistical Analysis</i> .....	119
<b>3.3.</b>	<b>Results</b> .....	121
3.3.1.	<i>Univariate analysis of the root morphological data</i> .....	121
3.3.2.	<i>Additive, synergistic and antagonistic effect of combined stress</i> .....	126
3.3.3.	<i>Root responses to the single and combined stress: a supervised analysis with PLS-DA</i> .....	128
<b>3.4.</b>	<b>Discussion</b> .....	132
3.4.1.	<i>Single stress determined different root type-related morphological responses</i> .....	132
3.4.2.	<i>Combined stress caused different root type-related morphological response respect to the single stress with non-additive effects</i> .....	134
3.4.3.	<i>Primary lateral RLR, primary and seminal root branching density discriminated the root phenotypes in drought and heat stress and their combination</i> .....	136
<b>3.5.</b>	<b>Conclusions</b> .....	137
	<b>CHAPTER 4: SINGLE AND COMBINED ABIOTIC STRESSORS AFFECT MAIZE RHIZOSPHERE BACTERIAL MICROBIOTA</b> .....	138
<b>4.1.</b>	<b>Introduction</b> .....	139
<b>4.2.</b>	<b>Material and Methods</b> .....	140
4.2.1.	<i>Study system</i> .....	140
4.2.2.	<i>Experimental design and sample collection</i> .....	142
4.2.3.	<i>DNA extraction and library preparation</i> .....	143

4.2.4.	<i>Raw reads processing</i> .....	144
4.2.5.	<i>Data analysis</i> .....	145
<b>4.3.</b>	<b>Results</b> .....	145
<b>4.4.</b>	<b>Discussion</b> .....	149
<b>4.5.</b>	<b>Supplementary material</b> .....	152
	<b>CONCLUSIONS AND FUTURE PERSPECTIVES</b> .....	156
	<b>ACKNOWLEDGEMENTS</b> .....	158
	<b>REFERENCES</b> .....	159
	<b>List of Figures</b> .....	200
	<b>List of Tables</b> .....	208

## **ABSTRACT**

The present PhD project is based on current issues related to the plant adaptation to climate change and can be summarized in two key words: multiple stresses and spatio-temporal responses of the plants.

Owing to sessile nature, plants are continually exposed to the abiotic and biotic stresses which co-occur in nature. Until now, the plant responses to the single stress factor have been extensively studied. Conversely, the plant adaptation to the combined stress, real condition of the agro- and eco-systems, has been little addressed by the scientific community in the face of the specificity of metabolic pathways and molecular mechanisms that are induced by the presence of such stressful combinations.

Abiotic and biotic stresses, moreover, change in space and time, resulting in a patchy of stressful areas of the surrounding physical environment to which plants should be adapt. In such highly dynamic and heterogeneous environments, the plants adopted strategies based on the within-plant phenotypic plasticity characterized by high morpho-physiological and molecular variability both intra-radical (different root types) and -foliar (heterophyllia) which produce spatio-temporal components of responses (different nutrient and water uptake among and along the root axis, induction rate of defense systems, etc.).

In this perspective, in order to understand the morpho-physiological and molecular responses of plants to combined stresses and how these responses occur at different spatial (location, age, root type) and temporal (temporal dynamics) scales, the present PhD project addressed these aspects in different case-study ranging from the adaptation of the rare and endemic *Salvia ceratophylloides* Ard. (Lamiaceae) to the plant-insect and root-soil interactions.

## RIASSUNTO

Il presente Progetto si fonda su ben affermate ed attuali problematiche inerenti l'adattamento delle piante ai cambiamenti climatici e può essere sintetizzato in due parole chiave: stress multipli e risposte spatio-temporali delle piante. A causa della loro natura sessile, le piante sono continuamente esposte agli stress sia abiotici sia biotici. Le risposte delle piante a tali fattori stressanti presi singolarmente sono stati estensivamente studiati. Viceversa, l'adattamento delle piante alla combinazione degli stress, condizione verosimile degli agro- ed eco-sistemi, è stata poco affrontata dalla comunità scientifica a fronte anche della specificità delle vie metaboliche e meccanismi molecolari che si instaurano in presenza di tali combinazioni stressanti. Gli stress abiotici e biotici, inoltre, variano nel tempo e nello spazio, determinando un mosaico di zone stressanti dell'ambiente fisico a cui le piante si devono adattare. In tali ambienti altamente dinamici ed eterogenei, le piante hanno adottato delle strategie basate sulla plasticità fenotipica intra-pianta caratterizzata da un'elevata variabilità morfo-fisiologica e molecolare intra-radiale (differenti tipi radicali) e fogliare (eterofillia) che genera delle componenti spatio-temporali delle risposte (diverso assorbimento dei nutrienti e dell'acqua tra e lungo gli assi radicali, velocità di induzione dei sistemi di difesa, ecc.).

In tale ottica, nel comprendere le risposte morfo-fisiologiche e molecolari delle piante agli stress combinati e di come tali risposte si presentano a diversa scala spaziale (posizione, età, tipo radicale) e temporale (dinamica temporale), il presente progetto di dottorato ha affrontato tali aspetti in differenti casi-studio che vanno dall'adattamento della rara ed endemica *Salvia ceratophylloides* Ard. (Lamiaceae) all'interazione pianta-insetto e radice-suolo.

**KEYWORDS:** multiple stresses; spatio-temporal plant responses; root microbiota; volatiloma; root morphology; within-plant variance; plant-insect interaction.

## **GENERAL INTRODUCTION**

### **Climate change.**

In according to The Intergovernmental Panel on Climate Change (IPCC), climate change refers “to a change in the state of the climate that can be identified (e.g., by using statistical tests) by changes in the mean and/or the variability of its properties, and that persists for an extended period, typically decades or longer”. Climate change may be due to natural internal processes or external forcing such as modulations of the solar cycles, volcanic eruptions and persistent anthropogenic changes in land use or in the composition of the atmosphere and consisting of changing concentrations of greenhouse gases in the atmosphere, rising temperatures, changes in precipitation patterns, and intensifying frequency of extreme weather events (Gray et al, 2016). The impact of climate change is not spatio-temporal equally distributed throughout the world. For instance, in Continental and Mediterranean Region there will be an increase in heat extremes, while in Atlantic and Boreal Region there will be an increase in heavy precipitation events, as Figure 1 shows.

Emerging evidence indicates that these climate change-related events will result in an increase of the stressful conditions for the plant/crop/forest growth, development and, ultimately, productivity in both natural and agro-ecosystems. Indeed, predictions indicated an increase of the burst herbivory and the drought stress and nutrient deficiency favored by climate change.

## Climate change impacts in Europe's regions

Climate change is projected to impact the availability of water in Europe, putting additional pressure on southern regions already facing water stress. Other parts of Europe are expected to face more frequent flooding events, while low-lying regions are at risk from storm surges and sea level rise.



### Mediterranean region

- Large increase in heat extremes
- Decrease in precipitation and river flow
- Increasing risk of droughts
- Increasing risk of biodiversity loss
- Increasing risk of forest fires
- Increased competition between different water users
- Increasing water demand for agriculture
- Decrease in crop yields
- Increasing risks for livestock production
- Increase in mortality from heat waves
- Expansion of habitats for southern disease vectors
- Decreasing potential for energy production
- Increase in energy demand for cooling
- Decrease in summer tourism and potential increase in other seasons
- Increase in multiple climatic hazards
- Most economic sectors negatively affected
- High vulnerability to spillover effects of climate change from outside Europe

### Boreal region

- Increase in heavy precipitation events
- Decrease in snow, lake and river ice cover
- Increase in precipitation and river flows
- Increasing potential for forest growth and increasing risk of forest pests
- Increasing damage risk from winter storms
- Increase in crop yields
- Decrease in energy demand for heating
- Increase in hydropower potential
- Increase in summer tourism

### Continental region

- Increase in heat extremes
- Decrease in summer precipitation
- Increasing risk of river floods
- Increasing risk of forest fires
- Decrease in economic value of forests
- Increase in energy demand for cooling

### Atlantic region

- Increase in heavy precipitation events
- Increase in river flow
- Increasing risk of river and coastal flooding
- Increasing damage risk from winter storms
- Decrease in energy demand for heating
- Increase in multiple climatic hazards

### Coastal zones and regional seas

- Sea level rise
- Increase in sea surface temperatures
- Increase in ocean acidity
- Northward migration of marine species
- Risks and some opportunities for fisheries
- Changes in phytoplankton communities
- Increasing number of marine dead zones
- Increasing risk of water-borne diseases

### Arctic region

- Temperature rise much larger than global average
- Decrease in Arctic sea ice coverage
- Decrease in Greenland ice sheet
- Decrease in permafrost areas
- Increasing risk of biodiversity loss
- Some new opportunities for the exploitation of natural resources and for sea transportation
- Risks to the livelihoods of indigenous peoples

### Mountain regions

- Temperature rise larger than European average
- Decrease in glacier extent and volume
- Upward shift of plant and animal species
- High risk of species extinctions
- Increasing risk of forest pests
- Increasing risk from rock falls and landslides
- Changes in hydropower potential
- Decrease in ski tourism

Source: EEA Report No 01/2017 — Climate change, impacts and vulnerability in Europe 2016.

**Figure 1** - Climate change impacts in Europe's regions (source: EEA Report No 01/2017 Climate change, impacts and vulnerability in Europe 2016).



An overview of the effects of climate change on agricultural productivity is illustrated in Figure 2:

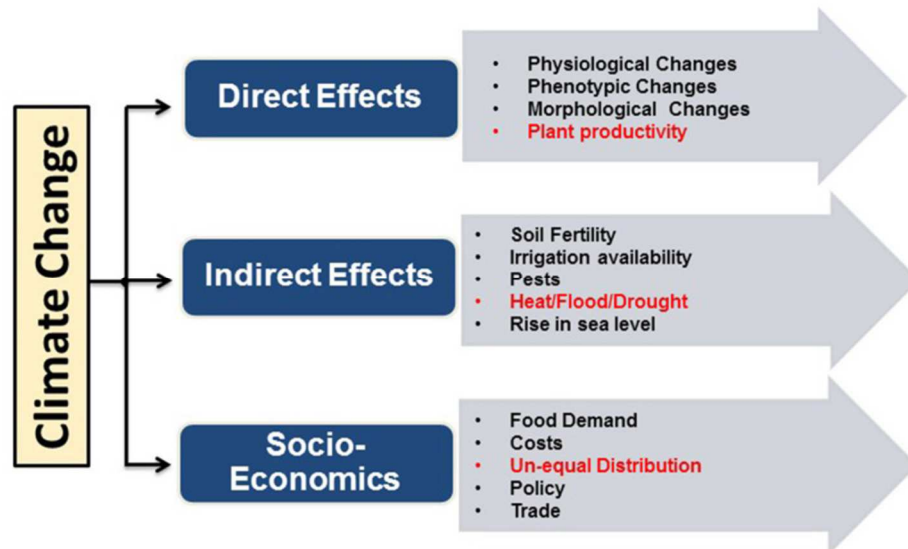


Figure 2 - Impact of climate change on agriculture (source: Ghatak et al, 2017).

### What is a plant stress?

Lichtenthaler (1996) defined plant stress as an adverse situation that impacts on plant's metabolism, growth or development. The stress is a physical state where a plant develops in non-ideal growth conditions (e.g. high or low temperature, drought, flooding, low nutrients), which inhibit its development, propagation and productivity (Madlung and Comai, 2004; Lambers et al, 2008). The environmental stresses for the plant growth can be grouped in abiotic and biotic stress.

The main abiotic stress for the plants are heat, high salinity, nutrient deficiency, cold and, above all, drought. Abiotic factors which induced the stress may be either physical or chemical and include water scarcity or abundance in soil, poor nutrient availability, pollutant, wind and UV radiation. Drought is one of the most critical abiotic stress that negatively affects plant growth and development (Farooq et al, 2012). For this reason, plants change their morphological structure, in order to survive in the existing environment (Wani et al. 2016a; Hossain et al. 2016; Sah et al. 2016). Morphological growth indices affected by drought stress are the leaf area, the plant height, dry matter and biomass production (Onyekachi et al, 2019). However, a considerable flexibility exists among crop species and even within species (Aroca, 2012). The reduction of the biomass is a common phenomenon under drought, whose levels differed among and within crop species (Aroca, 2012)

and among the plant organs also (Poorter and Nagel, 2000). These macroscopic effects on plants corresponded to physiological and biochemical changes such as alterations in water relations, decreased CO<sub>2</sub> assimilation, membrane structure damage, inhibition of enzyme activity, increased reactive oxygen species (ROS) generation (Tuba et al., 1996; Sarafis, 1998; Yordanov et al., 2003; Abid et al, 2018). Also the high or low temperature negatively impacts on the plant fitness and development (Wahid et al, 2007). For instance, the heat may slow down or inhibit germination, adversely affect photosynthesis, plant respiration, water relations and membrane fluidity, integrity or stability, alter levels of hormones and primary and secondary metabolites (Howarth, 2005; Smertenko et al, 1997). Low temperature may affect the amount and rate of water and nutrients uptake also (Kollist et al, 2019).

Biotic stresses include plant competition, pest (pathogens and insect) and animal attack; hence they are caused from living organisms which usually determined plant diseases and damages and, ultimately, the plant death. Pathogens (fungi, bacteria, and viruses) primarily caused diseases in plant characterized by different symptoms such as vascular wilts, leaf spots and cankers (Brown, 2015), while the insect feeding could also results in direct consumption of foliar tissues or photosynthates with negatively impacts in the physiology in the remaining leaf (Nabity and DeLucia, 2009). However, both biotic agents takes away nutrients from their host plant, leading to decreased plant vigor and, in extreme cases, death (Singla et al, 2016).

### **How do plants respond to stress?**

In order to cope with unfavorable environmental conditions, the plants have evolved various adaptations strategies to protect themselves through a variety of morphological, physiological and molecular mechanism (Devi et al, 2017).

The term “strategy” defines the manner in which a plant responds to a particular stress by the capacity to escape, avoid or tolerate/resist the stress and so they may survive (Hopkins and Hüner, 2009). If plant prevent the injury of stress by regulating its life cycle before the onset of stress, it is referred to stress escape (Levitt, 1980). For instance, Kumar and Abbo (2001) demonstrated that the

developing short-duration varieties of chickpea (*Cicer arietinum* L.) was an effective strategy for minimizing yield loss from terminal drought, as early maturity helps the crop to avoid the period of stress. When plants show the ability to avoid the stress injury by building up a barrier to prevent stress factors entering the plant, it is referred to stress avoidance (Blum, 2005). Avoidance mechanisms reduced the impact of a stress on the plant, although the stress exists in the environment (Hopkins and Hüner, 2009). A variety of adaptive traits involving the minimization of water loss (water savers) and optimization of water uptake (water spenders) allow to achieve the stress avoidance. The minimization is the reduction of transpiration, transpiration area, radiation absorption, etc.; while the optimization aims to maintain the water uptake through increased rooting, hydraulic conductance, etc. (Basu et al, 2016). Stress tolerance indicates that plants adapt to the stress environment by regulating their metabolism and repair the damage caused by stress by modifying their structure or function (Blum et al, 2005). Stress resistance is referred to the plant's ability to grow and survive during stress (Hopkins, 1999; Levitt, 1980; Price et al., 2002).

In relation to the stress intensity and duration, these stress-related plant strategies can be successful or not. In case of success, the plants pointed out the adaptation and/or acclimation as fitness process. Adaptation is a gradual and irreversible process, according to which individuals can reproduce adaptive traits in a given environment. Acclimation is a rapid and reversible phenotypic modification (morphological, physiological) of individuals exposed to environmental change. Hence, the difference between adaptation and acclimation is in the heritability of the plant morpho-physiological mechanisms: for the first process are heritable that increase the fitness of the organism in the stressful environment, while the acclimation implies no heritable physiological modifications due to a gradual exposure to the stress (Bhargava and Sawant, 2012; Hopkins and Hüner, 2009).

The capacity of plants to acclimate to changing environmental conditions reflects their phenotypic plasticity (i.e. the ability of a genotype to modify phenotype expression depending on the environment) (Hopkins and Hüner, 2009). Phenotypic plasticity allows plants to grow in diverse habitats and across environmental

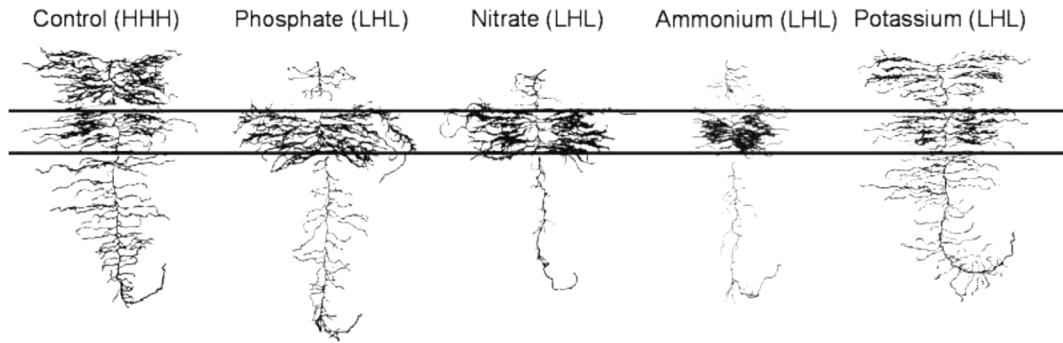
gradients (Givnish et al., 2002; Pan et al., 2006; Schurr et al., 2006; Robe et al., 2000; Sultan, 2003).

The enhanced plant fitness under variable environments by the different strategies is determined by an elaborate and complex combination of morphological, physiological and molecular plant responses as reported in the next paragraphs.

### **Morphological responses.**

Morphological response refers to the change of the plant form in terms of the length, surface area, branching, number, height and biometric parameters such as fresh and dry weight and their ratios.

Since the water reduction takes place in the soil, the first morphological responses occur at the root level. Some plants have the ability to increase root growth at the early stage of drought stress in order to absorb the water in deep soil (Hu and Xiong, 2014; Fang and Xiong, 2014). The root morphological responses to drought stress include the increases in elongation of individual roots (Jackson and Caldwell, 1989; Bilbrough and Caldwell, 1995; Zhang and Forde, 1998, 2000; Zhang et al, 1999) and total root length (van Vuuren et al, 1996; Hodge et al, 1999a, 2000c), the root production (Pregitzer et al, 1993; Hodge et al, 1999b, 2000d), and the extent of lateral branching (Larigauderie & Richards, 1994; Farley and Fitter, 1999b). These morphological mechanisms permitted a higher extraction of the water from the soil deeper strata and determined a higher plant resistance to the drought. Interesting root morphological modifications were observed in response to heterogeneous distribution of the nutrient in the soil as “nutrient patch”. In this respect, morphological plasticity as root proliferation is important for successful exploration of these nutrient-rich patches (Hodge, 2004). Mechanistically, the root proliferation involves the initiation of new lateral roots, as Drew and coworkers (1970) demonstrated in a series of classic experiments. Figure 3 shows barley root system exposed to high concentrations of phosphate, ammonium ( $\text{NH}_4^+$ ), nitrate ( $\text{NO}_3^-$ ) or potassium (K) in a localized soil area. Roots responded by increasing the length and number of primary laterals and secondary laterals to phosphate,  $\text{NH}_4^+$  and  $\text{NO}_3^-$  but not K (Drew, 1975; Drew et al, 1973; Drew and Saker, 1975, 1978).



**Figure 3** - Proliferation of primary and secondary laterals by barley (*Hordeum vulgare*) grown in solution culture with the middle root section exposed to a 100-fold greater concentration of phosphate, nitrate, ammonium or potassium ions compared with roots above or below (LHL). Controls were supplied with high concentration of nutrients in all zones (HHH). Abbreviations: H, high; L, low, referring to nutrient concentrations experienced by the top, middle and bottom sections of the root system. (source: Drew, 1975)

Besides the root, the drought reduced with more severe intensity the shoot dry weight in Asian red sage (*Salvia miltiorrhiza Bunge*) although that of the root system was also reduced resulting in an increase of the root/shoot dry weight ratio (Liu et al. 2011). Drought stress induces the reduction in rice growth and development also (Tripathy et al, 2000; Manikavelu et al, 2006). The reduction of the plant size in presence of drought is due to elongation and expansion cell process besides the biomass allocation. Indeed, the drought affects both elongation as well as expansion growth (Shao et al, 2008), and inhibits cell enlargement more than cell division (Jaleel et al, 2009). In addition, it alters the germination of rice seedlings (Jiang and Lafitte, 2007; Swain et al, 2014) and reduces number of tillers (Mostajeran and Rahimi-Eichi, 2009; Ashfaq et al, 2012; Bunnag and Pongthai, 2013) and plant height (Sarvestani et al, 2008; Ashfaq et al, 2012; Bunnag and Pongthai, 2013; Sokoto and Muhammad, 2014). In their experiment, Jaleel et al (2007) found that the water deficit caused the decrease of the stem length and total leaf area of *Catharanthus roseus* plants. Morphological changes are caused also by the heat stress. For example, Rollins et al (2013) in their study on barley noted that heat stress caused a considerably senescence of lower leaves.

Nutrient deficiency negatively impacted in the shoot morphology also. For example, the low nitrogen supply generally leads to early leaf senescence (Paul and Driscoll, 1997; Malamy and Ryan, 2001; Martin et al., 2002; Malamy, 2005; Wingler et al., 2006; Zhang, 2007, Kant, et al, 2011). Markhart (1985) compared leaf area expansion, dry weight, and water relations of *Phaseolus vulgaris* L. and

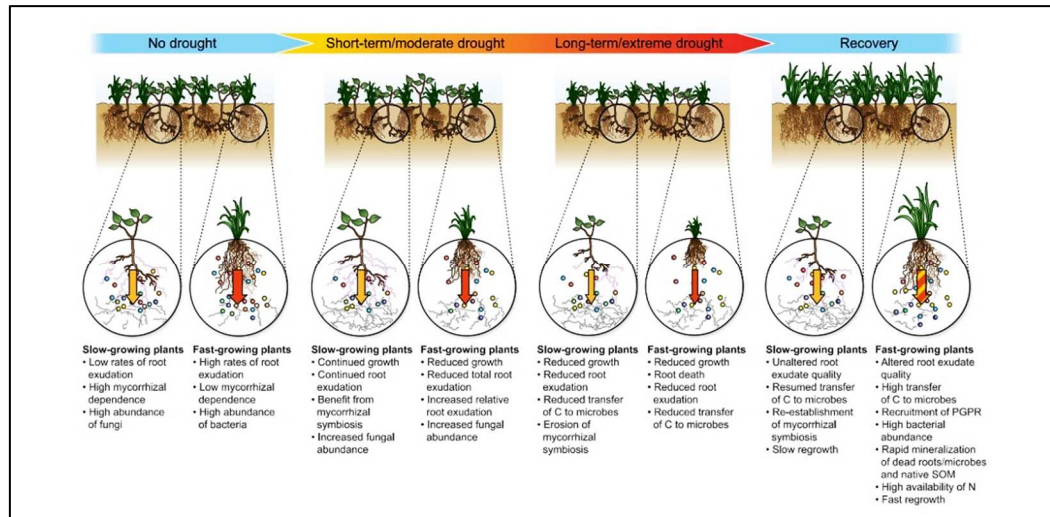
*P. acutifolius*, during a drying cycle in the greenhouse. The objective were to understand the characteristics which contribute to the superior drought tolerance of *P. acutifolius* compared to *Phaseolus vulgaris* L. He found that stomates of *P. acutifolius* closed at a much higher water potential than those of *P. vulgaris*, delaying dehydration of leaf tissue. Also, *P. acutifolius* had a more deeply penetrating root system, which also contributes to its drought tolerance.

### **Physiological responses.**

Faced with adverse environmental conditions such as drought stress, the first physiological response of plants is the stomatal closure in order to prevent the water loss by transpiration process (Ghatak et al., 2017) but, at the same time, it is the primary cause of the photosynthesis reduction in water stressed plants (Cornic and Massacci, 1996; Arve et al, 2011). However, the success of the plant physiological responses for the plant adaptation under stressed condition depends on plant species, growth stage, duration and intensity of stress (Jaleel et al, 2008). Ashraf and Harris (2013) showed that the overall photosynthetic capacity of a green plant could be reduced by a stress, because of all various components involved in the mechanism of photosynthesis (photosynthetic pigments and photosystems, the electron transport system, CO<sub>2</sub> reduction pathways) are severely affected. Stomatal closure and reduction of photosynthetic activity are also caused by biotic stresses (Bilgin et al, 2010; Melotto et al, 2016).

The allocation and partitioning of assimilated carbon provide resources for acclimation to environmental stress. Under water stress conditions the carbon assimilation in plants is typically reduced (Huang and Fu, 2000; Naudts et al., 2011; Roy et al., 2016; Ingrisch et al., 2018) as well as the carbon transfer to the roots and the rhizosphere (Fuchslueger et al., 2014a, 2016; Hasibeder et al., 2015; Karlowsky et al., 2018), resulting in a lower soil CO<sub>2</sub> efflux (Ruehr et al., 2009; Barthel et al., 2011; Burri et al., 2014). This leads to a weakening of plant–microbial interactions (Brüggemann et al., 2011) and the microbial mineralization of nitrogen and phosphorous are limited during drought (Stark and Firestone, 1995; Borken and Matzner, 2009; Delgado-Baquerizo et al., 2013; Fuchslueger et al., 2014b; Canarini and Dijkstra, 2015; Dijkstra et al., 2015). Several studies have shown that a shift of carbon allocation from the aboveground to the belowground plant organs exists

(Palta and Gregory, 1997; Huang and Fu, 2000; Burri et al., 2014) with an increase of the amounts of soluble sugars in the roots (Hasibeder et al., 2015; Karlowsky et al., 2018). This latter effect determine also the osmotic regulation for supporting the survival of root system (Sicher et al., 2012; Hasibeder et al., 2015) while maintaining the carbon demand for root respiration (Barthel et al., 2011). The allocation of resources to root exudates is an important plant strategy against stress, in particular in nutrient deficiency soils. Indeed, the root exudation process plays a key role in plant nutrient uptake (Mommer et al., 2016) and in the formation of stable soil organic carbon (Sokol et al., 2019). In addition, the root exudates form a direct communication pathway between plants and rhizosphere microbes and have the potential to influence plant tolerance and survival during severe abiotic stress (Williams and de Vries, 2020). In their study, Williams and de Vries (2020) proposed that species-specific responses in root exudation can underline ecosystem responses to drought. They argued that central differences in the responses of root exudation between species that exhibit more conservative traits and those with exploitative traits drive the responses of their associated microbial communities to drought, which in turn feeds back to their own regrowth and ultimately affects ecosystem form and function. Specifically, they postulate that fast-growing species show rapid physiological responses to drought, with tight coupling to their associated soil microbes, as Figure 4 illustrates.



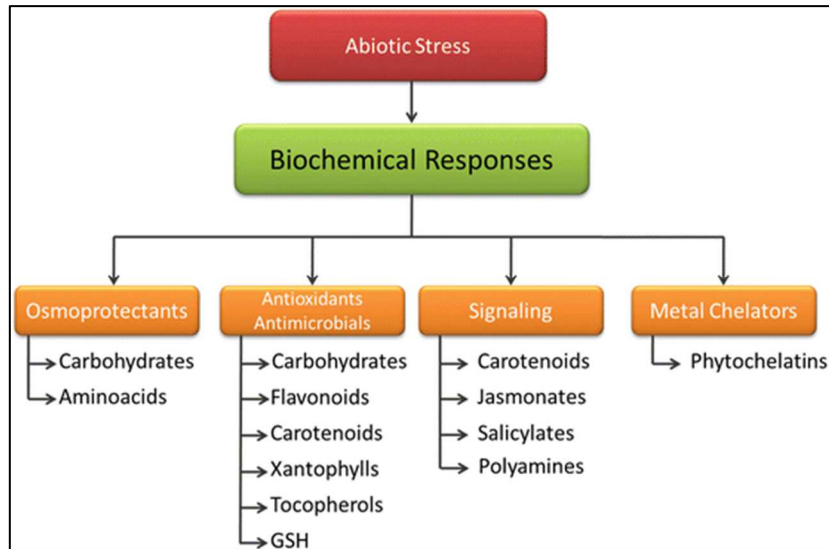
**Figure 4** - Hypothesized role of root exudates in the response of fast-growing and slow-growing plant species to drought and the potential consequences for ecosystem form and function. Arrows indicate exudation inputs into the soil, coloured dots indicate bacterial communities, thick grey lines represent decomposer fungi, and thin purple lines represent arbuscular mycorrhizal fungi. PGPR, plant growth-promoting rhizobacteria; SOM, soil organic matter (source: Williams and de Vries, 2020).

With regard to heat stress, Rollins et al. (2013) observed that in barley the photosynthetic performance was reduced and the leaf proteome changed.

### Metabolic and Molecular responses.

Under stress, plants generate signals for changing their metabolism (i.e. primary and secondary metabolism) and alter it in various ways (Hasanuzzaman et al, 2013). However, the association between metabolic variation and variation in morphological and physiological traits is largely unknown (García et al., 2015; Turner et al, 2016). Primary metabolites, such as carbohydrates, amino acids, and polyamines, are involved in the plant defense against herbivores and pathogens (Seigler, 1998). Plant secondary metabolites pointed out a specific role in the plant-stress interaction such as antioxidant, antimicrobial and signaling (Figure 5) (Arbona et al, 2015; Sarwart, 2017) playing a key role in plants defense (Gatehouse, 2002; Akula and Ravishankar, 2011).





**Figure 5** - Compound classes and roles exerted in response to abiotic stress.

Signaling metabolites include the reactive oxygen species (ROS) (Schmid-Hempel, 2003; Hoffmann, 2005; Lam et al, 2001; Maiti et al, 2018) and the release of some volatile organic compounds (VOCs), consisting mainly of terpenoids, fatty acid derivatives, and a few aromatic compounds, by herbivore-infested plants, that can attract natural enemies of the feeding insect, to reduce enemy pressure (Mithofer and Boland, 2012). Loughrin et al (1994) found that Cotton (*Gossypium hirsutum* L.) plants store large amounts of monoterpenes and sesquiterpenes in lysigenous glands. These constitutive compounds (rapid responses), as well as the green leafy volatiles (i.e. commonly emitted by green plants), are released immediately when the plant is damaged. Then, after several hours or on the next day of herbivore damage, the plants start to release herbivore-induced compounds and will continue to release these compounds for at least 3 days if damage continues (late-term responses).

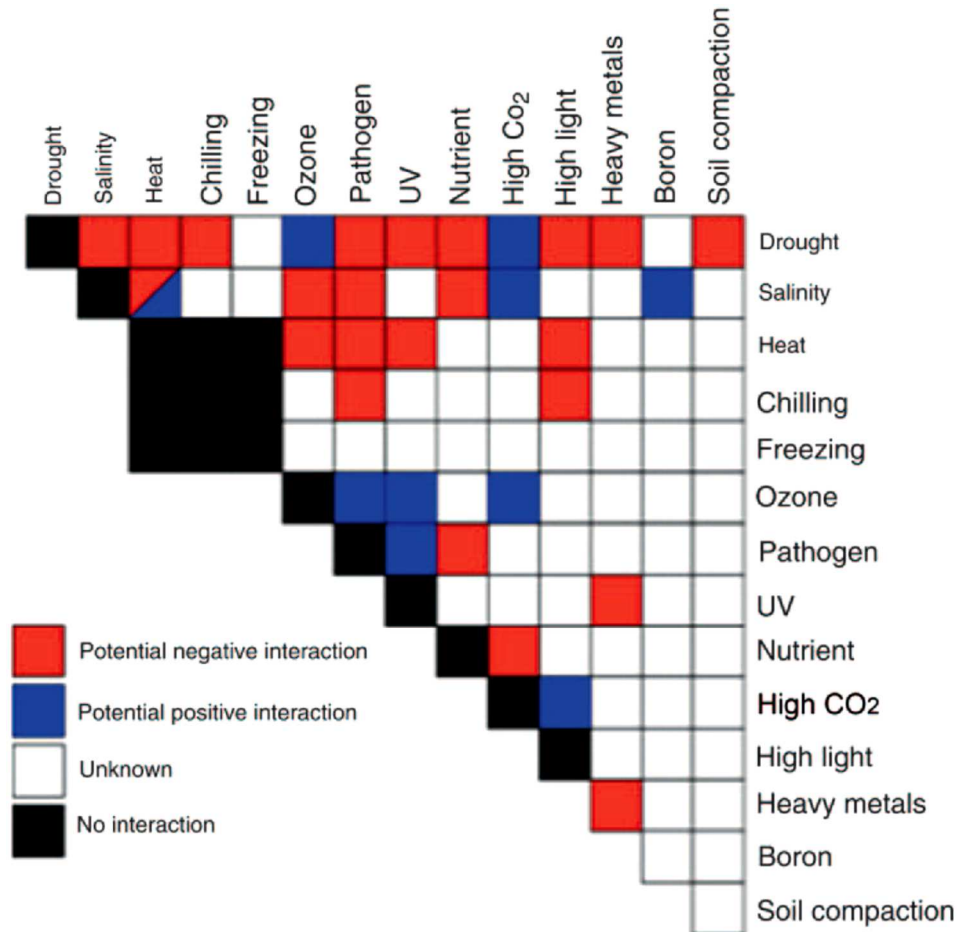
Plants responses are also controlled and regulated at the molecular level by changes in gene expression and many genes are involved (Cramer et al, 2011; Tardif et al., 2007; Kreps et al., 2002; Ingram et al., 1996; Walling, 2000). The complex molecular and biochemical signal transduction processes act in conjunction to regulate tolerance or sensitivity at the whole plant level, by alterations of defense-related genes and proteins at transcription, translation, and post-translational levels (Lee et al, 2020). The timely perception of the stress is a key step in plant defense,

in order to respond in a rapidly and efficiently (Rejeb et al, 2014). First, the sensors on the membrane perceive and capture the external drought stimuli. Then, the signals are transmitted down through multiple signal transduction pathways, resulting in the expression of drought-responsive genes. Signal transmitting pathways begin with a variety of secondary messengers such as  $Ca^{2+}$ , ROS, abscisic acid (ABA), phosphoglycerol, diacylglycerol, salicylic acid (SA), jasmonic acid (JA), and ethylene (ET) and transcriptional regulators (Kaur and Asthir, 2017). In their study, Bitá et al (2011) tried to explain the protective mechanisms and to identify candidate tolerance genes that could be used to improve tomato plants tolerance to heat stress. They used a gel-based transcript profiling method (e.g. cDNA-AFLP, an AFLP-based transcript profiling method that allows genome-wide expression analysis in any species (Vuylsteke et al, 2007)) and microarray analyses to compare the early response of the tomato meiotic anther transcriptome to moderate heat stress conditions (32°C) in a heat tolerant and a heat-sensitive tomato genotype. They concluded that the heat-tolerant genotype, in contrast to the heat-sensitive one, exhibits higher expression levels of genes involved in thermotolerance. Also, the constitutive gene expression profile of the tomato heat-tolerant genotype was different to that of the heat-sensitive one, indicating genetic differences in adaptation to the increase of the temperature. In the heat-tolerant genotype, the majority of changes in gene expression is represented by upregulation, while in the heat-sensitive genotype there is a general trend to down-regulate gene expression upon moderate heat stress (Bitá et al, 2011). The presumed functions associated with the genes identified indicate the involvement of heat shock, metabolism, antioxidant and development pathways.

### **Combined stresses and plant responses to multiple stresses.**

As sessile organisms, plants are continuously exposed to a multitude of biotic and abiotic stresses, that could be multiple, simultaneous or successive stresses, meaning at the same time or consecutively. From seed germination to senescence, there are no any location in the world where plants are isolated from environmental stress. Common combinations of two or more stresses, under natural conditions, are drought and salinity, salinity and heat, drought and heat, drought and high light

intensity, drought and heavy metals, drought and chilling salinity and nutrients (Suzuki et al, 2014). In addition to these abiotic stresses, the plants face the threat of infection by pathogens and attack by herbivore (Atkinson and Urwin, 2012). The various effects of different stress combinations are summarized in Figure 6 (Suzuki et al, 2014).



**Figure 6** - The stress matrix. Different combinations of potential environmental stresses that can affect crops in the field are showed in the form of a matrix. The matrix is color-coded to indicate stress combinations that are studied with a range of crops and their overall effect on plant growth and yield. [Adapted from Suzuki et al. (2014) and modified from Mittler (2006)].

Negative interaction means that plant growth is significantly reduced under both stresses, and the combination of stresses resulted in more injurious effects. For instance, Prasad et al (2011) evaluated the effects of drought, heat stress, and their combination on crop yield in spring wheat. Drought or heat stress caused a significant decrease in grain number, spikelet fertility, grain yield and harvest index as well as Chl contents. The combined effects of these stresses were greater than the effects of drought or heat stress alone. Positive interaction means that some

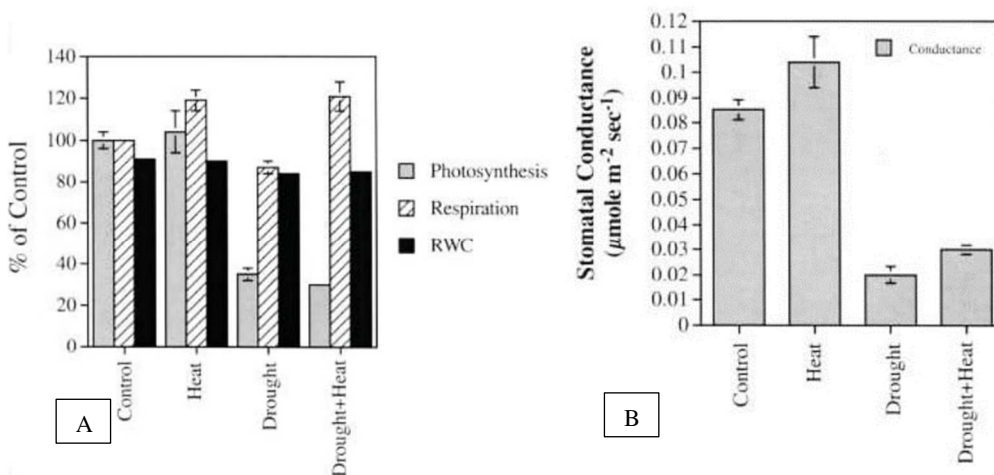
stress combinations might have beneficial effects on plants, when compared with each of the individual stresses applied separately (Suzuki et al, 2014).

Plants are subject to a “new state of stress” when two or more stresses occur concurrently (Mittler, 2006) and, for this reason, emerging evidences suggest that plant responses to a combination of stresses are “unique” from individual stress responses (Mittler, 2006; Mittler and Blumwald, 2010; Alameda et al., 2012; Atkinson & Urwin, 2012; Kasurinen et al., 2012; Srivastava et al., 2012; Perez-Lopez et al., 2013; Rivero et al., 2013; Pandey et al., 2015). In other words, combined stress responses are mostly non-additive effects (i.e., synergistic and antagonistic) and therefore the combined effects cannot be predicted based on results from single-stressor studies. A nonadditive antagonistic interaction can occur when the combined impact of two stressors is less than the sum of individual impacts, while an additive effect happens when the combined impact is simply equal to the sum of the impacts of individual stressors (Folt et al. 1999; Breitburg & Riedel 2005). A synergistic effect occurs when the impact of multiple stresses is greater than expected. An antagonistic effect occurs when the impact of multiple stresses is less than expected. Bansal et al (2013) studied the effects of drought stress and simulated bark-feeding herbivory at three levels of intensity (control, moderate and severe) on young *Pinus sylvestris* L. seedlings. They found that two stressors had synergistic impacts on specific leaf area and water-use efficiency, additive effects on height and root-shoot ratios, but antagonistic effects on photosynthesis, conductance and, most notably, on root, shoot and whole-plant biomass. However, the magnitude of the combined impacts depends on the relative intensities of each stressor (Bansal, 2013).

Prasad et al (2011) try to investigate the independent and combined effects of high temperature and drought stress during grain filling of two spring wheat (*Triticum aestivum* L.) cultivars (Pavon-76 and Seri-82). Their study showed that high temperature or drought stress individually decreased chlorophyll content, leaf photosynthesis, spikelet fertility, grain numbers and grain yield. The interaction between both stress was significant for total dry weight, harvest index and spikelet fertility, particularly when heat was severe. The combined effects of HT and

drought stress were greater than the additive effects of high temperature or drought stress alone for leaf chlorophyll content, grain number and harvest index.

The experiment of Rizhsky et al (2003) in which *Arabidopsis* was exposed to a combination of drought and heat stress demonstrated that heat stress was accompanied by enhanced respiration and opening of stomata, whereas drought was accompanied by suppression of photosynthesis and closure of stomata. In contrast, a combination of drought and heat stress resulted in the simultaneous enhancement of respiration and suppression of photosynthesis, as Figure 7A and 7B.



**Figure 7** (A) Photosynthetic activity and dark respiration, measured with a Li-Cor LI-6400 apparatus. (B) Stomatal conductance, measured with a Li-Cor LI-6400 apparatus [source: Rizhsky et al (2002)].

### Spatio-temporal components of plant responses to stress.

Plants live in a natural surroundings that is spatially and temporally heterogeneous in its biotic and abiotic properties (Ettema and Wardle, 2002; Hodge, 2005). Indeed, the soil-based resources required for plant growth, such as water and nutrient, are heterogeneously distributed (patchy) in time and space both in natural (Bell & Lechowicz 1991; Jackson and Caldwell 1993; Kleb & Wilson 1997, Farley and Fitter, 1999; James et al., 2009; Espeleta and Clark, 2007 ; Vandecar et al., 2011) and agricultural ecosystems (Tittonell et al., 2013; Serrano et al., 2017; Tittonell et al., 2005; Samaké et al., 2005; Zingore et al., 2007). These hydro-nutrient variabilities are observed at spatial scales ranging from a few millimeters (hot spot) (Parry et al., 2000), a few centimeters (Lynch, 1995) to several meters and may persist at time scale ranging from a few days to years (Van Vuuren et al.,

1995). Similarly to the belowground, the aboveground resources also varied in space and time. Examples raised from the sun and shade light patches observed within a plant canopy whose shape, lifetime, and amount of radiation play an important role for the plant growth and development (Baldochi and Collineau, 1994).

The environmental stresses (e.g. high light or temperature intensity, shade/cold, nutrient and/or water stress) intensified the natural heterogeneous distribution of the soil and atmosphere resources (water, nutrient, light) determining a patchily distribution and dynamic evolution of the abiotic and biotic stress in the physical environment of the plants. For example, soils with phosphorus deficiency are characterized by a higher phosphate availability at the upper layers and decreases with depth (Chu and Chang, 1966; Pothuluri et al., 1986); arid soils pointed out an extremely variable both in space and time of the soil moisture (Schwinning and Ehleringer, 2001).

At this spatial and temporal variations of the abiotic and biotic stress, the plants adopted a within-individual (or within-plant) phenotypic variance characterized by a spatial and temporal expression of the responses among their reiterated organs (i.e., distinct root types such as primary/adventitious, different leaves such as sun/shade or sessile/pedunculated, etc.) and along the different organs (nutrient and water uptake at apical vs basal root zones, local and systemic induced plant defenses, etc.). It means that plants pointed out a capacity to express the morpho-physiological and molecular responses at different locations within the organs and with different velocities. For examples, in bean root system, Rubio et al. (2004) observed a root-type and apical zone specific phosphorus uptake that was well highlighted in low P availability; the apical root regions showed higher capacity to absorb  $\text{NO}_3^-$  and a faster induction of the inducible high-affinity transport system verified at physiological and molecular levels in maize plants (Sorgonà et al., 2011); different water uptake capacity and growth rate among the distinct root classes could be important for the plant's adaptation to drought stress (Guo et al. 2008, Hund et al. 2009; Rewald et al. 2011); different responses among root types to combined P/drought stress (Ho et al. 2005) and root resistance (Roman-Aviles et

al. 2004) have been also observed; the within-plant heterogeneity in leaf quality affecting the herbivore behavior or performance (Denno and McClure, 1983). Although lesser studied, this within-plant spatio-temporal modulation of the plant responses to the patchily and dynamic physical environment could permit the plants to improve their fitness in stressed conditions and, above all, could be exploited by crop breeding.

## **Aims and Organization of thesis.**

Climate change imposes a big challenge to the scientific community because it affect the crop production in the near future. Changes in the precipitation intensity and frequency, temperature and number of heatwaves are expected to increase the abiotic and biotic stressful conditions in the agro-ecosystems, of which drought, heat and burst of herbivory are the most harmful for plant growth, development and yield.

The plant adaptation to the single stress (e.g. abiotic or biotic) is extensively studied at morphological, physiological and molecular scale until to provide genetic engineering strategies for increasing the tolerance/resistance to them. However, plant experienced more often multiple stressful conditions in nature than single ones, forcing it to make decisions fine-tuning of responses to allocate resources efficiently for responding to the more serious stress at any given point in time. Few studies on the impact of the stress combination revealed that plant responses are characterized by a “unique” suite of morpho-physiological and metabolic traits orchestrated by metabolic pathways network, signaling transduction, hormone interaction and gene expression, impossible to understand considering the single stress only. Plant responses to the multiple stress are further complicated owing to the strong dependence on the species, genotypes, and type, intensity, duration and frequency of stresses. All these aspects drive the scientific community to highlight how the plants tailor their responses to specific combined stress factors. Furthermore, the studies focused on the plant-stress interactions did not considered the spatio-temporal changes of the abiotic and biotic factors which result in patch and dynamic stressful areas of the physical environment, above all at microscale level (within the plant), to which the plants should be adapt.

In this framework, the present PhD thesis aimed to evaluate the plant morpho-physiological and metabolic responses to combined abiotic and biotic stress at different within-plant spatial levels and temporal scales. To achieve these aims, the present thesis includes the following four case-stud organized in different chapters where the within-plant responses to combined stress are evaluated at population, shoot and root level.



The first case-study investigates the role of the within-plant plasticity of the morpho-physiological and metabolic traits in the adaptation of two different rare populations of *Salvia ceratophylloides* in two different sites. Thanks to the multiple ecological roles of the within-plant variance, the results could provide some information on the population-level intraspecific diversity and the optimization of the growth and defenses machinery of this rare plant useful for its fitness improvement to specific habitats, and, ultimately, the in situ conservation.

The second case-study focus on the impact of the combined abiotic stress (drought and N limitation) and the herbivore infestation on within-plant variance at shoot level in tomato. Tomato production is heavily subjected to *Tuta absoluta* infestation and the induction of defense machinery by drought together with N limitation reduced the *Tuta* larvae growth. However, no information was available on the combined stress effects on the tomato plant and if there is a trade-off between the negative impact on *Tuta* pests and the plant growth. Specific objectives were to analyze the influence of the combined stress on tomato functional traits by the evaluation of the additive, synergistic or antagonistic effects and to verify the impact of the single and combined stress on the within-plant variance that is, as well know, fundamental in the alteration of plant-antagonist interactions.

The third and fourth case-study evaluates the influence of the single and combined stress on within-plant variability at the root level, the “hidden half” of plant and the lesser studied. The root system comprises several root types (primary, seminal, laterals, etc.), genetically determined, which, differentially respond to the environmental conditions so as to be considered markers for the breeding. In this respect, the impact of drought, heat stress and their combination on the growth and morphological parameters and the rhizosphere microbial community of different maize root types were evaluated.

The ultimate goal is to provide knowledge on how plants adapt to their environment characterized by multiple, co-occurring abiotic and biotic stress conditions and by a spatial and temporal heterogeneous distribution of resources (nutrients, water, light, etc.).

## **Chapter 1: The within-plant variation in the morpho-physiological traits and VOCs profile of the endemic rare *Salvia ceratophylloides* Ard. (Lamiaceae).**

*Adapted from: Rosa Vescio et al. The Assessment and the Within-Plant Variation of the Morpho-Physiological Traits and VOCs Profile in Endemic and Rare *Salvia ceratophylloides* Ard. (Lamiaceae) Plants 2021, 10(3), 474. <https://doi.org/10.3390/plants10030474>.*

**Abstract:** *Salvia ceratophylloides* (Ard.) is an endemic, rare, threatened plant species recently rediscovered in very few individuals in two different sites of South Italy. The study of within-plant variation is fundamental to understand the plant adaptation to the local conditions, especially in rare species, and consequently to preserve plant biodiversity. Here we reported the sub-individual morpho-ecophysiological and metabolic analysis of the *S. ceratophylloides* plants to understand the molecular mechanisms adopted to survive in these habitats and the different strategies applied. The *S. ceratophylloides* individuals exhibited different net photosynthetic rate, maximum quantum yield, light intensity for the saturation of the photosynthetic machinery, stomatal conductance, transpiration rate, leaf area, fractal dimension and some VOCs between the leaf sessile and petiolate. This within-plant plasticity was determined by the metabolite profiling and physiological traits more than morphological features and was depended on the site. These results provide empirical evidence of sharply ‘continuous’ within-plant variation of the morpho-physiological traits and VOCs profiles in *S. ceratophylloides* which could be due to adaptation to the local conditions.

**Keywords:** Gas exchanges, LMA, rare species, *Salvia ceratophylloides* Ard., VOC, within-plant plasticity

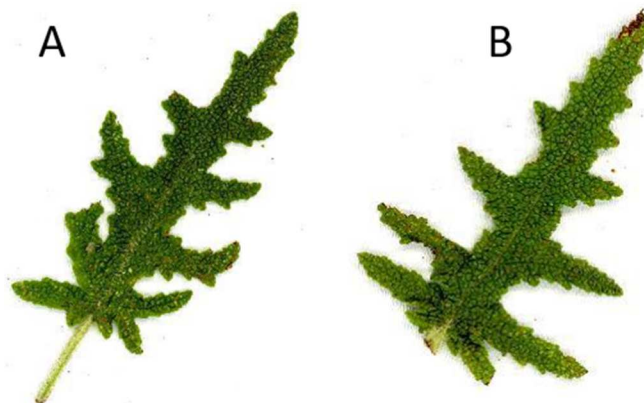
## 1.1. Introduction

*Salvia ceratophylloides* Ard. is a perennial herbaceous plant, endemic to Southern Calabria, declared as extinct in 1997 (Conti et al., 1997) and recently rediscovered in a hundred mature individuals distributed in two sites, 2 Km apart, around the Reggio Calabria hills (Crisafulli et al., 2010; Spampinato et al., 2011). Nowadays, the *S. ceratophylloides* population is threatened with extinction due to habitat modification and destruction by wild urbanization and agriculture (Spampinato et al., 2011). Furthermore, the spread of alien species, favored by climate change, establishes an additional threat factor (Laface et al., 2020; Musarella et al., 2020). The viability of endangered and rare species, as *S. ceratophylloides*, depends on their capability to maintain or even increase its fitness under short- and/or long-term continuous and climate change. Due to the rarity, the endemic species usually pointed out specific and narrow habitat requirements suggesting that their responses must occur only in the actual habitat determining local adaptation through phenotypic plasticity and/or genetic variation (Franks et al., 2014).

Although the results appeared sometimes contrasting, the plant phenotypic plasticity assumed a significant role in the viability of rare and endangered species. For example, Noel et al. (2007) observed a high degree of phenotypic plasticity that conferred an increased fitness in *Ranunculus nodiflorus* Ten. suggesting the maintenance of the micro-environment heterogeneity as habitat-based strategy for its conservation. By contrast, Westerband et al. (2020) observed low phenotypic plasticity in response to drought stress in *Schiedea obovate* (Sherff) W.L. Wagner & Weller, an endangered, endemic Hawaiian shrub, indicating a high risk of extinction in the future climate change scenarios. Based from earlier works of the Winn (1996a, 1996b) and the De Kroon's hypothesis (2005), which dealt with plant phenotypic plasticity at sub-individual level (i.e. organ or module), recently the 'within-plant' rather than "among-plant" phenotypic plasticity could represent the major source of population-level intraspecific diversity in several functional traits (Herrera, 2009; Herrera, 2017). Furthermore, the 'continuous within-plant' variation of homologous structures (i.e. leaves) rather than the 'discrete within-plant' variation (e.g. heterophylly, heterocarpy, and seed heteromorphism), could mainly contribute to population-level variability in evaluating the phenotypic

variance. Nevertheless, recent works pointed out the multiple ecological aspects of the ‘continuous within-plant’ variation such as the improvement of the exploitation of the heterogeneous-distributed resource (Osada et al., 2014; Ponce-Bautista, 2017), the adaptation to biotic and biotic gradients (Hidalgo et al., 2016). The spreading of the ecological breadth of species and individuals (Herrera et al., 2015; Dai et al., 2016), the increase of the functional diversity of populations (Herrera et al., 2015) and the alteration of plant-antagonist interactions (Sobral et al., 2014; Shimada et al., 2015; Wetzal et al., 2016; Wetzal et al., 2019). In spite, no quantitative characterization of the “continuous within-plant” plasticity in endangered and rare plant species was evaluated yet.

In this respect, we started a two years field study for the characterization of the *S. ceratophylloides* by leaf-level morpho-ecophysiological and metabolic analysis from its natural habitat. In particular, this species exhibited a leaf morphology characterized by contemporary presence (petiolate leaf, Picture 1.1A) and absence of petiole (sessile leaf, Picture 1.1B), which could suggest a potential within-plant variation. Further, the individuals of this species were located in two different sites distant <2 km apart suggesting no genetic variability between the two populations (Di Iorio et al., 2018) and indicating the phenotypic plasticity as the most driver for the local adaptation.



**Picture 1.1** - *S. ceratophylloides*: petiolate (A) and sessile leaf (B).

In particular, we focused on the photosynthetic performances as marker of tolerance and growth of species to predict the optimal habitat conditions for the conservation

of rare species (Aleric et al., 2005) but also to provide the capacity of plant adaptation to new conditions associated with climate change and the likely changes in plant communities (Tkemaladze et al., 2016). Further, we took in account the leaf mass per area (LMA) as a morphological trait strictly correlated with the functional syndrome and consequently to plant growth and development and, ultimately, plant fitness (Díaz et al., 2016). At the same time, metabolic profiles could provide information on the plant status and the plant-, microbial- and arthropode-plant communications (Holopainen et al., 2010). The evaluation of all these functional traits could offer useful information for effectively promoting translocation and mitigation operations to restore *Salvia ceratophylloides* rare plant species.

In this framework, the present study investigates the following questions: 1) does the continuous within-plant plasticity patterns of the morpho-physiological traits and metabolic profiles occur in *S. ceratophylloides* species? 2) Which of the morphological, physiological and metabolic traits are determinant for the continuous within-plant variation? Is the within-plant plasticity of *S. ceratophylloides* modified between the localities?

## **1.2. Materials and Methods**

### *1.2.1. Species and sites*

*Salvia ceratophylloides* Ard. was studied by Crisafulli et al.(2010) and Spampinato et al. (2011). Briefly, it is a perennial herb, scapose hemicryptophyte, with woody and upright stems with a dense pubescence of glandular and simple patent hairs (Figure 1.1C). The leaves are opposite pinnate-partite with toothed lobes and morphologically distinct in petiolate (basal, 12x4 cm long and less discrete pinnate lobes and presence of the petiole) and sessile (cauline, 3-4 x 1-2 cm long and more incise pinnate lobes, clasp the stem) (Figure 1.1C). Inflorescences are 20-30 cm in length and made up of 5–6 verticillaster each with 4–6 flowers.

*S. ceratophylloides* plants were studied in two different and closer sites (< 2 Km) located around the Reggio Calabria hills, Mosorrofa (Mo) (38° 5' 42.66" N latitude, 15°43' 18.66"E longitude) and Puzzi (Pu) (38° 4' 52.34" N latitude, 15° 42' 29.23"E longitude) (Southern Italy). Each site consisted in around 60 and 240 individuals for Mosorrofa and Puzzi, respectively. Further, Mosorrofa site is topographically

complex, and located in a little lateral valley of “Fiumara Mandarano” while Puzzi pointed out open and flatter terrains of “Fiumara S. Agata”. Both sites are characterized by layers of loose sand alternating with benches of soft calcarenites of Pliocene origin. The soils have a sandy texture with a basic pH and fall into the group Calcaric Cambisols (Pignatti, 2018).

Species identification is in agreement with Pignatti (2018) and specimens are deposited in the Herbarium of Mediterranean University of Reggio Calabria (acronym REGGIO).

The *S. ceratophylloides* location pointed out a Mediterranean climate with average annual temperatures of 18°C and average annual rainfall of 600 mm mostly in autumn-winter, and a dry period in summer. According to Rivas-Martínez (2019), the macro-bioclimate is “Mediterranean pluviseasonal oceanic” (upper thermos-Mediterranean thermotype and a lower subhumid ombrotype).

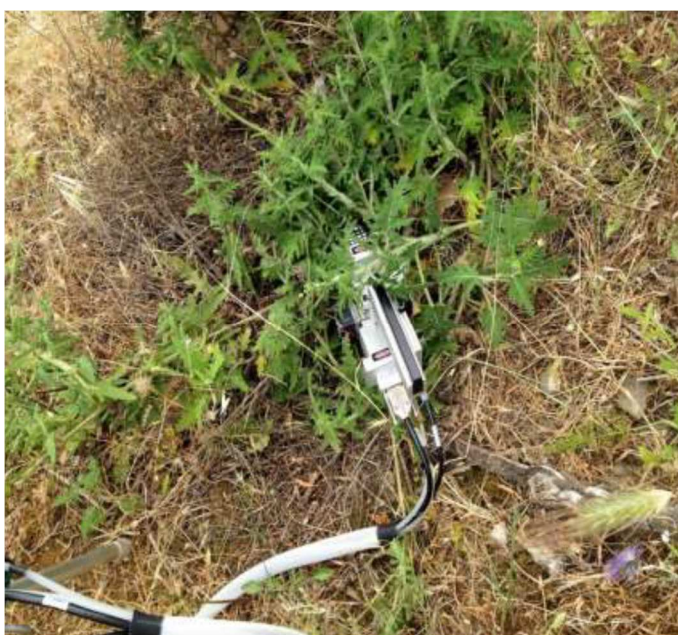
### *1.2.2. Measurements and samplings*

Measurements and samplings were conducted during the early summer (May-June) of 2016 and 2017 on two leaf types: 1) young, upper sessile leaves (S) (two to three nodes from the apex), about 6 months old and 2) old, lower petiolate leaves (P) (non-senescent leaves from fifth to sixth nodes from the apex), about 12 months old (Figure 1.1C). For the morphological and physiological analysis, 4-9 and 5-9 samples for petiolate and sessile leaves, respectively, were collected from at least 4 different plants in each site; while the metabolic analysis was carried out on 3 leaves of each type and site.

### *1.2.3. Physiological analysis*

The net photosynthetic light response curves were determined on leaf area using the LI-6400XT portable photosynthesis system (Li-Cor, Inc. Lincoln, Nebraska, USA, Picture 1.2) at the following irradiance levels: 2000, 1500, 800, 400, 200, 100, 30, 15, and 0  $\mu\text{mol m}^{-2} \text{s}^{-1}$ . The net photosynthesis was measured at 500  $\text{cm}^3 \text{min}^{-1}$  flow rate, 26 °C leaf temperature,  $\text{CO}_2$  concentration 400  $\mu\text{mol}(\text{CO}_2) \text{mol}(\text{air})^{-1}$  (controlled by  $\text{CO}_2$  cylinder). Each measurement was made with a minimum and maximum wait time of 120 and 200 s, respectively, and matching the

infrared gas analyzers for  $50 \mu\text{mol}(\text{CO}_2) \text{ mol}(\text{air})^{-1}$  difference in the  $\text{CO}_2$  concentration between the sample and the reference before every change in I. The leaf to-air vapor pressure difference (VPD) was set to 1.5 kPa, and continuously monitored around the leaf during measurements and maintained at a constant level by manipulating the humidity of incoming air as needed. The measurements are made on sunny days during 8:30 – 11:30 am. Finally, stomatal conductance ( $g_s, \text{mol H}_2\text{O m}^{-2} \text{ s}^{-1}$ ) and transpiration rate measurements ( $T, \text{mmol H}_2\text{O m}^{-2} \text{ s}^{-1}$ ) at each light intensities are evaluated.



**Picture 1.2** - Physiological analysis performed with LI-6400XT portable photosynthesis system.

#### *1.2.4. Morphological analysis*

After the physiological measurements, the same leaves were used for the morphological analysis. In particular, leaf fresh weight (LFW, g) and dry weight (LDW, g), determined by oven at  $70 \text{ }^\circ\text{C}$  for 2 days, and leaf area (LA,  $\text{cm}^2$ ) that was measured by WinRhizo Pro v. 4.0 software package (Instruments Régent Inc., Chemin Sainte-Foy, Québec, Canada) after scanned at a resolution of 300 dpi by WinRhizo STD 1600 (Instruments Régent Inc., Canada). Further, the fractal dimension of the leaf (FD) was obtained by the “fractal analysis module” through the WinRhizo software, based on the box-counting method with the following

settings: maximal pixel size (2.0mm), box sizes ranging from 2 to 32 and filters, and a length:width ratio smaller than 2.00. The FD provides information on the space occupation of the object: the fractal dimension approaches the value of 2 as the leaves become dense to the point of “filling in” a shape. For this reason, the FD was used to correlate the root architecture to the soil resource acquisition (Pignatti, 2018), but also as the correction parameter in the LAI-Light interception models (Jonckheere et al., 2006).

By these parameters, we also calculated the leaf mass per area (LMA, g LDW cm<sup>-2</sup> LA), strongly related to photosynthetic rate (Quero et al., 2006), growth rate (Ruíz-Robledo et al., 2005) and decomposition rate (Cornelissen et al., 1999); the leaf dry content (LDC, g dry weight/g fresh weight), strongly related with relative growth rate (Ryser et al., 1999), flammability (Pérez-Harguindeguy et al., 2013), and post-fire regeneration strategy (Saura-Mas et al., 2009); and leaf water content or leaf succulence (LWC, g H<sub>2</sub>O/cm<sup>2</sup> leaf area], which indicates the leaf water content in relation to its leaf area, directly correlated with the plant responses to abiotic stresses (Cruz et al., 2018).

#### *1.2.5. VOC analysis: HeadSpace/Solid-Phase Micro-Extraction (HS/SPME) GC-MS analysis*

The volatiles (VOCs) produced by petiolate and sessile leaves of *Salvia ceratophylloides* were chemically characterized using the HS/SPME method. One gram of plant material, per sample and replicate (N=3), was sealed in a 20 ml vial and allowed to equilibrate for 20 minutes at room temperature. Successively, the SPME gray fiber (StableFlex, divinylbenzene/Carboxen on polydimethylsiloxane coating; 50/30 µm coating; Supleco) was exposed to plant VOCs for 20 minutes to allow the VOCs adsorption on the fiber.

VOCs were identified using a Thermo Fisher gas chromatograph apparatus (Trace 1310) coupled with a single quadrupole mass spectrometer (ISQ LT). The capillary column was a TG-5MS 30 m×0.25 mm×0.25µm. Helium was used as carrier gas with a flow of 1 ml/min. Samples were injected in a split mode with a split ratio of 60. Injector and source were set at the temperature of 200°C and 260°C, respectively. The temperature ramp was settled as follow: 7 minutes at 45°C, from



45°C to 80°C with a rate of 10°C×min, from 80°C to 200°C with a rate of 20°C×min then isocratic for 3 minutes 200°C. Mass spectra were recorded in electronic impact (EI) mode at 70 eV, scanning the 45–500 m/z range.

Native raw chromatograms (RAW), previously converted in mzXML using the tool MSconvert of proteowizard (Chambers et al., 2012), were normalized for TIC intensity, aligned, deconvoluted and peak intensities extracted using the open source software XCMS (Tautenhahn et al., 2012). For peak analysis the GC/Single Quad (matchedFilter) pre-settled method was used.

After chromatograms processing and peak picking, features and normalized peak areas were imported to Excel for further statistical analysis. Compounds identification was carried out comparing the relative retention time and mass spectra of molecules with those of commercial libraries (NIST Mass Spectral Reference Library) and open source EI spectral libraries (Mass Bank of North America, Golm Metabolome Database) (Kopka et al., 2005; Horai et al., 2010).

#### 1.2.6. Statistical analysis

Light curves were fitted by nonlinear regression using the Ye (2007) model equation:

$$PN = \phi_{(I_0 - I_{comp})} \times \frac{1 - \beta \times I}{1 + \gamma \times I} \times (I - I_{comp}) \quad (1)$$

where:  $P_N$  – the net photosynthetic rate [ $\mu\text{mol}(\text{CO}_2) \text{ m}^{-2} \text{ s}^{-1}$ ];  $I$  – the photosynthetic photon flux density [ $\mu\text{mol}(\text{photon}) \text{ m}^{-2} \text{ s}^{-1}$ ];  $I_{comp}$  – the light compensation point [ $\mu\text{mol}(\text{photon}) \text{ m}^{-2} \text{ s}^{-1}$ ];  $\beta$  – the adjusting factor (dimensionless);  $\gamma$  – the adjusting factor (dimensionless);  $\phi_{(I_{comp} - I_{200})}$  – the quantum yield obtained at the range between  $I_{comp}$  and  $I_{200}$  [ $\mu\text{mol}(\text{CO}_2) \mu\text{mol}(\text{photon})^{-1}$ ]. The following leaf-level photosynthetic parameters were calculated by these equations (Ye, 2007):

$$P_{gmax} = \phi_{(I_0 - I_{comp})} \times \frac{1 - \beta \times I}{1 + \gamma \times I} \times (I - I_{comp}) + R_D \quad (2)$$

$$R_D = \phi_{(I_0 - I_{comp})} \times I_{comp} \quad (3)$$

$$I_{sat} = \sqrt{\frac{(\beta+\gamma) \times (1+\gamma \times I_{comp})}{\beta-1}} \gamma \quad (4)$$

$I_{sat}$  – the light saturation point [ $\mu\text{mol}(\text{photon}) \text{m}^{-2} \text{s}^{-1}$ ];  $P_{gmax}$  – the asymptotic estimate of the maximum gross photosynthetic rate [ $\mu\text{mol}(\text{CO}_2) \text{m}^{-2} \text{s}^{-1}$ ]; RD – the dark respiration rate [ $\mu\text{mol}(\text{CO}_2) \text{m}^{-2} \text{s}^{-1}$ ]. Finally, the  $\phi$  ( $I_{comp} - I_{200}$ ) was calculated as the slope of the linear regression of PN for values of I between  $I_{comp}$  and 200  $\mu\text{mol}(\text{photon}) \text{m}^{-2} \text{s}^{-1}$  representing the “maximum quantum yield”.

Finally, according to Lobo et al. (2013), we reported the  $I_{max}$  ( $\mu\text{mol}(\text{photon}) \text{m}^{-2} \text{s}^{-1}$ ) (light saturation point beyond which there is no significant change in  $P_N$ ) and the  $P_N(I_{max})$  ( $\mu\text{mol}(\text{CO}_2) \text{m}^{-2} \text{s}^{-1}$ ) (maximum value of  $P_N$  obtained at  $I = I_{max}$ ) instead of  $I_{sat}$  and  $P_{gmax}$  as more realistically adequate. We used a simple routine to minimize the error sum of squares (SSE) for fitting the models allowing the determination of equation parameters using the Microsoft Excel spreadsheet and Solver function (Microsoft Excel 2010). Non-linear regressions were repeated several times in order to minimize the sum of square of deviation between predicted and experimental values to less than 0.01% between two consecutive fits (Press et al., 2012).

In order to evaluate the effect of the Years (Y) (2016 and 2017), we used the one-way ANOVA on the gas exchange parameters, which quickly respond to the environmental conditions. Since the Years factor was not significant ( $p > 0.05$ ) for almost all the gas exchange traits (Table S1.1), all the morpho-physiological parameters were analyzed by two-way analysis of variance with the Leaf Type (LT) (sessile and petiolate) and Site (Sit) (Mosorrofa and Puzzi) as main factors and their interaction LtxSit. Then, Tukey’s test was used to compare the means of all the parameters of each LT and Sit. All data were tested for normality (Kolmogorov–Smirnov test) and homogeneity of variance (Levene median test) and, where required, the data were transformed.

For the comparison of the LMA and PN of *S. ceratophylloides* with that of different plant functional groups and *Salvia* spp., we used the  $I_{sat}$  and  $I_{comp}$  data obtained from Larcher et al. (2003) and Duursma et al. (2016) for evergreen angiosperm, Poorter et al. (2009) for evergreen shrub, de la Riva et al. (2016) for evergreen

species, Martins et al. (2017) for *S. officinalis*, Mommer et al. (2007) for *S. pratensis*, Paż-Dyderska et al. (2020) for *S. glutinosa*, Goergen et al. (2009) for *S. hispanica*, Knight et al. (2002) for *S. mohavensis*, *S. leucophylla*, *S. dorrii* var. *dorrii* and *S. mellifera*.

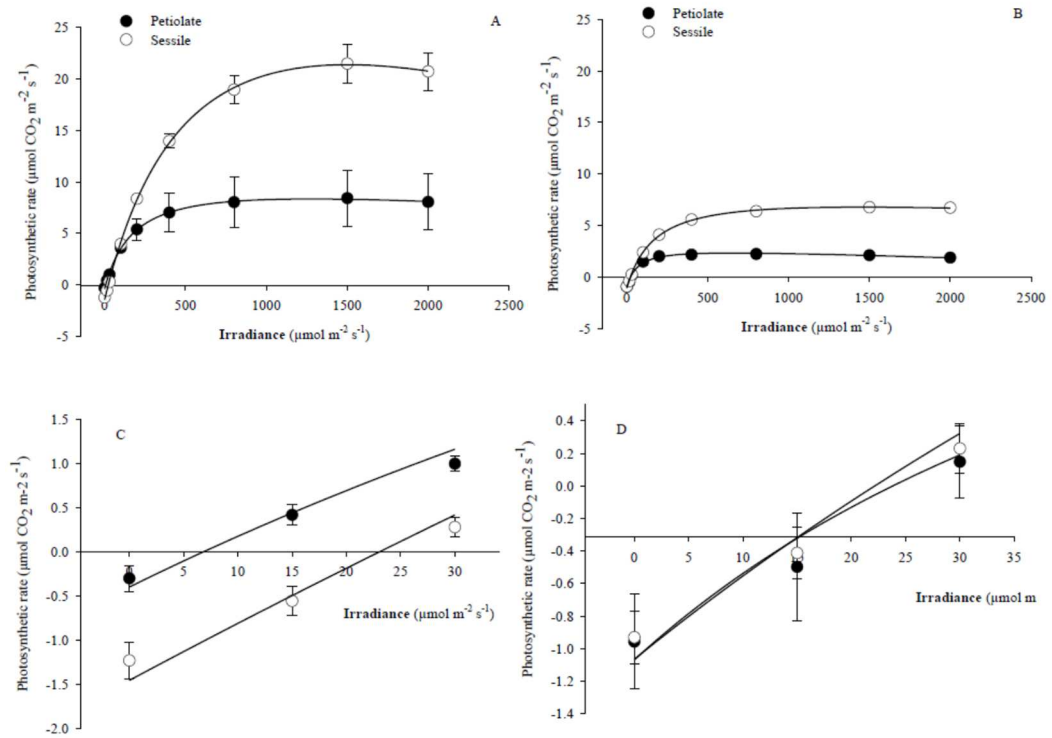
The TIC intensity normalized dataset obtained from metabolomic data analysis were classified through unsupervised Principal Component Analysis (PCA) where the output consisted of score plots to visualize the contrast among different samples. PCA analysis was carried out on all the features detected by the analysis. Successively, identified and annotated compounds were statistically analyzed through univariate two-way analysis of variance with the LT (sessile and petiolate) and Sit (Mosorrofa and Puzzi) as main factors. Then, the Tukey's test was used to compare the compound means of each leaf type and site ( $p < 0.05$ ).

### 1.3. Results

#### 1.3.1. Physiological performances and morphological traits of *S. ceratophylloides*.

The net photosynthetic rate ( $P_N$ ) and the photosynthetic photon flux density (I) curves of *S. ceratophylloides* leaves were well-fitted ( $R^2 > 0.95$  and  $P < 0.05$ ) and – described by Ye mathematical model (2007) (Figure 1.1). The parameters estimated by non-linear regression were reported in Table 1.1. As observed, the leaf type produced a significant and strong effect on the most photosynthetic parameters. In particular, the sessile leaves pointed out a higher  $I_{sat}$  ( $1578 \mu\text{mol}(\text{photon}) \text{m}^{-2} \text{s}^{-1}$ ),  $I_{max}$  ( $766 \mu\text{mol}(\text{photon}) \text{m}^{-2} \text{s}^{-1}$ ),  $P_{Nmax}$  ( $11.22 \mu\text{mol}(\text{CO}_2) \text{m}^{-2} \text{s}^{-1}$ ) and  $\phi$  ( $I_{comp} - I_{200}$ ) ( $0.030 \mu\text{mol}(\text{CO}_2) \mu\text{mol}(\text{photon})^{-1}$ ) level than petiolate ones which, in turn, showed a lower RD ( $0.69 \mu\text{mol}(\text{CO}_2) \text{m}^{-2} \text{s}^{-1}$  vs  $1.19 \mu\text{mol}(\text{CO}_2) \text{m}^{-2} \text{s}^{-1}$ ). This photosynthetic pattern was observed in all the parameters of both sites except for the  $P_{Nmax}$ , which was statistically different between the two leaf types in relation to the site ( $p < 0.05$  LTxSit interaction, Table 1.1): the petiolate leaves ( $6.85 \mu\text{mol}(\text{CO}_2) \text{m}^{-2} \text{s}^{-1}$ ) showed lower value respect to the sessile ones ( $19.70 \mu\text{mol}(\text{CO}_2) \text{m}^{-2} \text{s}^{-1}$ ) at Mo site. Further, the significant LTxSit interaction observed for the  $I_{comp}$  and RD indicated that the parameters difference between the leaf types is affected by site factor. Indeed, the  $I_{comp}$  of the sessile leaf was higher than

petiolate one ( $8$  vs  $22 \mu\text{mol}(\text{photon}) \text{m}^{-2} \text{s}^{-1}$ ) at Mo site only, and same pattern was observed for the RD ( $0.53$  vs  $1.40 \mu\text{mol}(\text{CO}_2) \text{m}^{-2} \text{s}^{-1}$ ) (Table 1.1).



**Figure 1.1** Leaf photosynthetic light-response curves measured on petiolate (●) and sessile leaves (○) of the *Salvia ceratophylloides* located at Mosorrofa (Mo) (A and C) Puzzi site (Pu) (B and D). The C and D panels showed the curves at lowest irradiance values. Data points represent means (N=4-9). Light curves were fitted by non-linear regression using the Ye et al. model (2007).

**Table 1.1** – Leaf-level photosynthetic parameters of different leaf types (P: petiolate; S: sessile) of *Salvia ceratophylloides* individuals of two sites (Mosorrofa, Mo; Puzzi, Pu) estimated by nonlinear regression using the Ye et al. model (2007). Different lower-case letters indicated significant differences at  $p < 0.05$  among the average within column (Tukey's test). Different capital case letters indicated statistical significant differences among the means along the rows ( $p < 0.05$ , Tukey's test).

	Leaf type (LT)	Site (Sit)		Leaf type average
		Mo	Pu	
<b>Icomp</b> [ $\mu\text{mol}(\text{photon})\text{m}^{-2}\text{s}^{-1}$ ]	P	8 <sup>b</sup>	26 <sup>a</sup>	<b>18<sup>x</sup></b>
	S	22 <sup>a</sup>	22 <sup>a</sup>	<b>22<sup>x</sup></b>
	<i>Site average</i>	<b>16<sup>A</sup></b>	<b>23<sup>A</sup></b>	
<b>Imax</b> [ $\mu\text{mol}(\text{photon})\text{m}^{-2}\text{s}^{-1}$ ]	P	312 <sup>b</sup>	310 <sup>b</sup>	<b>311<sup>y</sup></b>
	S	839 <sup>a</sup>	725 <sup>a</sup>	<b>766<sup>x</sup></b>
	<i>Site average</i>	<b>655<sup>A</sup></b>	<b>577<sup>A</sup></b>	
<b>Isat</b> [ $\mu\text{mol}(\text{photon})\text{m}^{-2}\text{s}^{-1}$ ]	P	1027 <sup>b</sup>	818 <sup>b</sup>	<b>911<sup>y</sup></b>
	S	1559 <sup>a</sup>	1588 <sup>a</sup>	<b>1578<sup>x</sup></b>
	<i>Site average</i>	<b>1323<sup>A</sup></b>	<b>1313<sup>A</sup></b>	
<b>PN(Imax)</b> [ $\mu\text{mol}(\text{CO}_2)\text{m}^{-2}\text{s}^{-1}$ ]	P	6.85 <sup>b</sup>	2.17 <sup>b</sup>	<b>4.25<sup>y</sup></b>
	S	19.70 <sup>a</sup>	6.51 <sup>b</sup>	<b>11.22<sup>x</sup></b>
	<i>Site average</i>	<b>14.00<sup>A</sup></b>	<b>4.96<sup>B</sup></b>	
<b>RD</b> [ $\mu\text{mol}(\text{CO}_2)\text{m}^{-2}\text{s}^{-1}$ ]	P	0.53 <sup>b</sup>	1.07 <sup>ab</sup>	<b>0.69<sup>y</sup></b>
	S	1.40 <sup>a</sup>	1.09 <sup>ab</sup>	<b>1.19<sup>x</sup></b>
	<i>Site average</i>	<b>1.01<sup>A</sup></b>	<b>1.08<sup>A</sup></b>	
$\Phi_{(\text{Icomp-200})}$ [ $\mu\text{mol}(\text{CO}_2)\mu\text{mol}(\text{photon})^{-1}$ ]	P	0.025 <sup>b</sup>	0.0095 <sup>c</sup>	<b>0.016<sup>y</sup></b>
	S	0.046 <sup>a</sup>	0.021 <sup>b</sup>	<b>0.030<sup>x</sup></b>
	<i>Site average</i>	<b>0.037<sup>A</sup></b>	<b>0.016<sup>B</sup></b>	

#Statistic analysis: two-way ANOVA with 4-9 replications (LT: leaf type; Sit: sites; LTxSit: Leaf type x Sites interaction); \* $0.05 > P < 0.01$ ; \*\* $0.01 > P < 0.001$ ; \*\*\* $0.001 > P$ ; NS not significant.

Figure S1.1 showed the comparisons of the Isat and the Icomp of *S. ceratophylloides* with those of different functional groups. The minimum Isat value of *S. ceratophylloides* fell between that of sclerophylls in habitat at a high light intensity and heliophytes, while the maximum one was within the range between heliophytes and C4 plants. The minimum Icomp value of *S. ceratophylloides* was located between epiphytes and spring geophytes, while the maximum one was between spring geophytes and heliophytes.

Table 1.2 and 1.3 reported the stomatal conductance and the transpiration rate of both leaves of *S. ceratophylloides* measured at 200 and 800  $\mu\text{mol}(\text{photon})\text{m}^{-2}\text{s}^{-1}$  corresponding to the light intensities around to the Imax values of the P and S

leaves, respectively. Similar to the photosynthetic pattern, the P leaves pointed out a significant lower stomatal conductance and transpiration rate than S at both light intensities. But this effect was different between the sites ( $p < 0.01$  for LTxSit interaction, Table 1.2 and 1.3): the S leaves showed higher levels of stomatal conductance and transpiration rate respect to the P ones only for the Mo site while any difference between the leaf type was produced in Pu site. Furthermore, the effect of the site was highly significant ( $p < 0.001$ , Tables 1.2 and 1.3) for both ecophysiological parameters with the Mo site showing the higher values than Pu one.

The leaf morphology of *S. ceratophylloides* was reported in Table 1.4. Leaf type affected the leaf fresh weight, leaf area, leaf water content, and fractal dimension, which were higher in petiolate leaves (Table 1.4.). This pattern, however, was modified in relation to the site for the LFW and LA only with higher values in the petiolate of Pu site only ( $p < 0.05$  LTxSit interaction, Table 1.4.). Finally, the site factor affected the LFW, the LDW, and the LWC and the Mo site showing the higher values (Table 1.4).

**Table 1.2** – Leaf-level stomatal conductance and transpiration rate of different leaf types (P: petiolate; S: sessile) of *Salvia ceratophylloides* individuals of two sites (Mosorrofa, Mo; Puzzi, Pu) measured at light intensity of  $200 \mu\text{mol m}^{-2} \text{s}^{-1}$ . Different lower-case letters indicated significant differences at  $p < 0.05$  among the average within column (Tukey’s test). Different capital case letters indicated statistical significant differences among the means along the rows ( $p < 0.05$ , Tukey’s test).

	Leaf type (LT)	Sites (Sit)		Leaf type average
		Mo	Pu	
<b>Stomatal conductance</b> (mol H <sub>2</sub> O m <sup>-2</sup> s <sup>-1</sup> )	P	0.032 <sup>b</sup>	0.016 <sup>b</sup>	<b>0.023<sup>y</sup></b>
	S	0.113 <sup>a</sup>	0.029 <sup>b</sup>	<b>0.059<sup>x</sup></b>
	<i>Site average</i>	<b>0.077<sup>A</sup></b>	<b>0.025<sup>B</sup></b>	
<b>Transpiration rate</b> (mol H <sub>2</sub> O m <sup>-2</sup> s <sup>-1</sup> )	P	0.87 <sup>b</sup>	0.55 <sup>b</sup>	<b>0.69<sup>y</sup></b>
	S	2.59 <sup>a</sup>	0.92 <sup>b</sup>	<b>1.52<sup>x</sup></b>
	<i>Site average</i>	<b>1.82<sup>A</sup></b>	<b>0.79<sup>B</sup></b>	

#Statistic analysis: two-way ANOVA with 4-9 replications (LT: leaf type; Sit: sites; LTxSit: Leaf type x Sites interaction); \* $0.05 > P < 0.01$ ; \*\* $0.01 > P < 0.001$ ; \*\*\* $0.001 > P$ ; NS not significant.

**Table 1.3** – Leaf-level stomatal conductance and transpiration rate of different leaf types (P: petiolate; S: sessile) of *Salvia ceratophylloides* individuals of two sites (Mosorrofa, Mo; Puzzi, Pu) measured at light intensity of 800  $\mu\text{mol m}^{-2} \text{s}^{-1}$ . Different lower-case letters indicated significant differences at  $p < 0.05$  among the average within column (Tukey's test). Different capital case letters indicated statistical significant differences among the means along the rows ( $p < 0.05$ , Tukey's test).

	Leaf type (LT)	Sites (Sit)		Leaf type average
		Mo	Pu	
<b>Stomatal conductance</b> (mol H <sub>2</sub> O m <sup>-2</sup> s <sup>-1</sup> )	P	0.032 <sup>b</sup>	0.016 <sup>b</sup>	<b>0.023<sup>y</sup></b>
	S	0.107 <sup>a</sup>	0.032 <sup>b</sup>	<b>0.059<sup>x</sup></b>
	<i>Site average</i>	<b>0.074<sup>A</sup></b>	<b>0.026<sup>B</sup></b>	
<b>Transpiration rate</b> (mol H <sub>2</sub> O m <sup>-2</sup> s <sup>-1</sup> )	P	0.83 <sup>b</sup>	0.55 <sup>b</sup>	<b>0.67<sup>y</sup></b>
	S	2.44 <sup>a</sup>	1.03 <sup>b</sup>	<b>1.53<sup>x</sup></b>
	<i>Site average</i>	<b>1.72<sup>A</sup></b>	<b>0.86<sup>B</sup></b>	

#Statistic analysis: two-way ANOVA with 4-9 replications (LT: leaf type; Sit: sites; LTxSit: Leaf type x Sites interaction); \*0.05>P<0.01; \*\*0.01>P<0.001; \*\*\*0.001>P; NS not significant.

**Table 1.4** – Biometric and morphological parameters of different leaf types (P: petiolate; S: sessile) of *Salvia ceratophylloides* individuals of two sites (Mosorrofa, Mo; Puzzi, Pu). Different lower-case letters indicated significant differences at  $p < 0.05$  among the average within column (Tukey's test). Different capital case letters indicated statistical significant differences among the means along the rows ( $p < 0.05$ , Tukey's test).

	Leaf type (LT)	Sites (Sit)		Leaf type average
		Mo	Pu	
<b>Leaf fresh weight</b> [g/leaf]	P	1.33 <sup>a</sup>	1.38 <sup>a</sup>	<b>1.36<sup>x</sup></b>
	S	1.40 <sup>a</sup>	0.43 <sup>b</sup>	<b>0.78<sup>y</sup></b>
	<i>Site average</i>	<b>1.37<sup>A</sup></b>	<b>0.77<sup>B</sup></b>	
<b>Leaf dry weight</b> [g/leaf]	P	0.23 <sup>a</sup>	0.22 <sup>b</sup>	<b>0.22<sup>x</sup></b>
	S	0.27 <sup>a</sup>	0.12 <sup>b</sup>	<b>0.17<sup>x</sup></b>
	<i>Site average</i>	<b>0.25<sup>A</sup></b>	<b>0.16<sup>B</sup></b>	
<b>Leaf area</b> [cm <sup>2</sup> ]	P	41.4 <sup>ab</sup>	54.4 <sup>a</sup>	<b>48.6<sup>x</sup></b>
	S	43.6 <sup>ab</sup>	19.9 <sup>b</sup>	<b>28.3<sup>y</sup></b>
	<i>Site average</i>	<b>32.2<sup>A</sup></b>	<b>42.6<sup>A</sup></b>	
<b>Leaf mass x area</b> [g m <sup>-2</sup> ]	P	55.4 <sup>a</sup>	44.1 <sup>a</sup>	<b>49.1<sup>x</sup></b>
	S	62.3 <sup>a</sup>	61.6 <sup>a</sup>	<b>61.8<sup>x</sup></b>
	<i>Site average</i>	<b>59.2<sup>A</sup></b>	<b>55.3<sup>A</sup></b>	
<b>Leaf dry content</b> [g dry weight/g fresh weight]	P	0.17 <sup>a</sup>	0.18 <sup>a</sup>	<b>0.18<sup>x</sup></b>
	S	0.19 <sup>a</sup>	0.28 <sup>a</sup>	<b>0.25<sup>x</sup></b>
	<i>Site average</i>	<b>0.18<sup>A</sup></b>	<b>0.24<sup>A</sup></b>	
<b>Leaf water content</b> [g H <sub>2</sub> O/cm <sup>2</sup> leaf area]	P	0.027 <sup>a</sup>	0.020 <sup>a</sup>	<b>0.023<sup>x</sup></b>
	S	0.025 <sup>b</sup>	0.016 <sup>b</sup>	<b>0.019<sup>y</sup></b>
	<i>Site average</i>	<b>0.026<sup>A</sup></b>	<b>0.017<sup>B</sup></b>	
<b>Fractal dimension</b>	P	1.67 <sup>a</sup>	1.73 <sup>a</sup>	<b>1.70<sup>x</sup></b>
	S	1.51 <sup>b</sup>	1.65 <sup>b</sup>	<b>1.56<sup>y</sup></b>
	<i>Site average</i>	<b>1.69<sup>A</sup></b>	<b>1.59<sup>A</sup></b>	

#Statistic analysis: two-way ANOVA with 4-9 replications (LT: leaf type; Sit: sites; LTxSit: Leaf type x Sites interaction); \* $0.05 > P < 0.01$ ; \*\* $0.01 > P < 0.001$ ; \*\*\* $0.001 > P$ ; NS not significant.

Figure S1.2 pointed out the value average ( $\pm$ SD) of LMA of *S. ceratophylloides* in comparison with that of the sun- and shade-species herbs, evergreen angiosperm, evergreen species, herbs, and different *Salvia* species. The LMA range of *S. ceratophylloides* fell in that of the herbs, evergreen species, *S. mellifera*, *S. hispanica*, *S. officinalis*, and sun species.

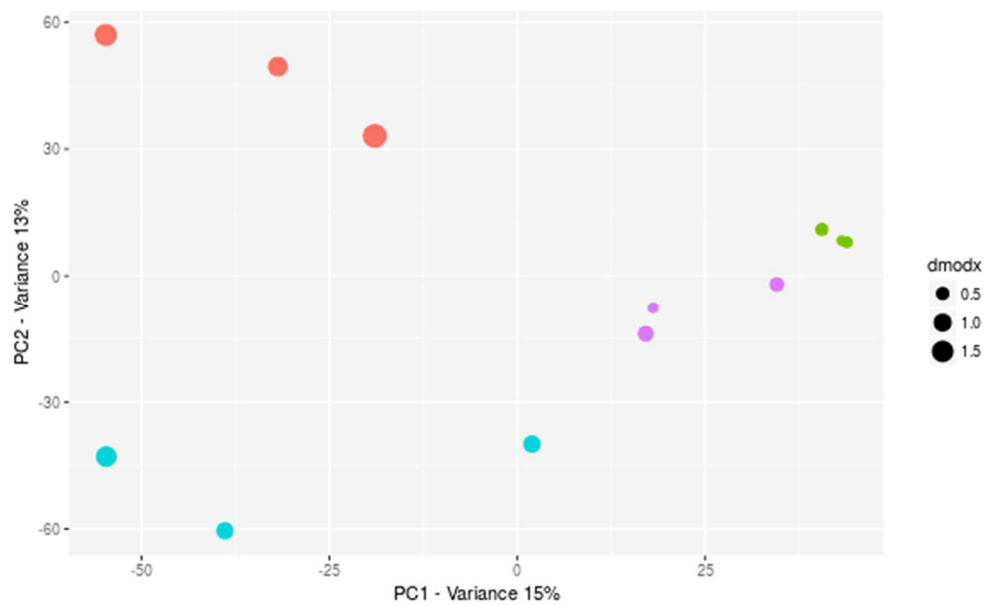


### 1.3.2. VOCs analysis of *Salvia ceratophylloides* in its habitat.

Figure 1.2 showed the PCA of GC-MS spectra of different leaves and sites of *Salvia ceratophylloides*. The two-dimensional PCA score plot revealed a separation in VOCs profile induced by leaf type but this difference was more evident in Mo site than Pu one. Nevertheless, the VOCs profile was also different between the two *Salvia* sites.

In table S1.1 are summarized the VOCs annotated by GC-MS: a total of 39 compounds were identified of which the most representative chemical class was the monoterpene with 17 constituents followed by sesquiterpene (7 chemicals), monoterpene alcohol (4), aldehyde (4), keton (3), alcohol (2), aliphatic esters (1) and ether (1).

Comparing the amount of the XCMS-extracted peak intensities of each chemical between the S and P leaf types, 13 compounds emitted by both P and S were statistically different (Table 1.5.). In particular, p-Cymene, Sabinene, Terpinolene,  $\beta$ -Pinene,  $\gamma$ -Terpinene,  $\alpha$ -Terpineol,  $\alpha$ -Cubebene,  $\alpha$ -Muurolene, Isovaleraldehyde, 5-Methylheptan-3-one, Pentan-3-one,  $\beta$ -tujone, and Dimethyl Sulfide were higher in S than P leaves. However, the higher emission of  $\beta$ -tujone and  $\alpha$ -Terpineol in S leaves was only observed in Mo site (significant LTxSit interaction, Table 1.5.) and the same pattern was revealed for D-germacrene, which was not modified by both leaf type and site as single factors. Only 6 compounds were differently affected by sites: p-Cymene,  $\alpha$ -Terpineol,  $\alpha$ -Copaene and  $\alpha$ -Cubebene were emitted in Pu more than Mo which, conversely, produced more  $\beta$ -tujone and Dimethyl Sulfide (Table 1.5).



**Figure 1.2** - Principal component analysis of untargeted metabolomics data from different leaves (sessile and petiolate) and sites (Mo and Pu) of *Salvia ceratophylloides* individuals: Mo-sessile (red), Mo-petiolate (green), Pu-sessile (blue) and Pu-petiolate (purple).

**Table 1.5.** - Chemical characterization of volatile organic compounds in fresh sessile and petiolate leaves of two sites (Mosorrofa, Mo; Puzzi, Pu) of *Salvia ceratophylloides* plants. Values represent peak areas.

	Compound	#Statistics	Sessile		Petiolate	
			Pu	Mo	Pu	Mo
1	p-Cymene	<b>LT 7.78*</b> <b>Sit 14.16**</b> LTxSit 0.21 <sup>NS</sup>	195813	82392	108569	19607
2	Pinocarvone	LT 0.04 <sup>NS</sup> <b>Sit 6.57*</b> LTxSit 0.07 <sup>NS</sup>	2406	987	2444	696
3	Sabinene	<b>LT 11.80**</b> Sit 0.34 <sup>NS</sup> LTxSit 1.70 <sup>NS</sup>	554775	873306	195242	73210
4	Terpinolene	<b>LT 12.40**</b> Sit 0.40 <sup>NS</sup> LTxSit 3.09 <sup>NS</sup>	128554	218320	62198	19784
5	β-Pinene	<b>LT 7.30*</b> Sit 0.47 <sup>NS</sup> LTxSit 1.73 <sup>NS</sup>	92968	150052	53391	35502
6	γ-Terpinene	<b>LT 5.40*</b> Sit 0.19 <sup>NS</sup> LTxSit 0.04 <sup>NS</sup>	16341	13366	4610	3508
7	α-Terpineol	<b>LT 8.13*</b> <b>Sit 12.91**</b> <b>LTxSit 9.04*</b>	10220 <sup>b</sup>	80003 <sup>a</sup>	11854 <sup>b</sup>	18054 <sup>b</sup>

8	D-Germacrene	LT 0.11 <sup>NS</sup> Sit 3.47 <sup>NS</sup> LTxSit <b>4.22*</b>	2554 <sup>a</sup>	169 <sup>b</sup>	1102 <sup>a</sup>	1218 <sup>a</sup>
9	$\alpha$ -Copaene	LT 0.62 <sup>NS</sup> Sit <b>11.05*</b> LTxSit 0.67 <sup>NS</sup>	3517	601	2385	625
10	$\alpha$ -Cubebene	LT <b>8.21*</b> Sit <b>19.35**</b> LTxSit 1.02	4460201	1371705	2247264	312465
11	$\alpha$ -Muurolene	LT <b>9.49*</b> Sit 0.56 <sup>NS</sup> LTxSit 0.99 <sup>NS</sup>	14382	15236	7105	1038
12	Isovaleraldehyde	LT <b>6.10*</b> Sit 0.52 <sup>NS</sup> LTxSit 0.52 <sup>NS</sup>	81876770	46391341	3426789	3466464
13	5-Methylheptan-3-one	LT <b>5.70*</b> Sit 0.21 <sup>NS</sup> LTxSit 0.08 <sup>NS</sup>	7776	8204	1578	3291
14	Pentan-3-one	LT <b>7.73*</b> Sit 2.44 <sup>NS</sup> LTxSit 1.20 <sup>NS</sup>	321989	649080	114170	171753
15	$\beta$ -tujone	LT <b>17.37**</b> Sit <b>6.21*</b> LTxSit <b>12.54**</b>	65370 <sup>b</sup>	168599 <sup>a</sup>	54660 <sup>b</sup>	36692 <sup>b</sup>

16	(3z)-3-Hexenyl acetate	LT 3.58NS Sit 5.09NS <b>LTxSit 5.46*</b>	1253 <sup>a</sup>	0 <sup>b</sup>	99 <sup>ab</sup>	122 <sup>ab</sup>
17	Dimethyl Sulfide	<b>LT 23.77**</b> <b>Sit 5.34*</b> LTxSit 1.40 <sup>NS</sup>	29866633	54386837	3926181	11857751

#Statistic analysis: two-way ANOVA with 4-9 replications (LT: leaf type; Sit: sites; LTxSit: Leaf type x Sites interaction); \*0.05>P<0.01; \*\*0.01>P<0.001; \*\*\*0.001>P; NS not significant.

## 1.4. Discussion

### 1.4.1. The assessment of the morpho-physiological traits of rare *Salvia ceratophylloides* Ard.

*Salvia ceratophylloides* Ard., endemic, rare, and critically endangered plant species, currently growing on some sites recently found, while it is extinct in the known sites of the last century (Crisafulli et al., 2010; Spampinato et al., 2011).

The knowledge of the morphological and ecophysiological traits are very important for understanding the habitat requirements for the conservation of the endemic species (Aleric et al., 2005) but also for providing their capacity to adapt to new environmental conditions associated with climate change and consequently to the plant communities distribution (Tkemaladze et al., 2016). The responses of these traits in *Salvia ceratophylloides* are reported here for the first time. In particular, we focused on two functional traits, the photosynthetic light-response curve and the leaf mass per area, which are indicative of the habitat preferences and responsive to the environmental conditions (Aleric et al., 2005; Poorter et al., 2009; de la Riva et al., 2016). The photosynthetic response curves to the PAR photon flux and, in particular, the Isat (818-1588  $\mu\text{mol}(\text{photon}) \text{m}^{-2} \text{s}^{-1}$ ) and Icomp values (8-26  $\mu\text{mol}(\text{photon}) \text{m}^{-2} \text{s}^{-1}$ ) suggested that *S. ceratophylloides* is well adapted to the sunny habitat. Indeed, the minimum and maximum values of the Isat fell within the range defined by sclerophyll of sunny habitat and C4 plants (Figure S1.1) and, the Icomp values were included between spring geophytes and heliophytes (Figure S1.1). The LMA values (44.1-55.4  $\text{g m}^{-2}$ ) of *S. ceratophylloides* are comprised in the LMA range of the herbs (Poorter et al., 2009) and evergreen species (de la Riva et al., 2016) (Figure S1.2) confirming that the LMA could be a trait related to the functional plant groups (Poorter et al., 2009). Comparing the different *Salvia* species, the LMA of *S. ceratophylloides* was similar to that of *S. mellifera*, *S. hispanica* and *S. officinalis* (Knight et al., 2002; Castrillo et al., 2005; Goergen et al., 2019) but lower than that of *S. mohavensis* and *S. dorrii* var. *dorrii* (Knight et al., 2002) and higher than that of *S. glutinosa* and *S. pratensis* (Mommer et al., 2007; Paż-Dyderska et al., 2020) (Figure S1.2). The different range of the LMA of *S. ceratophylloides* respect to that of some *Salvia* species, were probably correlated with its functional response to the environmental conditions, such as water and light availability (Poorter et al., 2009; de la Riva et al., 2016). For example, the higher LMA value in *S. mohavensis* and *S. dorrii* var. *dorrii* was

due to the adaptation to their native desert area (mountain ranges of the Mojave Desert of southern California, south-western Nevada, and northern Baja California Norte, Mexico) (Knight et al., 2002). Although the *S. pratensis* was strictly related to *S. ceratophylloides* (belong to the same sect. Plethiosphace: (Goergen et al., 2019) as distributed to the similar area (native from Europe: (Govaerts et al., 2003), it showed lower LMA value (Mommer et al., 2007) probably because of the different growing conditions of *S. pratensis* (pot and growth chamber) in Mommer's experiments. Finally, the LMA values ( $57 \text{ g m}^{-2}$ ) of *S. ceratophylloides* fell in the range of sun species (Figure S1.2.) confirming its preference to the open sunny habitat as for the most *Salvia* species (Castrillo et al., 2005; Nikolova et al., 2017).

#### *1.4.2. Do the within-plant patterns of the photosynthetic performance, morphological traits and metabolic profiles occur?*

Recently, the 'continuous' within-plant variation as an expression of intraspecific phenotypic plasticity is strongly taken into account for its role in plant evolution and ecology at individual, population, and community levels (Herrera, 2009; Herrera, 2017). For example, the sub-individual variation in leaf morpho-physiological traits allows the adaptation of each individual to optimize i) its capturing structures to the heterogeneous local environmental conditions such as light, temperature and CO<sub>2</sub> gradients within plant canopy in trees (Osada et al., 2014) and in perennial herbs (Herrera et al., 2015) and ii) its cost-expensive defenses against herbivory and pathogens (McKey, 1974; Meldau et al., 2012). Further, the knowledges of the leaf-level photosynthetic performances within the plant allows to scale at canopy level (Medrano et al., 2015) and to understand the competitive strategies for exploring the within-canopy heterogeneous light, and CO<sub>2</sub> availability. In this respect, the 'continuous' within-plant variation of *S. ceratophylloides* by comparing the morpho-physiological and metabolic traits of petiole and sessile leaves were here evaluated, for the first time at our knowledge.

The P and S leaf types of *S. ceratophylloides* exhibited a clear 'continuous' within-plant variability underlying that the metabolite profiling and physiological traits (10 out 10 parameters, considering the LTxSit interaction also; Table 1.1, 1.2 and 1.3, Figure 1.2) varied more than morphological features (4 out 7 parameters; Table 1.4). Why do *S. ceratophylloides* plants choose to invest in the physiological and metabolic capacity more

than size-related traits between S and P leaves? Since the phyllotaxy of *S. ceratophylloides* plants is opposite decussate (low self-shaded), the different photosynthetic machinery performances along the shoot axes could allow a well-optimized light use at low cost respect to the cost-expensive changes of morphological traits. This choice is supported by scientific evidence. For example, the plant physiological plasticity is more related to an enhanced ability to colonize gaps and open areas and, hence, exploiting the transient environmental resources at low cost by short-term adjustments, briefly the plant acclimatization (Niinemets et al., 2004; Meier et al., 2008; Marchiori et al., 2017; Puglielli et al., 2017). Conversely, the plant expensive morphological plasticity is more functional for the plant adaptation at the long-term and probably useful, for growing in forest understories (Niinemets et al., 2004; Meier et al., 2008; Marchiori et al., 2017; Puglielli et al., 2017; Valladares et al., 2000). Furthermore, the choice to invest in higher within-plant plasticity of the physiological traits than morphological ones was also reported by Herrera et al. (2015), which observed that the within-ramet variation in *Helleborus foetidus* L. was more due to the stomatal features than leaf size- and area-related traits causing an increase of seed number produced by each individual (Herrera, 2017).

Comparing the leaf types, the S pointed out a better photosynthetic performance by higher net photosynthetic rate and maximum quantum yield, higher  $I_{sat}$  (1578 vs 911  $\mu\text{mol}(\text{photon}) \text{m}^{-2} \text{s}^{-1}$ ) and higher stomatal conductance but they exhibited a lower leaf area and capacity to fill the space as evidenced by FD, respect than the P ones. Hence, a switch between the short-term low-expensive and the long-term high-expensive traits for the resource acquisition and use (light,  $\text{CO}_2$ ) in S (uppermost) and P leaves (lowest) respectively, was observed. Hence, the leaves placed at the top of the shoot of *S. ceratophylloides* facing high light intensity, temperature, and vapor pressure deficit, could use higher photon and  $\text{CO}_2$  fluxes for increased their carbon gains by high  $I_{sat}$  and stomatal conductance. The spatial distribution of more efficient structures or functions within plants to fit the micro-environmental heterogeneous conditions and to maximize the photosynthesis and carbon gain is already known in different plant species (Schurr et al., 2006). Further, the higher stomatal conductance, in turn, determined a higher transpiration rate that limited the leaf overheating, as reported by Lin et al. (2017) in dry areas species. The smaller size and shape of the sessile leaves (lower leaf area and fractal



dimension), mainly determined by lower water content, was further insurance, beneficial allied for avoiding leaf overheating by lower aerodynamic resistance (Lin et al., 2017; Leuzinger et al., 2007) but also for reducing the water loss by smaller total leaf area.

The within-plant variation of *S. ceratophylloides* was also observed in the VOCs composition and emission. Indeed, the S and P leaves were sharply separated by VOC-based metabolic profiles (Figure 1.2) suggesting different intensity and composition between two leaves. Further, the emission of 14 out of 39 identified VOCs was statistically increased in S leaves respect than P ones (Table 1.5 and Table S1.1). The VOCs with higher emission in sessile leaves included monoterpenes (p-Cymene, Sabinene, Terpinolene,  $\beta$ -Pinene,  $\gamma$ -Terpinene, and  $\alpha$ -Terpineol), sesquiterpenes (D-Germacrene,  $\alpha$ -Cubebene,  $\alpha$ -Muurolene) and green leaf volatiles ((3Z)-3-Hexenyl acetate) mostly involved in defenses against herbivory and pathogens (Pichersky et al., 2018) and in responses to abiotic stress (Loreto et al., 2010). The within-plant variation of VOCs emission in response to herbivory was already observed in wild and crop species (Frost et al., 2007; Rodriguez-Saona et al., 2009) but no evidence at field level was reported yet. Why do *S. ceratophylloides* plants defend the S more than P leaves by higher VOCs emission? Probably, the upper, younger, sessile leaves are more protected in views of its high performing photosynthetic machinery) and nutritive value (the high leaf dry content, although not statistical support) as suggested by optimal defense hypothesis (ODH) (McKey, 1974; Meldau et al., 2012). Overall these results pointed out the within-plant functional subdivision at morpho-physiological and metabolic levels of *S. ceratophylloides* mimicking what has been already observed in the wide crown of trees for heat tolerance (Slot et al., 2019), light acquisition and differential expression of genetic polymorphisms in sun and shade leaves of trees (de Casas et al., 2011) and defense responses to herbivory (Girón-Calva et al., 2014).

The within-plant variation of both morpho-physiological and metabolic traits was affected by site suggesting that *Salvia* plants were adapted to local conditions. Indeed, the morpho-physiological patterns of the S and P leaves changed between the two sites for most traits (on 12 that showed the leaf type factor as statistically significant, nine traits pointed out LTxSit interaction). The S leaves pointed out a higher photosynthetic rate, stomatal conductance, and transpiration rate associated with higher dark respiration and Icomp than P ones in the Mo site only. These results could be due to phenotypic plasticity

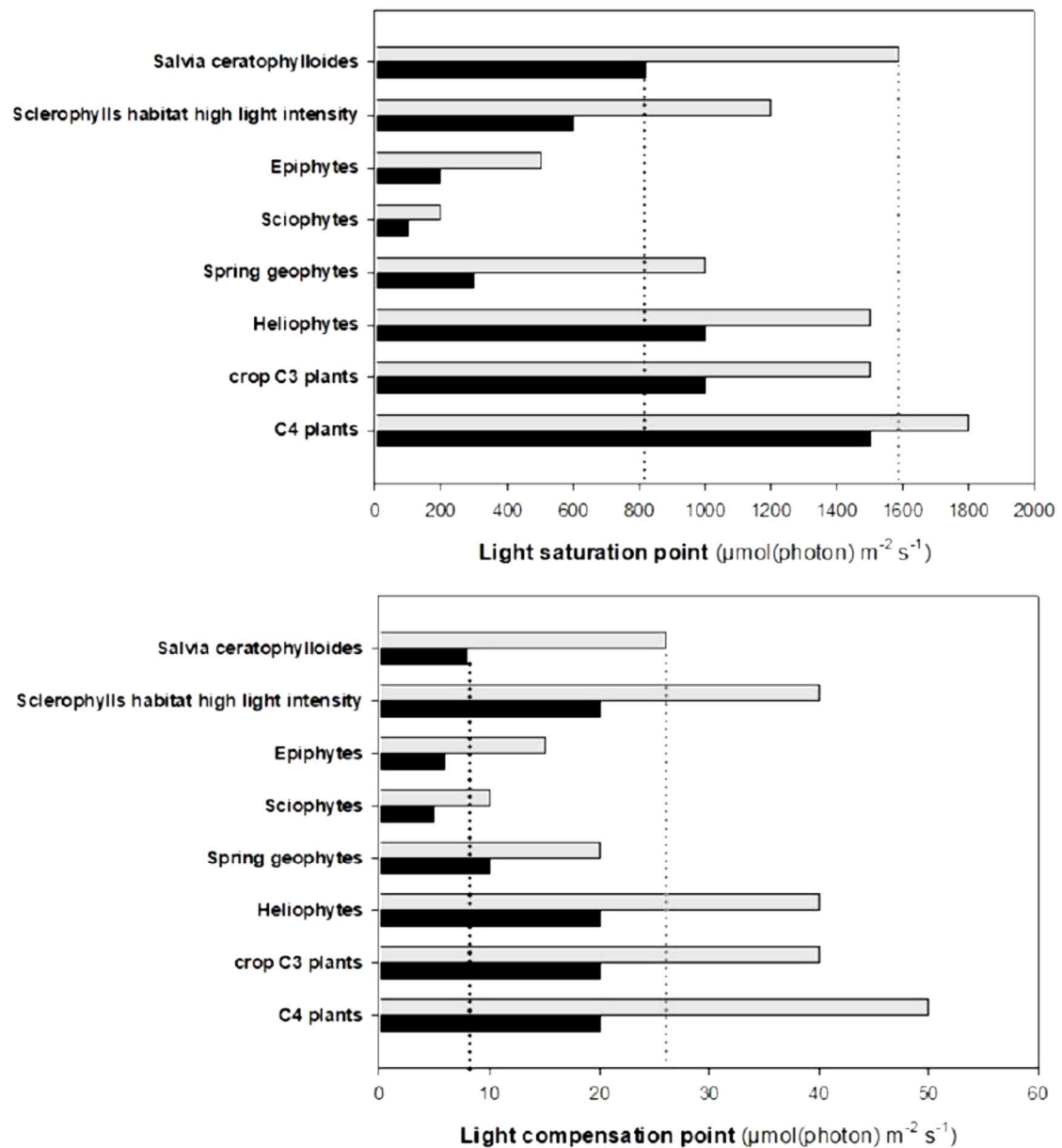
in response to local conditions (Alberto et al., 2013; Aitken et al., 2013) because preliminary results demonstrated a low genetic variability of *S. ceratophylloides* populations (Di Iorio et al., 2018). It was observed that the within-individual phenotypic plasticity responded to the microhabitat environmental heterogeneity or fine-grained (small-scale) environmental variations (Winn, 1996a; de Kroon et al., 2005; Osada et al., 2014; Ponce-Bautista et al., 2017) rather than macro-geographical or coarse-grained environmental variations (Herrera et al., 2015; Sobral et al., 2013; Bruschi et al., 2003). In this respect, we can hypothesize that the *S. ceratophylloides* individuals in the Mo site, showing a statistically significant within-plant leaf morpho-physiological variation, could face with a higher microhabitat environmental heterogeneity, especially for light intensity and/or temperature gradients (the most important abiotic stresses affecting the leaf growth), than Pu site. Opedal et al. (2015) observed that the microhabitat environmental heterogeneity increased with the topographically complex sites modifying the intraspecific traits of 16 plant species. The Pu site is characterized by flatter, more open terrains and higher altitude than Mo one, which conversely is placed at a lower altitude at the base of the valley, closed and with rough terrains (Figure 1.1) determining, probably, a short duration of light and steeply thermal and light gradients in the latter location. Unlike the morpho-physiological traits, the within-plant variation of metabolic profiles was lesser affected by the different sites. Indeed, the PCA pointed out that the metabolic profiles of S and P leaves were separate at both sites and only 4 single VOCs out 13 exhibited a statistically significant LtxSit interaction. Considering that the VOCs emission is more involved to the biotic stress (plant-plant, plant-herbivory, and plant-pathogen interactions) (Holopainen et al., 2010), probably the *Salvia* plants in both sites are faced to similar biotic environment heterogeneity or variability (predation, competition, etc.) differently to the abiotic ones (light, temperature, etc.), determining thus the maintaining of the same within-plant VOCs emission in *S. ceratophylloides* at both sites.

## 1.5. Conclusions

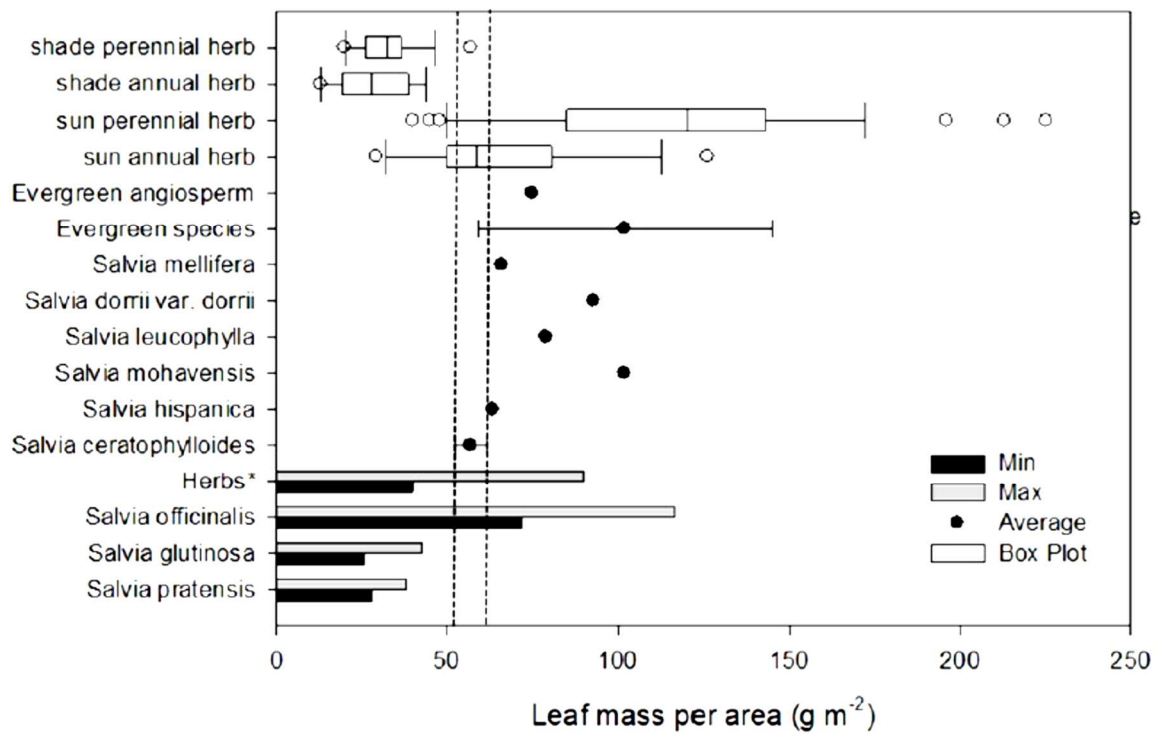
The eco-physiological adaptation of *S. ceratophylloides*, a rare and endangered plant species, to its habitat by functional traits was evaluated. The higher light saturation and compensation point and leaf mass per area indicated a sunny habitat preference of *S.*

*ceratophylloides*. These results suggested that for its in-situ conservation, lower competition (low density and diversity) especially with woody species (trees and shrubs), should be favored. However, the *S. ceratophylloides* habitat has been destroyed and continuously fragmented due to anthropogenic disturbance and environmental deterioration and, consequently, further and deepening study needs to identify the main stressful factors that threaten its growth, development, and fitness. For the artificial propagation, *ex-situ* conservation, we recommend growing the seedlings at least half sunlight ( $1200 \mu\text{mol (photons) m}^{-2} \text{s}^{-1}$ ).

Further, for the first time, the “continuous within-plant variation” of the morpho-physiological traits and metabolic profiles of endangered and rare plant species was assessed in the field. The results indicated that the physiologic and metabolic traits explained most of this within-plant plasticity which was also affected by the location. Indeed, the sessile and petiolate leaves of *S. ceratophylloides* showed different photosynthetic performances and metabolic profiles but the sub-individual variation of the photosynthetic-related parameters, differently to the volatilome, was exhibited in one site only. These within-plant patterns, probably related to the micro-environmental heterogeneity, could optimize the growth and defenses machinery for the fitness’s improvement to specific habitats. Overall, the magnitude of the within-plant variation should be taken into consideration when designing sampling schemes for the ecological studies of *S. ceratophylloides*.



**Figure S1.1** - Light saturation point ( $\mu\text{mol}(\text{photons}) \text{m}^{-2} \text{s}^{-1}$ ) (upper panel) and light compensation point ( $\mu\text{mol}(\text{photons}) \text{m}^{-2} \text{s}^{-1}$ ) (bottom panel) of different plant functional groups. The data [minimum (■) and maximum value (■)] are derived from Larcher (2003). The dotted lines are drawn for a better comparison with the minimum and maximum value of *Salvia ceratophylloides*.



**Figure S1.2** - Leaf mass per area ( $\text{g m}^{-2}$ ) of sun- and shade-species herbs, evergreen angiosperm and species, herbs and different *Salvia* species. The data of LMA of *Salvia* species, herbs, evergreen angiosperm and species are indicated by minimum (■) and maximum value (▒) or by the average (black plot point and the standard deviation where reported) and were derived from Martins et al. (2017) for *S. officinalis*, Mommer et al. (2007) for *S. pratensis*, Paz'-Dyderska et al. (2020) for *S. glutinosa*, Goergen et al. (2019) for *S. hispanica*, Knight and Ackerley (2002) for *S. mohavensis*, *S. leucophylla*, *S. dorrii* var. *dorrii* and *S. mellifera*, Poorter et al. (2009) for herbs, Duursma et al. (2016) for evergreen angiosperm and de la Riva et al. (2016) for evergreen species. Box plots point out the distribution of LMA values as observed for a wide range of sun- and shade-species herbs both annual and perennial, with the bottom and top part of the box indicating the 25<sup>th</sup> and 75<sup>th</sup> percentile, respectively, the two whiskers the 10<sup>th</sup> and the 90<sup>th</sup> percentile, respectively, and the horizontal line within the box the median value. The data for the box plot are derived by scientific literature as indicated in Table S1.1. The dotted lines were drawn for better comparisons and pointed out the range of LMA values of *Salvia ceratophylloides*.

**Table S1.1** – Two-way ANOVA results and chemical characterization of volatile organic compounds in fresh sessile and petiolate leaves of *Salvia ceratophylloides* harvested in two different sites (Mosorrofa, Mo; Puzzi, Pu). Values represent peak areas.

Compound	Chemical classes	#Statistics	Sessile		Petiolate		
			Pu	Mo	Pu	Mo	
Camphene	Monoterpene	LT	0.75 <sup>NS</sup>	468	141	130	184
		Sit	0.64 <sup>NS</sup>				
		LTxSit	1.25 <sup>NS</sup>				
Camphor		LT	2.78 <sup>NS</sup>	1776	368	606	34
		Sit	4.82 <sup>NS</sup>				
		LTxSit	0.86 <sup>NS</sup>				
Limonene		LT	5.30 <sup>NS</sup>	77187	72261	53128	19515
		Sit	1.33 <sup>NS</sup>				
		LTxSit	0.74 <sup>NS</sup>				
p-Cymene	LT	<b>7.78*</b>	195813	82392	108569	19607	
	Sit	<b>14.16**</b>					
	LTxSit	0.21 <sup>NS</sup>					
Pinocarvone	LT	0.04 <sup>NS</sup>	2406	987	2444	696	
	Sit	<b>6.57*</b>					
	LTxSit	0.07 <sup>NS</sup>					
Sabinene	LT	<b>11.80**</b>	554775	873306	195242	73210	
	Sit	0.34 <sup>NS</sup>					
	LTxSit	1.70 <sup>NS</sup>					
Terpinolene	LT	<b>12.40**</b>	128554	218320	62198	19784	
	Sit	0.40 <sup>NS</sup>					
	LTxSit	3.09 <sup>NS</sup>					

trans-Sabinene hydrate	LT Sit LTxSit	0.00 <sup>NS</sup> 0.28 <sup>NS</sup> 3.73 <sup>NS</sup>	3086	4773	5342	2381
trans- $\alpha$ -Ocimene	LT Sit LTxSit	0.56 <sup>NS</sup> 3.02 <sup>NS</sup> 0.04 <sup>NS</sup>	4784232	2005449	3790259	292998
$\alpha$ -Pinene	LT Sit LTxSit	1.04 <sup>NS</sup> 0.68 <sup>NS</sup> 0.60 <sup>NS</sup>	548	104	50	36
$\alpha$ -Terpinene	LT Sit LTxSit	0.01 <sup>NS</sup> 5.21 <sup>NS</sup> 6.02 <sup>NS</sup>	1116	1202	2418	22
$\alpha$ -Thujene	LT Sit LTxSit	3.83 <sup>NS</sup> 4.44 <sup>NS</sup> 3.74 <sup>NS</sup>	1186	114	153	108
$\beta$ -Myrcene	LT Sit LTxSit	2.54 <sup>NS</sup> 0.15 <sup>NS</sup> 0.01 <sup>NS</sup>	10189	8949	4114	2208
$\beta$ -Ocimene	LT Sit LTxSit	0.54 <sup>NS</sup> 3.61 <sup>NS</sup> 0.38 <sup>NS</sup>	3309	978	2059	868
$\beta$ -Phelladrene	LT Sit LTxSit	0.80 <sup>NS</sup> 3.86 <sup>NS</sup> 0.60 <sup>NS</sup>	1327	167	620	117

β-Pinene	<b>LT</b>	<b>7.30*</b>	92968	150052	53391	35502
	Sit	0.47 <sup>NS</sup>				
	LTxSit	1.73 <sup>NS</sup>				
γ-Terpinene	<b>LT</b>	<b>5.40*</b>	16341	13366	4610	3508
	Sit	0.19 <sup>NS</sup>				
	LTxSit	0.04 <sup>NS</sup>				
<hr/>						
cis-Pinen-3-ol	LT	1.40 <sup>NS</sup>	882	51	7	60
	Sit	1.13 <sup>NS</sup>				
	LTxSit	1.46 <sup>NS</sup>				
Eucalyptol	LT	0.42 <sup>NS</sup>	124492	278959	194614	53771
	Sit	0.00 <sup>NS</sup>				
	LTxSit	1.52 <sup>NS</sup>				
<b>monoterpene</b>						
<b>alcohol</b>						
Isoborneol	LT	1.48 <sup>NS</sup>	7041	156368	7160	46949
	Sit	4.42 <sup>NS</sup>				
	LTxSit	1.48 <sup>NS</sup>				
α-Terpineol	<b>LT</b>	<b>8.13*</b>	10220 <sup>b</sup>	80003 <sup>a</sup>	11854 <sup>b</sup>	18054 <sup>b</sup>
	<b>Sit</b>	<b>12.91**</b>				
	<b>LTxSit</b>	<b>9.04*</b>				
<hr/>						
D-Germacrene	LT	0.11 <sup>NS</sup>	2554 <sup>a</sup>	169 <sup>b</sup>	1102 <sup>a</sup>	1218 <sup>a</sup>
	Sit	3.47 <sup>NS</sup>				
	<b>LTxSit</b>	<b>4.22*</b>				
α-Caryophyllene	LT	0.62 <sup>NS</sup>	43235 <sup>a</sup>	19311 <sup>a</sup>	33115 <sup>a</sup>	8972 <sup>a</sup>
	Sit	3.43 <sup>NS</sup>				
	LTxSit	0.00 <sup>NS</sup>				
<b>Sesquiterpene</b>						
α-Copaene	LT	0.62 <sup>NS</sup>	3517	601	2385	625
	<b>Sit</b>	<b>11.05*</b>				
	LTxSit	0.67 <sup>NS</sup>				



$\alpha$ -Cubebene		LT <b>8.21*</b> Sit <b>19.35**</b> LTxSit 1.02	4460201	1371705	2247264	312465
$\alpha$ -Muurolene		LT <b>9.49*</b> Sit 0.56 <sup>NS</sup> LTxSit 0.99 <sup>NS</sup>	14382	15236	7105	1038
$\beta$ -Caryophyllene		LT 1.56 <sup>NS</sup> Sit 2.04 <sup>NS</sup> LTxSit 0.17 <sup>NS</sup>	30708	18290	19500	12669
$\beta$ -Copaene		LT 2.46 <sup>NS</sup> Sit 2.74 <sup>NS</sup> LTxSit 2.19 <sup>NS</sup>	1001	100	126	74
<hr/>						
(z)-Hex-3-en-1-ol	<b>Alcohol</b>	LT 0.06 <sup>NS</sup> Sit 4.29 <sup>NS</sup> LTxSit 0.06 <sup>NS</sup>	2721741	7008	2159260	8617
1-Octen-3-ol		LT 0.05 <sup>NS</sup> Sit 3.20 <sup>NS</sup> LTxSit 0.13 <sup>NS</sup>	22710	12017	23730	7653
<hr/>						
2-Propenal		LT 0.89 <sup>NS</sup> Sit 1.20 <sup>NS</sup> LTxSit 0.87 <sup>NS</sup>	900	94	153	88
Isovaleraldehyde	<b>aldehyde</b>	LT <b>6.10*</b> Sit 0.52 <sup>NS</sup> LTxSit 0.52 <sup>NS</sup>	81876770	46391341	3426789	3466464
Octenal		LT 2.94 <sup>NS</sup> Sit 1.40 <sup>NS</sup> LTxSit 0.16 <sup>NS</sup>	10441	7566	6602	5171

$\alpha$ -Methyl-n-Butanal		LT	5.19 <sup>NS</sup>	32740199	30174050	3454460	4492251
		Sit	0.00 <sup>NS</sup>				
		LTxSit	0.02 <sup>NS</sup>				
5-Methylheptan-3-one		<b>LT</b>	<b>5.70*</b>	7776	8204	1578	3291
		Sit	0.21 <sup>NS</sup>				
		LTxSit	0.08 <sup>NS</sup>				
Pentan-3-one	<b>Keton</b>	<b>LT</b>	<b>7.73*</b>	321989	649080	114170	171753
		Sit	2.44 <sup>NS</sup>				
		LTxSit	1.20 <sup>NS</sup>				
$\beta$ -tujone		<b>LT</b>	<b>17.37**</b>	65370 <sup>b</sup>	168599 <sup>a</sup>	54660 <sup>b</sup>	36692 <sup>b</sup>
		<b>Sit</b>	<b>6.21*</b>				
		<b>LTxSit</b>	<b>12.54**</b>				
(3z)-3-Hexenyl acetate	<b>Aliphatic esters</b>	LT	3.58 <sup>NS</sup>	1253 <sup>a</sup>	0 <sup>b</sup>	99 <sup>ab</sup>	122 <sup>ab</sup>
		Sit	5.09 <sup>NS</sup>				
		LTxSit	5.46*				
Dimethyl Sulfide	<b>ether</b>	<b>LT</b>	<b>23.77**</b>	29866633	54386837	3926181	11857751
		<b>Sit</b>	<b>5.34*</b>				
		LTxSit	1.40 <sup>NS</sup>				

#Statistic analysis: two-way ANOVA with 4-9 replications (LT: leaf type; Sit: sites; LTxSit: Leaf type x Sites interaction); \*0.05>P<0.01; \*\*0.01>P<0.001; \*\*\*0.001>P; NS not significant. Different lower-case letters indicated significant differences at p<0.05 among the average along the rows (Tukey's test) and they were only reported when the LTxSit interaction was significant. The bold identify the statistically significant factors and/or their interaction.

## **Chapter 2: Abiotic and biotic combined stress in tomato: additive, synergic and antagonistic effects and within-plant phenotypic plasticity.**

**Keywords:** within-plant phenotypic plasticity; combined stresses; synergic effects; metabolome; VOC

### **2.1. Introduction**

Owing to sessile nature, plants are continually exposed to abiotic (mainly drought, heat and salinity) and biotic stresses (pathogens and herbivory) whose intensity and frequency are expected to be increased by climate change. The effects of these stresses and how the plants respond to these stressful factors taken individually, have been extensively studied at both the morpho-physiological and molecular scale (Heil and Bostock, 2002; He et al., 2018) and plant community level (Maron and Crone, 2006; Mordecai, 2011). However, under field condition, these various biotic and abiotic factors are constantly changing during the plant life cycle and, above all, co-occur in nature (Pandey et al., 2017). Hence, the plants have to make decisions about fine-tuning their responses to allocate resources efficiently for responding to the more serious and different threats at any given point in time. Different studies have uncovered that plants evoke a “unique response” to the abiotic and biotic combined stresses compared to the single stress (see the reviews Mittler, 2006; Atkinson & Urwin, 2012; Suzuki et al., 2014; Pandey et al., 2015, 2017) revealing that the plant responses to combined stress pointed out “a new stress state” with mostly non-additive effects (i.e., synergistic and antagonistic). For example, the insect herbivory antagonized the heat responses in tomato (Havko et al., 2020), the emission of specific VOCs was synergized by the combination of aphid and drought stress in tomato plants (Catola et al., 2018) as well in the larvae of green alder sawfly (*Monsoma pulveratum*) and *Alnus glutinosa* interaction (Copolovici et al., 2014), some morphological traits of *Pinus sylvestris* were synergized while others antagonized in drought and simulate herbivory combination (Bansal et al., 2013). In addition to the “new stress state”, the plant responses to the stress are strictly dependent on the plant traits, genotypes, species, and type, intensity, frequency and duration of the stress suggesting

that more investigation are needed for a better understanding of the abiotic and pest herbivore interaction, the stress combination lesser studied.

The plant responses to the individual abiotic and biotic stress have been showed to observe a modulation (induced and constitutive) with a strong spatio-temporal component (local and systemic, transient and permanent) that determined a high “within-plant variation”. For example, the spatial scale of herbivore- induced changes can range from localized at the site of attack (Mason et al. 2017) to systemic throughout the entire plant or tissue type (Orians, 2005; Park et al., 2007; Pieterse et al., 2014) as well the light and heat gradients determined different responses within the tree canopy (Slot and Krause, 2019; de Casas and Vargas, 2011) or the nutrient deficiency caused different morpho-physiological responses among the root types (Rubio et al., 2004; Sorgonà et al., 2007). The temporal scale of the plant responses can also vary: rapid or long term, ontogenic-modulated (Boege and Marquis, 2005) and in some cases even trans- generational responses are evoked for the herbivory (Agrawal et al., 1999; Holeski, 2007) as well the abiotic stress (Kollist et al., 2019). The multiple ecological role of the ‘within-plant’ variation was recently pointed out in the adaptation to individual biotic and biotic gradients (Hidalgo et al., 2016) and the alteration of plant-antagonist interactions (Sobral and Guitián, 2014; Shimada and Takahashi, 2015; Wetzel and Kharouba, 2016; Wetzel and Meek, 2019) so much so that it was proposed as “functional trait itself” whose influences on ecosystem functioning still neglected (Herrera et al., 2015). In spite of this important role, the within-plant variation in response to the combined stress has been still no investigated at our knowledge.

Since 2006, the tomato production of the Mediterranean region is under attack by a newly introduced insect, *Tuta absoluta* (Desneux et al., 2010, 2011) whose larvae feed on leaves, stems and fruits causing severe damage to the tomato with decreases in production both in the field and greenhouse (Desneux et al., 2011). Studies revealed that the low nitrogen levels and drought stress inputs to tomato negatively affected the biological traits of the *T. absoluta* (Han et al., 2014; Larbat et al., 2016) but arised that the N deficiency and drought could be also unfavorable to the tomato plants suggesting to evaluate the trade-off between negative impact on *Tuta* pests and plant growth. In this respect, experiments were set up to study the spatial and temporal expressions of the morpho- physiological and metabolic responses of the tomato plants to the single and/or combined abiotic

(drought+N deficiency) and biotic stress. In particular, the present study investigates the following questions: 1) Are the morpho-physiological responses to individual stresses different from the combined ones in tomato plants? 2) Are additive, synergistic or antagonistic effects in the combined stress? 3) Do the tomato responses to the single and combined stress occurred at between- or within-plant levels?

## **2.2. MATERIAL AND METHODS**

### *2.2.1. Experimental procedure and Plant material*

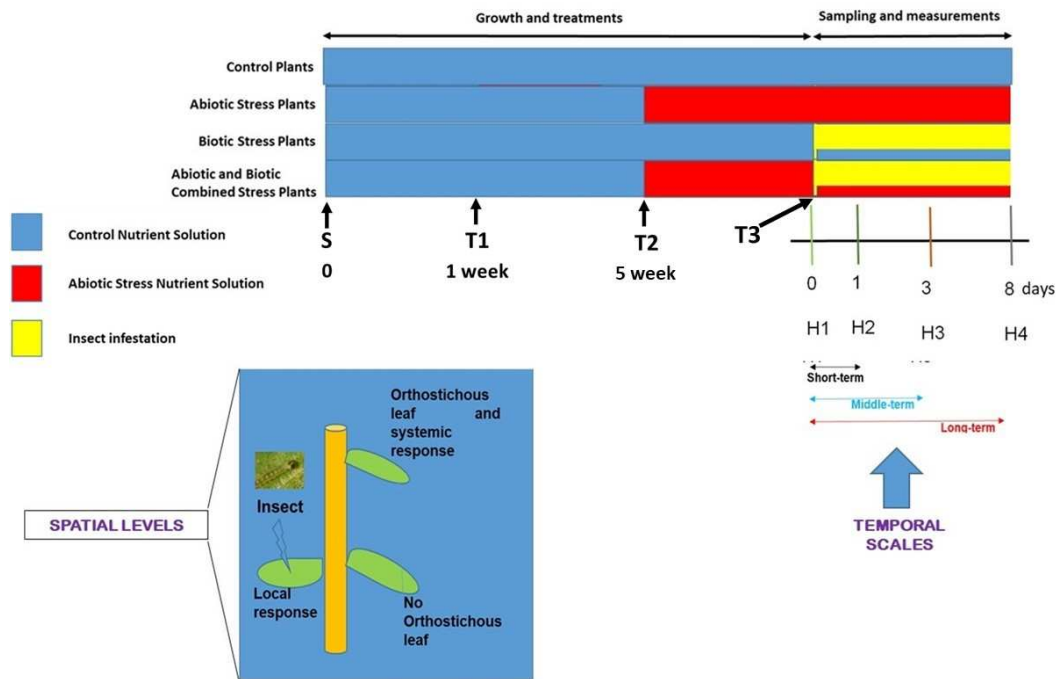
This study was constituted by two experimental sets addressing different but consequently related questions.

The first experiment, i.e. the ‘synergic, antagonistic and additive effects’, aimed to determine the tomato response to the single and combined stress and their temporal evolution and whether the responses to the combined stress were the results of the additive, synergistic or antagonistic effects of the single stress. For this purpose, the effects of the abiotic (drought and N deficiency) (ABIO), biotic (herbivores) (BIO) and combined stress (abiotic plus biotic stress) (COMB) and the time of exposure (0, 1, 3 and 8 days) on the morphological (leaf fresh and dry weight and water content), physiological (photosynthesis, stomatal conductance, transpiration rate and  $WUE_i$ ) and metabolic (VOC) plant traits were evaluated. The leaf fresh and dry weight are traits directly related to the plant status, while the leaf water content was strictly correlated with the plant drought tolerance (Ahmed et al., 2012) but also with the plant palatability (Schädler et al., 2003). The gas exchange traits (photosynthesis, stomatal conductance, transpiration and water use efficiency) are involved in the plant responses to drought and N deficiency (Flexas et al., 2018; Schwarz et al., 2002) and the photosynthesis is “...a *plant-driven response to the perception of stress rather than a secondary physiological response to tissue damage...*” highlighting a strict interactions between photosynthesis, ROS and hormonal signaling pathways for the plant response to insect herbivory (Kerchev et al., 2012). Finally, the VOCs, as direct and indirect defense, are emitted by plants subject to both abiotic and biotic stress (Holopainen and Gershenzon, 2010).

Tomato plants (*Solanum lycopersicum* L., cultivar nano S. Marzano) (provided by BAVICCHI S.p.a., ITALY) were exposed to the abiotic stress (nitrogen limitation and drought stress simulated by the use of PEG), biotic stress (two first instar larvae placed

in a leaf), or their combination and were considered as ‘stress condition’. The control group (CTR) was maintained at optimal N concentration and no drought and herbivory and it was considered as the ‘optimal condition’. For the morpho-physiological analysis, we used a randomized block design in which the entire experiment yielded a total of 4 (treatments) x 4 (time of exposure) x 2 (block) x 2 (replications) = 64 samples. The block was introduced because we used two experiments at two different times. A completely randomized design was used for the VOC profiling, in which the entire experiment was constituted by 4 (treatments) x 4 (time of exposure) x 3 (replicates) x 3 (measurements) = 144 samples. The replicates for the VOC were obtained in three different experiments. The second experiment, i.e. “within-plant phenotypic plasticity”, aimed to evaluate the within-plant variation of the tomato morpho-physiological and metabolic traits and how this within-plant phenotypic plasticity changed with each environmental conditions (optimal, abiotic, biotic and combined stress). For this aim, the environmental effects on tomato traits were evaluated on three mature leaves located at three different positions along the shoot axes for each treatment. For each treatment, we used a completely randomized design in which the entire experiments yielded a total of 3 (leaves) x 1 (time of exposure) x 3 (replicates) = 9 samples. For the gas exchanges traits only, we took two measurements for each leaf, hence the experiments provided 3 (leaves ) x 1 (time of exposure) x 2 (measurements) x 4 replicates = 24 samples.

The Figure 2.1 reported the experimental protocol schedule of both experiments including the plant growth, treatments and analysis.



**Figure 2.1** – Protocol schedule including tomato growth and treatments (S: plant seeding; T1: Plant transfer to hydroponic system; T2: abiotic treatment start; T3: *Tuta absoluta* larvae infestation) and plant sampling events (H1-H4: samplings and analysis). Analysis: morphological analysis (leaf fresh and dry weight, leaf water content), physiological (photosynthetic rate, stomatal conductance, transpiration rate and WUEi) and VOC profiling. The tomato responses were evaluated at temporal and spatial scales.

### 2.2.2. Growth condition

Tomato seeds were surface sterilized for 15 min in 10% (v/v) sodium hypochloride, rinsed with tap water and then were germinated in a Petri dish (diameter 90 mm) on filter paper with 0.1 mM CaSO<sub>4</sub>. After 7 d of germination (7 DAS), six seedlings of uniform size were transferred to eight hydroponic unit containing 4.5 L of the following aerated nutrient solution at 50% strength and adjusted to pH 6.0 with 0.1 M potassium hydroxide: 5mM KNO<sub>3</sub>, 1 mM NH<sub>4</sub>NO<sub>3</sub>, 1.44 mM MgSO<sub>4</sub>, 3.99 mM Ca(NO<sub>3</sub>)<sub>2</sub>, 0.97 mM KH<sub>2</sub>PO<sub>4</sub>, 1 mM K<sub>2</sub>SO<sub>4</sub>, 25 μM H<sub>3</sub>BO<sub>3</sub>, 50 μM KCl, 2 μM MnSO<sub>4</sub>, 4 μM ZnSO<sub>4</sub>\*7H<sub>2</sub>O, 0.5 μM CuSO<sub>4</sub>\*5H<sub>2</sub>O, 0.5 μM (NH<sub>4</sub>)Mo<sub>7</sub>O<sub>24</sub>\*4 H<sub>2</sub>O, 20 μM EDTA iron(III) sodium salt.



**Picture 2.1** - Hydroponic unit. Each color indicates a different treatment.

This nutrient solution (Nutritional recommendation for tomato” downloaded from Haifa website: <http://www.haifa-group.com/files/Guides/tomato/Tomato.pdf>) was adopted after preliminary experiments that compared different nutrient solutions on tomato growth and SPAD unit.





**Picture 2.2** – Plant growth differences between treatments (black is CTR, red is ABIO, yellow is BIO, red and yellow is COMB).

The hydroponic units were placed in a growth chamber at 24°C; 14 h photoperiod; photon flux rate of 300  $\text{mmol m}^{-2} \text{s}^{-1}$ ; 70% RH.

After 7 days (14 DAS), the nutrient solution was brought to 100% strength and the plants of each pot were reduced at four for the morpho-physiological analysis while they were left to six for the VOC and metabolomics analysis. The nutrient solution was renewed every 2 days.

### 2.2.3. Insect Rearing

The tomato leafminer *Tuta absoluta* (*Lepidoptera: Gelechiidae*) colony was maintained in climatic chambers (25°C, RH 70%, 16h light). It was kept in cages (Bugdorm® -

60x60x60 cm) and containing tomato plants. Sugar and water were provided *ad libitum* to adults in rearing cages.

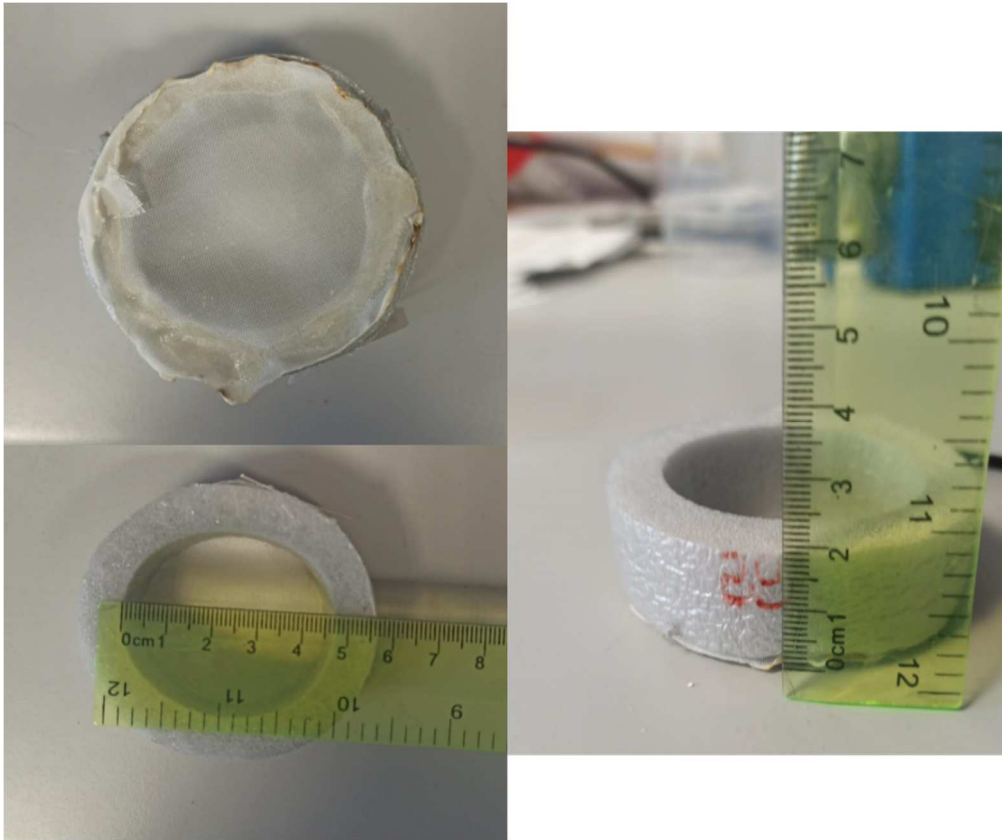
#### 2.2.4. Abiotic stress and Herbivory treatment

At 28 DAS, six hydroponic units continued to receive the same nutrient solution as described in growth condition while in two hydroponic units were added 5% (w/v) Polyethylene glycol 8000 (Sigma PEG8000) and 1 mM nitrogen for simulating the drought stress and nitrogen deficiency, respectively (ABIO group). The final PEG concentration was gradually achieved by the addition of 2.5% (w/v) PEG8000 every two days. The osmotic potential of the solutions, measured by a osmometer (Freezing point osmometer, Osmomat 3000, Gonotec), was -0.55 MPa for 5% PEG and -0.05 MPa for the control solution (0% PEG). To obtain 1 mM N for the nitrogen deficiency, the  $\text{NH}_4\text{NO}_3$  was not added and the  $\text{KNO}_3$  and  $\text{Ca}(\text{NO}_3)_2$  were reduced to 1 mM and 0.5 mM, respectively. In order to balance K and Ca, the  $\text{K}_2\text{SO}_4$  was increased to 3 mM and the 3.5 mM  $\text{CaSO}_4$  was added.

At 42 DAS, the six remaining hydroponic units were treated as following:

- 1) two hydroponic units were renewed the optimal nutrient solution (CTR group);
- 2) two hydroponic units were renewed the nutrient solution with N deficiency and PEG (ABIO group);
- 2) two hydroponic units received the optimal nutrient solution but the plants were infested with *Tuta* larvae to induce the biotic stress (BIO group);
- 3) two hydroponic units maintained the same nutrient solution with N deficiency and PEG and In addition the plants were infested by *Tuta* larvae (COMB group).

Preliminary experiments were conducted to individuate the PEG8000 and N concentrations used for simulating the drought stress and nitrogen deficiency for the entire experiment without plant death. The plant infestation was obtained by placing two first instar larvae of *Tuta* in the 1<sup>st</sup> fully-developed leaf (with 5 leaflets) from the bottom and to avoid larvae escaping, each infested leaf was then bagged with a nylon mesh of 4.7 cm diameter (Picture 2.3).



**Picture 2.3** - Larva bag with a nylon mesh.

We added herbivorous insects to plants (Picture 2.4) after 7 days of abiotic stress treatment in order to simulate the effects of a pest outbreak which are predicted to become more frequent with climate change (IPCC 2018).



**Picture 2.4** - Trap for *Tuta absoluta*'s larva.

## **2.2.5. First experimental set: synergic, antagonistic and additive effects.**

### *2.2.5.1. Measurements and samplings*

At 0 (42 DAS), 1 (43 DAS), 3 (45 DAS), and 8 days from the treatments (50 DAS), the measurements/samplings were realized in order to simulate the short-, middle- and long-time responses, respectively. The measurements for the gas exchange traits were carried out on terminal leaflet of 1<sup>st</sup> fully-developed leaf (in presence of larvae, we used lateral leaflets) while the whole plants was used for the morphological analysis. Three consecutively leaves for each treatments and time of exposure were sampled for the VOC.

### *2.2.5.2. Gas exchange measurements*

A calibrated portable photosynthesis system (LI-6400; LI-COR, Inc.; Lincoln, NE) was used to measure net CO<sub>2</sub> assimilation rate ( $A$ ,  $\mu\text{mol}(\text{CO}_2) \text{m}^{-2} \text{s}^{-1}$ ), stomatal conductance ( $g_s$ ,  $\text{mol H}_2\text{O m}^{-2} \text{s}^{-1}$ ), and transpiration rate ( $T$ ,  $\text{mmol H}_2\text{O m}^{-2} \text{s}^{-1}$ ). These gas exchange parameters were measured at  $500 \text{ cm}^3 \text{ min}^{-1}$  flow rate,  $26 \text{ }^\circ\text{C}$  leaf temperature, CO<sub>2</sub> concentration  $400 \mu\text{mol}(\text{CO}_2) \text{ mol}(\text{air})^{-1}$  (controlled by CO<sub>2</sub> cylinder), and  $1200 \mu\text{mol}$

$\text{m}^{-2}\text{s}^{-1}$  of photosynthetically active radiation supplied by the LED light source in the leaf chamber. Each measurement was made with a minimum and maximum wait time of 120 and 200 s, respectively, and matching the infrared gas analyzers for  $50 \mu\text{mol} (\text{CO}_2) \text{mol}(\text{air})^{-1}$  difference in the  $\text{CO}_2$  concentration between the sample and the reference before every change of plants. The leaf to-air vapor pressure difference (VPD) was set to 1.5 kPa, and continuously monitored around the leaf during measurements and maintained at a constant level by manipulating the humidity of incoming air as needed. All measurements were performed in growth chamber.

Finally, the water use efficiency intrinsic ( $\text{WUE}_i$ ) was calculated as the rate of photosynthesis ( $A$ ) divided by the rate of stomatal conductance to water ( $g_s$ ) (Seibt et al., 2008).

#### 2.2.5.3. Morphological measurements

All the leaves of the plants were harvested, immediately weighted to obtain the leaf fresh weight (LFW, g) and placed in an oven at  $70^\circ\text{C}$  for 2 days to determine the leaf dry weight (LDW, g).

By the above measurements, the leaf water content (LWC, %) was calculated as the following as reported in Jin et al. (2017):

$$\text{Leaf Water content (\%)} = (\text{LFW} - \text{LDW}) / \text{LFW} * 100 \quad (1)$$

#### 2.2.5.4. VOC analysis

Volatile organic compounds (VOCs) from three leaves per treatments and time of exposure were profiled by HS/SPME method. One leaf was sealed in a 20 ml hermetic vial with butyl lid and allowed to incubate for 20 minutes at room temperature. The fiber (50/30  $\mu\text{m}$  DVB/CAR/PDMS) (Supelco®, Bellefonte, PA, USA) was conditioned according to the supplier's instructions prior to its use and then was inserted into the headspace of the vial containing the sample for 20 minutes for the adsorption of a suitable and representative number of volatiles. The volatiles were desorbed by placing the fiber for 6 min into the injection port of the GC-MS system. All the SPME sampling and desorption conditions were identical for all the samples. Blanks were performed before first SPME extraction and randomly repeated during each series.

GC-MS analyses were performed with a Thermo Fisher TRACE 1300 gas chromatograph equipped with a DB-5 capillary column (30 m x 0.25 mm; coating thickness = 0.25  $\mu\text{m}$ , with 10 m of pre-column) and a Thermo Fisher ISQ LT ion trap mass detector (emission current: 10 microamps; count threshold: 1 count; multiplier offset: 0 volts; scan time: 1.00 second; prescan ionization time: 100 microseconds; scan mass range: 30–300 m/z; ionization mode: EI).

GC-MS data were obtained under the following analytical conditions: carrier gas Helium (He 99.99%); flow rate 1 ml/min; splitless. The initial oven temperature was 60°C for 3 min, after which it was raised to 240°C at 6 °C/min, where it was held for 3 min. The injection port, transfer line, and source temperatures were 250°C, 250°C, and 260°C, respectively.

Qualitative identification was performed using GC-MS reference libraries (NIST x.0). Linear retention indices (LRI) were determined from the retention times of a series of n-alkane mixture (C<sub>8</sub>-C<sub>20</sub>, Sigma Aldrich, Milan, Italy) analysed under identical conditions (Van den Dool & Kratz, 1963). Percentage of the studied compounds were calculated from the peak areas in the total ion chromatograms. The relative abundance of volatile compounds was relative to the total amount or released volatiles, after subtracting eventual contaminants.

#### **2.2.5.6. Statistical analysis**

##### *Morpho-physiological data*

By SPSS Inc., V. 10.0, 2002 (SPSS Inc., Evanston, IL, USA), all the morpho-physiological parameters were analyzed by ANOVA with the Treatment (Tr) (CTR, ABIO, BIO and COMB), Time of exposure (Ti) and Block (Bl) as main factors and the TrxTi as interaction. Then, Tukey's test was used to compare the means of all the parameters of each Tr and Ti. All data were tested for normality (Kolmogorov-Smirnoff test) and homogeneity of variance (Levene median test) and, where required, the data were transformed.

### *VOCs data*

The VOC dataset was elaborate using R statistical software 3.5 (R Core Team 2013). Differences among treatments, time of exposure and TrxTi interaction were inferred through PERMANOVA multivariate analysis (999 permutations) using the package *vegan*. Pairwise comparisons were calculated using a custom script and correcting P values using the False Discovery Rate (FDR) method.

In order to identify VOC key predictors that could constitute a molecular signature identification among the treatments within each time of exposure, we used a preliminary unsupervised (Principal Component Analysis, PCA) and then supervised analysis (Sparse Projection to Latent Structure-Discriminant Analysis, sPLS-DA) using the package *mixOmics* (Rohart et al., 2017). Statistical algorithms are detailed in Rohart et al. (2017) and they account for multiple comparisons inherent in biomarker datasets, where multiple classification features are considered for a relatively small number of specimens ( $p \gg n$ ). In particular, the sPLS-DA procedure constructs artificial latent components of the predicted dataset [VOCs Table denoted  $X(N \times P)$ ] and the response variable (denoted Y with categorical information of samples, e.g. CTR, ABIO, BIO and COMB). To predict the number of latent components (associated loading vectors) and the number of discriminants, for sPLS-DA, we used the *perf.plsda()* and *tune.splsda()* functions, respectively. We fine-tuned the model using 5-fold cross-validation repeated 10 times to estimate the classification error rates employing two metrics, overall error rates and balanced error rates (BER), between the predicted latent variables with the centroid of the class labels (categories considered in this study) and specifying the *max.dist* (which gave the minimal classification rate in this study).

### *Calculation of additive, synergistic or antagonistic effects in combined stress*

To determine if abiotic stress and herbivory treatments exerted additive, synergistic or antagonistic impacts on tomato traits, we used the Bansal et al. method (2013) and, specifically, we compared the observed effects (Ob) to expected additive effects (Ex) for the plants exposed to the abiotic stress and herbivory combination (COMB) at 3 and 8 days of treatments, only. The Ob effect sizes were calculated as the absolute value of:

$$Ob = (ob - \bar{x}_{CTR}) / \bar{x}_{CTR} \quad (2)$$

where ob is the measured trait value for each plants and treatment and  $\bar{x}_{CTR}$  is the mean trait value for the CTR plants.

The Ex additive effect sizes for the treatment COMB were define in two steps by first determining and then summing the independent effects (In) of each treatment. The In effect sizes were calculated as the absolute value of:

$$\text{Ind} = (\bar{x}_{\text{stress}} - \bar{x}_{\text{CTR}}) / \bar{x}_{\text{CTR}} \quad (3)$$

where  $\bar{x}_{\text{stress}}$  is the mean trait values from a single stress, and  $\bar{x}_{\text{CTR}}$  is the mean trait value for the CTR plants. Then, the Ex additive effect size for the COMB treatment were calculated using a multiplicative risk model as suggested by Darling et al. (2010), that is the sum of two In effects minus their product. Finally, the Ex additive values for COMB plants were compared to the actual Ob additive effects. In particular, we calculated a mean difference ( $\pm$  95% confidence interval) between the effect sizes of Ob and Ex was for COMB plants. When Ob-Ex  $>$  0 and the lower 95% confidence limit was greater than zero, then the impact from the combination of both stressor was classified as synergistic. Antagonistic effects were defined when the Ob-Ex  $<$  0 and the upper 95% confidence limit was less than zero. Finally, we classified additive effects when the 95% confidence interval crossed the zero line.

## **2.2.6. Second experiment: within-plant phenotypic plasticity**

### *2.2.6.1. Measurements and samplings*

The measurements and samplings were carried out at 8 days from the treatments (50 DAS) in the leaves located at three different positions (basal (B), intermediate (I) and apical leaf (A) placed at first, second and third node, respectively) along the shoot axes. Because the apical leaf, but not the intermediate, is linked to the basal one by vasculature connection (preliminary experiments using phloem dying as reported in Orians et al., 2000), we also considered the basal, intermediate and apical leaves as the local (L), no-orthostichous (nO) and orthostichous leaf (O), respectively. The basal or local leaf was used for placing the first instar larvae



Measurements for the gas exchange traits were carried out on two opposite leaflets of the basal/local (B/L), intermediate/noOrthostic (I/noO) and apical/orthostic leaf (A/O) placed at first, second and third node, respectively, and the same leaves were subsequently collected for the morphological analysis.

#### *2.2.6.2. Morpho-physiological Analysis*

All the morpho-physiological analysis were carried out as in the first experiment.

#### **2.2.6.3. Statistics**

##### *Within-plant variance of the morpho-physiological traits*

The within-plant variance of the morpho-physiological traits was evaluated as in Zywiec et al. (2012).

In order to estimate the partitioning of total variation of the morpho-physiological traits among- and within-treatments, we conducted Linear Mixed Models with treatments and plant nested within-treatments as random effects using the whole-plant data. The variance partitions among- and within-treatments and tests on the statistical significance of variance components were conducted using restricted maximum likelihood (REML).

In order to verify the effects of each treatments on morpho-physiological traits of different leaves within the plants, we analyzed the within-plant variation by applying a hierarchical partition to divide total variance into two levels of variation: among plants and among the leaves in the same plants (leaf nested within plant). All levels were considered as random effects, as required for variance partitioning. Analyses were conducted with the mixed procedure of SPSS. The replicate obtained for each leaflets sample allowed us to estimate measurement error and thus assess the variance component and statistical significance (Wald Z and p values) of this component between- and within-individual plants.

#### *2.2.6.4. Morpho-physiological data*

By SPSS Inc., V. 10.0, 2002 (SPSS Inc., Evanston, IL, USA), all the morpho-physiological parameters were analyzed by one way ANOVA with Tukey's test as post-hoc test ( $p < 0.05$ ).

## 2.3. RESULTS AND DISCUSSION

2.3.1. *Are the morpho-physiological responses to individual stresses different from the combined ones in tomato plants? Are additive, synergistic or antagonistic effects in the combined stress?*

The morpho-physiological results clearly indicated an opposite pattern of the tomato plant responses to the single stresses with the ABIO treatments showing more negative impact than the BIO one respect to the CTR plants (Figures 2.2 and 2.3). In particular, the leaf fresh and dry weight, leaf water content, photosynthetic rate and WUE were significantly reduced in ABIO plants respect to the control while no significant differences were observed in presence of herbivory except than leaf water content and WUE, only (Figures 2.2. and 2.3.; Tables 2.1. and 2.2.). It is known that the drought stress alone (English-Loeb et al., 1997; Patanè, 2011; Liang et al., 2020) and together with N deficiency (García et al., 1996, 2000, 2007) reduced the photosynthesis rate, the stomatal conductance and leaf water content with negatively consequence to the leaf growth of tomato plants through very clear molecular mechanisms (Tamburino et al., 2017; Gong et al., 2010). The BIO treatment did not produce modification of the morpho-physiologic traits in comparison to the control (Figures 2.2 and 2.3) and this no response to the herbivory falls in the highly variable effects observed in different plant-insect combination. For example, the leaf dry to fresh mass ratio was not changed by *Monsoma pulveratum* feeding on *Alnus glutinosa* (Copolovici et al. 2014) but a weakly negative effects in the soybean-natural herbivory interactions was observed (Grinnan et al., 2013). Further, the high variability in the plant response to the herbivory was observed for the photosynthesis that was sharply reduced (Zangerl et al. 2002), increased (Thomson et al. 2003) or not modified (Aldea et al. 2005; Copolovici et al., 2014). Probably, in this study, the *Tuta absoluta* could have caused ‘indirect effects’ in leaf tomato such as increase of the photosynthesis and water losses by transpiration rate with reduced WUE and leaf water content as also observed in soybean-japanese beetles and -corn earworm caterpillars interactions (Aldea et al., 2005). However, in a specific study of the *Tuta*-tomato interactions, the reduction leaflet growth was pointed out (Coqueret et al., 2017)

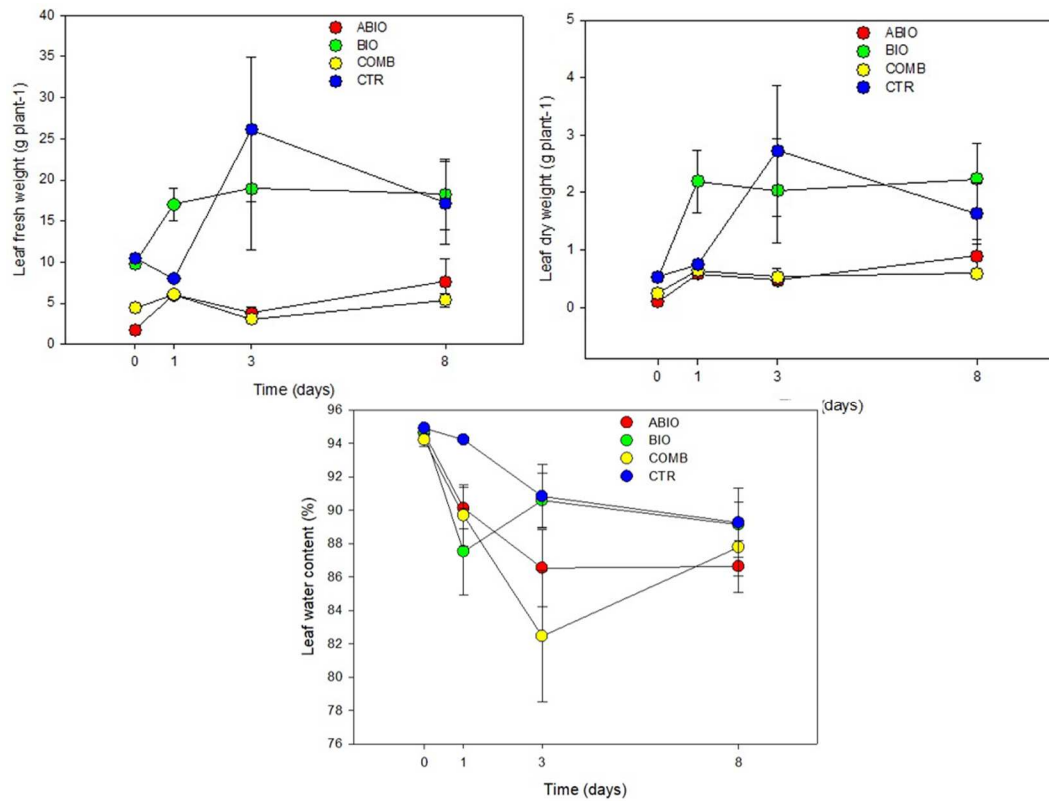
Although the plant responses to the drought, N deficiency and herbivory as individual stress are well understood, no information on their impact in the tomato plants as combined stress are detected. The combination of the abiotic stress (N deficiency and

drought) with herbivory by *Tuta* determined the highest reduction of the tomato morpho-physiological traits respect to the control plants (Figures 2.2 and 2.3; Tables 2.1 and 2.2). This overstate effect of the combined stress could be due to the interactive responses determined by cross-talk hormonal signal and regulation of defence-related genes. Indeed, in the interaction between *Solanum dulcamara* and the herbivory by specialist *Leptinotarsa decemlineata*, the antagonism of the specific herbivory-induced salicylic acid on the jasmonic acid (JA) prevailed on the synergism of the specific drought-induced ABA with consequent reduction of the defence responses observed at transcriptional levels (increase in the cell wall components and secondary metabolism) (Nguyen et al., 2018). Moreover, the tomato plants subjected to both drought and herbivory by *Spodoptera exigua* stresses pointed out an adaptive response with an increase of the genes related to the photosynthetic machinery and chlorophyll biosynthesis and, consequently, reduction of the secondary metabolite production (Nguyen et al., 2018).

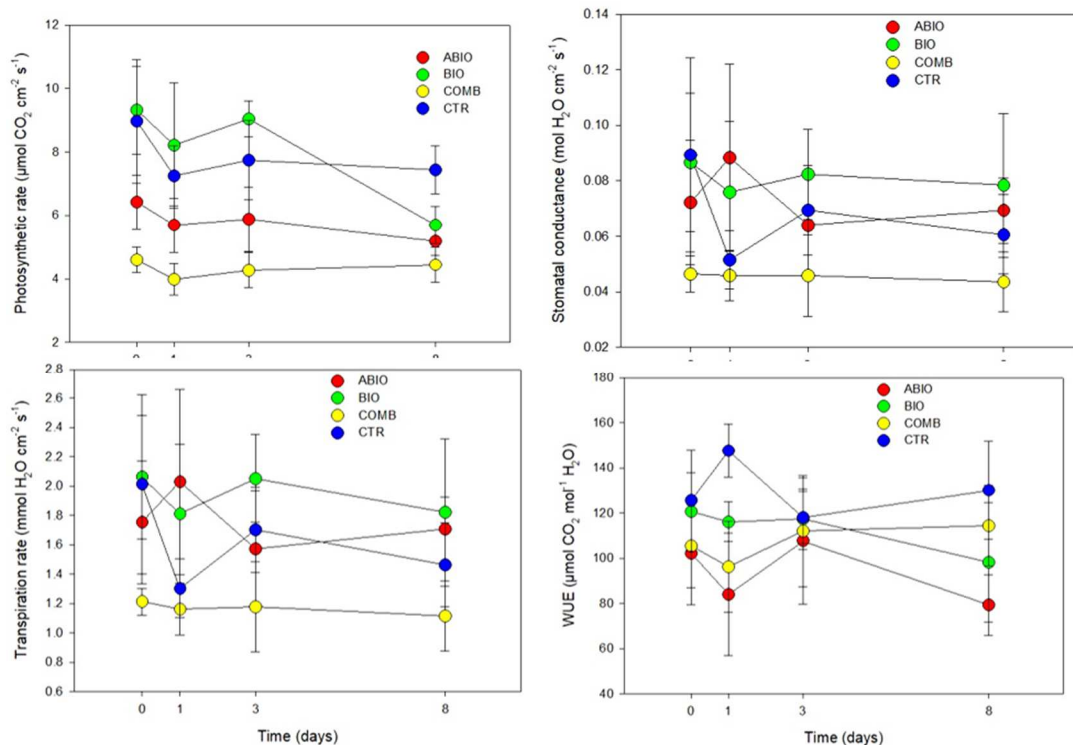
The temporal evolution of the plant responses to the environmental stresses results fundamental for the success of the plant adaptation although is an aspect less studied in the scientific literature. In the present work, differently to the single stress, the COMB treatment reduced the leaf fresh and dry weight at 3 days from the stress treatments, while the leaf water content and the physiological traits such as the photosynthetic rate, stomatal conductance and WUE respond faster by a reduction already at 1 day of treatment (Figures 2.2 and 2.3; Tables 2.1 and 2.2). Probably, the combined stress in tomato plants rapidly activated the stomatal closure to reduce the water losses caused by drought component with consequently reduction of the photosynthetic process which diminished the defence-related metabolites and all this subsequently translates into a lower leaf growth. However, this morpho-physiological pattern could be the final result of the signaling and molecular network which is instead activated in a very rapid responses (within second and minute) as observed in different abiotic- and biotic-stressed plants (Kollist et al., 2019).

To observe also that drought, N deficiency and herbivory by *Tuta* negatively affected more the physiological traits than morphological ones (Figures 2.2 and 2.3; Tables 2.1 and 2.2). The plant physiological plasticity is more related to an enhanced ability to exploit the transient environmental resources, such as water and nutrient patches, or to produce the defence responses (secondary metabolites) to the herbivory attack at low cost

by short-term adjustments (Mou et al., 2013; Marchiori et al. 2017; Puglielli et al. 2017; Wagner and Mitchell-Olds, 2018). Conversely, the plant morphological plasticity is more expensive and functional for the plant adaptation at the long-term (Mou et al., 2013; Wagner and Mitchell-Olds, 2018).



**Figure 2.2**– Morphological traits. Leaf fresh (g), dry (g) and water content (%) of tomato plants treated with different stress (ABIO, BIO, COMB) or not treated (CTR) for different time of exposure (0, 1, 3 and 8 days). The data and error bars indicated the mean and the error standard, respectively (N=4).



**Figure 2.3** – Gas exchange parameters. Photosynthetic rate ( $\mu\text{mol CO}_2 \text{ cm}^{-2} \text{ s}^{-1}$ ), Stomatal conductance ( $\text{mol H}_2\text{O cm}^{-2} \text{ s}^{-1}$ ), Transpiration rate ( $\text{mmol H}_2\text{O cm}^{-2} \text{ s}^{-1}$ ) and  $\text{WUE}_i$  ( $\mu\text{mol CO}_2 \text{ mol}^{-1} \text{ H}_2\text{O}$ ) of tomato plants treated with different stress (ABIO, BIO, COMB) or not treated (CTR) for different time of exposure (0, 1, 3 and 8 days). The data and error bars indicated the mean and the error standard, respectively (N=4).

**Table 2.1** - Results of two-way ANOVA [Treatment (Tr), Time (Ti), Block (Bl) TrxTi interaction (TrxTi)]. Statistics: F- and p-values. Within each root traits and time of exposure, the different letters indicated statistical differences among the means of the treatments ( $p < 0.05$ , test of Tukey).

Parameters	Statistics	Treatments (Tr)	Time (Ti)			
			t0	t1	t3	t8
<b>Leaf fresh weight</b>	Tr 10.92***	ABIO	a	a	b	b
	Ti 1.40 <sup>NS</sup>	BIO	a	a	a	a
	Bl 6.08*	COMB	a	a	b	b
	TrxTi 1.06 <sup>NS</sup>	CTR	a	a	a	a
<b>Leaf dry weight</b>	Tr 8.87***	ABIO	a	a	b	b
	Ti 2.91*	BIO	a	a	a	a
	Bl 17.17***	COMB	a	a	b	b
	TrxTi 1.26 <sup>NS</sup>	CTR	a	a	a	ab
<b>Leaf water content</b>	Tr 3.16*	ABIO	a	ab	ab	a
	Ti 12.01***	BIO	a	b	a	a
	Bl 52.15***	COMB	a	b	b	a
	TrxTi 1.50 <sup>NS</sup>	CTR	a	a	a	a

**Table 2.2** - Results of two-way ANOVA [Treatment (Tr), Time (Ti), Block (BI) TrxTi interaction (TrxTi)]. Statistics: F- and p-values. Within each root traits and time of exposure, the different letters indicated statistical differences among the mean of the treatments ( $p < 0.05$ , test of Tukey).

Parameters	Statistics	Treatments (Tr)	Time (Ti)			
			t0	t1	t3	t8
<b>Photosynthetic rate</b>	Tr 17.60 <sup>***</sup>	ABIO	a	b	bc	ab
	Ti 2.73 <sup>NS</sup>	BIO	a	a	a	ab
	BI 20.74 <sup>***</sup>	COMB	a	b	c	b
	TrxTi 0.76 <sup>NS</sup>	CTR	a	ab	ab	a
<b>Stomatal conductance</b>	Tr 5.38 <sup>**</sup>	ABIO	a	a	ab	a
	Ti 0.60 <sup>NS</sup>	BIO	a	a	a	a
	BI 61.82 <sup>***</sup>	COMB	a	b	b	a
	TrxTi 0.57 <sup>NS</sup>	CTR	a	ab	ab	a
<b>Transpiration rate</b>	Tr 6.94 <sup>**</sup>	ABIO	a	a	ab	ab
	Ti 0.79 <sup>NS</sup>	BIO	a	a	a	a
	BI 55.73 <sup>***</sup>	COMB	a	a	b	b
	TrxTi 1.13 <sup>NS</sup>	CTR	a	a	ab	ab
<b>WUE</b>	Tr 6.23 <sup>**</sup>	ABIO	a	b	a	b
	Ti 0.47 <sup>NS</sup>	BIO	a	b	a	b
	BI 136.54 <sup>***</sup>	COMB	a	b	a	ab
	TrxTi 1.52 <sup>NS</sup>	CTR	a	a	a	a

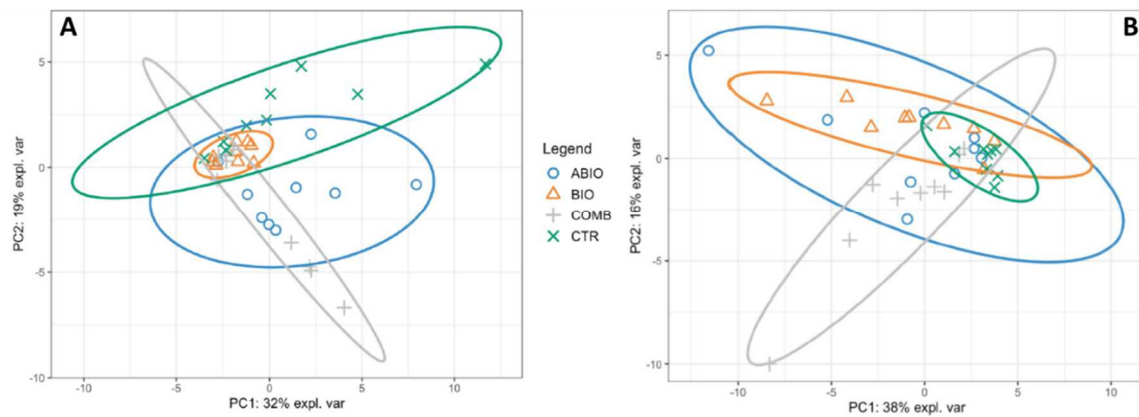
The VOC emission is an important plant defence process in response to the herbivory attack (Niinemets et al., 2013; Foti et al., 2020) and the abiotic stress also (Loreto and Schnitzler, 2010). HS/SPME GC-MS analysis revealed forty-five volatile compounds emitted by the tomato leaves exposed to the single (abiotic and biotic) and combined stress (Table 2.3). In particular, the volatile profile was mostly characterized by mono- (24% of the total) and sesquiterpenes (44%) but hydrocarbons (11%), ester (9%), alcohol (5%), ether (5%) and aldehyde (2%) were also present (Table 2.3). Volatile terpenoid metabolites have been recognized as having a range of specific roles in plant/environment and plant/plant interactions (Tholl, 2015) and, in particular, in the direct and indirect defence of tomato against the herbivory (Bleeker et al., 2012; Silva, 2017). Table 2.5 reported the volatiles from each treatment and time of exposure on the basis of % area of each peak over the total area of the chromatogram. In order to test the influence of the treatments and time of exposure on the volatile profiling, we run a multivariate approach that included, first, the Permanova and, then, the PCA and sPLSDA that permitted to

visualize the difference among the groups and to select informative and relevant volatiles. Permanova analysis indicated that the treatments, time of exposure and their interaction determined a significant difference in the volatilome of tomato plants (Table 2.5). Pairwise comparison among the treatments within each time of exposure revealed that the COMB treatment pointed out a volatile profile different to the control at 3 and 8 days of exposure, while the BIO at 8 days of exposure only ( $p_{\text{adjusted}} < 0.05$ ; Table 2.6). Since these two times of exposure pointed out differences among the treatments, we used the volatiles dataset from the four treatments at 3 and 8 days of exposure for running the PCA. Figure 2.4 showed the results of PCA where it is apparent that this multivariate analysis was not able to separate treatment groups owing to the high variability among samples. Therefore, data were further analysed using sPLS-DA at each time of exposure (3 and 8 days). At 3 days of exposure, the performance step of the sPLS-DA for the selection of the number of components suggested that 3 components were enough to sharply reduce the balanced error rate around 0.23 (Figure 2.5A). Further, the final model obtained by tuning process pointed out that the Component 1, 2 and 3 were constituted by 25, 19 and 31 volatiles, respectively (Figure 2.5B), but with a scarce discrimination among the treatments as highlighted by the sample plots on the first three components (Figures 2.5C and 2.5D). At 8 days of exposure, three components were selected with a balanced error rate around 0.28 and with a molecular signature composed of 16, 16 and 31 VOCs selected on the first three components, respectively (Figures 2.6A and 2.6B). The sample plots on the three components permitted to visualize a discrimination among the treatments with 60% of total explained variability split up by 32%, 15% and 13% for the first, second and third components, respectively (Figures 2.6C and 2.6D). In particular, plotting the first two components, the BIO was sharply separated from the control and COMB by the second component (Figure 2.6C). Conversely, the first and third components point out scarce discrimination among the treatments (Figures 2.6C and 2.6D). The 16 VOCs selected on the second component all had negative weight in the linear combination, and the followings were highly expressed in BIO: (E)-2 hexen-1 ol, (2E)-2-Hexenyl propionate, (+)-4-carene,  $\alpha$ -copaene, Hexyl propionate,  $\beta$ -phellandrene,  $\alpha$ -pinene, terpinolene,  $\beta$ -pinene, E  $\beta$ -caryophyllene (Figure 2.6E). However, the dodecane, 2,6,11-trimethyl was expressed in CTR while the  $\alpha$ -humulene and  $\alpha$ -terpinene and the  $\gamma$ -elemene and  $\delta$ -cadinene fell in the ABIO and COMB, respectively (Figure 2.6E).

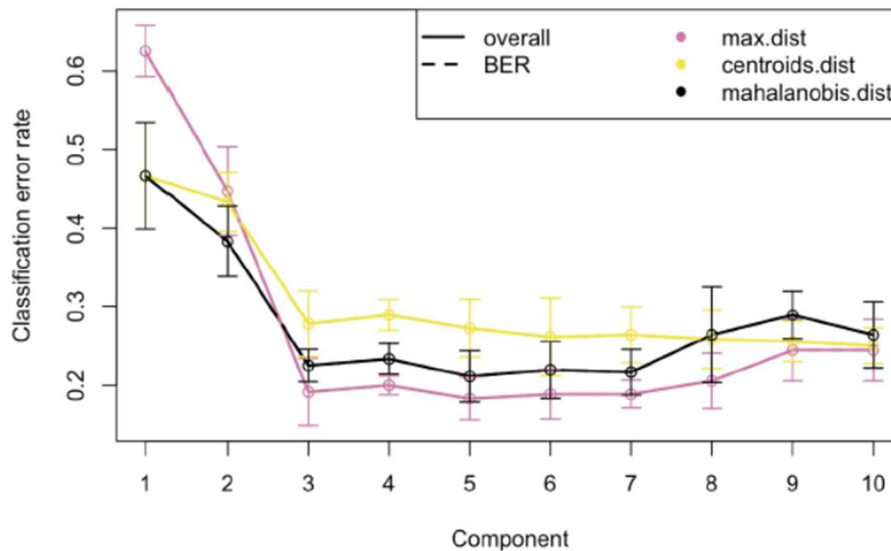
The (E)-2 hexen-1 ol (Deglow and Borden, 2011), (2E)-2-Hexenyl propionate (Ruther, 2000) and Hexyl propionate (Rodriguez-Saona et al., 2011) are green leaf volatiles which are released in response to different stress conditions to aid in plant defence against herbivory and bacterial and fungal pathogens (Muhammad et al, 2015; Ameye et al., 2018). The (+)-4-carene,  $\alpha$ -copaene,  $\beta$ -phellandrene,  $\alpha$ -pinene, terpinolene,  $\beta$ -pinene and E  $\beta$ -caryophyllene are terpenes, organic class mostly involved in the plant defence. For example, the (+)-4-carene,  $\alpha$ -copaene and  $\beta$ -phellandrene are the most abundant VOCs emitted by *Solanum* species in presence of *Bactericera cockerelli* herbivory (Mayo-Hernández et al., 2019) and terpinolene and E  $\beta$ -caryophyllene were mainly produced by tomato leaves infested with *Trialeurodes vaporariorum* (Ángeles López et al., 2012). Further, the  $\alpha$ -humulene was responsible of tomato repellence against *Bemisia tabaci* (Islam et al., 2017). The dodecane, 2,6,11-trimethyl that was highly expressed in CTR in this study (Figure 2.6.E), is confirmed as VOC emitted by healthy plants such as olive (Giunti et al., 2016). Interesting is that the  $\alpha$ -terpinene and  $\delta$ -terpinene were mainly discriminant of ABIO treatments (Figure 2.6E) confirming the results obtained in tomato plants (cv. Gan Liang Mao Fen 802 F1) fertilized with lower levels of N (Islam et al., 2017) and in drought-stressed *Thymus vulgaris* plants (Mahdavi et al., 2020). Finally, the present study revealed the VOCs emitted in multi-stressed tomato plants. In particular, the  $\gamma$ -muurolene,  $\delta$ -elemene,  $\delta$ -cadinene,  $\beta$ -elemene,  $\alpha$ -gauiene, z- $\beta$ -caryophyllene, aromadendrene,  $\gamma$ -elemene, 1,3,7 Nonatriene 4,8 dimethyl (3E)-, methyl salicylate,  $\beta$ -cadinene and myrcene were the compounds constituting the VOC blend emitted by tomato plants when exposed to combined N and drought stress with infestation by *Tuta absoluta* (Figures 2.6E and 2.6F). To note that the  $\gamma$ -elemene and  $\delta$ -cadinene were present in both components while the other volatiles were only observed in the Component 1 that is the lesser discriminant (Figures 2.6E and 2.6F). In *Gossypium arboreum*, the  $\delta$ -cadinene is a precursor of the cyclic secondary sesquiterpene aldehydes, including gossypol, that are insecticide (Tan et al., 2000) and it was also increased in Pot Marigold (*Calendula officinalis* L., Asteraceae) under water deficit (Emmati et al., 2018). Conversely to the  $\delta$ -cadinene, the  $\gamma$ -elemene was poor modified in the tomato leaves by stresses such as, for example, the pest (Ángeles López et al., 2012). Besides the  $\delta$ -cadinene and  $\gamma$ -elemene, the volatiles pointed out in the component 1 were interesting in plant response to the abiotic and biotic stress. The methyl salicylate was observed to



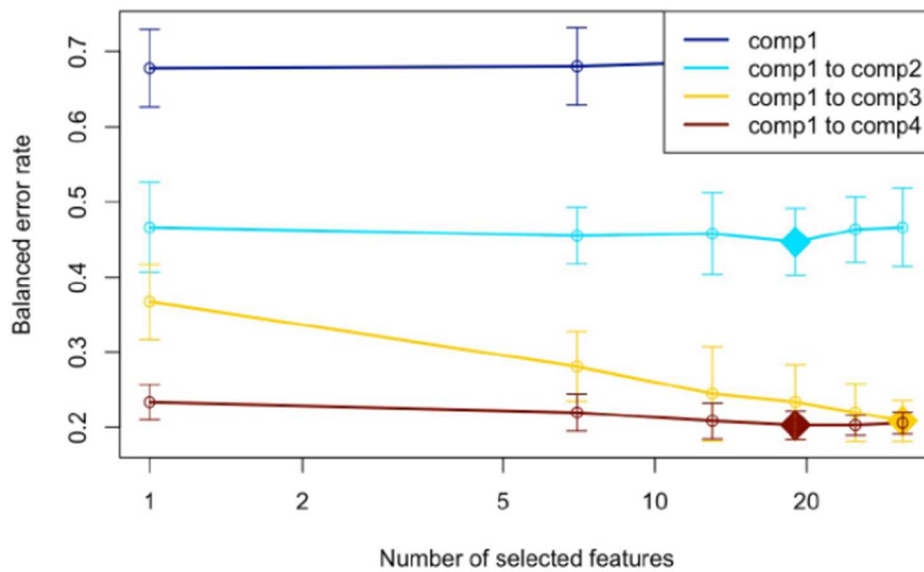
increase in double drought-stressed and aphid-infested tomato plants (Catola et al., 2018) but also in the drought-herbivory combination together with 1,3,7-Nonatriene, 4,8-dimethyl-, (3E)-, the two stress-specific VOC (Copolovici et al., 2014). The other volatiles were present in the VOC profiles of different plant species stressed with the combination of two or more stresses (Copolovici et al., 2014; Errard et al., 2015; Weldegergis et al., 2015).



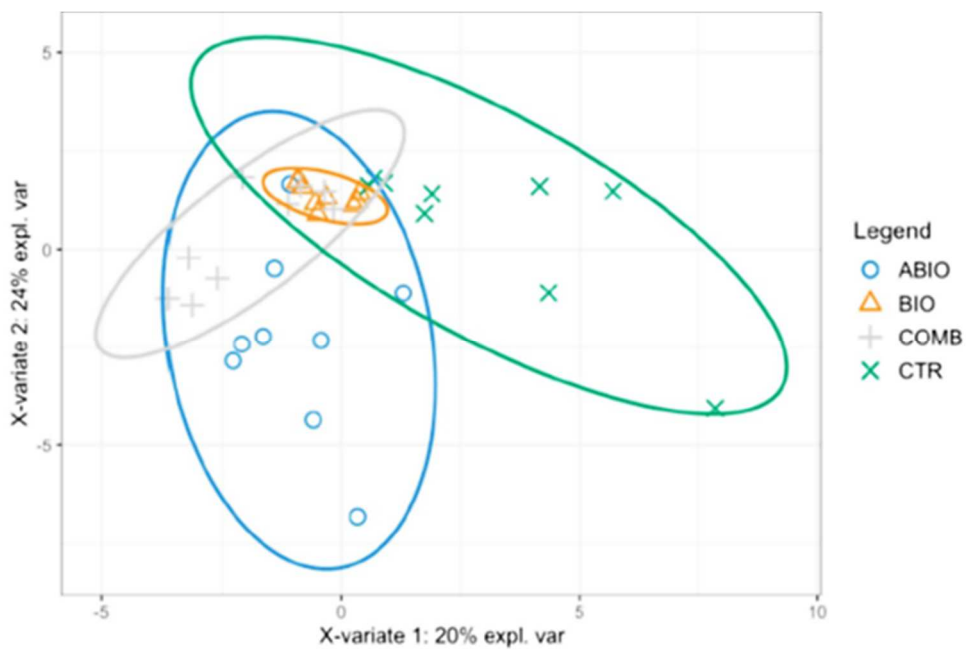
**Figure 2.4** - Principal component analysis applied to volatiles emission data obtained from tomato leaves treated with different stress (ABIO, BIO, COMB) or not treated (CTR) for 3 (A) and 8 days (B) of exposure.



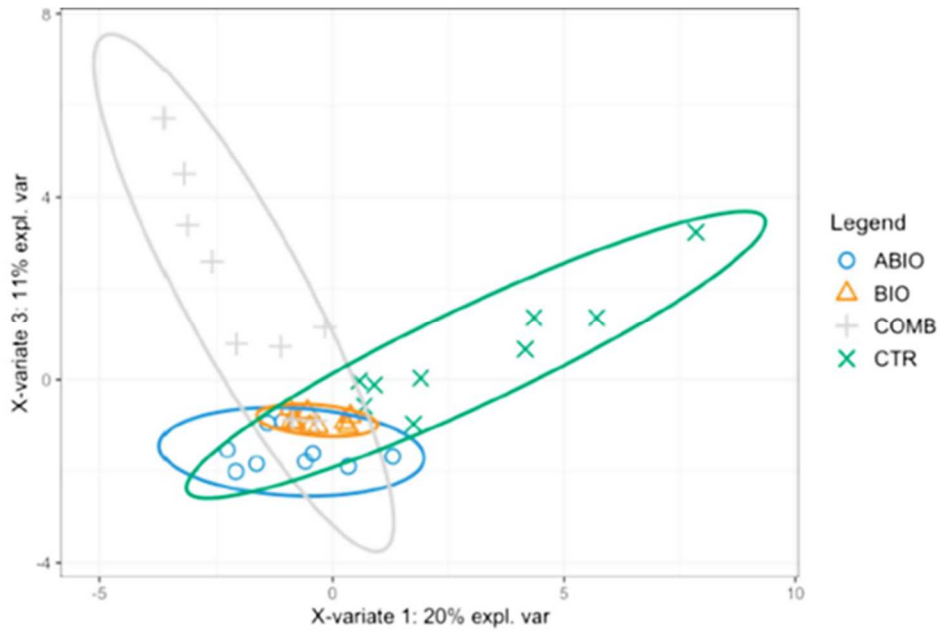
**Figure 2.5** A sPLS-DA of volatile profiles obtained in tomato plants exposed to different stress (ABIO, BIO, COMB) or not stress (CTR) for 3 days of exposure. Choosing the number of components in sPLS-DA by performance test.



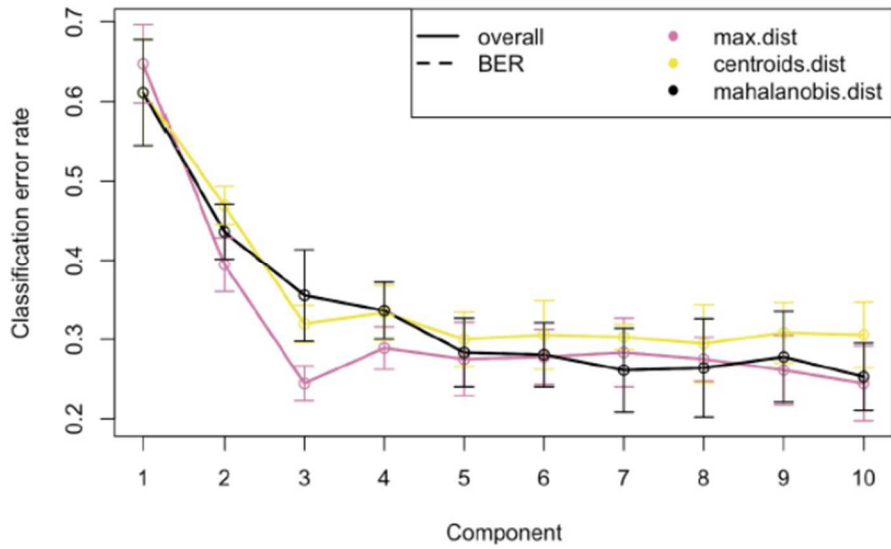
**Figure 2.5 B** Mean classification by overall and balanced error rate (5 cross-validation averaged 50 times) for each sPLS-DA component. Choosing the number of volatiles for each sPLS-DA components by tuning test (B).



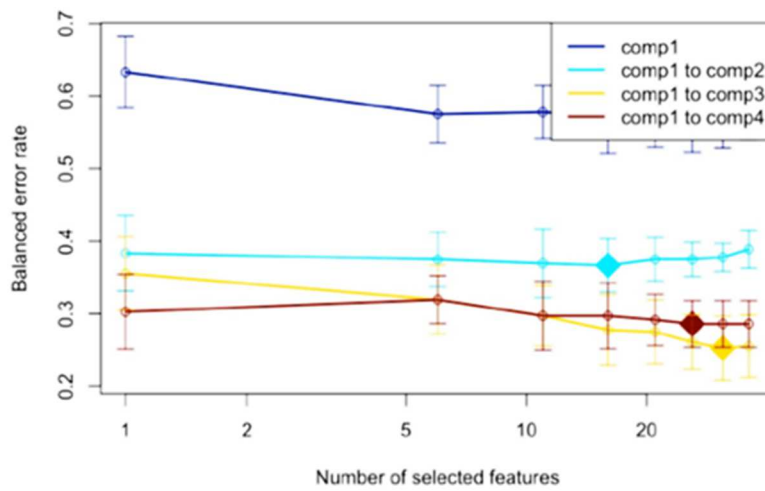
**Figure 2.5 C** Estimated classification balanced error rates for volatile dataset (5 cross-validation averaged 50 times) with respect to the number of selected volatiles for the sparse exploratory approaches. sPLS-DA sample plot for the different components using 95% confidence ellipses. Component 1 vs. Component 2.



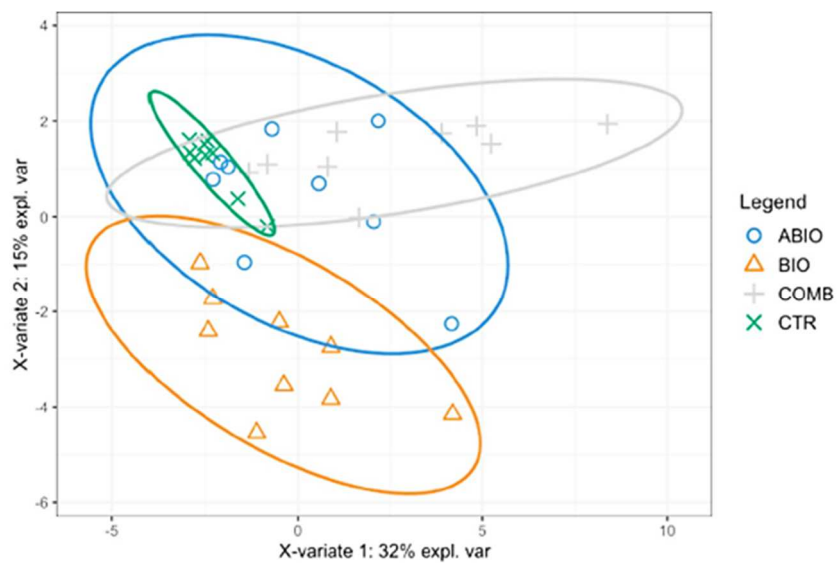
**Figure 2.5 D** Estimated classification balanced error rates for volatile dataset (5 cross-validation averaged 50 times) with respect to the number of selected volatiles for the sparse exploratory approaches. sPLS-DA sample plot for the different components using 95% confidence ellipses. Component 1 vs Component 3.



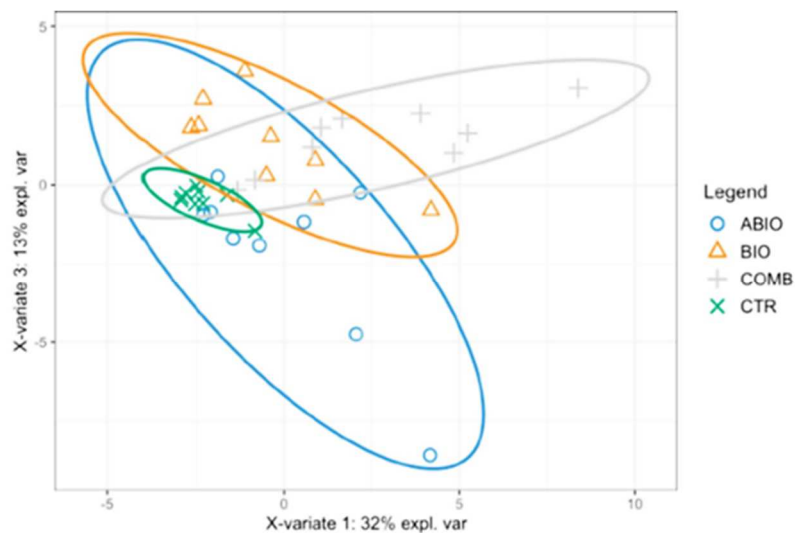
**Figure 2.6 A** sPLS-DA of volatile profiles obtained in tomato plants exposed to different stress (ABIO, BIO, COMB) or not stress (CTR) for 8 days of exposure. Choosing the number of components in sPLS-DA by performance test.



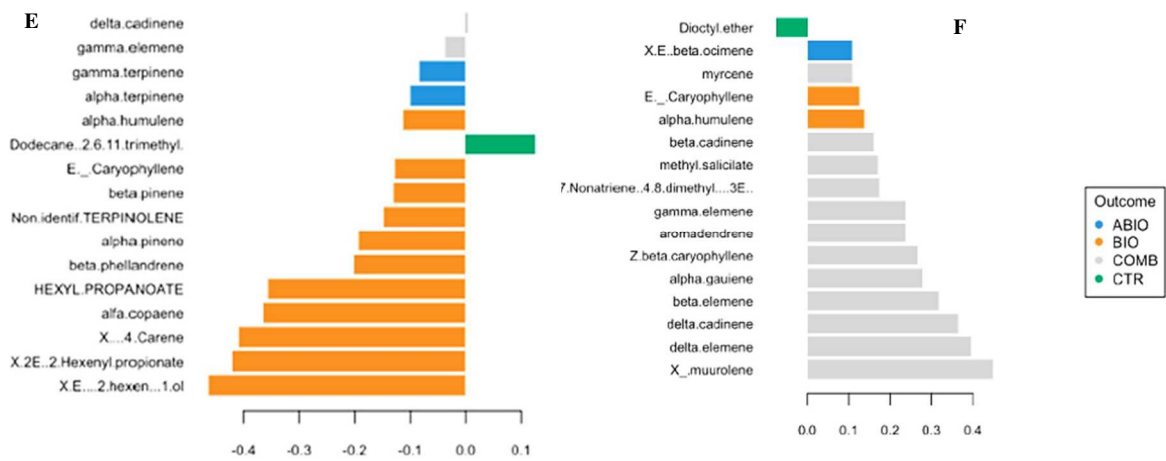
**Figure 2.6 B** Mean classification by overall and balanced error rate (5 cross-validation averaged 50 times) for each sPLS-DA component. Choosing the number of volatiles for each sPLS-DA components by tuning test.



**Figure 2.6 C** Estimated classification balanced error rates for volatile dataset (5 cross-validation averaged 50 times) with respect to the number of selected volatiles for the sparse exploratory approaches. sPLS-DA sample plot for the different components using 95% confidence ellipses. Component 1 vs. Component 2.

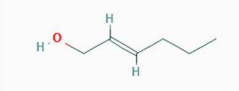
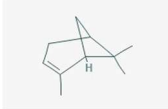
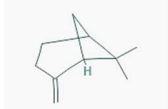
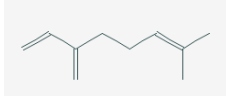
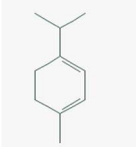
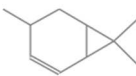

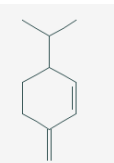
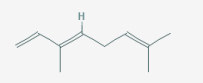


**Figure 2.6 D** Estimated classification balanced error rates for volatile dataset (5 cross-validation averaged 50 times) with respect to the number of selected volatiles for the sparse exploratory approaches. sPLS-DA sample plot for the different components using 95% confidence ellipses. Component 1 vs Component 3.

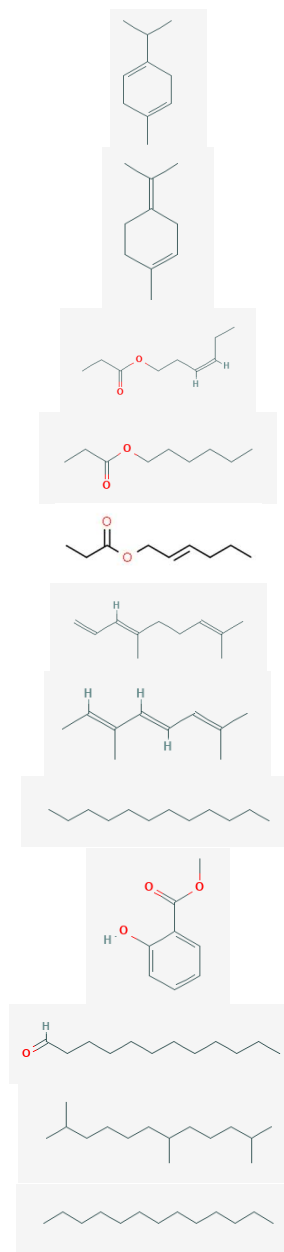


**Figure 2.6 E-F** Contribution plots by loading weights of the volatiles selected for the Component 2 (E) and Component 1 (F) of the sPLS-DA. The colour indicated the treatments for which the selected volatile has a maximal mean loading weight value.

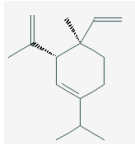
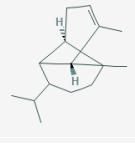
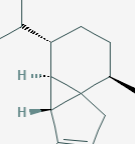
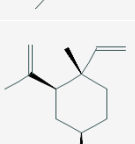
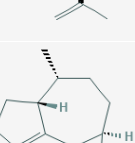
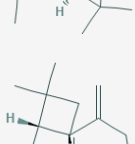
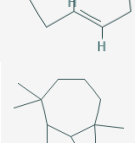
**Table 2.3** - Volatile organic compounds identified using gas chromatography/mass spectrometry (GC/MS) analysis by HS/SPME method in the leaves of the tomato plants treated with abiotic, biotic and combined stress. RT, retention time; KI, retention index.

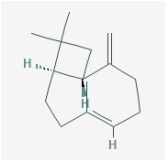
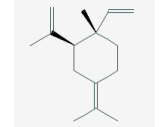
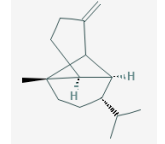
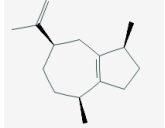
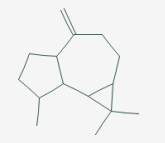
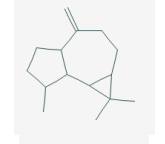
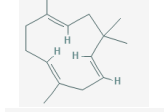
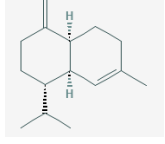
Common Name	IUPAC name	Class	RT (min)	KI	chemical structure
(E) - 2 hexen - 1 ol	(E)-hex-2-en-1-ol	Alcohol	5.97	873	
alpha pinene	2,6,6-trimethylbicyclo[3.1.1]hept-2-ene	monoterpene	7.36	939	
beta pinene	6,6-dimethyl-2-methylidenebicyclo[3.1.1]heptane	monoterpene	8.22	981	
Myrcene	7-methyl-3-methylideneocta-1,6-diene	monoterpene	8.61	993	
alpha terpinene	1-methyl-4-propan-2-ylcyclohexa-1,3-diene	monoterpene	8.85	1018	
(+)-4-Carene	4,7,7-Trimethylbicyclo[4.1.0]hept-2-ene	monoterpene	9.19	1022	
o - cymene	1-methyl-2-propan-2-ylbenzene	monoterpene	9.51	1026	
beta phellandrene	3-methylidene-6-propan-2-ylcyclohexene	monoterpene	9.59	1033	
(E) beta ocimene	(3E)-3,7-dimethylocta-1,3,6-triene	monoterpene	9.98	1050	

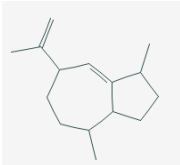
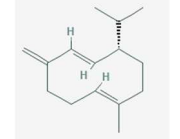
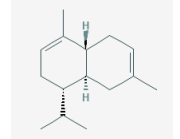
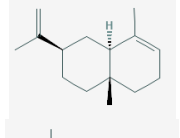
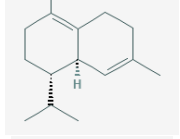
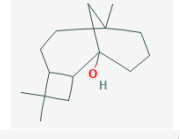
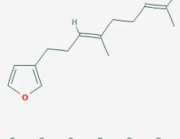
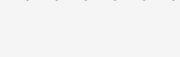

gamma terpinene	1-methyl-4-propan-2-ylcyclohexa-1,4-diene	monoterpene	10.30	1062
Terpinolene	1-methyl-4-propan-2-ylidenecyclohexene	monoterpene	11.05	1090
3-Hexen-1-ol, propanoate, (3Z)-	[(Z)-hex-3-enyl] propanoate	Ester	11.29	1103
Hexyl propanoate	hexyl propanoate	Ester	11.34	1110
(2E)-2-Hexenyl propanoate	[(E)-hex-2-enyl] propanoate	Ester	11.50	1112
1,3,7-Nonatriene, 4,8-dimethyl-, (3E)-	(3E)-4,8-dimethylnona-1,3,7-triene	hydrocarbon	11.67	1119
allo-ocimene	(4E,6E)-2,6-dimethylocta-2,4,6-triene	monoterpene	11.71	1133
Dodecane	dodecane	hydrocarbon	13.60	1200
methyl salicylate	methyl 2-hydroxybenzoate	Ester	13.69	1193
Dodecanal	dodecanal	Aldehydes	13.94	1204
Dodecane, 2,6,11-trimethyl-	2,6,11-trimethyldodecane	hydrocarbon	15.58	1275
Tridecane	tridecane	hydrocarbon	16.63	1302





delta elemene	(3R,4R)-4-ethenyl-4-methyl-1-propan-2-yl-3-prop-1-en-2-ylcyclohexene	sesquiterpene	17.00	1340	
alfa copaene	(2R,6R)-1,3-dimethyl-8-propan-2-yltricyclo[4.4.0.02,7]dec-3-ene	sesquiterpene	17.89	1376	
alfa cubebene	(5S,6R,7S,10R)-4,10-dimethyl-7-propan-2-yltricyclo[4.4.0.01,5]dec-3-ene	sesquiterpene	17.89	1344	
beta elemene	(1S,2S,4R)-1-ethenyl-1-methyl-2,4-bis(prop-1-en-2-yl)cyclohexane	sesquiterpene	18.22	1393	
alpha gurjunene	(1aR,4R,4aR,7bS)-1,1,4,7-tetramethyl-1a,2,3,4,4a,5,6,7b-octahydrocyclopropa[e]azulene	sesquiterpene	18.53	1410	
Z beta caryophyllene	(1S,4E,9S)-4,11,11-trimethyl-8-methylidenebicyclo[7.2.0]undec-4-ene	sesquiterpene	18.60	1416	
Longifolene	3,3,7-trimethyl-8-methylidenetricyclo[5.4.0.02,9]undecane	sesquiterpene	18.61	1404	

E $\beta$ -Caryophyllene	(1R,4E,9S)-4,11,11-trimethyl-8-methylidenebicyclo[7.2.0]undec-4-ene	sesquiterpene	18.88	1428	
gamma elemene	(1S,2S)-1-ethenyl-1-methyl-4-propan-2-ylidene-2-prop-1-en-2-ylcyclohexane	sesquiterpene	19.06	1431	
$\beta$ -copaene	(1S,6S,7S,8S)-1-methyl-3-methylidene-8-propan-2-yltricyclo[4.4.0.0 <sup>2,7</sup> ]decane	sesquiterpene	19.07	1431	
alpha guaiene	(1S,4S,7R)-1,4-dimethyl-7-prop-1-en-2-yl-1,2,3,4,5,6,7,8-octahydroazulene	sesquiterpene	19.35	1439	
aromadendrene	1,1,7-trimethyl-4-methylidene-2,3,4a,5,6,7,7a,7b-octahydro-1aH-cyclopropa[e]azulene	sesquiterpene	19.50	1445	
Alloaromadendrene	1,1,7-trimethyl-4-methylidene-2,3,4a,5,6,7,7a,7b-octahydro-1aH-cyclopropa[e]azulene	sesquiterpene	19.52	1462	
alpha humulene	(1E,4E,8E)-2,6,6,9-tetramethylcycloundeca-1,4,8-triene	sesquiterpene	19.61	1456	
$\gamma$ muurolene	(1S,4aS,8aR)-7-methyl-4-methylidene-1-propan-2-yl-2,3,4a,5,6,8a-hexahydro-1H-naphthalene	sesquiterpene	20.08	1477	

$\gamma$ gurjunene	1,4-dimethyl-7-prop-1-en-2-yl-1,2,3,3a,4,5,6,7-octahydroazulene	sesquiterpene	20.12	1477	
germacrene D	(1E,6E,8S)-1-methyl-5-methylidene-8-propan-2-ylcyclodeca-1,6-diene	sesquiterpene	20.31	1481	
beta cadinene	(1S,4aR,8aS)-4,7-dimethyl-1-propan-2-yl-1,2,4a,5,8,8a-hexahydronaphthalene	sesquiterpene	20.36	1500	
alpha selinene	(3R,4aR,8aR)-5,8a-dimethyl-3-prop-1-en-2-yl-2,3,4,4a,7,8-hexahydro-1H-naphthalene	sesquiterpene	20.41	1500	
delta cadinene	(1S,8aR)-4,7-dimethyl-1-propan-2-yl-1,2,3,5,6,8a-hexahydronaphthalene	sesquiterpene	21.01	1524	
caryophyllene alcohol	4,4,8-trimethyltricyclo[6.3.1.0 <sup>2,5</sup> ]dodecan-1-ol	Alcohol	21.87	1571	
Dendrolasin	3-[(3E)-4,8-dimethylnona-3,7-dienyl]furan	Ether	22.08	1575	
hexadecane	hexadecane	hydrocarbon	22.37	1600	
Dioctyl ether	1-octoxyoctane	Ether	23.69	1660	

Analyzing the tomato morpho-physiologic and metabolic responses to the combined stress is interesting to understand the additive (equal to the sum of the single-stress effects), synergistic (higher than expected) or antagonistic (lower than expected) effects of the single stress. In relation to the results of these effects, the signaling pathways and molecular mechanisms underlying the plant strategy in presence of simultaneous stress could be hypothesized. For example, the antagonistic effect of drought and insect herbivory could be explained by cross-talking interactions between JA and ABA signaling (Nguyen et al., 2018). In this respect, the additive, synergistic and antagonistic effects of abiotic (drought and N deficiency) and biotic stress in tomato plants were investigated by the Bansal et al. method (2013). In general, the physiological (photosynthesis, stomatal conductance and transpiration) and the metabolic (VOC) traits pointed out more synergistic effects than morphological ones especially at early time of exposure, i.e. at 1 and 3 days (Figure 2.7). In particular, a synergic effect was observed for the reduction of the physiological traits (photosynthesis, stomatal conductance and transpiration) (Table 2.2 and Figure 2.7) and for the increase of the VOC emission (Table 2.4 and Figure 2.7). The closure of the stomata is the first plant response to the water scarcity mediated by ABA that orchestrate a network of stress-responsive metabolites and gene expression (Takahashi et al., 2020). The ABA signaling pathways interact also with that of the JA one, the phytohormone that activate the signaling cascades for regulating downstream transcriptional responses to the herbivory (Nguyen et al., 2016; Yang et al., 2019) and, furthermore, it was observed that MeJA signaling is overlapped with ABA signaling in guard cells (Hossain et al., 2011). This interaction between the ABA and JA signaling pathway could have caused the synergic effect for the reduction of the physiological traits (Table 2.2 and Figure 2.7). However, besides the hormonal interactions, unique and novel molecular mechanisms were also found during the stress combination. For example, the transcriptome analysis revealed that a unique set of transcripts was altered in response to the combination of drought and nematode infection (Atkinson et al., 2013), drought, heat stress and virus (Prasch and Sonnewald, 2013), infection by *Botrytis cinerea*, herbivory by chewing larvae and drought stress (Coolen et al., 2016). The synergic effect on the reduction of the photosynthesis and transpiration (Table 2.2 and Figure 2.7) could be determined by the stomatal closure in addition to the herbivory-induced resource

reallocation to chemical defence (Nabity et al., 2009) that determined more intense dark respiration (Schmidt et al., 2009).

Differently to the physiological traits, the synergic effect was also involved in the increase of the VOC emission in COMB-treated tomato plants (Table 2.4 and Figure 2.7). This synergic effect could be due to diverse reasons. First, the improvement of the formation reactive oxygen species (ROS) by drought stress (Chaves et al., 2009) and nutrient deficiency (Shin et al., 2005) that could sensitizes the VOC response. Indeed, it is know that the VOCs are emitted by early signaling events involved the ROS during the herbivory (Arimura et al. 2011; Bruinsma et al. 2010; Wu and Baldwin 2009). Second, the abiotic stress and herbivory by *Tuta* could have improved the biosynthesis of VOCs by both hormone cross-talking and higher resource reallocation to chemical defence. For example, the ABA and JA, the phytohormones involved in the plant response to the drought and herbivory, pointed out cross-talking interactions (Nguyen et al., 2016; Yang et al., 2019; Hossain et al., 2011) and the reallocation of plant resources to defense by modification of the gene expression profiles after herbivory was also observed (Reymond et al., 2004; Thompson and Goggins, 2006; Bethany et al., 2014). Third, the improved VOC biosynthesis in presence of both stresses could increase their accumulation inside the leaf with consequent formation of a deeply partial pressure gradient between the atmosphere and substomatal cavities along which the VOCs could be highly emitted.

The antagonistic effect observed in the reduction of leaf water content, and for the leaf fresh and dry weight although not significant, at 1 days of treatment with combined stress (Table 2.1 and Figure 2.7) is clearly due to the prioritization of the plant response to the herbivory. Indeed, the tomato plants aimed to reduce the leaf water content more in presence of *Tuta* rather than in abiotic stress through a sharp increase of the leaf dry weight (Table 2.1 and Figure 2.2). Why? The water and the dry weight are strictly and negatively linked to the plant palatability towards the pest (Elger and Will, 2003); hence, the tomato plant in presence of the combined stress redirect the resource allocation towards the formation of carbon-based secondary compounds such as lignin, fibre and silica contents which contribute to leaf toughness and reduce palatability (Cornelissen & Thompson 1997; Grime et al. 1996).

**Table 2.4** - Volatile organic compounds (Area %) from the leaves of tomato plants detected in at least two replicates out of three at each sampling time and treatments.

Common name	t0				t1				t3				t8			
	ABIO	BIO	COMB	CTR	ABIO	BIO	COMB	CTR	ABIO	BIO	COMB	CTR	ABIO	BIO	COMB	CTR
(+)-4-Carene	1.161	2.199	1.508	2.438	1.916	2.054	1.300	2.062	1.570	2.081	0.872	1.882	1.321	1.898	1.443	1.717
(2E)-2-Hexenyl propionate	-	-	-	-	-	-	-	-	-	-	-	-	-	0.154	0.010	-
(E) - 2 hexen - 1 ol	4.689	10.781	2.015	8.795	2.270	4.651	7.857	8.242	1.035	4.897	5.640	11.923	0.558	13.908	8.854	12.541
(E) beta ocimene	0.066	0.510	0.280	0.682	0.584	0.252	1.945	5.035	0.603	0.401	0.925	0.401	0.966	0.348	0.780	0.168
1,3,7-Nonatriene, 4,8-dimethyl-, (3E)-	-	-	0.054	0.154	0.113	0.029	0.449	0.005	0.136	-	0.149	-	0.163	-	0.123	-
3-Hexen-1-ol, propanoate, (3Z)-	0.124	0.297	-	0.475	-	0.319	-	0.181	0.014	0.233	0.206	0.249	0.032	0.073	0.071	0.192
alfa copaene	0.087	0.018	0.031	0.036	0.073	0.040	0.032	0.040	0.059	0.021	0.080	0.015	0.026	0.048	0.033	0.049
alfa cubebene	-	0.005	0.002	-	0.002	-	0.002	-	-	-	-	-	0.002	-	-	-
Alloaromadendrene	-	0.002	0.006	0.003	-	-	-	-	0.005	-	-	-	-	-	-	-
allo-ocimene	0.094	0.146	0.135	0.160	0.207	0.135	0.433	0.129	0.190	0.065	0.221	0.189	0.222	0.056	0.167	0.117
alpha guaiene	0.135	0.138	0.248	0.073	0.182	0.037	0.281	0.073	0.134	0.049	0.221	0.029	0.084	0.024	0.108	0.023
alpha gurjunene	-	-	0.008	-	-	-	-	-	-	-	-	-	-	-	-	-
alpha humulene	0.948	1.486	2.592	0.724	2.089	0.569	2.882	0.821	1.896	0.713	1.815	0.340	0.707	0.427	1.204	0.363
alpha pinene	1.962	2.2232	1.720	2.613	2.596	2.630	1.988	5.089	2.333	2.488	1.968	4.479	2.521	2.233	2.249	2.519
alpha selinene	-	-	-	-	-	-	-	-	-	-	-	-	-	-	0.003	-
alpha terpinene	23.117	22.598	21.464	27.941	18.196	26.618	17.120	22.316	22.055	20.163	19.942	22.084	24.387	23.187	21.425	24.561
aromadendrene	-	-	0.100	0.033	0.114	-	0.168	0.017	0.149	0.147	0.094	0.013	0.025	0.004	0.084	0.045
beta cadinene	0.086	0.084	0.137	0.063	0.083	0.034	0.279	0.043	0.109	0.017	0.197	0.008	0.088	0.018	0.091	0.047
beta elemene	0.257	0.130	0.257	0.126	0.213	0.018	0.337	0.056	0.168	0.053	1.137	0.019	0.093	0.025	0.137	0.112
beta phellandrene	51.056	39.824	42.917	44.314	19.965	52.715	38.307	45.478	48.506	57.142	41.944	46.486	56.737	48.859	46.358	49.086

beta pinene	5.432	2.481	2.781	1.851	1.043	2.502	1.922	2.654	2.087	2.154	1.889	6.098	2.602	2.638	1.890	2.323
caryophyllene alcohol	-	-	0.007	-	-	0.032	1.601	-	-	0.007	-	-	-	0.004	0.002	-
delta cadinene	-	-	0.035	-	0.006	-	0.007	-	-	-	-	-	0.007	-	0.017	-
delta elemene	0.836	1.003	2.875	0.584	2.285	0.308	3.013	0.537	1.981	0.582	2.929	0.287	1.035	0.225	1.861	0.439
Diocetyl ether	-	-	-	-	-	-	-	-	-	-	-	0.099	-	-	-	0.449
dodecanal	0.111	-	-	-	-	-	-	-	-	-	-	-	-	-	-	-
Dodecane	0.118	-	-	-	-	-	-	-	-	-	-	-	-	-	-	-
Dodecane, 2,6,11-trimethyl-	0.158	0.050	0.022	0.059	0.023	0.062	0.012	0.044	0.020	0.072	0.045	0.016	0.018	0.004	0.017	0.050
E $\beta$ -Caryophyllene	5.271	10.632	15.863	4.919	12.195	4.189	11.917	4.980	11.114	5.483	10.191	4.347	4.550	2.705	7.376	2.304
hexadecane	0.088	-	-	0.015	-	-	-	-	-	-	-	-	-	-	-	-
Dendrolasin	-	0.202	0.189	0.215	0.133	0.520	0.130	-	0.553	0.124	0.843	0.084	0.162	0.260	0.156	0.846
gamma elemene	0.261	0.184	0.580	0.282	0.662	0.108	0.581	0.206	0.485	0.163	0.141	0.049	0.075	0.078	0.240	0.056
gamma terpinene	0.117	0.343	0.207	0.509	0.423	0.467	0.181	0.345	0.344	0.487	0.437	0.470	0.355	0.299	0.175	0.392
germacrene D	-	-	0.027	-	-	-	-	-	0.007	-	-	-	0.004	-	0.003	-
hexyl propionate	-	0.098	-	-	-	-	-	-	-	-	-	-	0.040	0.092	0.010	-
Longifolene	-	0.003	-	-	-	-	-	-	-	-	-	-	-	-	-	-
methyl salicylate	-	-	-	-	-	-	-	-	-	-	4.159	-	0.332	0.534	0.913	-
myrcene	3.089	4.035	3.299	2.183	3.791	1.344	6.460	1.280	3.735	2.015	3.459	1.620	2.424	1.588	3.700	1.159
o - cymene	-	-	-	-	0.207	-	-	-	0.215	-	-	-	-	-	-	0.073
terpinolene	0.306	0.389	0.348	0.396	0.416	0.277	0.474	0.246	0.272	0.368	0.290	0.348	0.361	0.267	0.329	0.282
tridecane	0.072	-	-	0.024	-	-	-	-	-	-	-	-	-	-	-	-
Z $\beta$ -Caryophyllene	0.021	-	0.088	0.055	0.098	0.048	0.092	0.035	0.056	0.044	0.084	0.008	0.015	0.010	0.050	0.052
$\beta$ -copaene	-	-	-	-	-	-	-	0.008	-	-	-	-	-	-	-	-
$\gamma$ gurjunene	-	-	0.004	0.001	0.007	-	0.019	-	0.014	-	-	0.001	0.010	-	-	0.001
$\gamma$ muurolene	0.081	0.056	0.197	0.029	0.098	0.001	0.207	0.056	0.137	0.005	0.113	-	0.068	0.015	0.115	0.004

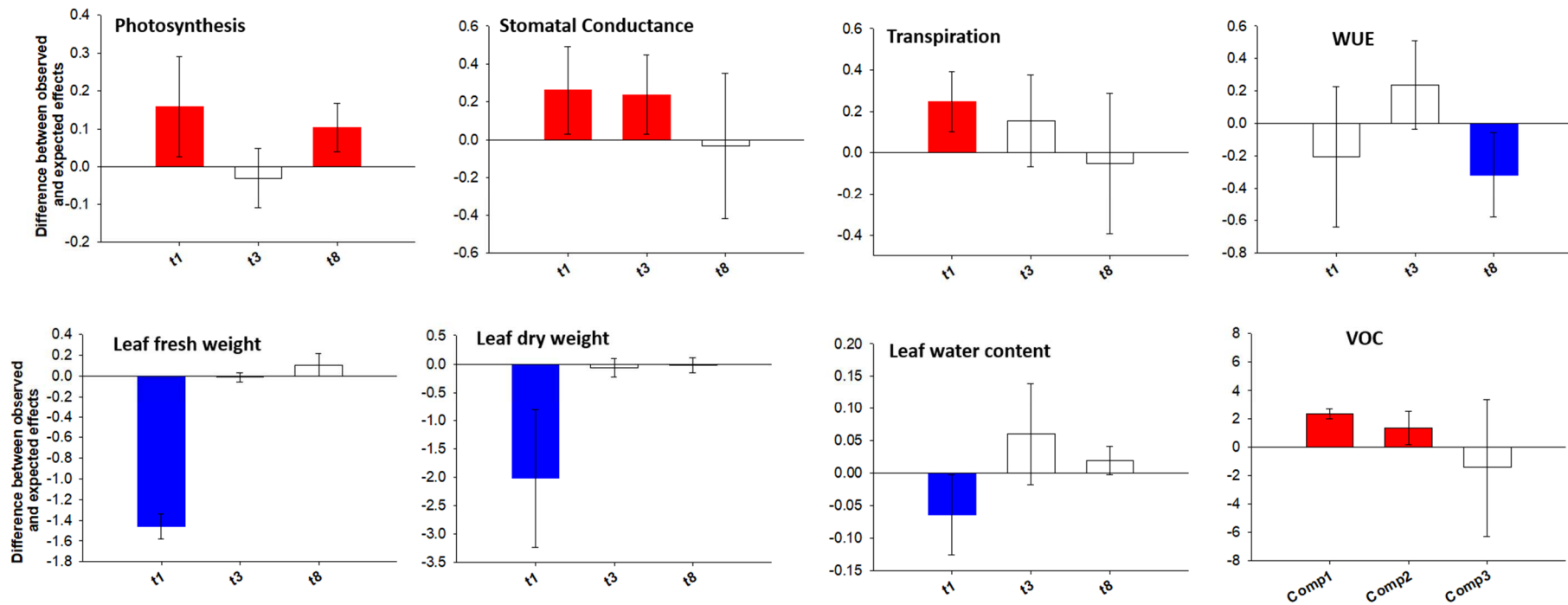
**Table 2.5** - Permanova results of the VOC emission of tomato plants exposed to different stress (Treatment) and Time of exposure (Ti).

	<b>Df</b>	<b>Sum of square</b>	<b>R2</b>	<b>F</b>	<b>Pr(&gt;F)</b>
<b>Treatments</b>	3	0.8661	0.06288	3.3117	0.003**
<b>Time</b>	1	0.2228	0.01618	2.5562	0.048*
<b>Treatments:Time</b>	3	0.8291	0.06020	3.1704	0.007**
<b>Residual</b>	136	11.8555	0.86075		
<b>Total</b>	143	13.7736	1.00000		

**Table 2.6** - PERMANOVA pairwise comparison between treatments within each time of exposure.

<b>Pairs</b>	<b>F. Model</b>	<b>R2</b>	<b>P value</b>	<b>P adjusted</b>
ABIO 0 vs BIO 0	2.368	0.129	0.065	0.152
ABIO 0 vs COMB 0	1.733	0.098	0.159	0.239
ABIO 0 vs CTR 0	1.917	0.107	0.145	0.229
ABIO 1 vs BIO 1	2.251	0.123	0.099	0.192
ABIO 1 vs COMB 1	1.684	0.095	0.150	0.234
ABIO 1 vs CTR 1	1.694	0.096	0.143	0.229
ABIO 3 vs BIO 3	1.067	0.063	0.289	0.350
ABIO 3 vs COMB 3	1.574	0.090	0.197	0.2670
ABIO 3 vs CTR 3	2.057	0.114	0.136	0.221
ABIO 8 vs BIO 8	1.656	0.094	0.190	0.267
ABIO 8 vs COMB 8	2.222	0.122	0.090	0.186
ABIO 8 vs CTR 8	4.258	0.210	0.018	0.070
BIO 0 vs COMB 0	0.722	0.043	0.473	0.515
BIO 0 vs CTR 0	0.240	0.015	0.831	0.838
BIO 1 vs COMB 1	2.429	0.132	0.066	0.153
BIO 1 vs CTR 1	1.313	0.076	0.259	0.320
BIO 3 vs COMB 3	1.654	0.094	0.186	0.267
BIO 3 vs CTR 3	1.959	0.109	0.122	0.201
BIO 8 vs COMB 8	4.734	0.228	0.024	0.082
BIO 8 vs CTR 8	9.793	0.380	0.004	0.040
COMB 0 vs CTR 0	0.705	0.042	0.473	0.515
COMB 1 vs CTR 1	3.053	0.160	0.027	0.088
COMB 3 vs CTR 3	5.218	0.246	0.006	0.042
COMB 8 vs CTR 8	9.034	0.361	0.001	0.040





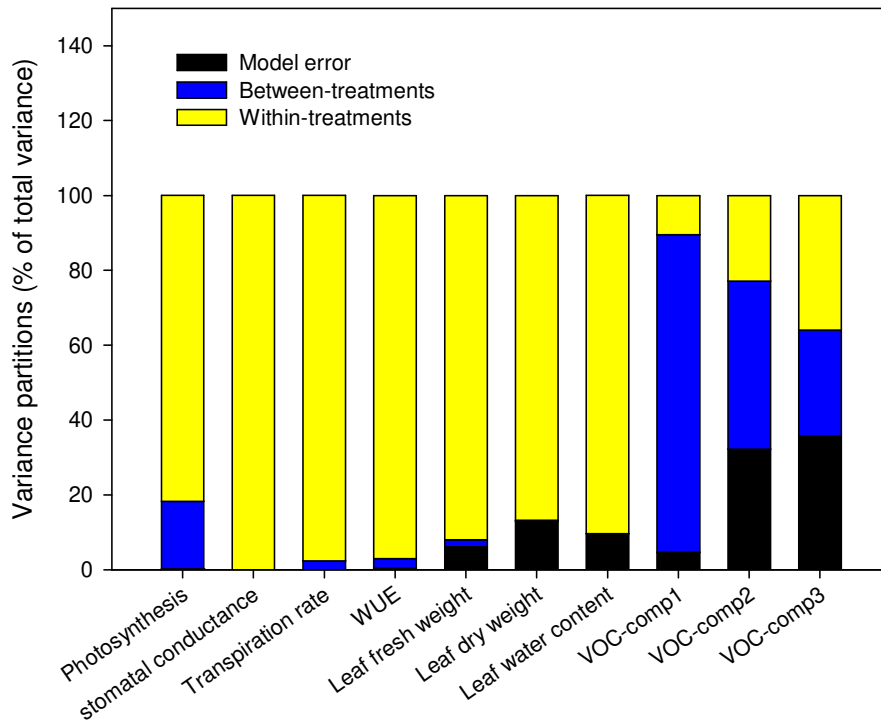
**Figure 2.7** - The combined impacts from abiotic (drought and N deficiency) and biotic stress (Infestation of *Tuta absoluta*) on morpho-physiological traits of tomato plants at 1, 3 and 8 days of treatment and VOC emission at 8 days of treatment.

The combined impact of single stressors was estimated as synergist (red colour), additive (white colour) or antagonistic (blue colour) (greater than, equal to or less than expected effects, respectively, based on single stressor effect sizes). The vertical and error bars represent, respectively, the mean and the 95% confidence interval of the overall effect size difference between the observed and expected additive effects from combined abiotic and biotic stress on morpho-physiological and metabolic traits of tomato plants. The zero line represents the expected additive effects from combined stressors. When the means (and their 95% confidence limits) were higher than or less than the zero line, they were considered synergistic or antagonistic, respectively.

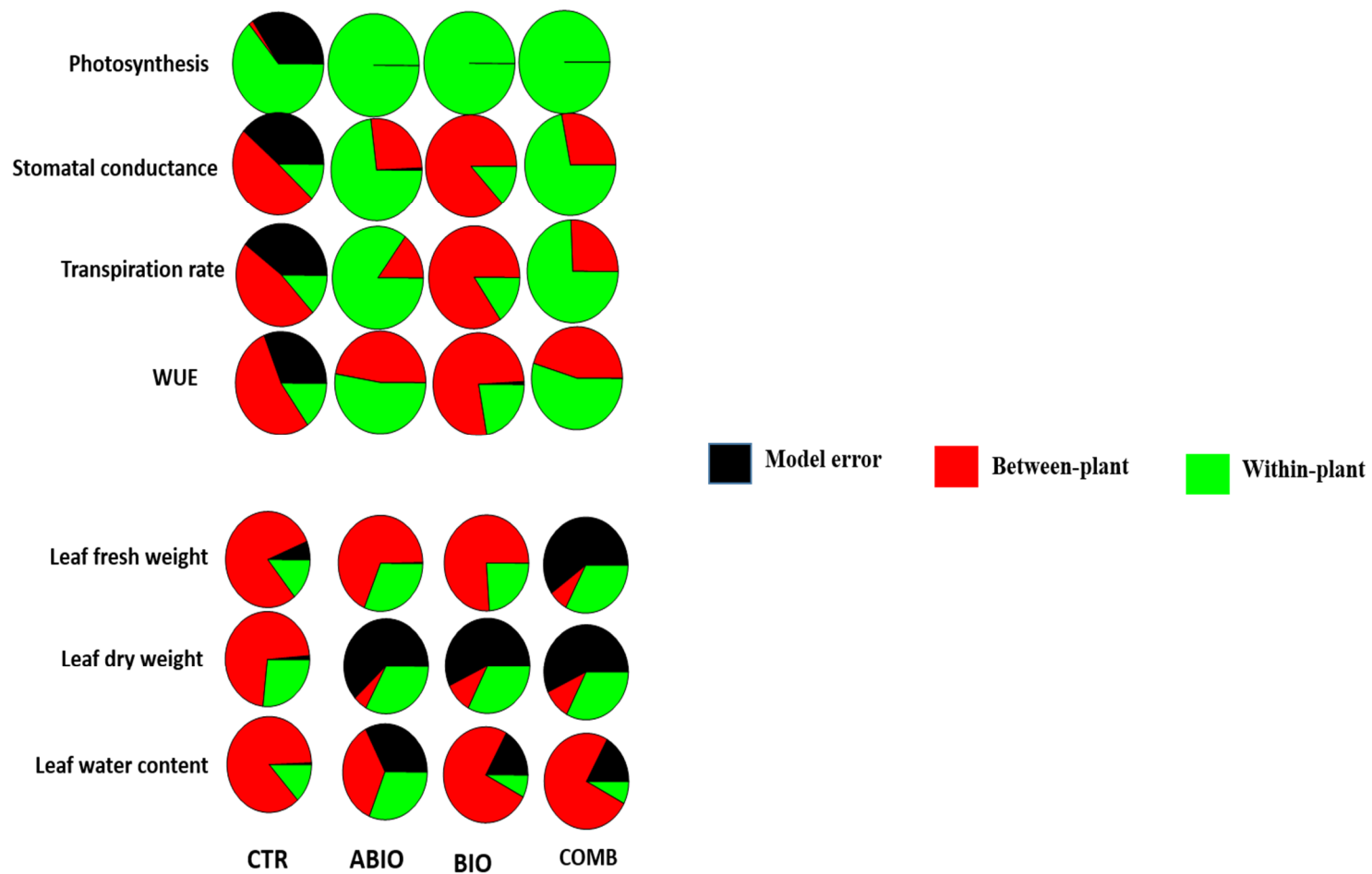
### *2.3.2. Do the tomato responses to the single and combined stress occurred at between- or within-plant levels?*

Recent studies pointed out the importance of the within-individual variation of the plant responses to the abiotic and biotic stress rather than that between-individual for the ecology at individual, population, and community levels (Herrera, 2009, 2017). For example, a higher within-plant variation of the morpho-physiological responses permitted an improvement of the exploitation of the heterogeneously-distributed resources such as light, CO<sub>2</sub>, nutrient (Osada, 2014; Herrera et al., 2015), an optimization of the cost-expensive defenses against herbivory and pathogens (McKey, 1974; Meldau et al., 2017), and an alteration of plant-antagonist interactions (Sobral and Guitián, 2014; Shimada and Takahashi, 2015; Wetzel and Kharouba, 2016; Wetzel and Meek, 2019). In this respect, we assessed, first, if the among-treatments variance of the morpho-physiological traits and VOC profiles of the tomato plants is more important than within-treatment one and, then, we evaluated the between- and within-plant variance for each treatment. To calculate the among- and within-treatments variance, we used the morpho-physiological traits and VOC observed at 8 days that is the time with wider and higher modifications of these traits (Tables 2.1 and 2.2; Figures 2.2, 2.3 and 2.6) and their measurements have been carried out in three mature leaves located at three different positions along the shoot axes. The contribution of the among- and within-treatment level to the total variance in mean of the morpho-physiological traits and VOC responses in the four treatments considered was estimated by Linear Mixed Models and statistically tested by restricted maximum likelihood (REML) (Figure 2.8). The results indicated that most variance

occurred at within-treatments, especially for the morpho-physiological traits but not for the VOCs (Figure 2.8). Hence, differently to the morpho-physiological traits, the emission of the VOCs was more dependent on the stress treatments rather than the individual plants. For this reason, only the morpho-physiological traits were used in the analysis of within-plant variation that was conducted applying a hierarchical partition to divide total variance into two levels of variation: among plants and among the leaves within the same plant. This analysis was performed for each single treatment in order to verify its effects to within-plant phenotypic plasticity. The variance partitions varied substantially among the different treatments and traits considered (Figure 2.9). In general, the physiological traits pointed out a higher within-plant variance (average 54%) while the morphological ones showed more between-plant variance (average 50%) (Figure 2.9). Why do the individual tomato plants modified more the leaf physiological than morphological traits within their shoot? Probably, the physiological traits being lesser expensive, could be faster modified in response to the abiotic and biotic stress; for example, rapid local and systemic responses through specific signaling pathways have been observed in presence of the light stress (Devireddy et al., 2018), the heat tolerance (Slot and Krause, 2019) and the herbivory (Girón-Calva and Li, 2014). Among the treatments, the stresses induced a higher within-plant variance than CTR: ABIO (average 58%), COMB (average 53%), BIO (average 31%) and CTR (average 22%) (Figure 2.9). The within-plant variation in stressful condition could permitted the improvement to exploit the stress-induced transient environmental and soil resources (Niinemets and Valladares, 2004; Meier and Leuschner, 2008; Marchiori and Machado, 2017; Puglielli and Catoni, 2017) and the optimization of the defences against herbivory (Frost and Appel, 2007; Rodriguez-Saona, et al., 2009).



**Figure 2.8** - Dissection of total variance components of the morpho-physiological traits and VOC responses at 8 days of treatments (control, abiotic stress, biotic stress, combined stress). Considering all treatments pooled, the contributions of treatment (blue color) and within-treatment (yellow color) level to the total variance in mean of the morpho-physiological traits and VOC responses in the four treatments considered were estimated by Linear Mixed Models.



**Figure 2.9** – Nested within-treatment variance partitions (% of the total) in the morpho-physiological responses of tomato plants to different abiotic and biotic stress. The between-plant variance comprise plant within treatment (red color) and the within-plant variance involved the leaves within plant within treatment (green color). The black color indicated the model error.

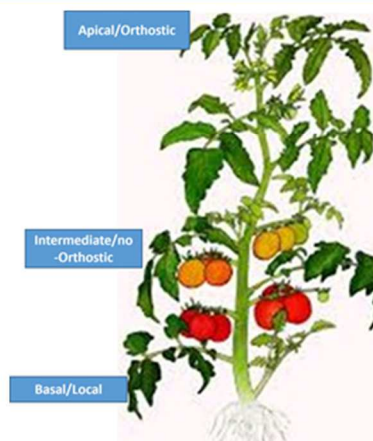
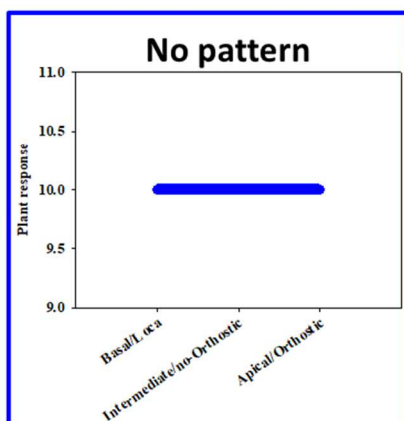
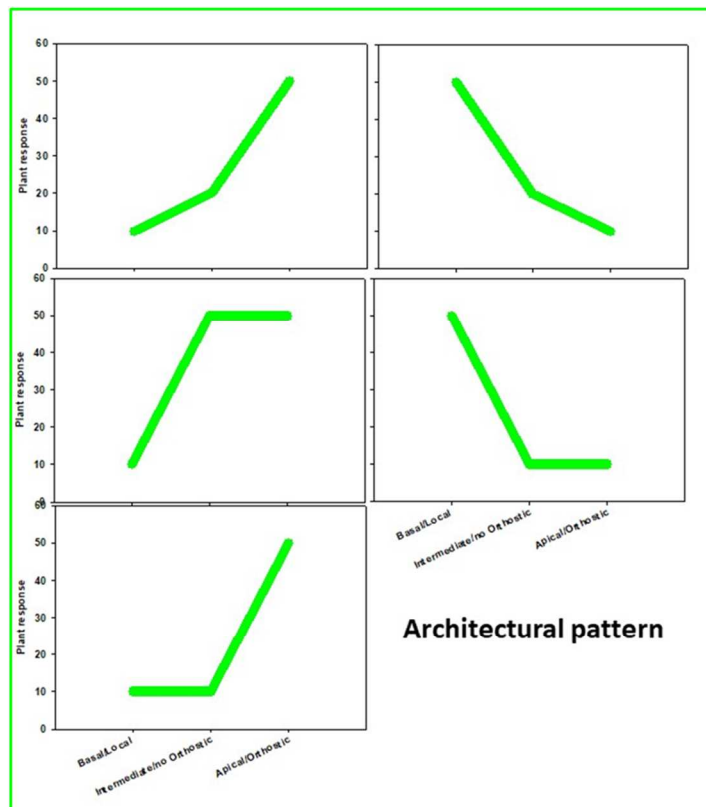
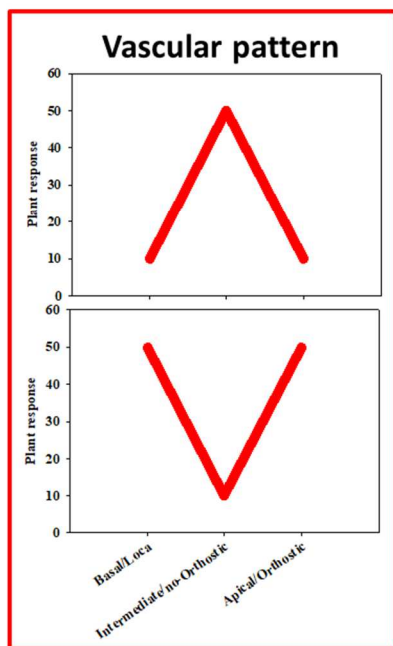
Considering that each treatment pointed out an important within-plant variation for the morpho-physiological traits, we asked if a well-defined spatial pattern of these responses among the leaves of the tomato shoot can be revealed. In this respect, by one-way ANOVA, we compared the effects of three mature leaves located at three different positions [basal (B), intermediate (I) and apical leaf (A) placed at first, second and third node, respectively] along the shoot axes on the morpho-physiological traits for each treatments. Further, the B, I and A leaf can be also considered as local (L), non-orthostichous (nO) and orthostichous leaf (O), respectively, because the apical leaf, but not the intermediate, is linked to the basal one by vasculature connection (Figure 2.10: preliminary experiments using phloem dyeing as reported in Orians et al., 2000). Hence, this leaf selection permitted us to evaluate which between the vascular (L vs O vs nO) or architectural patterns (B vs I vs A) determined the leaf-level spatial component of the within-plant phenotypic variability.



**Figure 2.10** - Degree of vascular connectivity among different leaf positions of tomato plants by method of Orians et al. (2000).

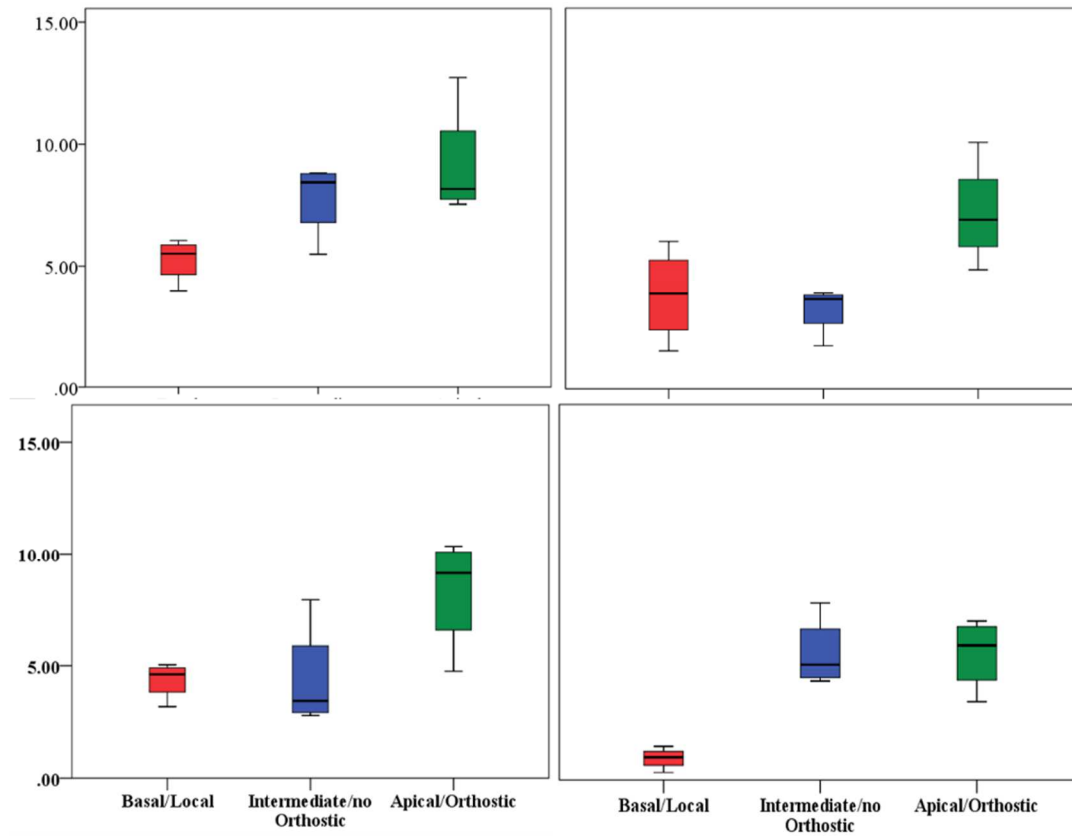
For example, the Figure 2.11 depicted the vascular or architectural pattern or no pattern of the tomato responses to each treatments. The Figure 2.12, 2.13, 2.14, 2.15, 2.16, 2.17 and 2.18 showed the results of physiological (photosynthesis, stomatal conductance, transpiration rate and WUEi) and morphological traits (leaf fresh and dry weight, leaf

water content) for each treatment. An overall result indicated that the ABIO and the COMB treatments significantly modified all the morpho-physiological traits of the three tomato leaves, except the leaf water content, differently to the CTR and BIO, except the photosynthetic rate (Figures 2.12, 2.13, 2.14, 2.15, 2.16, 2.17 and 2.18). Further, considering the results showed in the Figures 2.12, 2.13, 2.14, 2.15, 2.16, 2.17 and 2.18, the ABIO and COMB treatments determined an architectural pattern for the physiological responses (photosynthetic and transpiration rate, stomatal conductance and WUE) while the morphological ones pointed out a vascular pattern (Figures 2.12, 2.13, 2.14, 2.15, 2.16, 2.17 and 2.18 compared with Figure 2.11). The abiotic stress are known to strongly influence the plant photosynthetic traits in relation to the leaf position/age (Yamada et al., 1996; Schurr et al., 2006; Zhang et al., 2012) in order to preserve the highly valuable tissues, such as the young leaf. For example, the higher stomatal conductance in apical leaf determined a higher transpiration rate that limited the leaf overheating (Lin and Chen, 2017). The vascular pattern of the leaf fresh and dry weight in response to the COMB treatment could be due to the ABA-JA cross-talking signaling pathways (Nguyen et al., 2016; Yang et al., 2019; Hossain et al., 2011) which could be observed between the two vascular-connected leaves (local and orthostic). We can hypothesized that the *Tuta* larvae in the local leaf of tomato plants triggered by vascular connection, the signaling pathways which redirect the photosynthetic resource towards the defence compounds rather growth ones. This kind of hormone cross-talk signaling interaction among the different vascular-connected leaves within the plant was observed. For example, the abiotic stresses antagonized the immune responses by ABA-SA hormonal interaction in older leaves of *Arabidopsis* but this effect was suppressed in the younger leaf through a signaling component of the SA pathway (Berens et al., 2019).

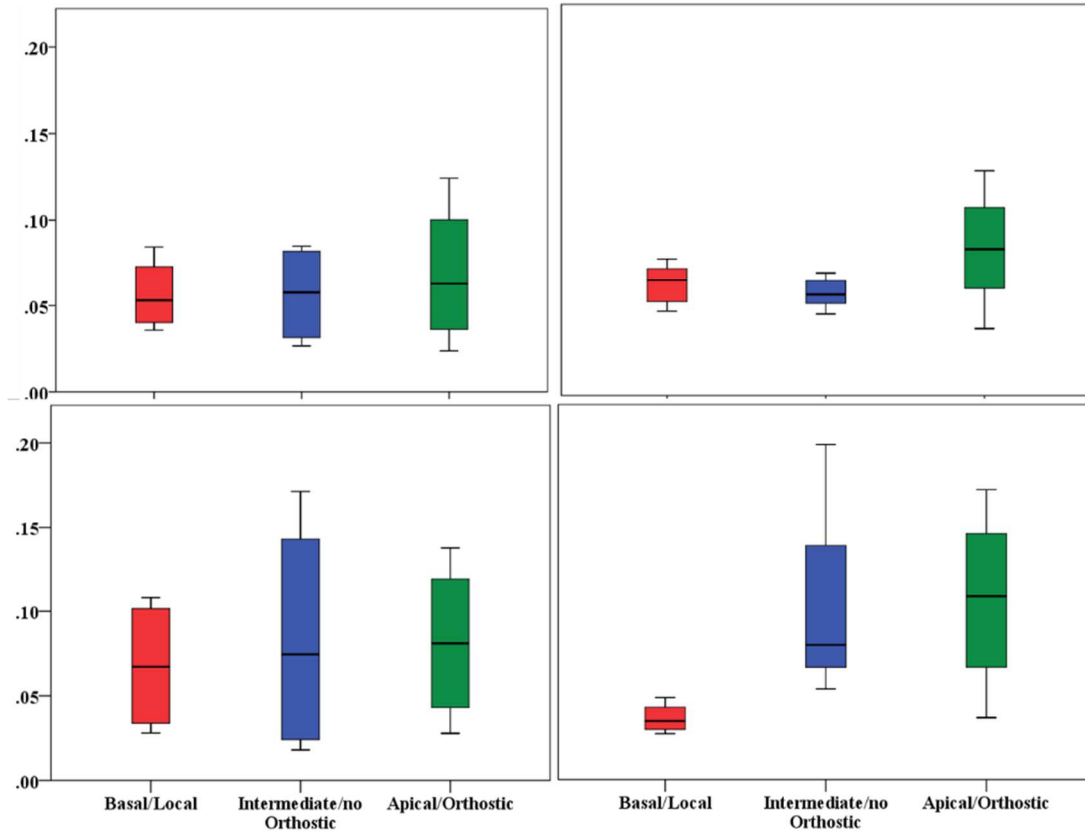


**Figure 2.11** – Tomato responses to the experimental conditions resembling the vascular pattern (red line) or architectural pattern (green line) or no pattern (blue line).

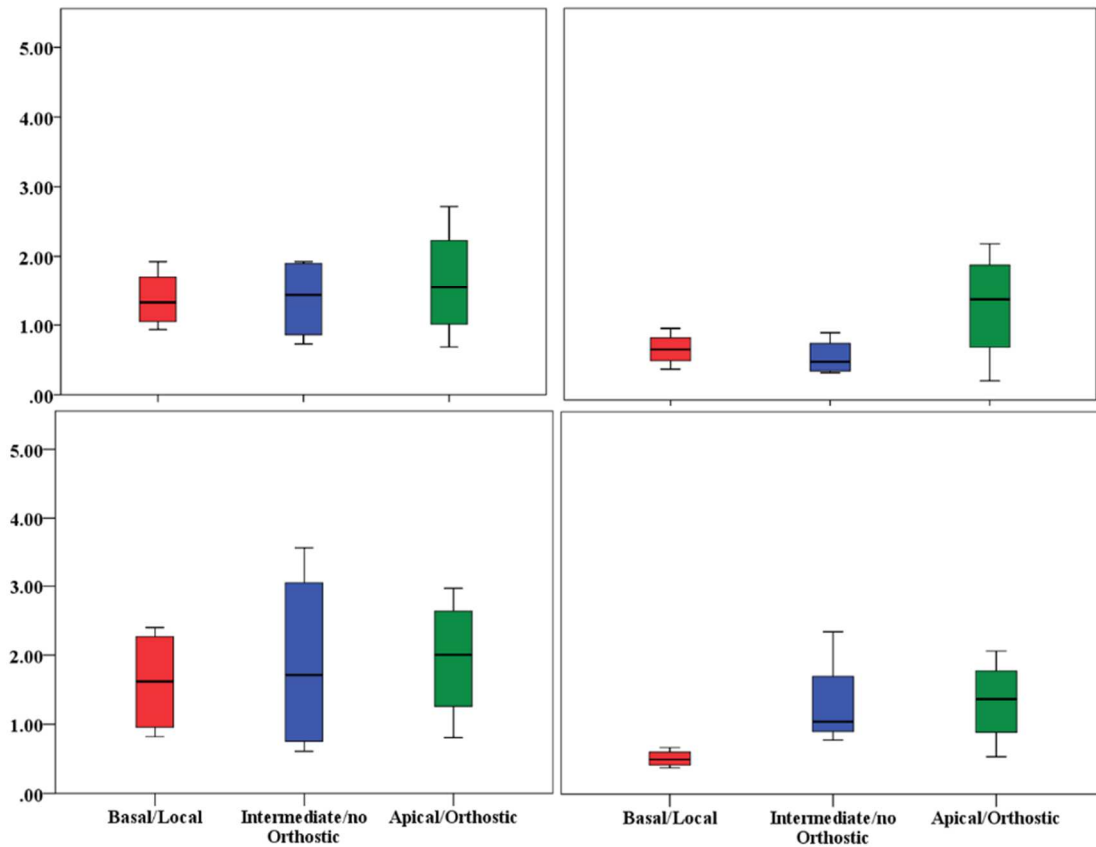




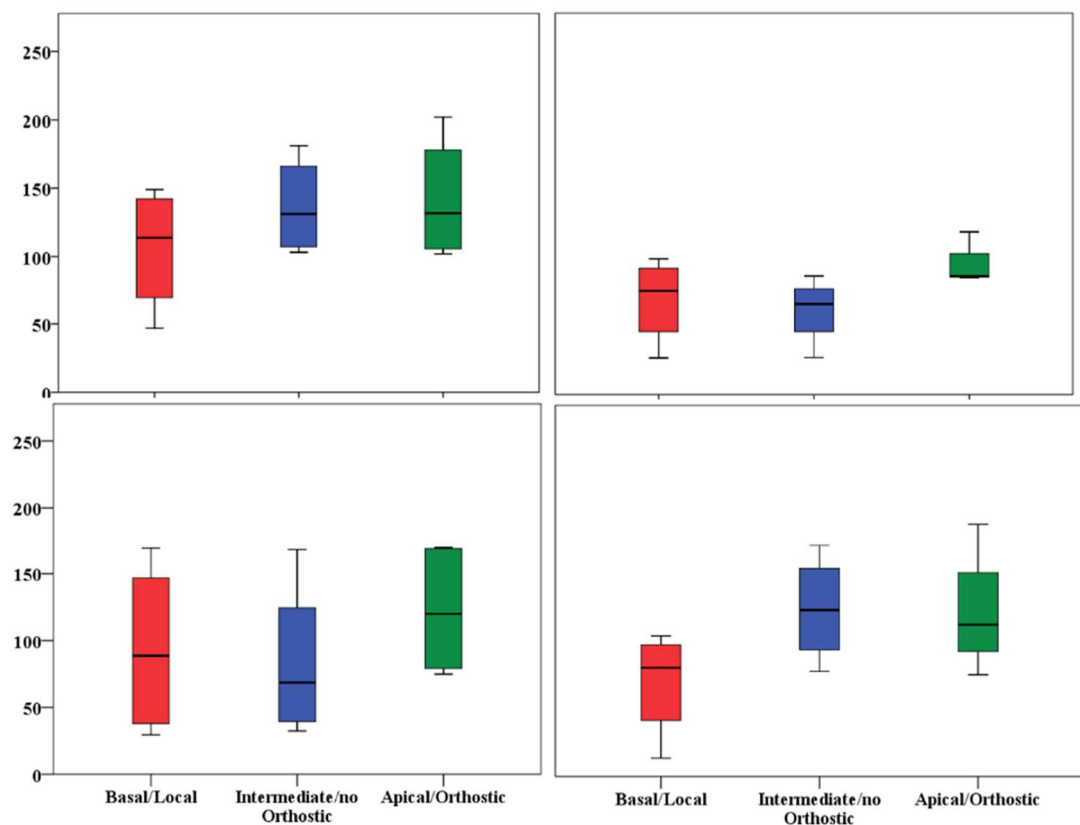
**Figure 2.12** – Photosynthetic rate of three different leaves of tomato plants exposed for 8 days at diverse stresses [abiotic (ABIO); biotic (BIO); combined (COMB)]. No stresses (CTR). The box plot indicated the minimum, first quartile, median, third quartile, and maximum value. Different letters indicated significant difference among the mean groups (N=8;  $p < 0.05$  test of Tukey). The values within the figure indicated the F statistic with the p values (\*\*\*)  $p < 0.001$  derived from one-way ANOVA.



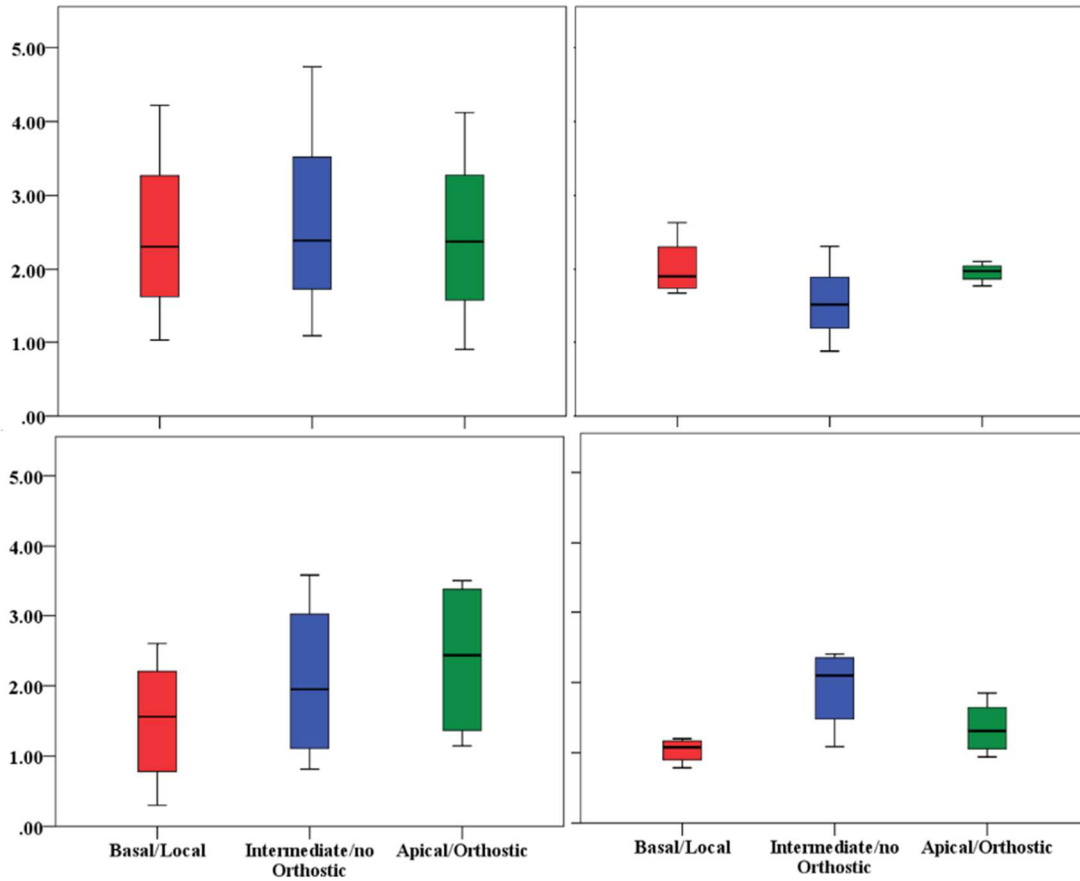
**Figure 2.13** – Stomatal conductance of three different leaves of tomato plants exposed for 8 days at diverse stresses [abiotic (ABIO); biotic (BIO); combined (COMB)]. No stresses (CTR). The box plot indicated the minimum, first quartile, median, third quartile, and maximum value. Different letters indicated significant difference among the mean groups (N=8;  $p < 0.05$  test of Tukey). The values within the figure indicated the F statistic with the p values (\*  $0.05 < p < 0.01$ ;  $0.01 < p < 0.001$ ; ns not significant) derived from one-way ANOVA.



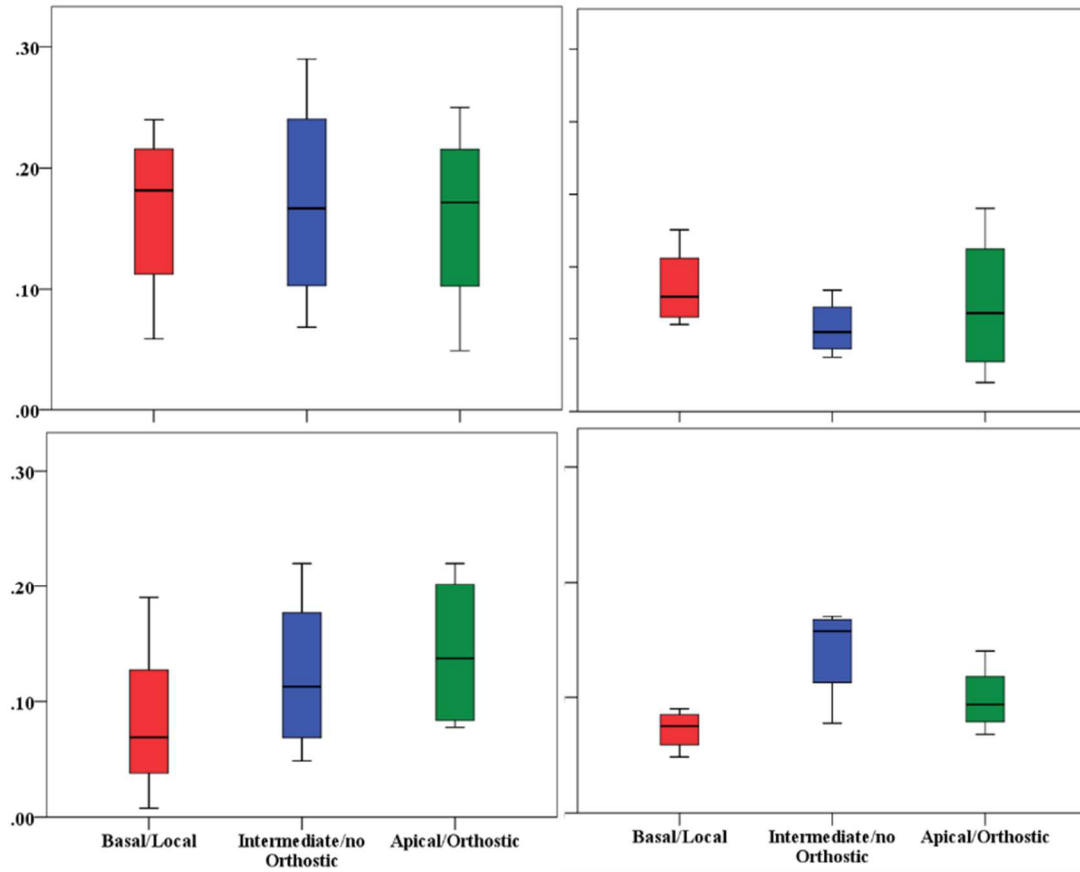
**Figure 2.14** – Transpiration rate of three different leaves of tomato plants exposed for 8 days at diverse stresses [abiotic (ABIO); biotic (BIO); combined (COMB)]. No stresses (CTR). The box plot indicated the minimum, first quartile, median, third quartile, and maximum value. Different letters indicated significant difference among the mean groups (N=8;  $p < 0.05$  test of Tukey). The values within the figure indicated the F statistic with the p values (\*  $0.05 < p < 0.01$ ;  $0.01 < p < 0.001$ ; ns not significant) derived from one-way ANOVA.



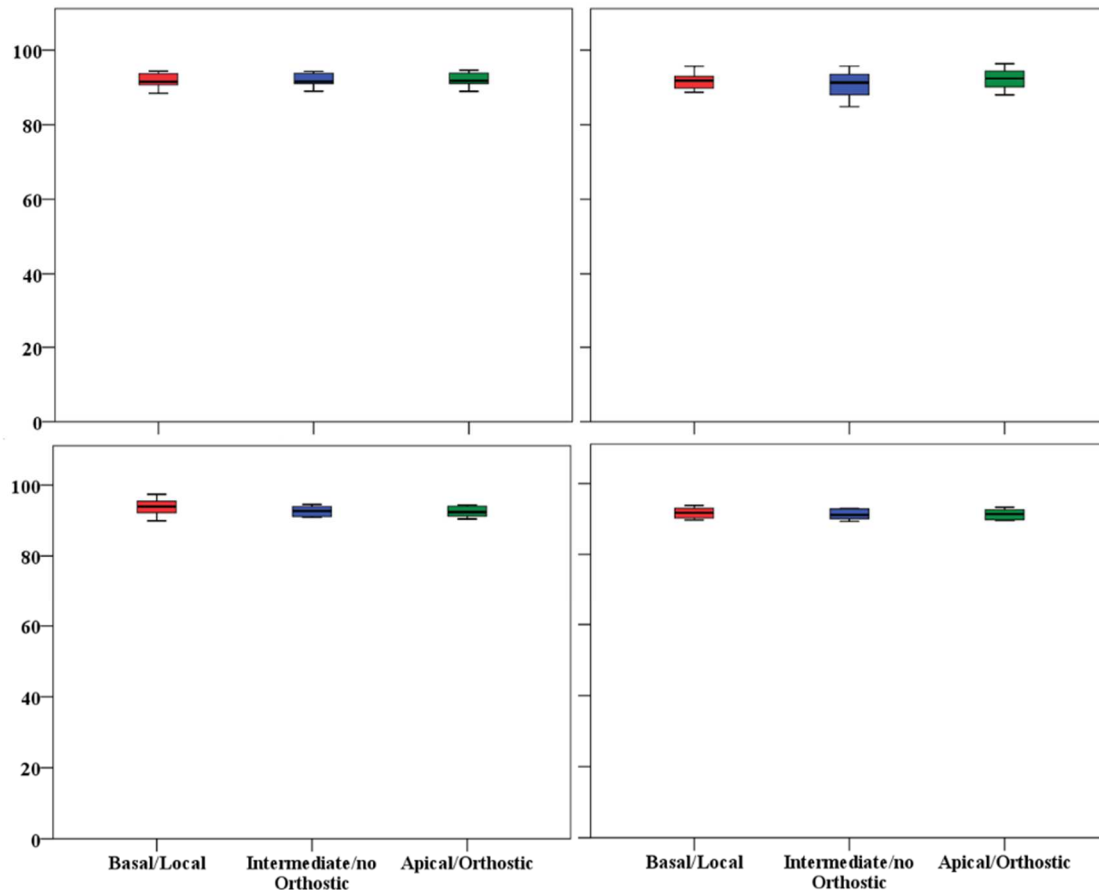
**Figure 2.15** – WUE<sub>i</sub> of three different leaves of tomato plants exposed for 8 days at diverse stresses [abiotic (ABIO); biotic (BIO); combined (COMB)]. No stresses (CTR). The box plot indicated the minimum, first quartile, median, third quartile, and maximum value. Different letters indicated significant difference among the mean groups (N=8; p<0.05 test of Tukey). The values within the figure indicated the F statistic with the p values (\* 0.05<p<0.01; ns not significant) derived from one-way ANOVA.



**Figure 2.16** – Leaf fresh weight of three different leaves of tomato plants exposed for 8 days at diverse stresses [abiotic (ABIO); biotic (BIO); combined (COMB)]. No stresses (CTR). The box plot indicated the minimum, first quartile, median, third quartile, and maximum value. Different letters indicated significant difference among the mean groups (N=8;  $p < 0.05$  test of Tukey). The values within the figure indicated the F statistic with the p values (\*  $0.05 < p < 0.01$ ; \*\*\*  $p < 0.001$ ; ns not significant) derived from one-way ANOVA.



**Figure 2.17** – Leaf dry weight of three different leaves of tomato plants exposed for 8 days at diverse stresses [abiotic (ABIO); biotic (BIO); combined (COMB)]. No stresses (CTR). The box plot indicated the minimum, first quartile, median, third quartile, and maximum value. Different letters indicated significant difference among the mean groups (N=8;  $p < 0.05$  test of Tukey). The values within the figure indicated the F statistic with the p values (\*  $0.05 < p < 0.01$ ; \*\*\* $p < 0.001$ ; ns not significant) derived from one-way ANOVA.



**Figure 2.18** – Leaf water content of three different leaves of tomato plants exposed for 8 days at diverse stresses [abiotic (ABIO); biotic (BIO); combined (COMB)]. No stresses (CTR). The box plot indicated the minimum, first quartile, median, third quartile, and maximum value. Different letters indicated significant difference among the mean groups (N=8; p<0.05 test of Tukey). The values within the figure indicated the F statistic with the p values (ns not significant) derived from one-way ANOVA.

## 2.4. Conclusions

The present study has been addressed to answer questions related to the tomato responses in presence of combined abiotic stress (drought and N deficiency) and herbivore infestation raised from previsions of burst herbivory and increased of drought stress and nutrient deficiency favored by climate change. First result was that the combination of drought, N deficiency and *Tuta* infestation caused a stronger negative impact on the tomato morpho-physiological traits and induced a specific VOC blend emission than single stress. Probably, hormone cross-talking regulating the signaling and metabolic systems of the plant responses could be evoked. Interestingly, differently to the single stress, the VOC blend emitted by tomato plants exposed to the COMB was characterized, besides to other, by the homoterpene 4,8-Dimethyl-1,3,7-nonatriene, a rare and

fundamental plant alarm volatiles, and by the methyl salicylate, a well-known herbivore-induced plant volatile which attract natural enemies and affect herbivore behavior.

Second result pointed out was the relatively rapid responses of the tomato plants to the COMB treatment and the synergistic effects for the physiological and VOC responses but antagonistics for the morphological ones. In this respect, no-additive effects of the single stress in tomato response to the combined stress are highlighted. This result is important because suggests that a “new stress state” characterized by specific signaling pathways and gene expression, probably orchestrated by hormone interactions, could be evoked in tomato plants stressed by the combination of drought, N deficiency and *Tuta* infestation. Finally, except for the VOC emission, the stressful conditions induced a higher within-plant variance in tomato with the abiotic and combined stress as the most influenced. The increase of the variability of the morpho-physiological responses within the tomato plants is very interesting considering the higher defense against the herbivore infestation and the maximization of the exploitation efficiency of the scarce soil resources observed in plant with high within-plant variance.

Overall, these results pointed out a “phenotypic picture” of the tomato plants subjected to the single and combined stress that is interesting and worthy to investigate at signaling pathways and gene expression levels for further understanding the physiological mechanisms.



## **Chapter 3: Single and Combined Abiotic Stress in Maize Root Morphology.**

*Adapted from: Rosa Vescio et al. Single and combined abiotic stress in maize root morphology. Plants 2021, 10(1), 5. <https://doi.org/10.3390/plants10010005>*

### **Abstract**

Plants are continually exposed to multiple stresses, which co-occur in nature and the net effects are frequently more non-additive (i.e., synergistic or antagonistic), suggesting “unique” responses respect to that of the individual stress. Further, plant stress responses are not uniform, showing a high spatial and temporal variability among and along the different organs. In this respect, the present work investigated the morphological responses of different root types (seminal, seminal lateral, primary, primary lateral) of maize plants exposed to single (drought and heat) and combined stress (drought + heat). Data were evaluated by a specific root image analysis system (WinRHIZO) and analyzed by uni- and multi-variate statistical analysis. The results indicated that primary roots and their laterals were the types more sensitive to the single and combined stresses while the seminal laterals specifically responded to the combined only. Further, antagonistic and synergistic effects were observed for the specific traits in the primary and their laterals and in the seminal lateral roots in response to the combined stress. These results suggested that maize root system modified specific root types and traits to face with different stressful environmental conditions highlighting that the adaptation strategy to the combined stress may be different from that of the individual ones. The knowledge of “unique or shared” responses of plants to multiple stress can be utilized to develop varieties with broad spectrum stress tolerance.

**Keywords:** combined stresses; drought stress; heat stress; maize; root morphology; root types

**List of abbreviations:** Partial Least Squares-Discriminant Analysis (sPLS-DA); Principal Component Analysis (PCA); Drought stress (D); Heat stress (H); Combined stress (Comb); Field Capacity (FC); Control (Con); Shoot Fresh Weight (ShFW); Shoot

Dry Weight (ShDW); Length (L); Surface Area (SA); Volume (V); Seminal root (S); Primary root (Pr); Seminal lateral root (SL); Primary Lateral roots (PL); Root Zone Formation (RZF); Branching Zone Formation (BZF); Branching Density (BD); Primary Fresh Weight (PrFW); Primary Dry Weight (PrDW); Seminal Fresh weight (SFW); Seminal Dry Weight (SDW); Primary Lateral Fresh Weight (PrLFW); Primary Lateral Dry Weight (PrLDW); Seminal Lateral Fresh Weight (SLFW); Seminal Lateral Dry Weight (SLDW); Root Fresh Weight (RFW); Root Dry Weight (RDW); Plant Fresh Weight (PFW); Plant Dry Weight (PDW); Root Length Ratio (RLR); Root Mass Ratio (RMR); Root Fineness (RF); Root Tissue Density (RTD); False Discovery Rate (FDR).

### **3.1. Introduction**

The European climate change scenarios will be characterized by extreme temperature, heat waves and warmer days along with dry days and droughts, especially in Southern Europe (Cardell et al., 2020). Emerging evidences indicate that these climate change-related events will negatively impact on the plant/crop/forest productivity in both natural and agro-ecosystems (Boisvenue et al., 2006; Niinemets et al., 2010; Lobell et al., 2012; Tito et al., 2018; Sultan et al., 2019; Ding et al., 2019). To date, the effects and the plant responses to each stressor have been extensively studied at both the morpho-physiological and molecular levels. For example, both drought and heat stress reduced the photosynthetic activity, modified the oxidative metabolism, inducing membrane instability (Fahad et al., 2017), changed the phosphoproteome (Hu et al., 2015) and, consequently affected grain yield and quality in maize (Sah et al., 2020). However, under field conditions, these abiotic stresses co-occur concurrently during the plant life cycle stimulating fine-tuned and early-prompted plant responses to allocate resources efficiently for the adaptation to the coexistent threats. Recent studies uncover that plants evoke a “unique response” to the drought and heat combined stresses (Mittler et al., 2006; Rivero et al., 2013; Pandey et al., 2015), suggesting that their effects are mostly non-additive (i.e., synergistic and antagonistic) and, therefore, cannot be predicted through single-stressor results. Although few studies have been performed so far, the impacts of the combined drought and heat stress on maize growth, development and yield production and quality have been pointed out (Hu et al., 2015; Hussain et al., 2019; Obata et al., 2015; Killi et al., 2017; Zhao et al., 2016). In particular, the maize responses to the

combined abiotic stress were mainly focused on the aerial part of plant and its reproductive organs, probably for breeding aims. To the best of our knowledge, no information on the maize root system responses to the combined drought and heat stress are available. This knowledge is even more interesting considering that single maize root types, such as the embryonic roots (primary and seminal) and the post-embryonic roots (nodal and lateral) (Hochholdinger et al., 2018), differently responded to environmental cues and could be a “source” of stress adaptation. For example, different responses among root types to drought stress (Zhan et al., 2015; Hund et al., 2008), allelochemicals (Abenavoli et al., 2004; Lupini et al., 2016), P deficiency (Rubio et al., 2004) and to combined N deficiency/drought stress (Lynch, 2013) were already reported. In this respect, a microcosm experiment was setup for studying several growth and morphological parameters of different root types in response to drought (30% of field capacity) and heat stress (32° air temperature) and their combination in maize plants. Further, the additive, synergic and antagonistic effects in combined drought and heat stress were also evaluated.

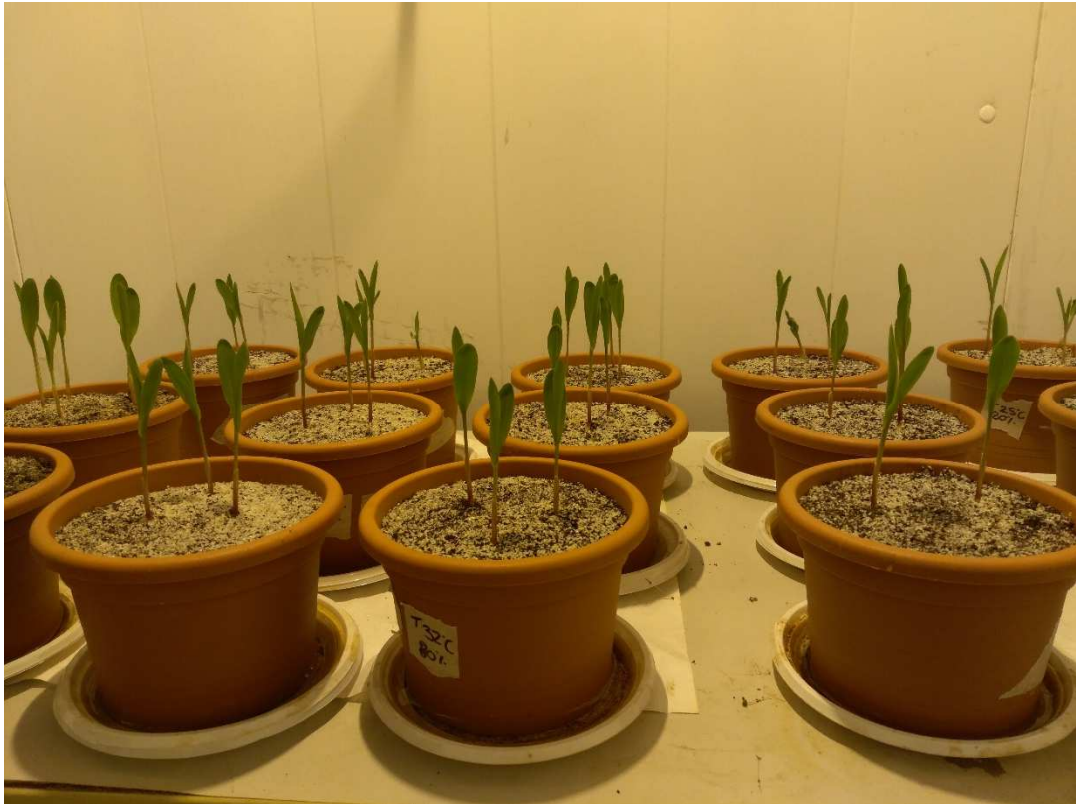
Considering the cooperation or the antagonism mechanisms of diverse root traits or phenes for the root phenotypes adaptations in diverse environments (York et al., 2013; Miguel et al., 2015; Rangarajan et al., 2018), the use of the multivariate approach for identifying the root architecture strategy in terms of functional traits and mechanisms, which operate independently or jointly, was raised (Bodner et al., 2013). In this respect, the maize root architecture responses to the single and combined stresses were evaluated with the sparse Partial Least Squares-Discriminant Analysis (sPLS-DA), a novel multivariate approach, which differently to the unsupervised methods (i.e., principal component analysis, the PCA) pointed out very satisfying predictive performances being able to select informative variables (Lê Cao et al., 2011).

Maize (*Zea mays* L.) is a major cereal crop and food for both humans and animals, widely used as resource for industrial use and for bio-energy production worldwide. It is highly productive under water suitable by irrigation, but water scarcity, high temperature, and their combination as observed in semi-arid environments caused a reduction on its yield and quality. Hence, the maize tolerance improvement to drought, heat, and their combination has become a challenge for the breeding programs (Chen et al., 2012).

## 3.2. Materials and Methods

### 3.2.1. Plant material and growth condition and treatments

The experiments were conducted at the University “Mediterranea” of Reggio Calabria, Italy. Maize seeds (*Zea mays* L.) (genotype KXB7554, provided by KWS Italia) were surface sterilized with 20% NaClO for 20 min, rinsed and then soaked in aerated deionized water at room temperature for 36h. Afterwards, five seeds were sown in each of sixteen sterilized pots (16 cm diameter x 12 cm height, Picture 3.1), which were filled with sand:soil mixture (70:30 v/v). The soil physico-chemical values were reported in Gelsomino et al. (2010).



**Picture 3.1** – Pots containing maize seedlings.

Then, the pots were randomly placed in the growth chamber at 25 °C, 70% relative humidity and  $350 \mu\text{mol m}^{-2} \text{s}^{-1}$  of photosynthetic photons flux density at plants' height (LI-190SA quantum sensor, Li-Cor, Lincoln, NE) with a 14 h photoperiod. The planted pots received, for two weeks, 200 mL of tap water every four days, necessary to compensate the water losses by evapotranspiration, as suggested by preliminary trials. After twelve days from seeding, five seedlings were thinned to one for each pot.

### 3.2.2. *Treatments*

From the third week, planting pots were subjected to stresses. In particular, eight pots were transferred to a second growth chamber with the same environmental conditions except for the temperature setted to 32 °C (Heat condition, H), whereas the remaining eight were left in the previous growth chamber at 25 °C. In four pots of both growth chambers were imposed drought stress (D) by the water withholding until to reach the theoretical fraction of 30% of field capacity (FC) measured by the gravimetric method. To the remaining pots, conversely, were ensured well-watered conditions in order to maintain the theoretical fraction of 80% FC. The desired percentage of FC was maintained by daily surface addition of water. Overall, the following treatments were imposed: drought (D) (25° and water at 30% FC), heat (H) (32 °C and water at 80% FC), combined (Comb) (32 °C and water at 30% FC) and control (Con) (25° and water at 80% FC).

### 3.2.3. *Morphological Root Analysis*

After 7 days of treatments, the seedlings were harvested and separated in shoot and root. The shoot fresh (ShFW, g) was measured and then the shoot dry weight (ShDW, g) were determined after oven-drying at 70 °C for 48 h.

After gently removing the adhering substrate, the root system was washed by tap water, paper-blotted and then stained with 0.1% toluidine blue solution for 5 min. Afterwards, it was divided into primary and seminal roots with their laterals and scanned at a resolution of 300 dpi (WinRhizo STD 1600, Instruments Régent Inc., Canada) with the WinRHIZO image analysis (WinRhizo STD 1600, Instruments Régent Inc., Canada). Then, the length (L, cm), surface area (SA, cm<sup>2</sup>) and volume (V, cm<sup>3</sup>) of the seminal (S) and primary axes (P) and seminal (SL) and primary lateral roots (PL) were measured by WinRhizo Pro v. 4.0 software package (Instruments Régent Inc., Canada). The number of both primary and seminal lateral roots was manually counted from the scanned image. The root and branching zone formation (RZF and BZF, respectively; cm) and the branching density (BD, n cm<sup>-1</sup>) were also measured and calculated, respectively, as reported by Drubvosky et al. (2012).



**Picture 3.2** – WinRHIZO image of primary root and its laterals.

The fresh and dry weights of the primary (PrFW, g and PrDW, g), seminal (SFW, g and SDW, g), primary lateral (PrLFW, g and PrLDW, g) and seminal lateral roots (SLFW, g and SLDW, g) were measured as reported above. The fresh (RFW, g) and dry weights (RDW, g) of root system were calculated as the sum of each root type, and the plant fresh (PFW, g) and dry weight (PDW, g) were calculated by the sum of the ShFW and RFW and the ShDW and RDW, respectively.

Finally, based on the above measurements, the root length ratio (RLR, root length/whole plant dry weight,  $\text{cm g}^{-1}$ ), root mass ratio (RMR, root dry weight/whole plant dry weight,  $\text{g g}^{-1}$ ), root fineness (RF, root length/root volume,  $\text{cm cm}^{-3}$ ) and root tissue density (RTD, root dry weight/root volume,  $\text{g cm}^{-3}$ ) were calculated for each root type. The functional

significance of these root parameters are reported on Ryser (1998). Further, according to Ryser and Lambers (1995), the RLR and its “morphological components” (RMR, RF, RTD) are related as follows:

$$RLR = RMR \times \frac{RF}{RTD} \quad (1)$$

#### 3.2.4. Statistical Analysis

All the experiment was arranged in a randomized complete design with four replicates per treatment.

All the root morphological parameters were firstly analyzed by one-way ANOVA followed by the Tukey’s test to compare the mean values among the treatments (Control, D, H and Comb) at  $p < 0.05$ .

To determine if the combination of the H and D stress exerted additive, synergistic or antagonistic impacts on root traits, we used the Bansal et al. method (2013) and, specifically, we compared the observed effects (Ob) to expected additive effects (Ex) for the plants exposed to the Comb treatment. The Ob effect sizes were calculated as the absolute value of:

$$Ob = \frac{(ob - \bar{x}Con)}{\bar{x}Con} \quad (2)$$

where ob is the measured trait value for each plant and treatment and  $\bar{x}Con$  is the mean trait value for the control plants.

The Ex additive effect sizes for the Comb treatment were defined in two steps by first determining and then summing the independent effects (Ind) of each treatment. The Ind effect sizes were calculated as the absolute value of:

$$Ind = \frac{(\bar{x}stress - \bar{x}Con)}{\bar{x}Con} \quad (3)$$

where  $\bar{x}stress$  is the mean trait values from each stress (H and D), and  $\bar{x}Con$  is the mean trait value for the control plants.

Then, the Ex additive effect size for the Comb treatment was calculated using a multiplicative risk model as suggested by Darling et al. (2010), i.e. the sum of two Ind effects minus their product. Finally, the Ex additive values for Comb treatment were compared to the actual Ob additive effects. In particular, we calculated a mean difference ( $\pm 95\%$  confidence interval) between the effect sizes of Ob and Ex for each seedling of the Comb treatment. When  $Ob-Ex > 0$  and the lower 95% confidence limit was greater than zero, the impact from the combination of both stressors was classified as synergistic. Conversely, the effects were antagonistic when the  $Ob-Ex < 0$  and the upper 95% confidence limit was less than zero, and additive when the 95% confidence interval crossed the zero line.

Furthermore, we analyzed the effects of the single and combined stresses on the entire dataset of the root morphological parameters using a multivariate approach with R statistical software 3.5 (R Core Team 2013). First, the differences among treatments were inferred through PERMANOVA multivariate analysis (999 permutations) using the package *vegan*. Pairwise comparisons among the groups were calculated using a custom script and correcting P values using the False Discovery Rate (FDR) method. In order to identify the root morphological key predictors that could constitute a root strategy among the treatments, we used a preliminary unsupervised (Principal Component Analysis, PCA) followed by the supervised analysis (Sparse Projection to Latent Structure-Discriminant Analysis, sPLS-DA) using the package *mixOmics* (Rohart et al., 2017). The *perf.plsda()* and *tune.splsda()* functions were used to predict the number of latent components (associated loading vectors) and the number of discriminants root traits for the sPLS-DA, respectively.

In particular, the optimal number of components was chosen by the averaged overall and balanced classification error rates with centroid distances over 50 repeats of 5-fold cross-validations (*perf.plsda()*). The optimal number of root traits for each component was then selected by the lowest average balanced classification error rate with centroids after tuning of the sPLS-DA model (*tune.plsda()*) using the selected number of components and 5-fold cross-validation with 50 repeats. Single samples were showed on a score plot and differentiated by treatments with color and 95% confidence ellipses. Furthermore, discriminant root traits were plotted according to their contribution weights to components 1, 2 and 3 of sPLS-DA and discriminated by treatments with color.



Finally, the Pearson product–moment correlations between the plant fresh and dry weight with the scores of the latent components determined by the sPLS-DA were run for verifying the root strategy for plant adaptation to the abiotic stress.

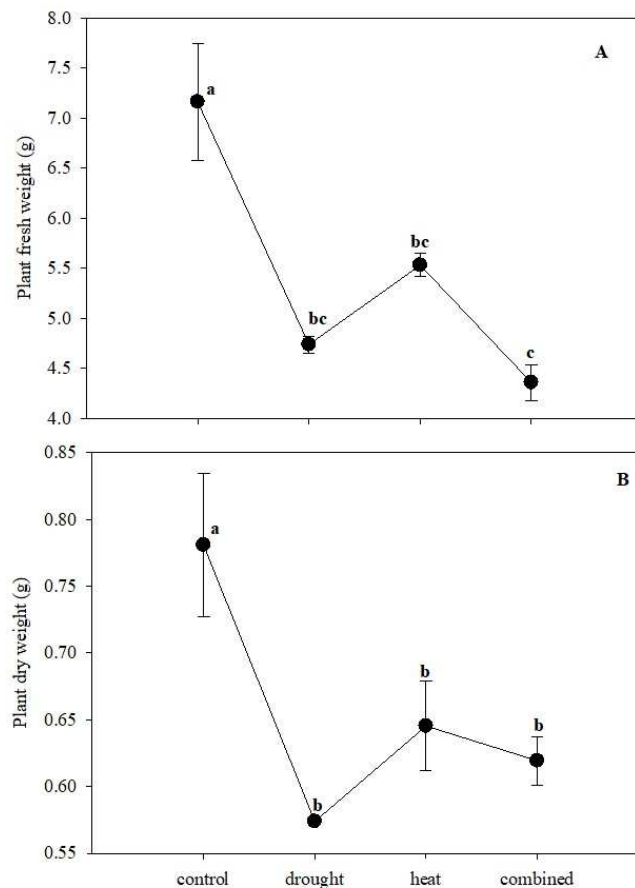
The statistical software was the SPSS Inc., V. 10.0, 2002 (SPSS Inc., Evanston, IL, USA).

### 3.3. Results

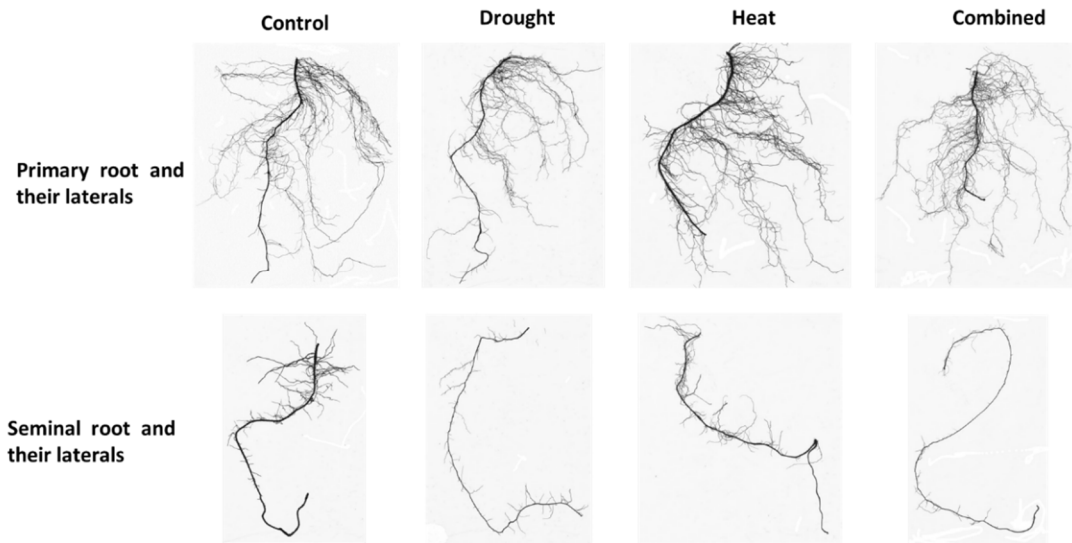
#### 3.3.1. Univariate analysis of the root morphological data

One-way ANOVA revealed that each stress (H and D), alone or in combination, significantly affected plant growth in terms of both fresh and dry weight. In particular, the combined stress reduced the fresh weight more than heat ones respect to the control but similarly to the drought stress. By contrast, all the stresses diminished the plant dry weight to at similar extent (Figure 3.1).

Figure 3.2 showed that the single root types of maize seedlings were also modified by single and combined abiotic stress.



**Figure 3.1** - The maize growth in terms of fresh (A) and dry weight (B) in presence of single (drought and heat stress) and combined stress. The bars represented the error standard (N = 4).



**Figure 3.2** - Primary and seminal roots and their laterals of maize seedlings exposed to drought, heat and their combination (Combined).

Out of the eleven traits of the primary roots, eight were significantly modified by stresses in comparison to the control (Table 3.1). The drought stress significantly increased the RLR, RMR, fineness, tissue density, branching zone reducing the branching density; conversely, the RLR and branching zone were not affected by heat stress, which, in turn, weakly increased and reduced the fineness and branching density, respectively (Table 3.1). The combined stress pattern was similar to the drought stress but with a sharply increase of the dry weight and, consequently, of both the RMR and tissue density (Table 3.1).

**Table 3.1** - Morphology of primary root of maize plants exposed to single (drought and heat) and combined stress (drought + heat).

Category	Parameters	Treatments			
		Control	Drought	Heat	Combined
<i>Biometric</i>	<b>Fresh weight(g)</b>	0.128 (0.008)a	0.131 (0.001) a	0.147 (0.001) a	0.162 (0.021) a
	<b>Dry weight (g)</b>	0.0111(0.0009)b	0.0116 (0.0006) b	0.0131(0.0003)b	0.0168 (0.0017) a
<i>Geometric</i>	<b>Length (cm)</b>	49 (1) a	71 (6) a	57 (4) a	66 (12) a
	<b>Surface area (cm<sup>2</sup>)</b>	9.460(0.009) a	10.669 (0.896) a	9.723 (0.587) a	10.415 (1.766) a
<i>Length components</i>	<b>RLR (cm g<sup>-1</sup>)</b>	63 (4) b	123 (12) a	83 (2) b	117 (15) a
	<b>RMR (g g<sup>-1</sup>)</b>	0.01381 (0.00016)c	0.01840 (0.00002) b	0.02004 (0.00051)b	0.02702 (0.00205) a
	<b>Fineness (cm cm<sup>-3</sup>)</b>	336 (11) c	531 (11) a	396 (8) b	500 (6) a
	<b>Tissue density (g cm<sup>-3</sup>)</b>	0.075 (0.007) c	0.097 (0.006) b	0.097 (0.003) b	0.117 (0.007) a
<i>Branching</i>	<b>Root zone formation (cm)</b>	9 (1) a,b	3 (1) b	9 (3) a	7 (1) a,b
	<b>Branching zone formation (cm)</b>	42 (2) b	65 (5) a	48 (1) a,b	64 (11) a
	<b>Branching density (n cm<sup>-1</sup>)</b>	4.961 (0.101) a	3.389 (0.051) c	4.276 (0.027) b	4.152 (0.284) b

Different letters along the rows indicated significant differences among the means at  $p < 0.05$  (Test of Tukey). The values within the brackets are the error standards ( $n = 4$ ).

The morphology of the seminal roots was lesser affected and not by all the stresses (Table 3.2). In particular, the drought stress reduced the fresh weight increasing the fineness only; the heat stress increased the fineness but, differently from the drought stress, raised the branching density (Table 3.2). Conversely, the combined stress did not modify the seminal root morphology respect to the control (Table 3.2).

**Table 3.2** - Morphology of seminal root of maize plants exposed to single (drought and heat) and combined stress (drought + heat).

Category	Parameters	Treatments			
		Control	Drought	Heat	Combined
<i>Biometric</i>	<b>Fresh weight (g)</b>	0.285 (0.031) a	0.172 (0.029)b	0.205(0.043)a,b	0.176 (0.018) b
	<b>Dry weight (g)</b>	0.021 (0.004) a	0.015 (0.003) a	0.014 (0.004) a	0.018(0.002)a
<i>Geometric</i>	<b>Length (cm)</b>	64 (7) a	64 (7) a	63 (8) a	51 (2) a
	<b>Surface area (cm<sup>2</sup>)</b>	11 (1) a	10 (1) a	12 (2) a	10 (1) a
<i>Length components</i>	<b>RLR(cm g<sup>-1</sup>)</b>	82 (13) a	103 (14) a	97 (14) a	83 (1) a
	<b>RMR (g g<sup>-1</sup>)</b>	0.027 (0.002) a	0.023 (0.002) a	0.027 (0.007) a	0.031(0.003)a
	<b>Fineness (cm cm<sup>-3</sup>)</b>	294 (47) b	463 (21) a	435 (55) a	362(24) a,b
	<b>Tissue density (g cm<sup>-3</sup>)</b>	0.094(0.007)a,b	0.064 (0.023) b	0.091 (0.003) a,b	0.124(0.001)a
<i>Branching</i>	<b>Root zone formation (cm)</b>	7 (1) a,b	8 (2) a,b	12 (3) a	6 (1) b
	<b>Branching zone formation (cm)</b>	54 (5) a	55 (6) a	57 (14) a	44 (3) a
	<b>Branching density (n cm<sup>-1</sup>)</b>	2.8 (0.1) b	2.9 (0.1) b	4.5 (0.4) a	3.0 (0.2) b

Different letters along the rows indicated significant differences among the means at  $p < 0.05$  (Test of Tukey). The values within the brackets are the error standards ( $n = 4$ ).

Seven traits of the primary lateral roots were differentially modified by the stress (Table 3.3). The RLR and fineness were increased by drought stress in comparison with the control, while the heat stress increased the fresh weight, length, surface area and RLR but not the fineness. The combined stress pointed out a significant and marked modification of the primary lateral root morphology increasing by 84%, 56%, 124%, 43% and 57% the length, surface area, RLR, fineness and average length, respectively (Table 3.3).

**Table 3.3** - Morphology of primary lateral root of maize plants exposed to single (drought and heat) and combined stress (drought + heat).

Category	Parameters	Treatments			
		Control	Drought	Heat	Combined
<i>Biometric</i>	<b>Fresh weight (g)</b>	0.212 (0.012) b	0.280 (0.047) a,b	0.315 (0.040) a	0.225 (0.001) a,b
	<b>Dry weight (g)</b>	0.022 (0.004) a	0.016 (0.001) a	0.021 (0.003) a	0.020 (0.001) a
<i>Geometric</i>	<b>Length (cm)</b>	557 (8) c	691 (35) b,c	757(82) b	1028 (33) a
	<b>Surface area (cm<sup>2</sup>)</b>	34.6 (0.7) b	37.2 (2.7) b	45.8 (4.8) a	53.3 (0.1) a
	<b>number (n)</b>	208 (16) a	225 (14) a	200 (2) a	247 (27) a
	<b>Average length (cm)</b>	2.860 (0.136) b	3.076 (0.039) b	3.640 (0.384) a,b	4.486 (0.578) a
<i>Length components</i>	<b>RLR (cm g<sup>-1</sup>)</b>	736 (41) c	1195 (63) b	1125 (75) b	1650 (90) a
	<b>RMR (g g<sup>-1</sup>)</b>	0.0324 (0.0079) a	0.0220 (0.0003) a	0.0308 (0.0031) a	0.0330(0.0016)a
	<b>Fineness (cm cm<sup>-3</sup>)</b>	3257 (44) c	4018 (56) b	3512 (76) c	4670 (288) a
	<b>Tissue density (g cm<sup>-3</sup>)</b>	0.134 (0.027) a	0.093 (0.005) a	0.097 (0.005) a	0.093 (0.006) a

Different letters along the rows indicated significant differences among the means at  $p < 0.05$  (Test of Tukey). The values within the brackets are the error standards ( $n = 4$ ).

The seminal lateral roots were affected by the stress in eight out of ten traits (Table 3.4). However, the single stress lesser influenced these root types which reduced the RMR (drought stress) and the dry weight and surface area (heat stress) in comparison to the control (Table 3.4). Conversely, the combined stress strongly affected the seminal lateral roots, reducing the dry weight, length, surface area and RMR and increasing the fineness (Table 3.4).

**Table 3.4** - Morphology of seminal lateral roots of maize plants exposed to single (drought and heat) and combined stress (drought + heat).

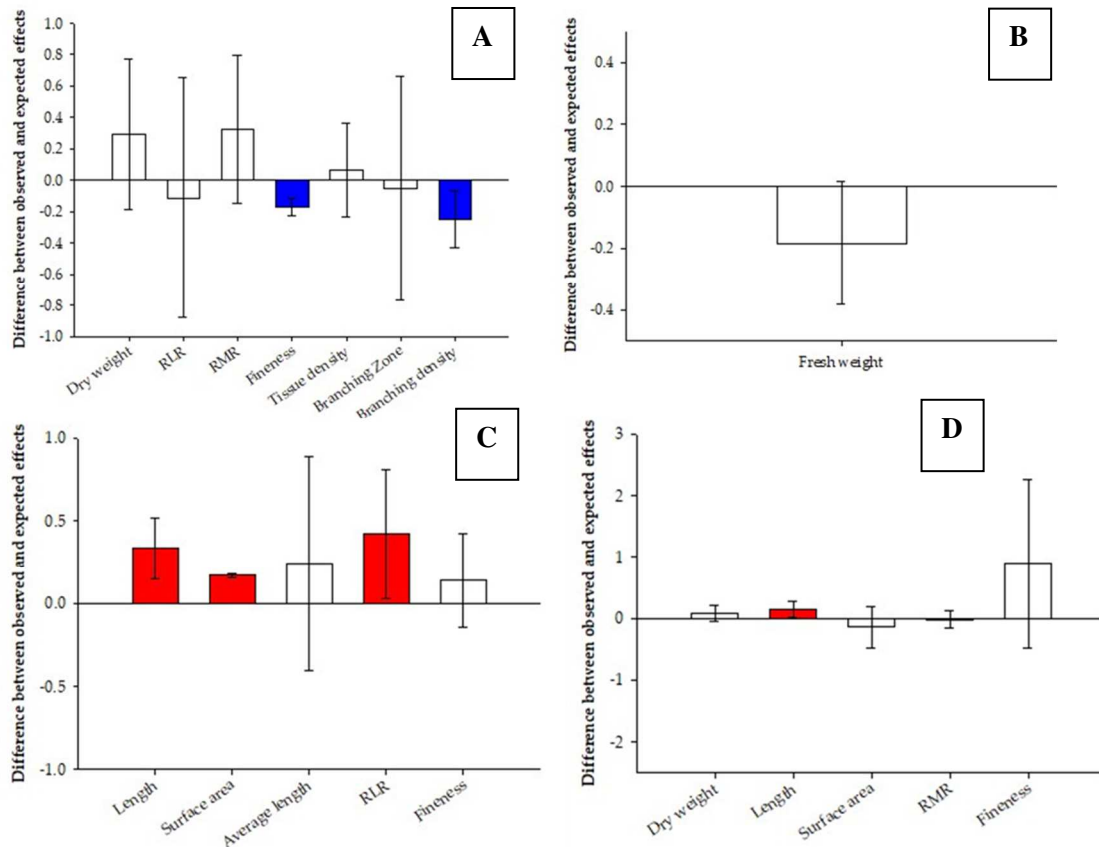
Category	Parameters	Treatments			
		Control	Drought	Heat	Combined
<i>Biometric</i>	<b>Fresh weight (g)</b>	0.0600(0.0114) a,b	0.0355 (0.0048) b	0.1323 (0.0459) a	0.0149(0.0002)b
	<b>Dry weight (g)</b>	0.0051 (0.0010) a	0.0035(0.0006)a,b	0.0025(0.0008) b	0.0013(0.0002)b
<i>Geometric</i>	<b>Length (cm)</b>	113 (7) a	104 (1) a,b	105 (13) a,b	79 (14) b
	<b>Surface area (cm<sup>2</sup>)</b>	8.5 (1.3) a	7.5 (0.1) a	3.7 (0.6) b	4.5 (0.9) b
	<b>number (n)</b>	149 (21) a,b	169 (18) a,b	202 (23) a	134 (5) b
	<b>Average length (cm)</b>	0.872 (0.151) a	0.707 (0.081) a	0.563 (0.136) a	0.530 (0.094) a
<i>Length components</i>	<b>RLR (cm g<sup>-1</sup>)</b>	147 (1) a,b	178 (2) a	151 (12) a,b	128 (19) b
	<b>RMR (g g<sup>-1</sup>)</b>	0.0066 (0.0010) a	0.0032 (0.0001) b	0.0041(0.0015)a,b	0.0021(0.0003)b
	<b>Fineness (cm cm<sup>-3</sup>)</b>	2728 (48) b	2416 (0) b	3630 (376) b	6283 (1176) a
	<b>Tissue density (g cm<sup>-3</sup>)</b>	0.095 (0.004) a	0.085 (0.015) a	0.101 (0.036) a	0.102 (0.022) a

Different letters along the rows indicated significative differences among the means at  $p < 0.05$  (Test of Tukey). The values within the brackets are the error standards ( $n = 4$ ).

### *3.3.2. Additive, synergistic and antagonistic effect of combined stress*

In order to evaluate the non-additive effects on the root traits significantly modified by the combined stress, we used the multiple risk model (Darling et al., 2010) that eluded the over-inflated response estimated by a simple additive model.

The response to the combined stress in maize root types were the result of the additive, synergistic and antagonistic effects of the single stress depending on the root types and traits (Figure 3.3). Indeed, a significant increase in the fineness and a decrease in the branching density in the primary roots under the combined stress (Table 3.1) was the result of an antagonistic effect of the single stress, whereas an additive effect was evoked for the enhance of dry weight, RLR, RMR, tissue density and branching zone (Figure 3.3A). The increase of the fresh weight in the seminal root, the only trait significantly modified by the combined stress (Table 3.2), was the result of the additive effect (Figure 3.3B). A synergistic effect could justify the increase of the length, surface area in the primary lateral roots exposed to the combined stress while an additive effect for the RLR, fineness and average length (Figure 3.3C). Finally, the only increase in the length of the seminal lateral roots in response to the combined stress was due to a synergistic effect, whereas an additive effect was responsible for the modifications of the dry weight, surface area, RMR and fineness (Figure 3.3D).



**Figure 3.3** - The combined impacts from drought and heat stress on selected traits of root primary (A), seminal (B), primary lateral (C) and seminal lateral (D) of maize plants. The combined impact of single stressors was estimated as synergist (red colour), additive (white colour) or antagonistic (blue colour) (greater than, equal to or less than expected effects, respectively, based on single stressor effect sizes). The vertical and error bars represent, respectively, the mean and the 95% confidence intervals of the overall effect size difference between the observed and expected additive effects from combined drought and heat on root traits of maize plants. The zero line represents the expected additive effects from combined stressors. When the means (and their 95% confidence limits) were higher than or less than the zero line, they were considered synergistic or antagonistic, respectively.

### 3.3.3. Root responses to the single and combined stress: a supervised analysis with PLS-DA.

A PERMANOVA analysis revealed that all the treatments determined a significant difference ( $p = 0.001$ ) in the root morphology as reported in Table 3.5. The Pairwise PERMANOVA comparisons suggested that the combined and drought stress but not the heat ones triggered significant difference respect to the control. Furthermore, the drought stress caused a different root morphology in comparison to both the heat and combined stress (Table 3.5).



**Table 3.5** - Results of the PERMANOVA analysis testing the root morphology of maize plants against the stress treatment.

<b>Factor</b>	<b>df</b>	<b>R<sup>2</sup></b>	<b>F</b>	<b>p</b>
Stress treatment	3	0.669	8.096	<0.001
Residual	12	0.331		
Total	15	1.000		

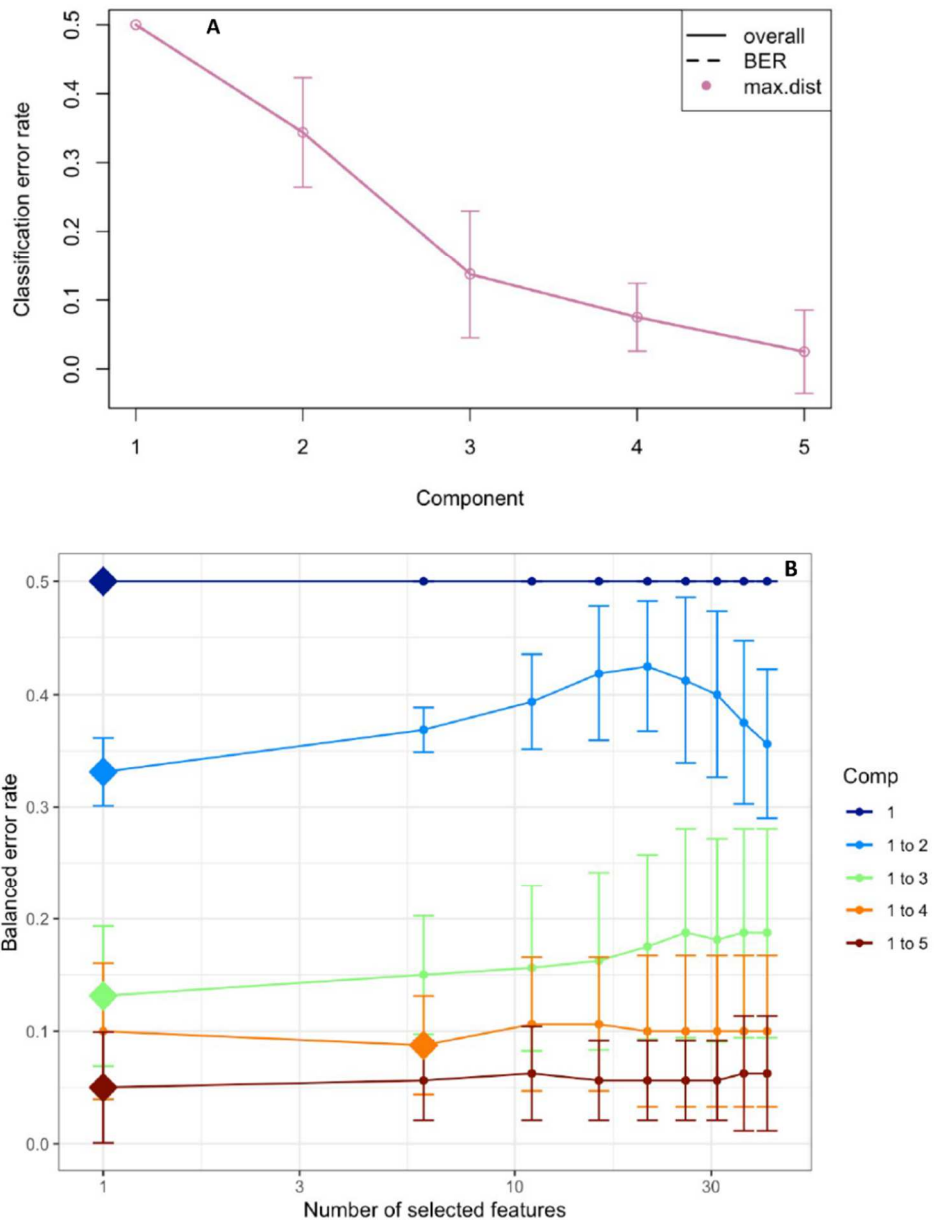
<b>Pairwise contrasts</b>				
	<b>F model</b>	<b>R<sup>2</sup></b>		<b>p</b>
C vs D	9.262	0.607		0.031
C vs H	3.878	0.393		0.053
C vs HD	15.926	0.726		0.027
D vs H	7.056	0.540		0.034
D vs HD	13.677	0.695		0.023
H vs HD	7.7520	0.564		0.054

In order to select informative and relevant root traits, we used the sparse Partial Least Squares-Discriminant Analysis (sPLSDA), a multivariate method characterized by a very satisfying predictive performance for the multiclass classification in plant biological studies (Lê Cao et al., 2011; Jiang et al., 2014).

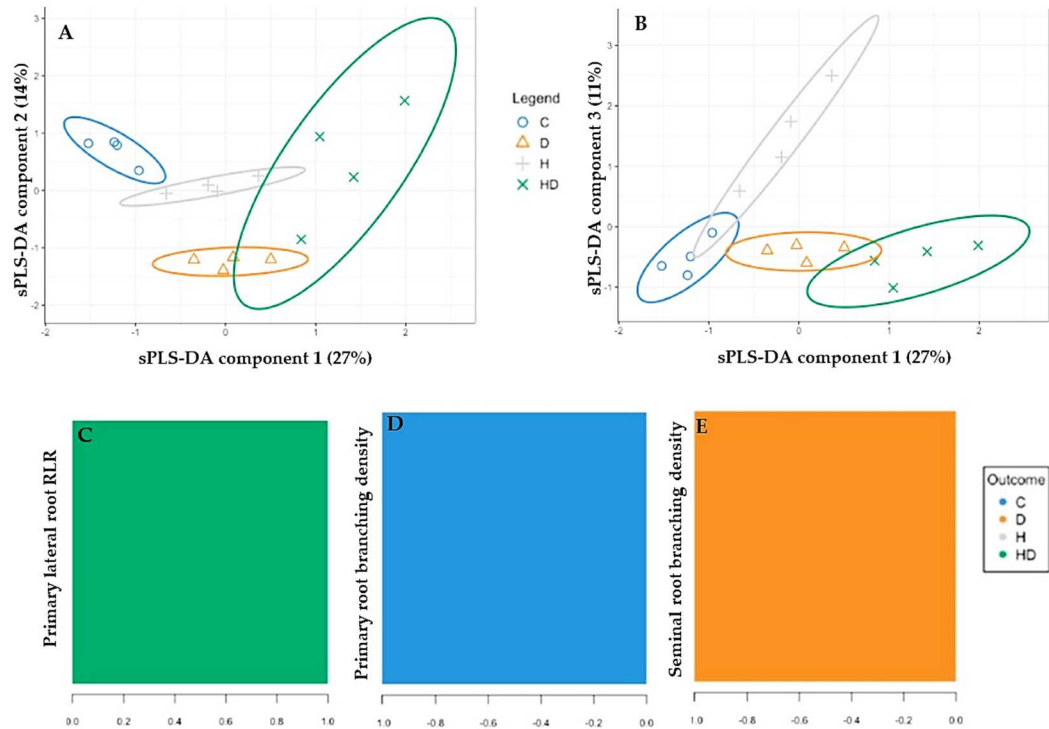
The performance step for the selection of the number of components suggested that 3 were enough to sharply reduce the balanced error rate (Figure 3.4A). Further, the final model obtained by tuning process pointed out that each component was constituted by one root morphological trait with a BER around 0.18 (Figure 3.4B). The sample plots on the three components permitted to visualize a sharply discrimination among the treatments with 52% of total explained variability split up by 27%, 14% and 11% for the first, second and third components, respectively (Figure 3.5A and 3.5B). In particular, plotting the first two components the combined and, at lesser extent, the drought stress were sharply separated from the control by the first component, whereas the second component discriminated the drought and, at lesser degree, the heat plants respect to the control (Figure 3.5A).

The addition of the third component permitted to separate the heat plants from the control ones (Figure 3.5B).

Figure 3.5C, 3.5D and 3.5E showed the selected root traits and relative loading weights for each component and the colour indicated the treatments for which the selected root traits has a maximal mean loading weight value. In particular, the root traits identified as performants for the sPLS-DA model were the primary lateral RLR in the combined stress, primary root branching density in the control and seminal root branching density in the drought stress for the first, second and third components, respectively (Figure 3.5C, 3.5D and 3.5E).



**Figure 3.4** - Choosing the number of components in sPLS-DA by performance test (A). Mean classification by overall and balanced error rate (5 cross-validation averaged 50 times) for each sPLS-DA component. Choosing the number of root traits for each sPLS-DA component by tuning test (B). Estimated classification balanced error rates for root morphology data set (5 cross-validations averaged 50 times) with respect to the number of selected root traits for the sparse exploratory approaches.



**Figure 3.5** - *sPLS-DA* sample plot for the different components using 95% confidence ellipses: (A) Component 1 vs. Component 2, (B) Component 1 vs. Component 3. Contribution plots by loading weights of the root traits selected for each *sPLS-DA* component: (C) Component 1, (D) Component 2, (E) Component 3.

### 3.4. Discussion

#### 3.4.1. Single stress determined different root type-related morphological responses

Drought as well as heat stress affected the primary root more than the other types. Indeed, differently from the seminal root, the primary improved its length both in term of absolute (LR) and relative value (RLR) but with different intensities: higher in drought than heat plants. The primary root is the very early dominant type in maize seedlings determining the early vigor and, by deepening in the subsoil strata, the survival under water deficit and higher air temperature (Hund et al., 2008; Landi et al., 1998). Further, the rooting depth is a phene very interesting as it confers drought tolerance/resistance in several plant species such as rice (Uga et al., 2013) and wheat (Wasson et al., 2012) improving the subsoil water capture. In order to evaluate the “morphological pattern” determining the increase in the RLR, trait that better than absolute length has been related to the plant’s potential for water and nutrient acquisition under stress conditions (Ryser, 1995), we estimated its “morphological components”, that is RMR, fineness and tissue density. In

according to Ryser and Lambers (1995), the higher RLR could be due to an increase of the RMR and/or fineness and/or decrease of the tissue density as explained by the equation 1. The results indicated that the increase of RLR in the primary root, under both single stress conditions, was due to a concomitant enhancement of the biomass allocation (RMR) and fineness, accompanied by a higher RTD trait positively correlated with the degree of lignification and cell wall thickness (Ciamporova et al., 1998; Wahl et al., 2000; Hummel et al., 2007). Hence, the maize seedlings under both the drought and heat stress, increased the length of the primary root, which appeared more fineness and, at the same time, thickness, useful traits to penetrate the hard soil layers under water stress (Chimungu et al., 2015). To note that, the RLR of the primary root under the drought stress was also higher than to heat ones and this difference was due to a higher fineness rather than biomass allocation variation (Table 3.1). Extensive transcriptomic and proteomic studies revealed specific transcripts and proteins related with cell wall extension properties in the primary root of maize seedlings exposed to the water stress (see reference in Yamaguchi et al., 2010; Voothuluru et al., 2020). Therefore, according to our results, the drought stress could induced a different molecular mechanism respect to the heat one, which differently regulated the elongation of the primary roots as observed in this study.

The seminal root axes were the lesser modified by the single stresses, which determined an increase in their fineness only (Table 3.2). The maize seminal roots responded to the drought and heat stress by reducing their emergence angle and length that resulted in the soil deepening (Hund et al., 2008; Lynch, 2013). These results were not observed in this study, probably, for the pot volume that limited the soil exploration.

Besides the primary and seminal root axes, the laterals, as post-embryonic roots arising from these axes, played an important role for the water acquisition from the soil allowing an improvement of the soil exploration due to their higher surface to volume ratio (Yu et al., 2019). Differently to the seminal lateral roots, the primary laterals were more modified by both single stresses: the drought-stressed plant pointed out similar lateral length to the heat plants but with a higher fineness (Table 3.3 and 3.4). Again, the trait “fineness” was differently regulated by drought respect

to the heat stress allowing a higher surface soil contact of the laterals, fundamental for water uptake. To note that, although the length of the primary lateral roots was increased, the branching density was decreased in both stressed plants. This reduction, associated with an increase of length the primary lateral roots constituted an important root “phenotypic pattern”, which improved drought resistance in maize plants by reducing both the intra-plant competition for the photosynthates and the capture of mobile soil resources such as water (Zhan et al., 2015).

#### *3.4.2. Combined stress caused different root type-related morphological response respect to the single stress with non-additive effects*

The recent studies on combined stress, such as drought and heat, were focused on the morpho-physiological and molecular responses of plant aerial traits such as yield and quality (Prasad et al., 2011; Liu et al., 2019), plant growth (Vile et al., 2012), foliar chemistry (Oriani et al., 2019) and leaf physiology (Hussain et al., 2019; Tricker et al., 2018). Conversely, very few studies have focused on the root system responses to combined stress and no information are available for the different root types. Here, for the first time, the responses of the single root types of maize seedlings to the combined stress were reported. It induced a similar morphological pattern to the single stresses resembling those of the drought and heat stress for the primary and seminal root axes and those of the heat for the primary lateral roots only. Conversely, the morphology of seminal lateral roots of the combined stress was completely different from that of the single stresses: length and biomass were sharply inhibited. Probably, the water scarcity exacerbated by the heat rendered not useful the exploration and resource exploitation of the topsoil strata; hence, the maize plants engaged their internal resource towards the root classes, such as the primary and its laterals, mainly localized in the subsoil to reach the water reserve.

Analyzing the pattern of the combined stress on the root traits is interesting to understand their additive (equal to the sum of the single-stress effects), synergistic (higher than expected) or antagonistic (lower than expected) effects. Besides a useful information on morphological pattern, these could provide a hypothesis on the signaling pathways and molecular mechanisms underlying the plant strategy in

presence of simultaneous stress. For example, the synergistic effect of NaCl and ABA in *Arabidopsis thaliana* was induced by the expression of *Responsive-to-Dehydration 29A (RD29A)* that cannot be explained by the sum of responses to the single stresses (Lee et al., 2016). Furthermore, the antagonistic effect of drought and insect herbivory could be explained by synergistic interactions between JA and ABA signaling (Nguyen et al., 2016). In our study, the combined stress produced mostly additive effects, but synergistic and antagonistic effects for specific trait and root types were also observed (Figure 3.3) suggesting, for these latter, an unique molecular and signaling interaction mechanisms. These results were below discussed for their ecological role, and plant fitness in environment characterized by co-occurring drought and heat stress. Differently to the seminal and their lateral roots, primary lateral root traits were mostly synergized whereas those related to the primary root axes were antagonized (Figure 3.3). Why non-additive effects (synergistic and antagonistic ones) were observed in the primary and their lateral respect to the seminal roots? Their different locations within the soil environment that caused diverse efficiency for the resource acquisition could be hypothesized. Indeed, the primary and their lateral roots are placed in the water-rich subsoil strata making these root types more important under water scarcity due to lesser rainfall/irrigation, further aggravated by a simultaneous heat stress. The root deepening during drought stress was revealed in maize plants (Hund et al., 2008; Lynch, 2013; Wasson et al., 2012). However, our results pointed out that combined stress antagonized the fineness and the branching density of the primary roots (Figure 3.3A). Probably, the thicker primary roots could be more useful for deeper penetration in soil compacted caused by both drought and heat stress (Bengough et al., 2011; Nosalewicz et al., 2014). At the same time, the reduction of the branching density of the primary root axes along with the root deepening is a useful strategy for the root adaptation in water scarcity environments as observed by (Lynch, 2018). Next to the antagonistic effects in the primary roots, the synergistic effects were observed on the length, surface area and RLR traits of the primary lateral roots (Figure 3.3C). Sustained by the soil penetration of the thicker primary roots, the longer laterals with higher surface contacts with soil could increase the exploration

of the subsoil strata characterized by higher soil moisture under combined drought and heat stress.

*3.4.3. Primary lateral RLR, primary and seminal root branching density discriminated the root phenotypes in drought and heat stress and their combination.*

Currently, for understanding the root strategy for the plant adaptation to abiotic stress, the multivariate analysis were applied. This suitable method allowed to identify the efficient and meaningful “multi-trait classifiers” of the root systems (Bodner et al., 2013) and the detection of the functional root traits and mechanisms, which operate independently or jointly. For example, the principal component analysis (PCA) permitted to identify the root ideotypes in drought stress for the peanut landraces (Tella et al., 2014), sugar beet genotypes (Romano et al., 2013), bean landraces (Abenavoli et al., 2016) and soybean genotypes (Zuffo et al., 2020). Conversely, the sparse PLS-DA, a supervised technique, made efficient the trait selection and dimension reduction simultaneously by imposing sparsity to the solution (Chung et al., 2010), making it a novel approach to investigate high dimensional and redundant root data.

The sPLS-DA clearly separated the root phenotypes of the combined and, to a lesser degree, the drought stress from that of the control by component 1 (Figure 3.5A). This component showed high positive loading for the RLR of the primary lateral roots and the combined stress was the group for which the selected variable had a maximal mean value. Hence, the root phenotypes of the combined stress were different from that of the control plants as firstly suggested by Permanova analysis and the RLR of the primary lateral roots was the triggering root trait as pointed out from sPLS-DA. As already described, this trait, which expresses the relative investment of the plant in root length, was strictly related to the soil resource availability and hence for their capture (Ryser and Lambers, 1995; Ryser et al., 2000), depended on the nutrient availability (Sorgonà et al., 2007; Freschet et al., 2015) and drought stress (Romano et al., 2013). The components 2 and 3 separated the root phenotypes of the drought stress plants from that of the control and heat ones, respectively (Figure 3.5A and 3.5B). The primary and seminal root branching densities were the root traits with a maximal negative mean value for the control



and drought group, respectively confirming that the inter-branch length could play a fundamental role in the drought stress condition (Zhan et al., 2015; Lynch, 2018).

### **3.5. Conclusions**

The present study pointed out, for the first time, the responses of different root types to the combined abiotic stress in maize seedlings.

The single and combined stress caused fine variations in growth and morphology of the single root types in the maize root phenotype. The seminal roots were the least modified root types, whereas the primary and their lateral roots were stimulated with an increase of the length together with higher biomass allocation and fineness by the single stress conditions. The combined stress determined similar effects but associated with a specific inhibition of growth and morphology of the seminal lateral roots. Non-additive effects (synergistic and antagonistic) were only observed in the primary and their lateral roots under the combined stress suggesting that single molecular mechanisms could be underlying their growth and morphological responses. Further, the results of sPLS-DA supported the idea that the primary and their lateral roots could be the “root type” with an important role for the adaptation to the combined abiotic stress.

## **Chapter 4: Single and combined abiotic stressors affect maize rhizosphere bacterial microbiota**

*Adapted from: Rosa Vescio et al. Single and combined abiotic stressors affect maize rhizosphere bacterial microbiota. Rhizosphere 2021, 17(1). <https://doi.org/10.1016/j.rhisph.2021.100318>*

### **Abstract**

Rhizosphere microbiomes are influenced by abiotic stresses, but we know a little about their response to combinations of stresses. In this study we tested: (i) if drought and heat stress influence the maize rhizosphere microbial community; (ii) if the combination of drought and heat has a different outcome compared to a single stress; (iii) if rhizosphere microbiota clusters according to root class and root zone. We setup a microcosm system using maize as model plant. We exposed plants to drought, heat stress and their combination, and used 16S amplicon-sequencing to reconstruct bacterial communities of different root classes (crown and primary) and root zones (apical, sub-apical and basal). We found both drought and heat affect the structure of rhizosphere bacterial communities. The combination of these stressors also influenced the structure of rhizosphere microbial communities, but this effect did not differ compared to the single stresses. Interestingly, we found differences in microbial communities inhabiting the rhizosphere of crown and primary roots in the control treatment, but this difference disappeared once stresses were applied. Stress also lead to an increased abundance of beneficial organisms.

**Keywords:** drought; heat; root class; root zone; 16S rRNA; metabarcoding

#### 4.1. Introduction

Abiotic stressors are a major limiting factor for crop production worldwide (Mantri *et al.* 2012; Wien 2020). Variation in water availability and increasing of global air temperature are major abiotic stresses posed by climate changes (IPCC 2019). As result, the increase in air temperature and drought events are likely to become more frequent and severe (Spinoni *et al.* 2018). Recent development in plant microbiome research highlighted the potential of plant-associated microbial communities in alleviating the negative effects of changes in water availability and air temperatures (Hussain, Mehnaz and Siddique 2018; Naylor and Coleman-Derr 2018; Saikkonen, Nissinen and Helander 2020).

Plants play an active role in selecting their own microbiota and can recruit beneficial organisms in response to stresses, especially in the rhizosphere (Berendsen, Pieterse and Bakker 2012; Turner, James and Poole 2013; Rolfe, Griffiths and Ton 2019). Both drought (Naylor and Coleman-Derr 2018) and high air temperatures (van der Voort *et al.* 2016) can produce a change in the structure of rhizosphere microbiomes. For example, the rhizosphere of plants under drought stress is enriched with plant growth promoting bacteria mainly belonging to the classes Actinobacteria and Firmicutes (Marasco *et al.* 2012; Edwards *et al.* 2018; Fitzpatrick *et al.* 2018; Xu *et al.* 2018; Simmons *et al.* 2020). While drought can influence the rhizosphere microbiome directly (via reduction of available water) and indirectly (via the host plant), air temperature only influences the rhizosphere microbiome indirectly (via the host plant). These two different pathways are likely to produce big differences in rhizosphere responses; however, to date, the differential response of rhizosphere microbiomes to heat and water stress has not yet been determined. Furthermore, the combination of heat and water stress commonly occurs in field conditions, and this has an additive detrimental effect on plant growth (Pandey *et al.* 2017). However, the combination of drought and heat on rhizosphere microbiomes has yet to be examined.

The plant root system comprises different root classes, usually classified accordingly to their ontogenesis (i.e. primary, nodal, lateral), each one characterized by distinct developmental, physiological and functional signatures (Waisel and Eshel 2002; Hodge *et al.* 2009; Tai *et al.* 2016), and different responses to

environmental stresses determining a large within-root phenotypic plasticity. For example, different root classes vary in their response to nutrient deficiency (Rubio, Sorgonà and Lynch 2004; Sorgonà, Abenavoli and Cacco 2005; Sorgonà *et al.* 2007), allelopathy (Abenavoli *et al.* 2004; Lupini *et al.* 2016) and drought (Romano *et al.* 2013; Abenavoli *et al.* 2016). In addition to this diversification among root classes, roots show differences in functionality in different root zones (Rubio, Sorgonà and Lynch 2004; Sorgonà *et al.* 2010, 2011). Along the root axis, morphological and functional differences in root architecture reflect the relationship between roots and their environment, with variation in nutrient uptake, water transport, carbon exudation, proton/hydroxyl excretion and respiration (Hodge *et al.* 2009). Although the physiological and morphological differences between root classes and in different root zones are widely reported, their microbiome remains currently little explored.

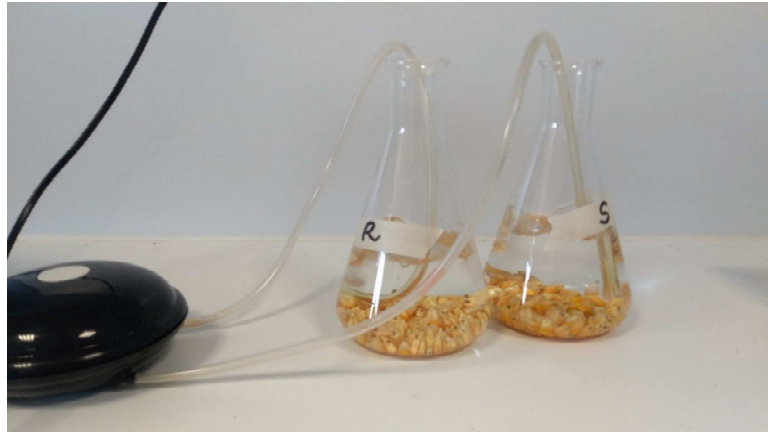
In this study, we exposed maize plants to drought and heated air, alone and combined, and we characterized the rhizosphere bacterial community in three root zones (apical, subapical and basal) for two different root classes (primary and crown). We hypothesize that drought and increased air temperatures influence the composition of rhizosphere bacterial microbiome differently due to the difference in direct and indirect influences on bacterial microbiome composition, and this response will vary with root class and zone. We also hypothesize that the combination of drought and heat will produce a unique rhizosphere microbiome signature.

## **4.2. Material and Methods**

### *4.2.1. Study system*

Soil was collected from the top 10cm layer of an uncultivated field located at the *information hidden for double-blind peer-review (coordinates hidden for double-blind peer-review* Table S4.1), and coarsely sieved (4mm mesh). Pots were filled with a mix of 1 part collected field soil and 2 parts of quartz sand (Ø 1-2 mm, Croci Trading Company s.r.l., Italy, autoclaved for 3 hours at 121°C, allowed to cool overnight and then other 3 hours at 121°C). Maize seeds (genotype KXB7554, provided by KWS Italia) were surface sterilized with 20% bleach solution for 20

minutes and rinsed with deionized water 5 times. Seed germination was synchronized by soaking seeds in deionized water for 24h (Picture 4.1) and providing air flow through an air pump. We selected maize as model species because: (i) it is an economically important crop and model species for research; (ii) it has been used as model for abiotic stress research; (iii) it has well-defined root classes and zones.



**Picture 4.1** – Maize seeds in deionized water, soaked for 24h.

#### 4.2.2. Experimental design and sample collection

We conducted an experiment testing the effects of two levels of water availability nested in two levels of air temperature on the diversity and composition of the rhizosphere microbiome. Maize plants (*Zea mays* L.) were exposed to two levels of air temperature (25°C and 32°C), and two levels of water availability (30% and 80% of soil field capacity, corresponding to a severe drought and no drought). The experiment was split into two blocks to account for the variability introduced by working with two climatic chambers. Each block contained 3 replicates and were temporally distinct: once the first block was harvested the second block was set up, and the air temperature treatments were inverted between the two chambers. The entire experiment yielded a total of 4 treatments (2 water availability treatments × 2 air temperature treatments) × 6 (replicates) 24 plants. Pairs of plants exposed to the same treatment in the two different blocks were grouped together, and for both we collected two root classes (primary and crown root) that were divided into three zones (apical, sub-apical and basal) yielding a total of 72 samples.

To start each block, after 24 hours of soaking, 5 maize seeds were sown in 1L pots filled with the soil mix. Three replicates of each treatment were then randomly distributed within two climatic chambers both initially set at 25°C, 70% relative humidity and a 14:10 light:dark photoperiod and left to grow for 2 weeks. During this timeframe each pot was weighted every two days and watered to guarantee a minimum of 80% of soil field capacity. Fifteen days after sowing, plants were exposed to the 30% field capacity and 32°C air temperature treatments for 7 days. Heat stress was applied by increasing the air temperature to 32°C (Hussain et al., 2019) in one climatic chamber. Drought stress was imposed at 30% soil field capacity (Hussain et al., 2019) by reducing water availability from 80% to 30% of the pot capacity (determined by weighing the pots) (Anderson, et al., 2018) for plants in both climatic chambers. With preliminary trials, we determined the amount of water necessary to reach 30% and 80% of field capacity on the same soil used for this experiment. During the experiment, we maintained 30% or 80% of field capacity (according to the treatment) by weighting pots twice a day, calculating the difference in weight compared to our target (either 30% or 80% of field capacity), and compensating this difference with distilled water.

At the end of stress exposure, we measured photosynthetic rate and stomatal conductance to confirm that treated plants were actually stressed (see Supplementary material). Plants were then removed from pots (Picture 4.2) and gently shaken to remove bulk soil.



**Picture 4.2** – Root and bulk soil.

The root system was divided into primary and crown roots. Each root class was then divided into three zones: apical (portion from the root tip to the first lateral root), subapical (following the apical portion, same length, but including lateral roots) and basal (same length as the others but excised starting from stem). To extract rhizosphere soil, root sections were put in a 2ml tube containing 300  $\mu$ l of lysis buffer (10 mM Tris, 100 mM NaCl, 10 mM EDTA, 0.5% SDS), and vortexed at maximum speed for 2 minutes (McPherson *et al.* 2018). Roots were then discarded, and rhizosphere samples were stored at  $-80^{\circ}\text{C}$  before being processed using 16S rRNA metabarcoding procedures (Abdelfattah *et al.* 2018).

#### *4.2.3. DNA extraction and library preparation*

Samples were homogenized with the lysis buffer using two 1 mm $\emptyset$  stainless steel beads per tube, with the aid of a bead mill homogenizer set at 30 Hz for 2 min (TissueLyzer II, Qiagen). Total DNA was extracted using a phenol-chloroform protocol. DNA quality and quantity were checked with a Nanodrop 2000 instrument

(Thermo Fisher Scientific Inc., USA). DNA was extracted also from non-template control samples, where experimental samples were replaced by 100  $\mu$ l of nuclease-free water, in order to account for contamination of reagents or instruments.

PCR amplifications were performed in a reaction mixture containing  $\sim$ 20ng of template DNA, 1X KAPA HiFi HotStart ReadyMix (KAPA Biosystems, USA), 0.5  $\mu$ M of 515F and 806R primers (Aprill *et al.* 2015; Parada, Needham and Fuhrman 2016), and nuclease free water was added to create a final volume of 12.5  $\mu$ L. Amplifications were performed in a Mastercycler Ep Gradient S (Eppendorf, Germany) with an initial denaturation at 94°C for 3 minutes, followed by 35 cycles of denaturation at 94°C for 45 seconds, 50°C for 60 seconds, 72°C for 90 seconds and a final extension step at 72 °C for 10 minutes. All PCR reactions included three non-template control wells, where DNA was replaced with nuclease-free water to check for contamination of PCR reagents. PCR products were inspected for correct amplification on 1% agarose gel. PCR products were then purified with Agencourt AMPure XP kit (Beckman and Coulter, Brea, CA, USA), following the manufacturer's instruction. A short-run PCR was performed on purified samples in order to include the Illumina i7 and i5 indices using the producer's protocol (Nextera XT, Illumina, San Diego, CA, USA). Amplicons were purified again with Agencourt AMPure XP kit as reported above and their concentration was quantified using a Qubit 3.0 fluorometer (Thermo Fisher Scientific Inc., USA). Samples were pooled together at equimolar rations and sequenced with an Illumina MiSeq platform (Illumina, San Diego, CA, USA) using the 300PE chemistry. No non-template control sample yielded a band after PCR, and the few reads retrieved from sequencing were lost after quality filtering.

#### *4.2.4. Raw reads processing*

De-multiplexed forward and reverse reads were merged using the PEAR 0.9.1 algorithm using default parameters (Zhang *et al.*, 2014). Data handling was carried out using QIIME 1.9.1 (Caporaso *et al.*, 2012), and we quality-filtered reads using default parameters, discarded chimeric sequences and binned OTUs with VSEARCH 2.14.2 (Rognes *et al.*, 2016). OTUs coming from amplification of chloroplast DNA were discarded from the downstream analyses. Taxonomy was



assigned to each OTU through the BLAST method by querying the SILVA database (v. 132) (Quast et al., 2012).

#### 4.2.5. Data analysis

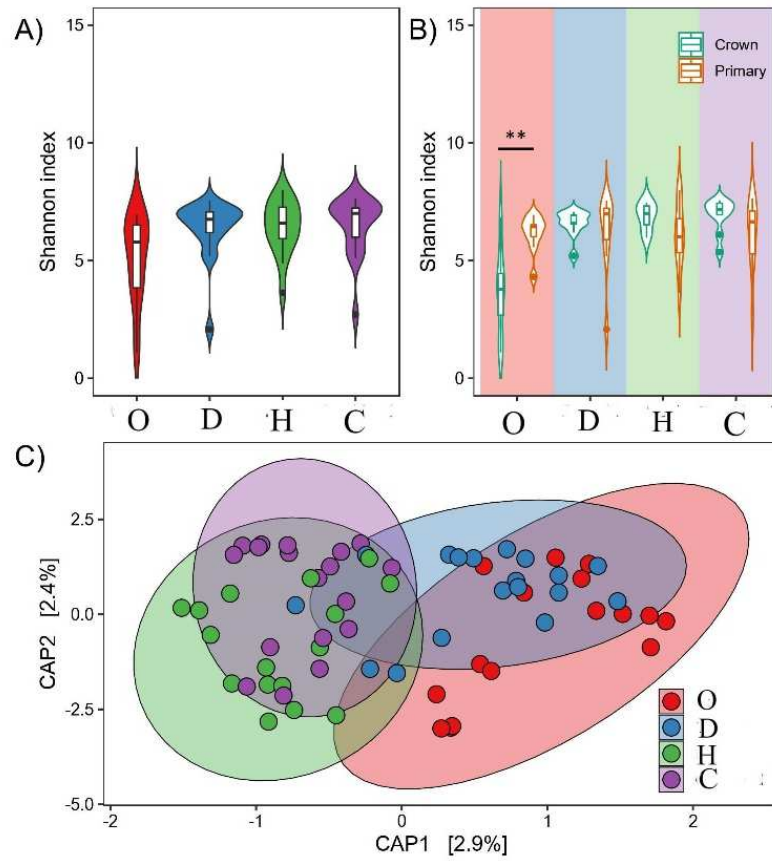
Data analysis was performed using R statistical software 3.5 (R Core Team 2013) with the package *phyloseq* (McMurdie and Holmes, 2013). Shannon index was calculated using the package *vegan* (Dixon 2003), and comparison among groups was performed by fitting a linear mixed-effect model to account for the nested design, specifying the formula `treatment * root_class * root_zone * (1|root_class/root_zone) + (1|temperature/water)`. Models were fit using the *lmer()* function under the *lme4* package (Bates *et al.* 2015) and the package *emmeans* was used to infer pairwise contrasts (corrected using False Discovery Rate, FDR).

Furthermore, we studied the effects of the same factors on the structure of the microbial communities using a multivariate approach. Distances between pairs of samples, in terms of community composition, were calculated using a Bray-Curtis matrix, and then visualized using Canonical Analysis of Principal Coordinates (CAP) procedure. Differences between groups were inferred through PERMANOVA multivariate analysis (999 permutations, stratified using the factors “root\_class/root\_zone” and “temperature/water”). Pairwise comparisons were calculated using a custom script and correcting *P* values using the FDR method. We used the R package *DESeq2* (Love, Huber and Anders 2014) to search for OTUs differentially abundant between each treatment groups and the control. First, we built a model using *treatment*, *root class* and *root zone* as factors, and then we extracted the appropriate contrasts (Stress/Control) for each treatment group. OTUs significantly more abundant in the stressed group were identified by filtering the contrast table by  $\log_2\text{FoldChange} > 1$  and  $P_{\text{adj}} < 0.05$ .

### 4.3. Results

The linear mixed-effects model analysis revealed that microbial rhizosphere Shannon diversity only varied significantly with the interaction between treatment and root class (Table 4.1). Specifically, primary roots had a higher diversity than

crown roots ( $P=0.003$ , Figure 4.1B), but this difference disappeared with reduced water availability and increased temperature ( $P>0.05$ , Figure 4.1B).



**Figure 4.1.** Comparison of Shannon diversity index between (A) treatments and (B) root classes within treatments. (C) CAP (Canonical Analysis of Principal coordinates) ordination using a Bray-Curtis distance matrix of samples.  $**P=0.003$ .

**Table 4.1.** Results from the mixed-effect linear model testing the Shannon diversity index against treatment, root class, root zone and their interactions.

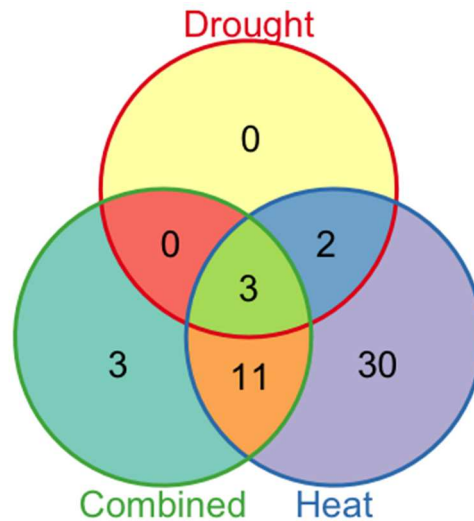
<b>Factor</b>	<b>df</b>	<b>F</b>	<b>P</b>
Treatment (T)	3	2.379	0.497
Root class (RC)	1	0.001	0.967
Root zone (RZ)	2	0.028	0.985
T x RC	3	16.171	<b>0.001</b>
T x RZ	6	5.118	0.528
RC x RZ	2	0.994	0.608
T x RC x RZ	6	5.874	0.437

We used a multivariate approach (PERMANOVA) to test the influence of treatments, root class, and root zone on the structure of microbial communities, and we found similar results to microbial diversity. We found a significant effect of treatment ( $P=0.005$ ) and the interaction between treatment and root class ( $P<0.001$ ) on the structure of rhizosphere microbiome in our experiment (Table 4.2). In both primary and crown roots, we consistently found that the microbial community of stressed plants was different from control ones and, also, between drought and heat plants (Table S4.2 and S4.3). However, the rhizosphere microbial community of plants exposed to both single stressors (drought and heat) was not different from the one of plant exposed to their combination (Tables S4.2 and S4.3). Furthermore, for each treatment group, we tested for differences between root classes. We found that the microbiota of primary and crown roots was different in control ( $P=0.001$ ), but not in any treatment ( $P>0.05$ , Table S4.4).

**Table 4.2.** Results from PERMANOVA analysis testing the effects of treatment, root class, root zone and their interactions on the structure of maize rhizosphere bacterial communities.

<b>Factor</b>	<b>df</b>	<b>R<sup>2</sup></b>	<b>F</b>	<b>P</b>
Treatment (T)	3	0.065	1.616	<b>0.005</b>
Root type (RC)	1	0.012	0.953	0.491
Root zone (RZ)	2	0.026	0.987	0.451
T x RC	3	0.091	2.267	<b>0.001</b>
T x RZ	6	0.079	0.99	0.501
RC x RZ	2	0.036	1.358	0.065
T x RC x RZ	6	0.095	1.184	0.06

Given the differential response of rhizosphere microbiome and the increased bacterial diversity as response to plant stress, we took a closer look to the bacterial taxa that were significantly more abundant in stressed plant compared to the control group (Figure 4.2). As general response among the three stresses, we found an increase of three bacterial groups: *Solirubrobacter*, *Massilia*, *Agrobacterium*. While we did not found a specific response to the drought treatment, the treatment with heated air increased the abundance of: *Blastococcus*, *Bosea* (2 OTUs), *Burkholderia*, *Caulobacter* (3 OTUs), *Conexibacter*, *Dactylosporangium*, *Flavisolibacter*, *Leptothrix*, *Massilia* (5 OTUs), *Mesorhizobium*, *Micromonospora* (3 OTUs), *Niastella*, *Phenylbacterium*, *Pseudomonas*, *Segetibacterium*, *Solirubrobacter* and 5 unidentified OTUs. On the other hand, when comparing the plant exposed to combined stress to the control, we found a higher abundance of *Rhizobacter*, and 2 unidentified OTUs. Furthermore, 11 OTUs were more abundant in both heat and combined stress treatments: *Acidovorax*, *Bryobacter*, *Massilia*, *Paraburkholderia*, *Pelomonas*, *Rubrobacter*, *Sphingomonas* (2 OTUs), and 3 unidentified OTUs. Two OTUs had a higher abundance in both heat and drought treatments: *Pelomonas* and *Paraburkholderia*.



**Figure 4.2.** Venn diagram representing the number of OTUs (Operational Taxonomic Units) differentially more abundant as response to specific stressors compared to the control group.

#### 4.4. Discussion

Here, we show that drought and heat stresses induce changes on maize rhizosphere bacterial microbiome. Previous studies, indeed, revealed the effect of various environmental stress on rhizosphere microbiome: drought (Marschner et al,2005; Cherif et al. 2015; Nuccio et al., 2016; Naylor et al., 2017; Santos-Medellín et al., 2017; Fitzpatrick et al., 2018; Timm et al., 2018), metal-deficiency (Timm et al., 2018), shading (Timm et al., 2018), and nitrogen-deficiency (Allison and Martiny, 2008; Roesch et al., 2008; Zhu et al., 2016). Our study supports the effects of plant stressors on rhizosphere microbial assemblages. Furthermore, we tested, for the first time, whether the combination of drought and heat stress produces a different outcome on the rhizosphere microbiome compared to the single stressors. While stress combination was different when compared to the control group, it was not different from the effects of single stressors.

Our results also showed that, in the control group, the rhizosphere of primary and crown roots is inhabited by different bacterial communities. Few previous studies, mostly based on total count and/or trophic strategy and/or culture-dependent techniques only, suggested that different root classes are associated with a different microbiome in the rhizosphere (Gochnauer et al., 1989; De Leij et al.,1994; Marschner et al., 2005) and, in particular, Sivasithamparam et al. (1979) reported that maize adventitious and seminal roots have similar diversity of bacteria, but the

adventitious roots have lower fungal diversity. The only paper focused on root classes soil-based microbiomes, reported nodal roots of *Brachypodium distacum* showing a different structure of bacterial and fungal communities compared to seminal roots (Kawasaki et al., 2016). However, Kawasaki et al. (2016) focused on non-stressed plants while our study included single and combined abiotic stress. Our results supported the differentiation of rhizosphere bacterial microbiome according to root classes. Interestingly, if we extend the same analysis to the stress treatments, the difference between root classes disappears. Currently we have a very narrow knowledge on this topic, so it is hard to outline an explanatory framework for this effect. We are confident that future studies can expand our results and provide a mechanistic explanation.

Here we also tested the hypothesis that different root zones, within each root class, would be associated to different microbial communities. In our study, we did not find differences in microbial community composition between different zones of the same root class. Following the evidence that different root zones produce different exudates (Walker et al., 2003), we would expect to observe differences in microbial assembly along the root axis. To our knowledge, a single previous study tested the hypothesis that the rhizosphere microbiome associated with different root zones would respond differently to drought stress (Simmons et al., 2020), and they also found no differences between root zones. Previous studies showed that rhizosphere microorganisms can quickly assimilate root exudates, buffering their influence on rhizosphere microbiomes (Dennis, et al., 2010). This mechanism might explain our results by itself. However, we should also consider a caveat of our study: we focused on a single species and genotype. Thus, it is difficult to generalize our results to other species, but we are confident that future research can focus on multiple species and genotypes to clarify this aspect. Another possible caveat of our study is that sub-apical roots have elongation zones that are morphologically and functionally similar to the apical zone, and this might have hidden differences in the microbiome composition between these two root zones. However, this does not explain why we did not observe differences between the apical and basal zones.

While each stressor influenced the rhizosphere microbiome in a different way, the analysis of microbial community highlighted that in the control group the microbial community differed between crown and primary roots, but this difference was not found in any of the stressed groups. Previous research found that plants can recruit beneficial microbes in the rhizosphere in an effort to alleviate stress (Lareen et al., 2016), and this can be the mechanism behind our observation. To test this possibility, we focused on the taxa that become significantly more abundant as consequence of plant stress. Indeed, we found that several microbial taxa that were differentially more abundant in our treatment groups are actually associated to plant beneficial organisms: *Massilia* (Ofek et al., 2012), *Solirubrobacter* (Yang et al., 2012; Franke-Whittle et al., 2015), *Burkholderia* (Suárez-Moreno et al., 2012), *Caulobacter* (Luo et al., 2019), *Mesorhizobium* (Laranjo, Alexandre and Oliveira 2014), *Micromonospora* (Martínez-Hidalgo et al., 2015), *Rhizobacter* (Lugtenberg and Kamilova, 2009), *Paraburkholderia* (Kaur et al., 2017), *Sphingomonas* (Khan et al., 2014, 2017). Furthermore, we found a higher abundance of three genera, *Agrobacterium*, *Pseudomonas* and *Acidovorax*, which are widely known host both pathogenic but also beneficial bacterial species.

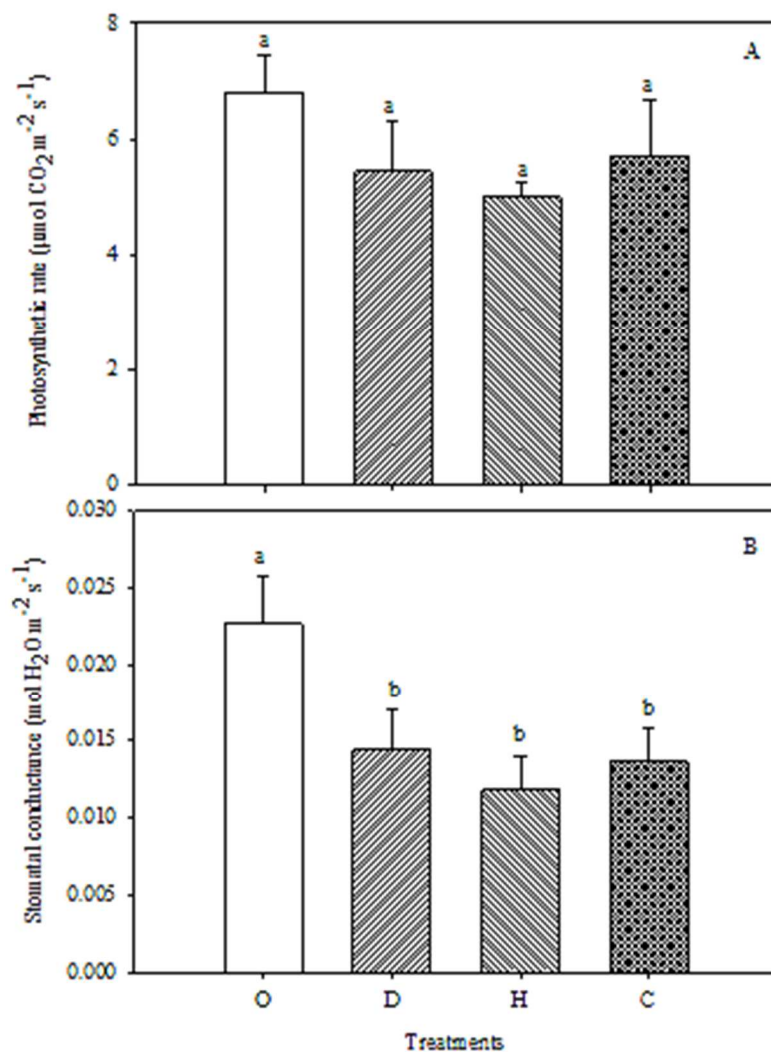
Our study brings a novel view to the ecology of plant-associated microorganisms. We showed that root class is an important factor in shaping the rhizosphere bacterial microbiome, and that the presence of plant stressors reduces the differences between root classes. Although more studies on a large set of plant species and genotypes are necessary, our results can contribute in increasing the predictability of plant-microbe relationship, which is an important interaction for securing the productivity of our crops. More generally, our results contribute to the knowledge on the effects of climate changes on crops, showing that two of the major plant stressors caused by climate change influence the plant-microbiome interactions. This has potential impact on the current trend of crafting agricultural practices around an holistic vision of plants-microbe-environment interactions.

#### 4.5. Supplementary material

The photosynthetic rate and stomatal conductance was measured on intact leaves using the LI-COR LI-6400 system (LI-COR Inc.; Lincoln, NE) with a leaf temperature of 26 °C, a CO<sub>2</sub> concentration of 400 μmol(CO<sub>2</sub>) mol(air)<sup>-1</sup> (controlled by CO<sub>2</sub> cylinder), an air flow rate of 500 cm<sup>3</sup> min<sup>-1</sup>, and 1200 μmol m<sup>-2</sup>s<sup>-1</sup> of photosynthetically active radiation supplied by the LED light source. Each measure was taken between 120 and 200 seconds of waiting time. Between measures, the difference in the CO<sub>2</sub> concentration between the sample and the reference was matched to 50 μmol(CO<sub>2</sub>) mol(air)<sup>-1</sup>. The leaf to-air vapor pressure difference (VPD) was set to 1.5 kPa, and continuously monitored around the leaf during measurements and maintained at a constant level by manipulating the humidity of incoming air as needed. All measurements were performed inside a growth chamber. For each treatment we measured six plants, and for each plant we recorded the mean value of two measures on different leaves. Data was analysed using one-way ANOVA, and contrasts were inferred using Fisher's LSD post hoc test.

Results show that photosynthetic rate was not influenced by treatments (F=1.0780; df=3; P=0.38 - Fig. S4.1A), while we observed differences in stomatal conductance between control and all treatments (F=3.51; df=3; P=0.034 - Fig S4.1B). The stomatal conductance decreased by -20%, -26% and -16% in plants exposed to drought, heat and combined stress, respectively (Fig. S4.1B). Similar results were obtained in Hussain et al. (2019). This confirms that our treatments were successful in inducing stress to maize plants.





**Figure S4.1** – Photosynthetic rate ( $\mu\text{mol}(\text{CO}_2) \times \text{m}^{-2} \times \text{s}^{-1}$ ) and stomatal conductance ( $\text{gs, mol H}_2\text{O} \times \text{m}^{-2} \times \text{s}^{-1}$ ) of maize plants exposed for seven days to drought (D), heat (H) and their combination (C). The control (O) was obtained in presence of optimal water and temperature (see Materials and Methods). Different letters indicate significant differences between treatments (Fisher's LSD test).

**Table S4.1** - Soil physical and chemical characteristics.

Soil texture	sand 36.0%, silt 32.0%, clay 32.0%
Bulk density	$1.23 \pm 0.04$ kg/dm <sup>3</sup>
pH <sub>water</sub>	$7.2 \pm 0.2$
pH <sub>KCl</sub>	$6.4 \pm 0.1$
Total organic Carbon (C)	$19.3 \pm 0.4$ g/kg dry soil
Total Nitrogen (N)	$1.8 \pm 0.2$ g/kg dry soil
C:N ratio	10.7
NH <sub>4</sub> <sup>+</sup>	$17.1 \pm 1.0$ mg/kg dry soil
NO <sub>3</sub> <sup>-</sup>	$13.0 \pm 1.0$ mg/kg dry soil
Olsen P	$18.3 \pm 2.3$ mg/kg dry soil
Total CaCO <sub>3</sub>	$8.4 \pm 1.0$ g/kg dry soil
Active CaCO <sub>3</sub>	$3.9 \pm 0.2$ g/kg dry soil
Cation Exchange Capacity (CEC)	$17.1 \pm 1.7$ cmol/kg dry soil
Electrical Conductivity (EC) 1:2 at 25°C	$0.165 \pm 0.004$ dS/m

**Table S4.2** - PERMANOVA pairwise comparison between treatments in primary roots.

<b>Pair</b>	<b>FDR corrected <i>P</i> value</b>
Control – Drought	<b>0.005</b>
Control – Heat	<b>0.001</b>
Control – Combined	<b>0.002</b>
Drought – Heat	<b>0.03</b>
Drought – Combined	0.308
Heat – Combined	0.094

**Table S4.3** - PERMANOVA pairwise comparison between treatments in crown roots.

<b>Pair</b>	<b>FDR corrected <i>P</i> value</b>
Control – Drought	0.006
Control – Heat	0.005
Control – Combined	0.004
Drought – Heat	0.03
Drought – Combined	0.253
Heat – Combined	0.073

**Table S4.4** - PERMANOVA pairwise comparison between root classes (primary vs crown) within each treatment.

<b>Pair</b>	<b>FDR corrected <i>P</i> value</b>
Control	<b>0.001</b>
Drought	0.200
Heat	0.055
Combined	0.273

## Conclusions and Future Perspectives

In consideration to the aims of the present PhD thesis focused on the evaluation of the plant morpho-physiological and metabolic responses to environmental conditions characterized by combined abiotic and biotic stress and how these responses occur at different within-plant spatial levels and temporal scales, the results of the research activities permit us to rise three main considerations.

First. The different spatial expression of the morpho-physiological performances within the plant contributed to the plant fitness in the specific and delicate habitats such as those of the rare plants. This result has been observed in *Salvia ceratophylloides*, a rare and endangered plant species, and specifically in a population that faces with high microhabitat environmental heterogeneity. Differently to the morpho-physiological traits, the volatilome showed a within-plant variability independently to the site of the *S. ceratophylloides* populations suggesting that the sites are characterized by a lower heterogeneous distribution of the biotic stress.

Second. The combination of the abiotic and biotic stress has been more harmful than single stress on the growth and on the physiological tomato responses with antagonistic and synergistic effects, respectively, but non-additive ones. Further, the tomato in presence of the combined stress emitted a different blend of VOCs respect to the single stress. These results suggest a “new stress state” of the tomato plants exposed to the combined stress which is worthy to deep molecular investigation. Interestingly is that the combined stress affected the morpho-physiological traits differently in relation to the position of the leaves along the shoot axis and/or to their vascular connection determining, hence, a high within-plant variance. The higher spatial expression of the morpho-physiological responses within the plant in presence of the combined stress could permit a better optimization of the growth and defence resources with improvement of the plant adaptation to the heterogeneous and multiple stressful environmental conditions. Further targeted experiments to verify the within-plant morpho-physiological variability as functional trait in the plant fitness in field are worthy of investigation.

Third. As observed for the aerial part of the plant, the root system also pointed out a within-root variability in responses to the combined stress, mainly drought and

heat. The primary root and their laterals have been more responsive to both the single and combined stress with antagonistic and synergistic effects, respectively, but only the seminal lateral roots have been more sensitive to the combined stress with synergized effects. In particular, these responses have been due to the alteration of specific root traits of whose the root length ratio of the primary lateral roots was the main discriminant for the combined stress. Besides the root morphology, the combined stress modified also the root microbiome differently to the single stress and with a root type specific response.

Overall, these results indicated specific morpho-physiological and metabolic responses to the combined stress with a well-defined within-plant pattern which determined a “new stress state” of which the underlying molecular mechanisms orchestrated by a network of metabolic pathways, signaling transduction, hormone interaction and gene expression, are worthy to be investigate.

## **ACKNOWLEDGEMENTS**

I thank my tutor, Prof. Agostino Sorgonà, for its precious support during the entire doctorate course.

I also like to thank Prof. Alison Bennett from The Ohio State University for its hospitality and PhD Antonino Malacrinò who helped and advised me during my period in USA. I would like to thank those who supported my during the lab analysis: Dr Antonino Zumbo, PhD Beatrix Petrovicova, PhD Fabrizio Araniti, PhD Antonio Lupini, PhD Giulia Giunti, PhD Giovanna Settineri, PhD Antonio Mauceri, PhD Giuseppe Badagliacca and Dr Luana De Rimini.

Special thanks to Davide, my parents and baby Salvatore.

## REFERENCES

1. Abdelfattah A, Malacrino A, Wisniewski M, Cacciola SO, Schena L (2018) Metabarcoding: A powerful tool to investigate microbial communities and shape future plant protection strategies. *Biol Control*. **120**: 1-10.
2. Abenavoli MR, Sorgonà A, Albano S, Cacco G (2004) Coumarin differentially affects the morphology of different root types of maize seedlings. *J Chem Eco*. **30**:1871–83.
3. Abenavoli MR, Leone M, Sunseri F, Bacchi M, Sorgonà A. (2016) Root phenotyping for drought tolerance in bean landraces from Calabria (Italy). *J. Agron. Crop. Sci*. **202**: 1–12.
4. Abid M, Ali S, Qi LK, Zahoor R, Tian Z, Jiang D, Dai T (2018) Physiological and biochemical changes during drought and recovery periods at tillering and jointing stages in wheat (*Triticum aestivum L.*). *Sci Rep*. **8**(1): 1-15.
5. Agrawal AA, Laforsch C, Tollrian R (1999) Transgenerational induction of defences in animals and plants. *Nature*. **401**: 60–63.
6. Ahmed IM, Dai H, Zheng W, Cao F, Zhang G, Sun D, Wu F (2013) Genotypic differences in physiological characteristics in the tolerance to drought and salinity combined stress between Tibetan wild and cultivated barley. *Plant Physiol. Bioch*. **63**: 49-60.
7. Aitken SN, Whitlock MC (2013) Assisted gene flow to facilitate local adaptation to climate change. *Annu Rev Ecol Evol Syst*. **44**: 367–388.
8. Akula R, Ravishankar GA (2011) Influence of abiotic stress signals on secondary metabolites in plants. *Plant signaling & behavior*. **6**(11): 1720-1731.
9. Alameda D, Anten NPR, Villar R (2012) Soil compaction effects on growth and root traits of tobacco depend on light, water regime and mechanical stress. *Soil and Tillage Research*. **120**: 121–129
10. Alberto FJ, Aitken SN (2013) Potential for evolutionary responses to climate change—evidence from tree populations. *Global Change Biol*. **19**: 1645–1661.
11. Aldea M, Hamilton JG, Resti JP, Zangerl AR, Berenbaum MR, Delucia EH (2005) Indirect effects of insect herbivory on leaf gas exchange in soybean. *Plant Cell Environ*. **28**: 402-411.

12. Aleric KM, Kirkman LK (2005) Growth and photosynthetic responses of the federally endangered shrub, *Lindera melissifolia* (Lauraceae), to varied light environments. *Am J Bot.* **92**: 682–689.
13. Allison SD, Martiny JBH (2008) Resistance, resilience, and redundancy in microbial communities. *Proc Nat Acad Sci.* **105**:11512–9.
14. Ameye M, Allmann S, Verwaeren J, Smagghe G, Haesaert G, Schuurink RC, Audenaert K (2018) Green leaf volatile production by plants: a meta-analysis. *New Phytol.* **220**: 666-683.
15. Anderson SM, Puertolas J, Dodd IC (2016) Does irrigation frequency affect stomatal response to drying soil? *Acta Hortic.* **1197**:133–8.
16. Apprill A, McNally S, Parsons R, Weber L (2015) Minor revision to V4 region SSU rRNA 806R gene primer greatly increases detection of SAR11 bacterioplankton. *Aquat Microb Ecol.* **75**:129–37.
17. Arbona V, Gómez-Cadenas A (2015) Metabolomics of disease resistance in crops. *Curr Issues Mol Biol.* **19**:13–29
18. Arimura GI, Ozawa R, Maffei ME (2011) Recent advances in plant early signaling in response to herbivory. *Int J Mol Sci.* **12**:3723–3739.
19. Aroca R (2012) Plant responses to drought stress. From morphological to molecular features, pp. 1-5.
20. ARSSA. I suoli della Calabria – Carta dei suoli in scala 1:250.000 della Regione Calabria. Rubettino Editore: Soveria Mannelli, 2003, pp. 387.
21. Arve LE, Torre S, Olsen JE, Tanino KK (2011) Stomatal responses to drought stress and air humidity. In: *Abiotic stress in plants-Mechanisms and adaptations*. IntechOpen.
22. Ashfaq M, Haider MS, Khan AS, Allah SU (2012) Breeding potential of the basmati rice germplasm under water stress condition. *African J Biotec.* **11**(25): 6647-6657.
23. Ashraf M, Harris PJ (2013) Photosynthesis under stressful environments: an overview. *Photosynthetica.* **51**(2): 163-190.
24. Atkinson NJ, Lilley CJ, Urwin PE (2013) Identification of genes involved in the response of *Arabidopsis* to simultaneous biotic and abiotic stresses. *Plant Physiol.* **162**: 2028–2041.



25. Atkinson NJ, Urwin PE (2012) The interaction of plant biotic and abiotic stresses: from genes to the field. *J Exp Bot.* **63**: 3523–3543.
26. Baldocchi D, Collineau S (1994) The physical nature of solar radiation in heterogeneous canopies: spatial and temporal attributes. *Exploitation of Environmental Heterogeneity by Plants. Ecophysiological Processes Above-and-Belowground.* 21-71.
27. Bansal S, Hallsby G, Löfvenius MO, Nilsson MC (2013) Synergistic, additive and antagonistic impacts of drought and herbivory on *Pinus sylvestris*: leaf, tissue and whole-plant responses and recovery. *Tree Physiol.* **33**:451-463.
28. Bhargava S, Sawant K (2013) Drought stress adaptation: metabolic adjustment and regulation of gene expression. *Plant breeding.* **132**(1): 21-32.
29. Barthel M, Sturm P, Knohl A (2011) Soil matrix tracer contamination and canopy recycling did not impair <sup>13</sup>CO<sub>2</sub> plant–soil pulse labelling experiments. *Isotopes Environ Health Stud.* **47**(3): 359-371.
30. Basu S, Ramegowda V, Kumar A, Pereira A (2016) Plant adaptation to drought stress. *F1000Research.* **5**.
31. Bates D, Mächler M, Bolker B, Walker S (2015) Fitting linear mixed-effects models using lme4. *J Stat Softw.* **67**:1–48.
32. Bengough AG, McKenzie BM, Hallett PD, Valentine TA (2011) Root elongation, water stress, and mechanical impedance: A review of limiting stresses and beneficial root tip traits. *J Exp Bot.* **62**: 59–68.
33. Berendsen RL, Pieterse CMJ, Bakker PAHM (2012) The rhizosphere microbiome and plant health. *Trends Plant Sci.* **17**:478–86.
34. Berens ML, Wolinska KW, Spaepen S, Ziegler J, Nobori T, Nair A, Krüler V, Winkelmüller TM, Wang Y, Mine A, Becker D, Garrido-Oter R, Schulze-Lefert P, Tsuda K (2019) Balancing trade-offs between biotic and abiotic stress responses through leaf age-dependent variation in stress hormone cross-talk. *Proc Nat Acad Sci.* **116**: 2364-2373.
35. Bilbrough CJ, Caldwell MM (1995) The effects of shading and N status on root proliferation in nutrient patches by the perennial grass *Agropyron desertorum* in the field. *Oecologia.* **103**: 10– 16.
36. Bilgin DD, Zavala JA, Zhu J, Clough SJ, Ort DR, De Lucia EH (2010)

Biotic stress globally downregulates photosynthesis genes. *Plant Cell Environ.* **33**(10): 1597-1613.

37. Bitá CE, Zenoni S, Vriezen WH, Mariani C, Pezzotti M, Gerats T (2011) Temperature stress differentially modulates transcription in meiotic anthers of heat-tolerant and heat-sensitive tomato plants. *BMC genomics.* **12**: 384.

38. Bleeker PM, Mirabella R, Diergaarde PJ, VanDoorn A, Tissier A, Kant MR, Prins M, de Vos M, Haring MA, Schuurink RC (2012) Improved herbivore resistance in cultivated tomato with the sesquiterpene biosynthetic pathway from a wild relative. *Proc Natl Acad Sci.* **109**: 20124-20129.

39. Blum A (2005) Drought resistance, water-use efficiency, and yield potential – are they compatible, dissonant, or mutually exclusive? *Aust J Agric Res* **56**: 1159–1168.

40. Bodner G, Leitner D, Nakhforoosh A, Sobotik M, Moder K, Kaul HP (2013) A statistical approach to root system classification. *Front Plant Sci.* **4**: 292.

41. Boege and Marquis (2005) Facing herbivory as you grow up: the ontogeny of resistance in plants. *Trends Ecol Evol.* **20**: 441 – 44

42. Boisvenue C, Running SW (2006) Impacts of climate change on natural forest productivity. Evidence since the middle of the 20th century. *Glob Chang Biol.* **12**: 862–882.

43. Borken W, Matzner E (2009) Reappraisal of drying and wetting effects on C and N mineralization and fluxes in soils. *Glob Change Biol.* **15**: 808–824.

44. Breitburg D, Riedel G (2005) Multiple stressors in marine systems. In: Norse E, Crowder L editors. *Marine conservation biology*. Island Press, Washington D.C. pp. 416–431.

45. Brown JK (2015) Durable resistance of crops to disease: a Darwinian perspective. *Annu Rev Phytopathol.* **53**: 513–539.

46. Brüggemann N, Gessler A, Kayler Z, Keel SG, Badeck F, Barthel M, Bahn M (2011) Carbon allocation and carbon isotope fluxes in the plant-soil-atmosphere continuum: a review. *Biogeosciences*, **8**(11): 3457-3489.

47. Bruinsma M, van Broekhoven S, Poelman EH, Posthumus MA, Muller MJ, van Loon JJA, Dicke M (2010) Inhibition of lipoxygenase affects induction of both direct and indirect plant defences against herbivorous insects. *Oecologia.* **162**: 393–

404.

48. Bruschi P, Grossoni P, Bussotti F (2003) Within- and among-tree variation in leaf morphology of *Quercus petraea* (Matt.) Liebl. natural populations. *Trees*. **17**: 164–172.

49. Bunnag S, Pongthai P (2013) Selection of rice (*Oryza sativa* L.) cultivars tolerant to drought stress at the vegetative stage under field conditions. *Am J Plant Sci*. **4**(09): 1701.

50. Burri S, Sturm P, Baur T, Barthel M, Knohl A, Buchmann N. (2014) The effect of physical back-diffusion of  $^{13}\text{CO}_2$  tracer on the coupling between photosynthesis and soil  $\text{CO}_2$  efflux in grassland. *Isotopes Environ Health Stud*, **50**(4): 497-513.

51. Canarini A, Dijkstra FA (2015) Dry-rewetting cycles regulate wheat carbon rhizodeposition, stabilization and nitrogen cycling. *Soil Biol Biochem*. **81**: 195–203.

52. Caporaso JG, Lauber CL, Walters WA, Berg-Lyons D, Huntley J, Fierer N, Owens SM, Betley J, Fraser L, Bauer M, Gormley N, Gilbert JA, Smith G, Knight R (2012) Ultra-high-throughput microbial community analysis on the Illumina HiSeq and MiSeq platforms. *ISME J*. **6**:1621–4.

53. Cardell MF, Amengual A, Romero R, Ramis C (2020) Future extremes of temperature and precipitation in Europe derived from a combination of dynamical and statistical approaches. *Int J Climatol*. **40**: 4800–4827.

54. Castrillo M, Vizcaino D, Moreno E (2005) Specific leaf mass, fresh: dry weight ratio, sugar and protein contents in species of *Lamiaceae* from different light environments. *Rev Biol Trop*. **53**: 23-8.

55. Catola S, Centritto M, Cascone P, Ranieri A, Loreto F, Calamai L, Balestrini R, Guerrieri E (2018) Effects of single or combined water deficit and aphid attack on tomato volatile organic compound (VOC) emission and plant-plant communication. *Environ Exp Bot*. **153**: 54-62

56. Chambers MC, Maclean B (2012) A cross-platform toolkit for mass spectrometry and proteomics. *Nat Biotechnol*. **30**: 918–920.

57. Chaves MM, Flexas J, Pinheiro C (2009) Photosynthesis under drought and salt stress: regulation mechanisms from whole plant to cell. *Ann Bot*. **103**: 551–560

58. Chen JP, Xu WW, Velten J, Xin ZG, Stout J (2012) Characterization of maize inbred lines for drought and heat tolerance. *J. Soil Water Conserv.* **67**: 354–364.
59. Cherif H, Marasco R, Rolli E, Ferjani R, Fusi M, Soussi A, Mapelli F, Blilou I, Borin S, Boudabous A (2015) Oasis desert farming selects environment-specific date palm root endophytic communities and cultivable bacteria that promote resistance to drought. *Environ Microbiol Rep.* **7**: 668–78.
60. Chimungu, JG, Loades KW, Lynch JP (2015) Root anatomical phenes predict root penetration ability and biomechanical properties in maize (*Zea Mays*). *J Exp Bot.* **66**: 3151–3162.
61. Chu WK, Chang SC (1966) Surface activity of inorganic soil phosphorus. *Soil Sci.* **101**: 459–464
62. Chung D, Keles S (2010) Sparse Partial Least Squares classification for high dimensional data. *Stat App Genet Mol Boil.* **9**: 17.
63. Ciamporova M, Dekankova K, Ovecká M (1998) Intra- and interspecific variation in root length, root turnover and the underlying parameters. In: Lambers H, Poorter H, VanVuuren MMI (eds) Variation in plant growth. Physiological mechanisms and ecological consequences. Backhuys Publishers, Leiden, pp 57–69.
64. Conti F, Manzi A, Pedrotti F (1997) Dipartimento di Botanica ed Ecologia, Università degli Studi di Camerino, Camerino. Associazione Italiana per il World Wildlife fund. Liste Rosse Regionali delle Piante d'Italia.
65. Coolen S, Proietti S, Hickman R, Davila Olivas NH, Huang PP, Van Verk MC, Van Pelt JA, Wittenberg AH, De Vos, M, Prins M, Van Loon JJ, Aarts, MG, Dicke M, Pieterse CM, Van Wees SC (2016), Transcriptome dynamics of *Arabidopsis* during sequential biotic and abiotic stresses. *Plant J*, **86**: 249-267.
66. Copolovici L, Kännaste A, Rimmel T, Niinemets Ü (2014) Volatile organic compound emissions from *Alnus glutinosa* under interacting drought and herbivory stresses. *Environ Exp Bot.* **100**: 55–63.
67. Coqueret V, Le Bot J, Lariat R, Desneux N, Robin C, Adamowicz S (2017) Nitrogen nutrition of tomato plant alters leafminer dietary intake dynamics. *J Insect Physiol.* **99**: 130-138.
68. Cornelissen JHC, Thompson K (1997) Functional leaf attributes predict

- litter decomposition rate in herbaceous plants. *New Phytol.* **135**: 109–114.
69. Cornelissen JHC, Pérez-Hargundeguy N (1999) Leaf structure and defence control litter decomposition rate across species and life forms in regional floras on two continents. *New Phytol.* **143**: 191–200.
70. Cornic G, Massacci A (1996) Leaf photosynthesis under drought stress. In: *Photosynthesis and the Environment*. Springer, Dordrecht. pp. 347–366.
71. Cramer GR, Urano K, Delrot S, Pezzotti M, Shinozaki K (2011) Effects of abiotic stress on plants: a systems biology perspective. *BMC Plant Biol.* **11**(1): 1–14.
72. Crisafulli A, Cannavò S, Maiorca G, Musarella CM, Signorino G, Spampinato G (2010) Aggiornamenti floristici per la Calabria. In: *Informatore Botanico Italiano*. **42**: 431–442.
73. Cruz AFS, Adiel F, Silva ÊFDF, Santos JDS, Lira RMD (2018) Stress index, water potentials and leaf succulence in cauliflower cultivated hydroponically with brackish water. *Rev Bras Eng Agr Amb.* **22**: 622–627.
74. Dai C, Liang XJ, Ren J, Liao M, Li J, Galloway LF (2016) The mean and variability of a floral trait have opposing effects on fitness traits. *Ann Bot.* **117**: 421–429.
75. Darling ES, McClanahan TR, Côté IM (2010) Combined effects of two stressors on Kenyan coral reefs are additive or antagonistic, not synergistic. *Conserv Lett.* **3**: 122–130.
76. Denno RF, McClure MS (1983) *Variable Plants and Herbivores in Natural and Managed systems*. Academic Press, New York, pp 291–341.
77. de Casas RR, Vargas, P, Pérez-Corona E, Manrique E, García-Verdugo C, Balaguer L (2011) Sun and shade leaves of *Olea europaea* respond differently to plant size, light availability and genetic variation. *Funct Ecol.* **25**: 802–812.
78. de Kroon H, Huber H, Stuefer JF, Van Groenendael JM (2005) A modular concept of phenotypic plasticity in plants. *New Phytol.* **166**: 73– 82.
79. de la Riva EG, Olmo M, Poorter H, Ubersa JL, Villar R (2016) Leaf Mass per Area (LMA) and Its relationship with leaf structure and anatomy in 34 mediterranean woody species along a water availability gradient. *PLoS One.* **11**: e0148788.

80. De Leij FAAM, Whipps JM, Lynch JM (1994) The use of colony development for the characterization of bacterial communities in soil and on roots. *Microb Ecol.* **27**:81–97.
81. Deglow E, Borden J (2011) Green leaf volatiles disrupt and enhance response to aggregation pheromones by the ambrosia beetle, *Gnathotrichus sulcatus* (Coleoptera: Scolytidae). *Can J Forest Res.* **28**: 1697-1705.
82. Delgado-Baquerizo M, Maestre FT, Gallardo A, Bowker MA, Wallenstein MD, Quero JL (2013) Decoupling of soil nutrient cycles as a function of aridity in global drylands. *Nature.* **502**: 672–676
83. Dennis PG, Miller AJ, Hirsch PR. (2010) Are root exudates more important than other sources of rhizodeposits in structuring rhizosphere bacterial communities? *FEMS Microbiol Ecol.* **72**: 313–27.
84. Desneux N, Wajnberg E, Wyckhuys KAG, Burgio G, Arpaia S, Narváez-Vasquez CA, González-Cabrera J, Catalán Ruescas D, Tabone E, Frandon J, Pizzol J, Poncet C, Cabello T, Urbaneja A (2010) Biological invasion of European tomato crops by *Tuta absoluta*: ecology, geographic expansion and prospects for biological control. *J Pest Sci.* **83**: 197–215.
85. Desneux N, Luna MG, Guillemaud T, Urbaneja A (2011) The invasive South American tomato pinworm, *Tuta absoluta*, continues to spread in Afro-Eurasia and beyond - the new threat to tomato world production. *J Pest Sci.* **84**: 403–408.
86. Devi EL, Kumar S, Singh TB, Sharma SK, Beemrote A, Devi CP, Wani S (2017). Adaptation strategies and defence mechanisms of plants during environmental stress. In: Medicinal plants and environmental challenges, pp. 359-413. Springer, Cham.
87. Devireddy AR, Zandalinas SI, Gómez-Cadenas A, Blumwald E, Mittler R (2018) Coordinating the overall stomatal response of plants: rapid leaf-to-leaf communication during light stress. *Sci Signal.* **11**: 518
88. Di Iorio A, Vescio R, Sorgonà A, Vanetti I, Binelli G, Spampinato G. The rediscovery of an endemic sage species in Calabria (Italy): an assessment of genetic diversity and structure in *Salvia ceratophylloides* Ard. (Lamiaceae). In: Book of Abstract, p 61. 113° Congresso della Società Botanica Italiana. V International

Plant Science Conference (IPSC). Fisciano (SA), Italy, 12-15 September 2018.  
ISBN: 978-88-85915-22-0

89. Díaz S, Kattge J, Cornelissen JH, Wright IJ, Lavorel S, Dray S, Garnier E (2016) The global spectrum of plant form and function. *Nature*. **529**: 167-171.
90. Ding Y, Liang S, Peng S (2019) Climate change affects forest productivity in a typical climate transition region of China. *Sustainability*. **11**: 2856.
91. Dijkstra FA, He M, Johansen MP, Harrison JJ, Keitel C (2015) Plant and microbial uptake of nitrogen and phosphorus affected by drought using <sup>15</sup>N and <sup>32</sup>P tracers. *Soil Biol Biochem*. **82**: 135–142
92. Dixon P (2003) VEGAN, a package of R functions for community ecology. *J Veg Sci*. **14**: 927–30.
93. Doussan C, Pagès L, Pierret (2003) A soil exploration and resource acquisition by plant roots: an architectural and modelling point of view. *Agronomie EDP Sciences*. **23**: 419-431.
94. Drew MC, Nye PH (1970) The supply of nutrient ions by diffusion to plant roots in soil: III. Uptake of phosphate by roots of onion, leek, and rye-grass. *Plant Soil*. pp. 545-563.
95. Drew MC, Saker LR, Ashley TW (1973) Nutrient supply and the growth of the seminal root system in barley. *J Exp Bot*. **24**: 1189–1202.
96. Drew MC (1975) Comparison of the effects of a localized supply of phosphate, nitrate, ammonium and potassium on the growth of the seminal root system, and the shoot, in barley. *New Phytol*. **75**: 479–490.
97. Drew MC, Saker LR (1978) Nutrient supply and the growth of the seminal root system in barley. *J Exp Bot*. **29**: 435–451
98. Dubrovsky JG, Forde BG (2012) Quantitative analysis of lateral root development: pitfalls and how to avoid them. *Plant Cell*. **24**: 4–14.
99. Duursma RA, Falster DS (2016) Leaf mass per area, not total leaf area, drives differences in above-ground biomass distribution among woody plant functional types. *New Phytol*. **212**: 368-376.
100. Edwards JA, Santos-Medellín CM, Liechty ZS, Nguyen B, Lurie E, Eason S, Phillips G, Sundaresan V (2018) Compositional shifts in root-associated bacterial and archaeal microbiota track the plant life cycle in field-grown rice. Gore J (ed.).

*PLOS Biol.* **16**: e2003862.

101. Elger A, Willby NJ (2003) Leaf dry matter content as an integrative expression of plant palatability: the case of freshwater macrophytes. *Funct Ecol.* **17**: 58-65.
102. English-Loeb G, Stout MJ, Duffey SS (2020) Drought stress in tomatoes: changes in plant chemistry and potential nonlinear consequences for insect herbivores. *Oikos.* **1997**: 456-68.
103. Errard A, Ulrichs C, Kühne S, Mewis I, Drungowski M, Schreiner M, Baldermann S (2015) Single- versus multiple-pest infestation affects differently the biochemistry of tomato (*Solanum lycopersicum* ‘Ailsa Craig’). *J Agr Food Chem.* **63**: 10103-10111.
104. Espeleta JF, Clark DA (2007) Multi-Scale variation in fine-root biomass in a tropical rain forest: a seven-year study. *Ecol. Monogr.* **77**: 377-404.
105. Ettema CH, Wardle DA (2002) Spatial soil ecology. *Trends Ecol Evol.* **17**(4): 177-183.
106. Fahad S, Bajwa AA, Nazir U, Anjum SA, Farooq A (2017) Crop production under drought and heat stress: plant responses and management options. *Front. Plant Sci.* **8**: 1147.
107. Fang Y, Xiong L (2015) General mechanisms of drought response and their application in drought resistance improvement in plants. *Cell Mol Life Sci.* **72**(4): 673-689.
108. Farley RA, Fitter AH (1999) The responses of seven co-occurring woodland herbaceous perennials to localized nutrient-rich patches. *J Ecol.* **87**(5): 849-859.
109. Farooq M, Hussain M, Wahid A, Siddique KHM (2012). Drought stress in plants: an overview. *Plant responses to drought stress.* 1-33.
110. Flexas J, Carriquí M, Nadal M (2018) Gas exchange and hydraulics during drought in crops: who drives whom? *J Exp Bot.* **69**: 3791–3795.
111. Fitzpatrick CR, Copeland J, Wang PW, Guttman DS, Kotanen PM, Johnson MT (2018) Assembly and ecological function of the root microbiome across angiosperm plant species. *Proc Natl Acad Sci.* **115**: E1157–65.
112. Folt CL, Chen CY, Moore MV, Burnaford J (1999) Synergism and antagonism among multiple stressors. *Limnol Oceanog.* **44**, 864– 877.



113. Foti V, Araniti F, Manti F, Alicandri E, Giuffrè AM, Bonsignore CP, Castiglione E, Sorgonà A, Covino S, Paolacci AR, Ciaffi M, Badiani M (2020) Profiling volatile terpenoids from Calabrian Pine stands infested by the Pine processionary Moth. *Plants*. **9**: 1362.
114. Franke-Whittle IH, Manici LM, Insam H, Stres B (2015) Rhizosphere bacteria and fungi associated with plant growth in soils of three replanted apple orchards. *Plant Soil*. **395**:317–33.
115. Franks SJ, Weber JJ, Aitken SN (2014) Evolutionary and plastic responses to climate change in terrestrial plant populations. *Evol Appl*. **7**:123-139.
116. Freschet GT, Swart EM, Cornelissen JHC (2015) Integrated plant phenotypic responses to contrasting above- and below-ground resources: key roles of specific leaf area and root mass fraction. *New Phytol*. **206**: 1247–1260.
117. Frost CJ, Appel HM (2007) Within-plant signalling via volatiles overcomes vascular constraints on systemic signalling and primes responses against herbivores. *Ecol Lett*. **10**: 490–498.
118. Fuchslueger L, Bahn M, Fritz K, Hasibeder R, Richter A (2014a) Experimental drought reduces the transfer of recently fixed plant carbon to soil microbes and alters the bacterial community composition in a mountain meadow. *New Phytol*. **201**: 916–927.
119. Fuchslueger L, Kastl EM, Bauer F, Kienzl S, Hasibeder R, LadreiterKnauss T (2014b) Effects of drought on nitrogen turnover and abundances of ammonia-oxidizers in mountain grassland. *Biogeosciences*. **11**: 6003–6015.
120. García AL, Fuentes V, Gallego J (1996) Influence of nitrogen supply on osmoregulation in tomato (*Lycopersicon esculentum* Mill.) plants under moderate water stress. *Plant Sci*. **115**: 33–38.
121. García AL, Fuentes V, Nicolas N (2000) Interactive effect of nitrogen and long-term moderate water stress on water relations in tomato (*Lycopersicon esculentum* Mill.) plants. *J Plant Physiol*. **156**: 563–566.
122. García AL, Marcelis L, Garcia-Sanchez F, Nicolas N, Martínez V (2007) Moderate water stress affects tomato leaf water relations in dependence on the nitrogen supply. *Biol Plant*. **51**: 707–712.
123. García GA, Dreccer MF, Miralles DJ, Serrago RA (2015) High night

temperatures during grain number determination reduce wheat and barley grain yield: A field study. *Glob. Change Biol.* **21**: 4153–4164.

124. Gatehouse JA (2002) Plant resistance towards insect herbivores: a dynamic interaction. *New phytol.* **156**(2): 145-169.

125. Ghatak A, Chaturvedi P, Weckwerth W (2017) Cereal crop proteomics: systemic analysis of crop drought stress responses towards marker-assisted selection breeding. *Fron Plant Sci.* **8**: 757.

126. Gelsomino A, Tortorella D, Cianci V, Petrovičová B, Sorgonà A, Piccolo A, Abenavoli MR (2010) Effects of a biomimetic iron-porphyrin on soil respiration and maize root morphology as by a microcosm experiment. *J Plant Nutr Soil Sc.* **173**: 399–406.

127. Girón-Calva PS, Li T, Koski TM, Klemola T, Laaksonen T, Huttunen L, Blande JD (2014) A role for volatiles in intra- and inter-plant interactions in birch. *J Chem Ecol.* **40**: 1203–1211.

128. Giunti G, Benelli G, Conte G, Mele M, Caruso G, Gucci R, Flamini G, Canale A (2016) VOCs-mediated location of olive fly larvae by the braconid parasitoid *Psytalia concolor*: A multivariate comparison among VOC bouquets from three olive cultivars. *Biomed Res Int.* **2016**.

129. Givnish TJ (2002) Ecological constraints on the evolution of plasticity in plants. *Evol Ecol.* **16**(3): 213-242.

130. Gochnauer MB, McCully ME, Labbé H (1989) Different populations of bacteria associated with sheathed and bare regions of roots of field-grown maize. *Plant Soil.* **114**: 107–20.

131. Goergen PCH, Lago I, Durigon A, Roth GFM, Scheffel LG, Slim T, Engineer A (2019) Performance of Chia on different sowing dates: characteristics of growth rate, leaf area index, shoot dry matter partitioning and grain yield. *J Agric Sci.* **11**: 252-263.

132. Gong P, Zhang J, Li H, Yang C, Zhang C, Zhang X, Khurram Z, Zhang Y, Wang T, Fei Z, Ye Z (2010) Transcriptional profiles of drought-responsive genes in modulating transcription signal transduction, and biochemical pathways in tomato. *J Exp Bot.* **61**: 3563–75.

133. Govaerts R (2003) World checklist of selected plant families database in

Access: 1-216203. The board of trustees of the Royal Botanic Gardens, Kew.

134. Gray SB, Brady SM (2016) Plant developmental responses to climate change. *Dev Biol.* **419**(1): 64-77.
135. Grime JP, Cornelissen JHC, Thompson K, Hodgson JG (1996) Evidence of a causal connection between antiherbivore defence and the decomposition rate of leaves. *Oikos.* **77**: 489–494.
136. Grinnan R, Carter TE, Johnson MTJ (2013) The effects of drought and herbivory on plant–herbivore interactions across 16 soybean genotypes in a field experiment. *Ecol Entomol.* **38**: 290-302.
137. Guo B, Chen ZY, Lee RD, Scully BT (2008) Drought stress and preharvest aflatoxin contamination in agricultural commodity: genetics, genomics and proteomics. *J Int Plant Biol.* **50**(10): 1281-1291.
138. Han P, Lavoit AV, Le Bot J, Amiens-Desneux E, Desneux N (2014) Nitrogen and water availability to tomato plants triggers bottom-up effects on the leafminer *Tuta absoluta*. *Sci Rep.* **4**: 4455.
139. Hasanuzzaman M, Nahar K, Fujita M (2013a) Plant response to salt stress and role of exogenous protectants to mitigate salt-induced damages. In: Ahmed P, Azooz MM, Prasad MNV (eds) *Ecophysiology and responses of plants under salt stress*. Springer, New York, pp 25–87
140. Hasibeder R, Fuchslueger L, Richter A, Bahn M (2015) Summer drought alters carbon allocation to roots and root respiration in mountain grassland. *New Phytol.* **205**(3): 1117-1127.
141. Havko NE, Das MR., McClain AM, Kapali G, Sharkey TD, Howe GA (2020) Insect herbivory antagonizes leaf cooling responses to elevated temperature in tomato. *Proc Nat Acad Sci.* **117**: 2211-2217.
142. He M, He CQ, Ding NZ (2018) Abiotic stresses: general defenses of land plants and chances for engineering multistress tolerance. *Front Plant Sci.* **9**:1771.
143. Hedge, I.C. (1972) Notes on *Salvia*. Flora Europaea. In: Tutin TG et al (eds), *Salvia* L. Vol. 3. Cambridge Univ Press. pp 188-192.
144. Heil M, Bostock RM (2002) Induced systemic resistance (ISR) against pathogens in the context of induced plant defences. *Ann Bot.* **89**: 503–512.
145. Herrera CM (2009) Multiplicity in unity: plant subindividual variation and

interactions with animals. University of Chicago Press, Chicago, USA.

146. Herrera CM (2017) The ecology of subindividual variability in plants: patterns, processes, and prospects. *Web Ecol.* **17**: 51–64.
147. Herrera CM, Medrano M, Bazaga P (2015) Continuous within plant variation as a source of intraspecific functional diversity: patterns, magnitude, and genetic correlates of leaf variability in *Helleborus foetidus* (Ranunculaceae). *Am J Bot.* **102**: 225–232.
148. Hidalgo J, Rubio de Casas R, Muñoz MA (2016) Environmental unpredictability and inbreeding depression select for mixed dispersal syndromes. *BMC Evol Biol.* **16**: 71.
149. Ho MD, Rosas JC, Brown KM, Lynch JP (2005) Root architectural tradeoffs for water and phosphorus acquisition. *Funct Plant Biol.* **32**(8): 737–748.
150. Hochholdinger F, Yu P, Marcon C (2018) Genetic control of root system development in maize. *Trends Plant Sci.* **23**: 79–88.
151. Hodge A, Robinson D, Griffiths BS, Fitter AH (1999a) Why plants bother: root proliferation results in increased nitrogen capture from an organic patch when two grasses compete. *Plant Cell Environ.* **22**: 811–820.
152. Hodge A, Robinson D, Griffiths BS, Fitter AH (1999b) Nitrogen capture by plants grown in N-rich organic patches of contrasting size and strength. *J Exp Bot.* **50**: 1243–1252.
153. Hodge A, Stewart J, Robinson D, Griffiths BS, Fitter AH (2000c) Spatial and physical heterogeneity of N supply from soil does not influence N capture by two grass species. *Funct Ecol.* **14**: 645–653.
154. Hodge A, Stewart J, Robinson D, Griffiths BS, Fitter AH (2000d) Competition between roots and soil micro-organisms for nutrients from nitrogen-rich patches of varying complexity. *J Ecol.* **88**: 150–164.
155. Hodge A (2004) The plastic plant: root responses to heterogeneous supplies of nutrients. *New Phytol.* **162**: 9–24.
156. Hodge A, Berta G, Doussan C, Merchan F, Crespi M (2009) Plant root growth, architecture and function. *Plant Soil.* **321**: 153–87.
157. Hoffmann A, Hammes E, Plieth C, Desel C, Sattelmacher B, Hansen UP (2005) Effect of CO<sub>2</sub> supply on formation of reactive oxygen species in *Arabidopsis*

*thaliana. Protoplasma.* **227**(1): 3-9.

158. Holeski LM (2007) Within and between generation phenotypic plasticity in trichome density of *Mimulus guttatus*. *J Evol Biol.* **20**: 2092–2100.

159. Holopainen JK, Gershenzon J (2010) Multiple stress factors and the emission of plant VOCs. *Trends Plant Sci.* **15**:176-84.

160. Hopkins WG (1999) Introduction to plant physiology. (No. Ed. 2). John Wiley and Sons.

161. Hopkins WG, Hüner NPA (2009) Introduction to Plant Physiology. 4th Edition. John Wiley and Sons, Inc., Hoboken, USA.

162. Horai H, Arita M, Kanaya S, Nihei Y, Ikeda T, Suwa K, Oda Y, Ojima Y, Tanaka K, Tanaka S, Aoshima K, Oda Y, Kakazu Y, Kusano M (2010) MassBank: a public repository for sharing mass spectral data for life sciences. *J Mass Spectrom.* **45**: 703-714.

163. Hossain MA, Munemasa S, Uraji M, Nakamura Y, Mori Izumi C, Murata Y (2011) Involvement of endogenous abscisic acid in Methyl Jasmonate-induced stomatal closure in *Arabidopsis*. *Plant Physiol.* **156**: 430-438.

164. Hossain MA, Wani SH, Bhattacharjee S, Burritt DJ, Tran LSP (2016) Drought stress tolerance in plants, Volume 2.

165. Howarth CJ (2005) Genetic improvements of tolerance to high temperature. In: Ashraf M, Harris PJC (Eds.) Abiotic Stresses: Plant Resistance through breeding and molecular approaches. Howarth Press Inc. New York.

166. Hu X, Wu L, Zhao F, Zhang D, Li N, Zhu G, Li C, Wang W (2015) Phosphoproteomic analysis of the response of maize leaves to drought, heat and their combination stress. *Front. Plant Sci.* **6**: 298.

167. Hu H, Xiong L (2014) Genetic engineering and breeding of drought-resistant crops. *Annu Rev Plant Biol.* **65**:715–741.

168. Huang B, Fu J (2000) Photosynthesis, respiration, and carbon allocation of two cool-season perennial grasses in response to surface soil drying. *Plant Soil.* **227**: 17–26.

169. Hummel I, Vile D, Violle C, Devaux J, Ricci B, Blanchard A, Garnier E, Roumet C (2007) Relating root structure and anatomy to whole-plant functioning in 14 herbaceous Mediterranean species. *New Phytol.* **173**: 313–321.

170. Hund A, Fracheboud Y, Soldati A, Stamp P (2008) Cold tolerance of maize seedlings as determined by root morphology and photosynthetic traits. *Eur. J. Agron.* **28**: 178–185.
171. Hund A, Ruta N, Liedgens M (2009) Rooting depth and water use efficiency of tropical maize inbred lines, differing in drought tolerance. *Plant Soil.* **318**(1): 311-325.
172. Huot B, Yao J, Montgomery BL, He SY (2014) Growth–defense tradeoffs in plants: a balancing act to optimize fitness. *Mol Plant.* **7**: 1267-1287.
173. Hussain HA, Men S, Hussain S, Chen Y, Ali S, Zhang S, Zhang K, Li Y, Xu Q, Liao C, Wang L (2019) Interactive effects of drought and heat stresses on morpho-physiological attributes, yield, nutrient uptake and oxidative status in maize hybrids. *Sci Rep.* **9**: 3890.
174. Hussain SS, Mehnaz S, Siddique KHM (2018) Harnessing the plant microbiome for improved abiotic stress tolerance. In *Plant Microbiome: Stress Response* (pp. 21-43). Springer, Singapore.
175. Ingram J, Bartels D (1996) The molecular basis of dehydration tolerance in plants. *Ann Rev Plant Biol.* **47**(1): 377-403.
176. Ingrisch J, Bahn M (2018) Towards a comparable quantification of resilience. *Trends Ecol Evol.* **33**(4): 251–259.
177. IPCC (2019) Climate Change and Land: An IPCC Special Report on Climate Change, Desertification, Land Degradation, Sustainable Land Management, Food Security, and Greenhouse Gas Fluxes in Terrestrial Ecosystems.
178. Islam MN, Hasanuzzaman ATM, Zhang ZF, Zhang Y, Liu TX (2017) High level of nitrogen makes tomato plants releasing less volatiles and attracting more *Bemisia tabaci* (Hemiptera: Aleyrodidae). *Front Plant Sci.* **8**: 466.
179. Jackson RB, Caldwell MM (1989) The timing and degree of root proliferation in fertile-soil microsites for three cold-desert perennials. *Oecologia.* **81**: 149–153.
180. Jackson RB, Caldwell MM (1993) Geostatistical patterns of soil heterogeneity around individual perennial plants. *J Ecol.* **81**: 683–692
181. Jaleel CA, Gopi R, Sankar B, Gomathinayagam M, Panneerselvam R (2008)

- Differential responses in water use efficiency in two varieties of *Catharanthus roseus* under drought stress. *Comptes Rendus Biologies*. **331**(1): 42-47.
182. Jaleel CA, Manivannan P, Wahid A, Farooq M, Al-Juburi HJ, Somasundaram R, Panneerselvam R (2009). Drought stress in plants: a review on morphological characteristics and pigments composition. *Int J Agric Biol*. **11**(1): 100-105.
183. James JJ, Mangold JM, Sheley RL, Svejcar T (2009) Root plasticity of native and invasive Great Basin species in response to soil nitrogen heterogeneity. *Plant Ecology*. **202**(2): 211-220.
184. Jiang M, Wang C, Zhang Y, Feng Y, Wang Y, Zhu Y (2014) Sparse Partial-least-squares Discriminant Analysis for different geographical origins of *Salvia miltiorrhiza* by 1H-NMR-based metabolomics. *Phytochem Anal*. **25**: 50–58.
185. Jiang W, Lafitte R (2007). Ascertain the effect of PEG and exogenous ABA on rice growth at germination stage and their contribution to selecting drought tolerant genotypes. *Asian J Plant Sci*. **6**: 684-687.
186. Jin X, Shi C, Yu CY, Yamada T, Sacks EJ (2017) Determination of leaf water content by visible and near-infrared spectrometry and multivariate calibration in *Miscanthus*. *Front Plant Sci*. **8**: 721.
187. Jonckheere I, Nackaerts K, Muys B, van Aardt J, Coppin P (2006) A fractal dimension-based modelling approach for studying the effect of leaf distribution on LAI retrieval in forest canopies. *Ecol Model*. **97**: 179-195.
188. Kant S, Bi YM, Rothstein SJ (2011) Understanding plant response to nitrogen limitation for the improvement of crop nitrogen use efficiency. *J Exp Bot*. **62**(4): 1499-1509.
189. Karlowsky S, Augusti A, Ingrisich J, Hasibeder R, Lange M, Lavorel S, Gleixner G (2018) Land use in mountain grasslands alters drought response and recovery of carbon allocation and plant-microbial interactions. *J Ecol*. **106**(3): 1230-1243.
190. Kasurinen A, Biasi C, Holopainen T, Rousi M, Maenpaa M, Oksanen E (2012) Interactive effects of elevated ozone and temperature on carbon allocation of silverbirch (*Betula pendula*) genotypes in an open-air field exposure. *Tree Physiol*. **32**:737–751.

191. Kaur G, Asthir B (2017) Molecular responses to drought stress in plants. *Biol Plant*. **61**(2): 201-209.
192. Kaur C, Selvakumar G, Ganeshamurthy AN (2017) *Burkholderia* to *Paraburkholderia*: the journey of a plant-beneficial-environmental bacterium. In: *Recent advances in applied microbiology* (pp. 213-228). Springer, Singapore.
193. Kawasaki A, Donn S, Ryan PR, Mathesius U, Devilla R, Jones A, Watt M (2016) Microbiome and exudates of the root and rhizosphere of *Brachypodium distachyon*, a model for wheat. Budak H (ed.). *PLoS One*. **11**: e0164533.
194. Kerchev PI, Fenton B, Foyer CH, Hancock RD (2012) Plant responses to insect herbivory: interactions between photosynthesis, reactive oxygen species and hormonal signalling pathways. *Plant Cell Environ*. **35**: 441-453.
195. Khan AL, Waqas M, Kang SM, Al-Harrasi A, Hussain J, Al-Rawahi A, Lee IJ, Al-Khiziri S, Ullah I, Ali L (2014) Bacterial endophyte *Sphingomonas* sp. LK11 produces gibberellins and IAA and promotes tomato plant growth. *J Microbiol*. **52**: 689-95.
196. Khan AL, Waqas M, Asaf S, Kamran M, Shahzad R., Bilal S, Kim YH, Al-Rawahi A, Al-Harrasi A (2017) A plant growth-promoting endophyte *Sphingomonas* sp. LK11 alleviates salinity stress in *Solanum pimpinellifolium*. *Environ Exp Bot*. **133**: 58-69.
197. Killi D, Bussotti F, Raschi A, Haworth M (2017) Adaptation to high temperature mitigates the impact of water deficit during combined heat and drought stress in C3 sunflower and C4 maize varieties with contrasting drought tolerance. *Physiol. Plant*. **159**: 130-147.
198. Knight CA, Ackerly DD (2002) An ecological and evolutionary analysis of photosynthetic thermotolerance using the temperature dependent increase in fluorescence. *Oecologia*. **130**: 505-514.
199. Kollist H, Zandalinas SI, Sengupta S, Nuhkat M, Kangasjärvi J, Mittler R (2019) Rapid responses to abiotic stress: priming the landscape for the signal transduction network. *Trends Plant Sci*. **24**: 25-37
200. Kopka J, Schauer N, Krueger S, Birkemeyer C, Usadel B, Bergmüller E, Willmitzer L, Fernie AR, Steinhauser D (2005) GMD@ CSB. DB: the Golm metabolome database. *Bioinformatics*. **21**: 1635-1638.



201. Kreps JA, Wu Y, Chang HS, Zhu T, Wang X, Harper JF (2002) Transcriptome changes for *Arabidopsis* in response to salt, osmotic, and cold stress. *Plant Physiol.* **130**(4): 2129-2141.
202. Kumar J and Abbo S (2001) Genetics of flowering time in chickpea and its bearing on productivity in semiarid environments. *Adv Agron.* **72**: 107-138.
203. Laface VLA, Musarella CM, Ortiz AC, Canas RQ, Cannavò S, Spampinato G (2020) Three new alien taxa for Europe and a chorological update on the alien vascular flora of Calabria (Southern Italy). *Plants.* **9**: 1181.
204. Lam M, Oleinick NL, Nieminen AL (2001) Photodynamic therapy-induced apoptosis in epidermoid carcinoma cells: reactive oxygen species and mitochondrial inner membrane permeabilization. *J Biol Chem.* **276**(50): 47379-47386.
205. Lambers H, Chapin FS, Pons TL (2008) Plant physiological ecology. Springer Science & Business Media.
206. Landi P, Albrecht B, Giuliani M, Sanguineti MC (1998) Seedling characteristics in hydroponic culture and field performance of maize genotypes with different resistance to root lodging. *Maydica.* **43**: 111–116.
207. Laranjo M, Alexandre A, Oliveira S (2014) Legume growth-promoting rhizobia: An overview on the *Mesorhizobium* genus. *Microbiol Res.* **169**: 2–17.
208. Larbat R, Adamowicz S, Robin C, Han P, Desneux N, Le Bot J (2016) Interrelated responses of tomato plants and the leaf miner *Tuta absoluta* to nitrogen supply. *Plant Biol (Stuttg).* **18**: 495-504.
209. Larcher W (2003) Physiological Plant Ecology. Ecophysiology and stress physiology of functional groups. 4th ed. Springer. Heidelberg, Germany.
210. Lareen A, Burton F, Schäfer P (2016) Plant root-microbe communication in shaping root microbiomes. *Plant Mol Biol.* **90**: 575–87.
211. Larigauderie A, Richards JH (1994) Root proliferation characteristics of seven perennial arid-land grasses in nutrient-enriched microsites. *Oecologia.* **99**(1-2): 102-111.
212. Lawlor DW (2013) Genetic engineering to improve plant performance under drought: physiological evaluation of achievements, limitations, and possibilities. *J Exp Bot.* **64**(1): 83-108.

213. Lê Cao KA, Boitard S, Besse P (2011) Sparse PLS discriminant analysis: biologically relevant feature selection and graphical displays for multiclass problems. *BMC Bioinform.* **12**: 253.
214. Lechowicz MJ, Bell G (1991) The ecology and genetics of fitness in forest plants. II. Microspatial heterogeneity of the edaphic environment. *J Ecol.* pp. 687-696.
215. Levitt J (1980) Responses of plants to environmental stress. Volume 1. Chilling, freezing, and high temperature stresses. Academic Press.
216. Lee SY, Boon N.J, Webb AA, Tanaka RJ (2016) Synergistic activation of RD29A via integration of salinity stress and Abscisic Acid in *Arabidopsis thaliana*. *Plant Cell Physiol.* **57**: 2147–2160.
217. Leuzinger S, Korner C (2007) Tree species diversity affects canopy leaf temperatures in a mature temperate forest. *Agr Forest Meteorol.* **146**: 29–37.
218. Liang G, Liu J, Zhang J, Guo J (2020) Effects of drought stress on photosynthetic and physiological parameters of tomato. *J Amer Soc Hort Sci.* **145**: 12-17.
219. Lichtenthaler HK (1996) Vegetation stress: an introduction to the stress concept in plants. *Plant Physiol.* **148**: 4–14.
220. Lin H, Chen Y, Zhang H, Fu P, Fan Z (2017) Stronger cooling effects of transpiration and leaf physical traits of plants from a hot dry habitat than from a hot wet habitat. *Funct Ecol.* **31**: 2202–2211.
221. Liu H, Wang X, Wang D, Zou Z, Liang Z (2011) Effect of drought stress on growth and accumulation of active constituents in *Salvia miltiorrhiza Bunge*. *Ind Crop Prod.* **33**(1): 84-88.
222. Liu H, Able AJ, Able JA (2019) Genotypic performance of Australian durum under single and combined water-deficit and heat stress during reproduction. *Sci Rep.* **9**: 14986.
223. Lobell DB, Gourджи SM (2012) The influence of climate change on global crop productivity. *Plant Physiol.* **160**: 1686–1697.
224. Lobo F, de Barros MP, Dalmagro HJ, Dalmolin ÂC, Pereira WE, De Souza EC, Ortíz, CR (2013) Fitting net photosynthetic light-response curves with Microsoft Excel - a critical look at the models. *Photosynthetica.* **51**: 445–456.

225. López YIÁ, Martínez-Gallardo NA, Ramírez-Romero R, López MG, Sánchez-Hernández C, Délano-Frier JP (2012) Cross-kingdom effects of plant-plant signaling via volatile organic compounds emitted by tomato (*Solanum lycopersicum*) plants infested by the greenhouse whitefly (*Trialeurodes vaporariorum*). *J Chem Ecol.* **38**: 1376-1386.
226. Loreto F, Schnitzler, P (2010) Abiotic stresses and induced BVOCs. *Trends Plant Sci.* **15**: 154-166.
227. Loughrin JH, Manukian A, Heath RR, Turlings TC, Tumlinson JH (1994) Diurnal cycle of emission of induced volatile terpenoids by herbivore-injured cotton plant. *Proc Nat A Sci.* **91**(25): 11836-11840.
228. Love MI, Huber W, Anders S. Moderated estimation of fold change and dispersion for RNA-seq data with DESeq2. *Genome Biol* 2014;**15**:550.
229. Lugtenberg B, Kamilova F. Plant-Growth-Promoting Rhizobacteria. *Annu Rev Microbiol* 2009;**63**:541–56.
230. Luo D, Langendries S, Mendez SG, De Ryck J, Liu D, Beirinckx S, Willems A Goormachtig S (2019) Plant Growth Promotion driven by a novel *Caulobacter* strain. *Mol Plant-Microbe Interact.* **32**: 1162–74.
231. Lupini A, Sorgonà A, Princi MP, Sunseri F, Abenavoli MR (2016) Morphological and physiological effects of trans-cinnamic acid and its hydroxylated derivatives on maize root types. *Plant Growth Regul.* **78**: 263–273.
232. Lynch JP (1995) Root architecture and plant productivity. *Plant Physiol.* **109**(1): 7.
233. Lynch JP (2013) Steep, cheap and deep: An ideotype to optimize water and N acquisition by maize root systems. *Ann Bot.* **112**: 347–357.
234. Lynch JP (2018) Rightsizing root phenotypes for drought resistance. *J Exp Bot.* **69**: 3279–3292.
235. Madlung A, Comai L (2004) The effect of stress on genome regulation and structure. *Ann Bot.* **94**: 481-495.
236. Mahdavi A, Moradi P, Mastinu A (2020) Variation in terpene profiles of *Thymus vulgaris* in water deficit stress response. *Molecules.* **25**: 1091.
237. Maiti AK, Spoorthi BC, Saha NC, Panigrahi AK (2018) Mitigating peroxynitrite mediated mitochondrial dysfunction in aged rat brain by

- mitochondria-targeted antioxidant MitoQ. *Biogerontology*. **19**(3–4): 271–286
238. Malamy JE, Ryan KS (2001) Environmental regulation of lateral root initiation in *Arabidopsis*. *Plant Physiol.* **12**: 899–909.
239. Malamy JE (2005) Intrinsic and environmental response pathways that regulate root system architecture. *Plant Cell Environ.* **28**: 67–7.
240. Manikavelu A, Nadarajan N, Ganesh SK, Gnanamalar RP, Babu RC (2006) Drought tolerance in rice: morphological and molecular genetic consideration. *Plant Growth Regul.* **50**: 121–138.
241. Mantri N, Patade V, Penna S, Ford R, Pang E (2012) Abiotic stress responses in plants: present and future. In *Abiotic stress responses in plants* (pp. 1–19). Springer, New York.
242. Marasco R, Rolli E, Ettoumi B, Vigani G, Mapelli F, Borin S, Zocchi G (2012) A drought resistance-promoting microbiome is selected by root system under desert farming. *PLoS One.* **7**: e48479.
243. Marchiori PER, Machado EC, Sales CR, Espinoza-Núñez E, Magalhães Filho JR, Souza GM, Ribeiro RV (2017) Physiological plasticity is important for maintaining sugarcane growth under water deficit. *Front Plant Sci.* **8**: 2148.
244. Markhart AH (1985) Comparative water relations of *Phaseolus vulgaris* L. and *Phaseolus acutifolius* Gray. *Plant Physiol.* **77**(1): 113–117.
245. Maron JL, Cron E (2006) Herbivory: effects on plant abundance, distribution and population growth. *Proc R Soc B.* **273**: 2575–2584
246. Marschner P, Grierson PF, Rengel Z (2005) Microbial community composition and functioning in the rhizosphere of three *Banksia* species in native woodland in Western Australia. *Appl Soil Ecol.* **28**: 191–201.
247. Martin T, Oswald O, Graham IA (2002) *Arabidopsis* seedling growth, storage lipid mobilization, and photosynthetic gene expression are regulated by carbon: nitrogen availability. *Plant Physiol.* **128**: 472–481.
248. Martínez-Hidalgo P, Galindo-Villardón P, Trujillo ME, Igual JM, Martínez-Molina E (2015) Micromonospora from nitrogen fixing nodules of alfalfa (*Medicago sativa* L.). A new promising Plant Probiotic Bacteria. *Sci Rep.* **4**: 6389.
249. Martins F, Oliveira Í, Afonso S, Ferreira H, Goncalves B (2017) Leaf morpho-physiological dynamics in *Salvia officinalis* L. var. *purpurascens*. *Turk J*

*Biol.* **41**: 134-144.

250. Mason CJ, Villari C, Keefover-Ring K, Jagemann S, Zhu J, Bonello P, Raffa KF (2017) Spatial and temporal components of induced plant responses in the context of herbivore life history and impact on host. *Funct Ecol.* **31**: 2034– 2050.
251. Mayo-Hernández J, Ramírez-Chávez E, Molina-Torres J, Guillén-Cisneros ML, Rodríguez-Herrera R, Hernández-Castillo F, Flores-Olivas A, Valenzuela-Soto JH (2019) Effects of *Bactericera cockerelli* herbivory on volatile emissions of three varieties of *Solanum lycopersicum*. *Plants.* **8**: 509.
252. McKey D (1974) Adaptive patterns in alkaloid physiology. *Am Nat.* **108**: 305–320.
253. McMurdie PJ, Holmes S (2013) phyloseq: An R package for reproducible interactive analysis and graphics of microbiome census data. Watson M (ed.). *PLoS One.* **8**: e61217.
254. McPherson MR, Wang P, Marsh EL, Mitchell RB, Schachtman DP (2018) Isolation and Analysis of microbial communities in soil, rhizosphere, and roots in perennial grass experiments. *J Vis Exp.* **137**: e57932
255. Medrano H, Tomás M (2015) From leaf to whole-plant water use efficiency (WUE) in complex canopies: limitations of leaf WUE as a selection target. *Crop J.* **3**: 220-228.
256. Meier IC, Leuschner C (2008) Genotypic variation and phenotypic plasticity in the drought response of fine roots of European beech. *Tree Physiol.* **28**: 297–309.
257. Meldau S, Erb M, Baldwin IT (2012) Defence on demand: mechanisms behind optimal defence patterns. *Ann Bot.* **110**: 1503–1514.
258. Melotto M, Underwood W, Koczan J, Nomura K, He SY (2006) Plant stomata function in innate immunity against bacterial invasion. *Cell.* **126**(5): 969-980.
259. Miguel MA, Postma JA, Lynch JP (2015) Phenotypic synergism between root hair length and basal root growth angle for phosphorus acquisition. *Plant Physiol.* **167**: 1430–1439.
260. Mithöfer A, Boland W (2012) Plant defense against herbivores: chemical aspects. *Ann Rev Plant Biol.* **63**: 431-450.

261. Mittler R (2006) Abiotic stress, the field environment and stress combination. *Trends Plant Sci.* **11**: 15–19.
262. Mittler R, Blumwald E (2010) Genetic engineering for modern agriculture: challenges and perspectives. *Ann Rev Plant Biol.* **61**: 443–462
263. Mommer L, Wolters-Arts M, Andersen C, Visser EJ, Pedersen O (2007) Submergence-induced leaf acclimation in terrestrial species varying in flooding tolerance. *New Phytol.* **176**: 337-345.
264. Mommer L, Hinsinger P, Prigent-Combaret C, Visser EJ (2016) Advances in the rhizosphere: stretching the interface of life. *Plant Soil.* **407**: 1–8.
265. Mordecai EA (2011) Pathogen impacts on plant communities: unifying theory, concepts, and empirical work. *Ecol Monogr.* **81**: 429–441.
266. Mostajeran A, Rahimi-Eichi V (2009) Effects of drought stress on growth and yield of rice (*Oryza sativa L.*) cultivars and accumulation of proline and soluble sugars in sheath and blades of their different ages leaves. *Agric Environ Sci.* **5**(2): 264-272.
267. Mou P, Jones RH, Tan Z, Bao Z, Chen H (2013) Morphological and physiological plasticity of plant roots when nutrients are both spatially and temporally heterogeneous. *Plant Soil.* **364**: 373–384.
268. Muhammad H, Zamri Z, Ismanizan I (2015) Green leaf volatiles: biosynthesis, biological functions and their applications in biotechnology. *Plant Biotechnol J.* **13**: 727-739.
269. Musarella CM, Stinca A, Cano-Ortíz A, Laface, LA, Petrilli R, Esposito A, Spampinato G (2020) New data on the alien vascular flora of Calabria (Southern Italy). *Annali di Botanica.* **10**: 55-66.
270. Nability PD, Zavala JA, DeLucia EH (2009) Indirect suppression of photosynthesis on individual leaves by arthropod herbivory. *Ann Bot.* **103**: 655-663.
271. Naudts K, Van den Berge J, Janssens IA, Nijs I, Ceulemans R (2013) Combined effects of warming and elevated CO<sub>2</sub> on the impact of drought in grassland species. *Plant Soil.* **369**: 497–507.
272. Naylor D, Coleman-Derr D (2018) Drought stress and root-associated bacterial communities. *Front Plant Sci.* **8**: 2223.
273. Naylor D, DeGraaf S, Purdom E, Coleman-Derr D (2017) Drought and host

- selection influence bacterial community dynamics in the grass root microbiome. *ISME J.* **11**: 2691–704.
274. Nguyen D, Poeschl Y, Lortzing T, Hoogveld R, Gogol-Döring A, Cristescu SM, Steppuhn A, Mariani C, Rieu I, van Dam NM (2018) Interactive responses of *Solanum dulcamara* to drought and insect feeding are herbivore species-specific. *Int J Mol Sci.* **19**: 3845.
275. Nguyen D, Rieu I, Mariani C, van Dam NM (2016) How plants handle multiple stresses: hormonal interactions underlying responses to abiotic stress and insect herbivory. *Plant Mol Biol.* **91**: 727–740.
276. Niinemets U (2010) Responses of forest trees to single and multiple environmental stresses from seedlings to mature plants: past stress history, stress interactions, tolerance and acclimation. *For Ecol Manag.* **260**: 1623–1639.
277. Niinemets U, Kännaste A, Copolovici L (2013) Quantitative patterns between plant volatile emissions induced by biotic stresses and the degree of damage. *Front Plant Sci.* **4**: 262.
278. Niinemets U, Valladares F (2004) Photosynthetic acclimation to simultaneous and interacting environmental stresses along natural light gradients: optimality and constraints. *Plant Biol.* **6**: 254–268.
279. Nikolova M, Aneva I (2017) European species of genus *Salvia*: Distribution, chemodiversity and biological activity. In: *Salvia Biotechnology*. Springer Cham. pp. 1-30.
280. Noel F, Machon N, Porcher E (2007) No genetic diversity at molecular markers and strong phenotypic plasticity in populations of *Ranunculus nodiflorus*, an endangered plant species in France. *Ann Bot J.* **99**: 1203-12.
281. Nosalewicz A, Lipiec J (2014) The effect of compacted soil layers on vertical root distribution and water uptake by wheat. *Plant Soil.* **375**: 229–240.
282. Nuccio EE, Anderson-Furgeson J, Estera KY, Pett-Ridge J, De Valpine P, Brodie EL, Firestone MK (2016) Climate and edaphic controllers influence rhizosphere community assembly for a wild annual grass. *Ecology.* **97**: 1307–18.
283. Obata T, Witt S, Lisek J, Palacios-Rojas N, Florez-Sarasa I, Yousfi S, Araus JL, Cairns JE, Fernie Alisdair R (2015) Metabolite profiles of maize leaves in

drought, heat, and combined stress field trials reveal the relationship between metabolism and grain yield. *Plant Physiol.* **169**: 2665–2683.

284. Ofek M, Hadar Y, Minz D (2012) Ecology of root colonizing *Massilia* (*Oxalobacteraceae*). *PLoS One.* **7**: e40117.

285. Onyekachi OG, Boniface OO, Gemlack NF, Nicholas N (2019) The effect of climate change on abiotic plant stress: a review. Abiotic and biotic stress in plants.

286. Opedal ØH, Armbruster WS, Graae BJ (2015) Linking small-scale topography with microclimate, plant species diversity and intra-specific trait variation in an alpine landscape. *Plant Ecol Divers.* **8**: 305-315.

287. Orians CM (2005) Herbivores, vascular pathways, and systemic induction: facts and artifacts. *J Chem Ecol.* **31**: 2231–2242

288. Orians CM, Schweiger R, Dukes JS, Scott ER, Müller C (2019) Combined impacts of prolonged drought and warming on plant size and foliar chemistry. *Ann. Bot.* **124**: 41–52.

289. Osada N, Yasumura Y, Ishida A (2014) Leaf nitrogen distribution in relation to crown architecture in the tall canopy species, *Fagus crenata*. *Oecologia.* **175**: 1093–1106.

290. Palta JA, Gregory PJ (1997) Drought affects the fluxes of carbon to roots and soil in <sup>13</sup>C pulse-labelled plants of wheat. *Soil Biol Biochem.* **29**:1 395–1403.

291. Pan X, Geng Y, Zhang W, Li B, Chen J (2006) The influence of abiotic stress and phenotypic plasticity on the distribution of invasive *Alternanthera philoxeroides* along a riparian zone. *Acta Oecologica.* **30**(3): 333-341.

292. Pandey P, Irulappan V, Bagavathiannan MV, Senthil-Kumar M (2017) Impact of combined abiotic and biotic stresses on plant growth and avenues for crop improvement by exploiting physio-morphological traits. *Front Plant Sci.* **8**: 537.

293. Pandey P, Ramegowda V, Senthil-Kumar M (2015) Shared and unique responses of plants to multiple individual stresses and stress combinations: physiological and molecular mechanisms. *Front Plant Sci.* **6**: 723

294. Parada AE, Needham DM, Fuhrman JA (2016) Every base matters: assessing small subunit rRNA primers for marine microbiomes with mock communities, time series and global field samples. *Environ Microbiol.* **18**: 1403–



- 14.
295. Park SW, Kaimoyo E, Kumar D, Mosher S, Klessig DF (2007) Methyl salicylate is a critical mobile signal for plant systemic acquired resistance. *Science*. **318**: 113–116.
296. Parry S, Renault P, Chadoeuf J, Chenu C, Lensi R (2000) Particulate organic matter as a source of variation in denitrification in clods of soil. *Europ J Soil Sci*. **51**(2): 271-281.
297. Patanè C (2011) Leaf area index, leaf transpiration and stomatal conductance as affected by soil water deficit and vpd in processing tomato in semi arid mediterranean climate. *J Agron Crop Sci*. **197**: 165–176.
298. Paul MJ, Driscoll SP (1997) Sugar repression of photosynthesis: the role of carbohydrates in signalling nitrogen deficiency through source: sink imbalance. *Plant Cell Environ*. **20**:110–116
299. Paż-Dyderska S, Dyderski MK, Szwaczka P, Brzezicha M, Bigos K, Jagodziński AM (2020) Leaf traits and aboveground biomass variability of forest understory herbaceous plant species. *Ecosystems*. **23**: 555–569.
300. Pérez-Harguindeguy N, Diaz S, Lavorel S, Poorter H, Craine J, Reich PB, Sack L, Conti G, Vaieretti MV (2013) New handbook for standardized measurement of plant functional traits worldwide. *Aust J Bot*. **61**: 167–234.
301. Perez-Lopez U, Miranda-Apodaca J, Munoz-Rueda A, Mena-Petite A (2013) Lettuce production and antioxidant capacity are differentially modified by salt stress and light intensity under ambient and elevated CO<sub>2</sub>. *J Plant Physiol*. **170**: 1517–1525.
302. Pichersky E, Raguso RA (2018) Why do plants produce so many terpenoid compounds? *New Phytol*. **220**: 692–702.
303. Pieterse CM, Zamioudis C, Berendsen RL, Weller DM, Van Wees SC, Bakker PA (2014) Induced systemic resistance by beneficial microbes. *Annu Rev Phytopathol*. **52**: 347– 375.
304. Pignatti S (2018) Flora d'Italia: In 4 Volumi. Volume 3: Flora d'Italia & Flora Digitale, 2nd ed.; Edagricole-Edizioni Agricole di New Business Media srl: Milano. ISBN 978-88-506-5244-0.
305. Ponce-Bautista A, Valverde PL, Flores J, Zavala-Hurtado A, Vite F, López-

- Ortega G, Pérez-Hernández MA (2017) Photosynthetically active radiation and carbon gain drives the southern orientation of *Myrtillocactus geometrizans* fruits. *Plant Biol.* **19**: 279–285.
306. Poorter H, Niinemets U (2009) Causes and consequences of variation in leaf mass per area (LMA): a meta-analysis. *New Phytol.* **182**: 565–88.
307. Poorter H, Nagel O (2000) The role of biomass allocation in the growth response of plants to different levels of light, CO<sub>2</sub>, nutrients and water: a quantitative review. *Aust J Plant Physiol.* **27**: 595–607.
308. Pothuluri JV, Kissel DE, Whitney DA, Thien SJ (1986) Phosphorus uptake from soil layers having different soil test phosphorus levels. *Agron J.* **78**: 991–994.
309. Prasad PVV, Pisipati SR, Momcilovic I, Ristic Z (2011) Independent and combined effects of high temperature and drought stress during grain filling on plant yield and chloroplast EF-Tu expression in spring wheat. *J Agron Crop Sci.* **197**: 430–441.
310. Prasch CM, Sonnewald U (2013) Simultaneous application of heat, drought, and virus to *Arabidopsis* plants reveals significant shifts in signaling networks. *Plant Physiol.* **162**: 1849–1866.
311. Pregitzer KS, Hendrick RL, Fogel R (1993) The demography of fine roots in response to patches of water and nitrogen. *New Phytol.* **125**: 575–580.
312. Press WH, Teukosky SA (1992) Numerical recipes in C. The art of scientific computing, 2nd ed. Cambridge University Press, Cambridge.
313. Price AH, Cairns JE, Horton P, Jones HG, Griffiths H (2002) Linking drought-resistance mechanisms to drought avoidance in upland rice using a QTL approach: progress and new opportunities to integrate stomatal and mesophyll responses. *J Exp Bot.* **53**: 989–1004.
314. Puglielli G, Catoni R, Spoletini A, Varone L, Gratani L (2017) Short-term physiological plasticity: trade-off between drought and recovery responses in three Mediterranean *Cistus* species. *Ecol Evol.* **7**: 10880–10889.
315. Quast C, Pruesse E, Yilmaz P, Yilmaz P, Gerken J, Schweer T, Yarza P, Glöckner FO, Peplies J (2012) The SILVA ribosomal RNA gene database project: improved data processing and web-based tools. *Nucleic Acids Res.* **41**: D590–6.
316. Quero JL, Villar R, Marañón T, Zamora R (2006) Interactions of drought

and shade effects on seedlings of four *Quercus* species: physiological and structural leaf responses. *New Phytol.* **170**: 819–834.

317. Rangarajan H, Postma JA, Lynch JP (2018) Co-optimization of axial root phenotypes for nitrogen and phosphorus acquisition in common bean. *Ann Bot.* **122**: 485–499.

318. Rejeb IB, Pastor V, Mauch-Mani B (2014) Plant responses to simultaneous biotic and abiotic stress: molecular mechanisms. *Plants.* **3**(4): 458-475.

319. Rewald B, Ephrath JE, Rachmilevitch S (2011) A root is a root is a root? Water uptake rates of *Citrus* root orders. *Plant Cell Environ.* **34**: 33–42

320. Reymond P, Bodenhausen N, Van Poecke RMP, Krishnamurthy V, Dicke M, Farmer EE (2004) A conserved transcript pattern in response to a specialist and a generalist herbivore. *Plant Cell.* **16**: 3132-47.

321. Rizhsky L, Liang H, Mittler R (2003) The water-water cycle is essential for chloroplast protection in the absence of stress. *J Biol Chem.* **278**: 38921– 38925.

322. Rivas-Martínez S (2019) Global Bioclimatics (Clasificación Bioclimática de la Tierra). <http://www.globalbioclimatics.org/book/publications.htm>.

323. Rivero RM, Mestre TC, Mittler R, Rubio F, Garcia-Sanchez F, Martinez V (2013) The combined effect of salinity and heat reveals a specific physiological, biochemical and molecular response in tomato plants. *Plant Cell Environ.* **37**: 1059–1073.

324. Robe WE, Griffiths H (2000) Physiological and photosynthetic plasticity in the amphibious, freshwater plant, *Littorella uniflora*, during the transition from aquatic to dry terrestrial environments. *Plant Cell Environ.* **23**(10): 1041-1054.

325. Rodriguez-Saona C, Parra L, Quiroz A, Isaacs R (2011) Variation in highbush blueberry floral volatile profiles as a function of pollination status, cultivar, time of day and flower part: implications for flower visitation by bees. *Ann Bot.* **107**: 1377-1390.

326. Rodriguez-Saona CR, Rodriguez-Saona LE, Frost, (2009) Herbivore-induced volatiles in the perennial shrub, *Vaccinium corymbosum*, and their role in inter-branch signaling. *J Chem Ecol.* **35**: 163–175.

327. Roesch LFW, Camargo FAO, Bento FM, Triplett EW (2008) Biodiversity of diazotrophic bacteria within the soil, root and stem of field-grown maize. *Plant*

*Soil*. **302**: 91–104.

328. Rognes T, Flouri T, Nichols B, Quince C, Mahé F (2016) VSEARCH: a versatile open source tool for metagenomics. *Peer J*. **4**: e2584.

329. Rohart F, Gautier B, Singh A, Lê Cao KA (2017) mixOmics: An R package for omics feature selection and multiple data integration. *PLoS Comput Biol*. **13**: e1005752.

330. Rolfe SA, Griffiths J, Ton J (2019) Crying out for help with root exudates: adaptive mechanisms by which stressed plants assemble health-promoting soil microbiomes. *Curr Opin Microbiol*. **49**: 73–82.

331. Rollins JA, Habte E, Templer SE, Colby T, Schmidt J, von Korff M (2013) Leaf proteome alterations in the context of physiological and morphological responses to drought and heat stress in barley (*Hordeum vulgare* L.). *J Exp Bot*. **64**: 3201–3212.

332. Romano A, Sorgonà A, Lupini A, Araniti F, Stevanato P, Cacco G, Abenavoli MR (2013) Morpho-physiological responses of sugar beet (*Beta vulgaris* L.) genotypes to drought stress. *Acta Physiol Plant*. **35**: 853–865.

333. Roy SK, Cho SW, Kwon SJ, Kamal A, Kim SW, Oh MW, Woo SH (2016). Morpho-physiological and proteome level responses to cadmium stress in sorghum. *PLoS One*. **11**(2): e0150431.

334. Rubio G, Sorgonà A, Lynch JP (2004) Spatial mapping of phosphorus influx in bean root systems using digital autoradiography. *J Exp Bot*. **55**: 2269–80.

335. Ruehr NK, Offermann CA, Gessler A, Winkler JB, Ferrio JP, Buchmann N, Barnard RL (2009) Drought effects on allocation of recent carbon: from beech leaves to soil CO<sub>2</sub> efflux. *New Phytol*. **184**(4): 950-961.

336. Ruíz-Roblet J, Villar R (2005) Relative growth rate and biomass allocation in ten woody species with different leaf longevity using phylogenetic independent contrasts (PICs). *Plant Biol*. **7**: 484–494.

337. Ruther J (2000) Retention index database for identification of general green leaf volatiles in plants by coupled capillary gas chromatography–mass spectrometry. *J Chromatogr*. **890**: 313-319.

338. Ryser P (1998) Intra- and interspecific variation in root length, root turnover and the underlying parameters. In: Inherent variation in plant growth: physiological

mechanisms and ecological consequences. Leiden: Backhuys Publishers. pp. 441–465.

339. Ryser P, Aeschlimann U (1999) Proportional dry-mass content as an underlying trait for the variation in relative growth rate among 22 Eurasian populations of *Dactylis glomerata* s.l. *Funct Ecol.* **13**: 473–482.

340. Ryser P, Eek L (2000) Consequences of phenotypic plasticity vs. interspecific differences in leaf and root traits for acquisition of aboveground and belowground resources. *Am J Bot.* **87**: 402–411.

341. Ryser P, Lambers H (1995) Root and leaf attributes accounting for the performance of fast- and slow-growing grasses at different nutrient supply. *Plant Soil.* **170**: 251–265.

342. Sarafis V (1998) Chloroplast: A structural approach. *J Plant Physiol.* **152**: 248–264.

343. Sah SK, Reddy KR, Li J (2016) Abscisic acid and abiotic stress tolerance in crop plants. *Front Plant Sci.* **7**: 571.

344. Sah RP, Chakraborty M, Prasad K (2020) Impact of water deficit stress in maize: Phenology and yield components. *Sci Rep.* **10**: 2944.

345. Saikkonen K, Nissinen R, Helander M. (2020) Toward comprehensive plant microbiome research. *Front Ecol Evol.* **8**.

346. Samaké O, Smaling E, Kropff MJ, Stomph TJ, Kodio A (2005). Effects of cultivation practices on spatial variation of soil fertility and millet yields in the Sahel of Mali. *Agric Ecosyst Environ.* **109**(3-4): 335-345.

347. Santos-Medellín C, Edwards J, Liechty Z, Nguyen B, Sundaresan V (2017) Drought stress results in a compartment-specific restructuring of the rice root-associated microbiomes. Ausubel FM (ed.). *MBio.* **8**

348. Sarvestani ZT, Pirdashti H, Sanavy SA, Balouchi H (2008) Study of water stress effects in different growth stages on yield and yield components of different rice (*Oryza sativa* L.) cultivars. *Pak J Biol Sci.* **11**(10): 1303-1309.

349. Sarwat M (2017) *Stress Signaling in Plants: Genomics and Proteomics Perspective, Volume 2*. Springer.

350. Saura-Mas S, Shipley B, Lloret F (2009) Relationship between post-fire regeneration and leaf economics spectrum in Mediterranean woody species. *Funct*

*Ecol.* **23**: 103–110.

351. Schädler M, Jung G, Auge H, Brandl R (2003). Palatability, decomposition and insect herbivory: patterns in a successional old-field plant community. *Oikos*. **103**: 121-132.

352. Schmidt L, Schurr U, Röse UR (2009) Local and systemic effects of two herbivores with different feeding mechanisms on primary metabolism of cotton leaves. *Plant Cell Environ.* **32**: 893-903.

353. Schurr U, Walter A, Rascher U (2006) Functional dynamics of plant growth and photosynthesis—from steady-state to dynamics—from homogeneity to heterogeneity. *Plant Cell Environ.* **29**: 340-352.

354. Schwarz D, Kläring HP, van Iersel MW, Ingram KT (2002) Growth and Photosynthetic response of tomato to nutrient solution concentration at two light levels. *J Am Soc Hort Sci.* **127**: 984-990

355. Shao HB, Chu LY, Jaleel CA, Zhao CX (2008) Water-deficit stress-induced anatomical changes in higher plants. *Comptes rendus biologiques.* **331**(3): 215-225.

356. Shimada T, Takahashi A, Shibata M, Yagihashi T (2015) Effects of within plant variability in seed weight and tannin content on foraging behavior of seed consumers. *Funct Ecol.* **29**: 1513–1521.

357. Shin R, Berg RH, Schachtman DP (2005) Reactive oxygen species and root hairs in *Arabidopsis* root response to nitrogen, phosphorus and potassium deficiency. *Plant Cell Physiol.* **46**: 1350-7.

358. Schmid-Hempel P (2003). Variation in immune defence as a question of evolutionary ecology. *Proc R Soc B.* **270**: 357–366.

359. Schwinning S, Ehleringer JR (2001) Water use trade-offs and optimal adaptations to pulse-driven arid ecosystems. *J Ecol.* **89**(3): 464-480.

360. Seibt U, Rajabi A, Griffiths H, Berry JA (2008) Carbon isotopes and water use efficiency: sense and sensitivity. *Oecologia.* **155**: 441-454.

361. Seigler DS (1998) Plant secondary metabolism. Springer Science & Business Media.

362. Serrano J, Silva J, Shahidian S, Silva LL, Sousa A, Baptista F (2017) Differential vineyard fertilizer management based on nutrient, s spatio-temporal variability. *J Soil Sci plant Nutr.* **17**(1),+: 46-61.

363. Sicher RC, Timlin D, Bailey B (2012) Responses of growth and primary metabolism of water-stressed barley roots to rehydration. *J Plant Physiol.* **169**: 686–695.
364. Silva DB, Weldegergis BT, Van Loon JJ, Bueno VH (2017) Qualitative and quantitative differences in herbivore-induced plant volatile blends from tomato plants infested by either *Tuta absoluta* or *Bemisia tabaci*. *J Chem Ecol.* **43**: 53–65.
365. Simmons T, Styer AB, Pierroz G, Gonçalves AP, Pasricha R, Hazra AB, Coleman-Derr D (2020) Drought drives spatial variation in the millet root microbiome. *Front Plant Sci.* **11**: 559.
366. Singla J, Krattinger SG, Wrigley CW, Faubion J, Corke H, Seetharaman K (2016) Biotic stress resistance genes in wheat. In: Wrigley CW, Faubion J, Corke H, Seetharaman K. Encyclopedia of Food Grains. Oxford. Elsevier. pp. 388-392.
367. Sivasithamparam K, Parker CA, Edwards CS (1979) Rhizosphere microorganisms of seminal and nodal roots of wheat grown in pots. *Soil Biol Biochem.* **11**: 155–60.
368. Slot M, Krause GH, Krause B, Hernández GG, Winter K (2019) Photosynthetic heat tolerance of shade and sun leaves of three tropical tree species. *Photosynth Res.* **141**: 119–130.
369. Smertenko A, Draber P, Viklicky V, Opatrny Z (1997) Heat stress affects the organization of microtubules and cell division in *Nicotiana tabacum* cells. *Plant Cell Environ.* **20**: 1534–1542.
370. Sobral M, Guitián J, Larrinaga AR (2014) Seed predators exert selection on the subindividual variation of seed size. *Plant Biol.* **16**: 836–842.
371. Sobral M, Guitián J, Guitián P, Larrinaga AR (2013) Selective larchure along a latitudinal gradient affects subindividual variation in plants. *Plos One.* **8**: 74356.
372. Sokol NW, Kuebbing SE, Karlsen-Ayala E, Bradford MA (2019). Evidence for the primacy of living root inputs, not root or shoot litter, in forming soil organic carbon. *New Phytol.* **221**(1): 233-246.
373. Sokoto MB, Muhammad (2014) A Response of rice varieties to water stress in Sokoto, Sudan Savannah Nigeria. *J Biosci Med.* **2**(1): 68-74
374. Sorgonà A, Abenavoli MR, Cacco G (2005) A comparative study between

two citrus rootstocks: Effect of nitrate on the root morpho-topology and net nitrate uptake. *Plant Soil*. **270**: 257–67.

375. Sorgonà A, Cacco G, Di Dio L, Schmidt W, Perry PJ, Abenavoli MR (2010) Spatial and temporal patterns of net nitrate uptake regulation and kinetics along the tap root of *Citrus aurantium*. *Acta Physiol Plant*. **32**: 683–93.

376. Sorgonà A, Lupini A, Mercati F, Di Dio L, Sunseri F, Abenavoli M (2011) Nitrate uptake along the maize primary root: an integrated physiological and molecular approach. *Plant Cell Environ*. **34**: 1127–40.

377. Sorgonà A, Abenavoli MR, Gringeri PG, Cacco G (2007) Comparing morphological plasticity of root orders in slow- and fast-growing citrus rootstocks supplied with different nitrate levels. *Ann. Bot*. **100**: 1287–1296.

378. Spampinato G, Crisafulli A, Cannavò S, Maiorca G, Musarella CM, Signorino G (2011) Notes on *Salvia ceratophylloides* Ard. (Lamiaceae). In: *Informatore Botanico Italiano*. **43**: 381–458.

379. Spinoni J, Vogt J V, Naumann G, Barbosa P, Dosio A (2018) Will drought events become more frequent and severe in Europe? *Int J Climatol*. **38**: 1718–36.

380. Srivastava G, Kumar S, Dubey G, Mishra V, Prasad SM (2012) Nickel and ultraviolet-B stresses induce differential growth and photosynthetic responses in *Pisum sativum* L. seedlings. *Biol Trace El Research*. **149**: 86–96.

381. Stark JM, Firestone MK (1995) Mechanisms for soil moisture effects on activity of nitrifying bacteria. *Appl Environ Microbiol*. **61**: 218–221.

382. Suárez-Moreno ZR, Caballero-Mellado J, Coutinho BG, Coutinho BG, Mendonça-Previato L, James EK, Venturi V (2012) Common features of environmental and potentially beneficial plant-associated *Burkholderia*. *Microb Ecol*. **63**: 249–66.

383. Sultan SE (2003) Phenotypic plasticity in plants: a case study in ecological development. *Evol Develop*. **5**(1): 25–33.

384. Sultan B, Defrance D, Iizumi T (2019) Evidence of crop production losses in West Africa due to historical global warming in two crop models. *Sci. Rep*. **9**: 12834.

385. Suzuki N, Rivero RM, Shulaev V, Blumwald E, Mittler R (2014), Abiotic and biotic stress combinations. *New Phytol*. **203**: 32–43.



386. Swain P, Anumalla M, Prusty S, Marndi BC, Rao GJN (2014) Characterization of some Indian native land race rice accessions for drought tolerance at seedling stage. *Aust J Crop Sci.* **8**(3).
387. Tai H, Lu X, Opitz N, Paschold A, Lithio A, Marcon C, Hochholdinger F (2016) Transcriptomic and anatomical complexity of primary, seminal, and crown roots highlight root type-specific functional diversity in maize (*Zea mays* L.). *J Exp Bot.* **67**: 1123–35.
388. Takahashi F, Kuromori T, Urano K, Yamaguchi-Shinozaki K, Shinozaki K (2020) Drought stress responses and resistance in plants: from cellular responses to long-distance intercellular communication. *Front Plant Sci.* **11**: 556972.
389. Tamburino R, Vitale M, Ruggiero A, Sassi M, Sannino L, Arena S, Grillo S (2017) Chloroplast proteome response to drought stress and recovery in tomato (*Solanum lycopersicum* L.). *BMC Plant Biol* **17**: 40.
390. Tan XP, Liang WQ, Liu CJ, Luo P, Heinstejn P, Chen XY (2000) Expression pattern of (+)-delta-cadinene synthase genes and biosynthesis of sesquiterpene aldehydes in plants of *Gossypium arboreum* L. *Planta.* **210**: 644-51.
391. Tardif G, Kane NA, Adam H, Labrie L, Major G, Gulick P, Laliberté JF (2007). Interaction network of proteins associated with abiotic stress response and development in wheat. *Plant Mol Biol.* **63**(5): 703-718.
392. Tautenhahn R, Patti GJ, Rinehart D, Siuzdak G (2012) XCMS Online: a web-based platform to process untargeted metabolomic data. *Anal Chem.* **84**: 5035-5039.
393. Tellah S, Badiani M, Trifilò P, Lo Gullo MA, Ounane G, Ounane SM, Sorgonà A (2014) Morpho-physiological traits contributing to water stress tolerance in a peanut (*Arachis hypogaea* L.) landraces collection from the Algerian Maghreb. *Agrochimica.*, **58**: 126–147.
394. Tholl D (2015) Biosynthesis and biological functions of terpenoids in plants. In *Biotechnology of isoprenoids* (pp. 63-106). Springer, Cham. **148**: 63–106.
395. Thompson GA, Goggin FL (2006) Transcriptomics and functional genomics of plant defence induction by phloem-feeding insects. *J Exp Bot.* **57**: 755-66.
396. Thomson VP, Cunningham SA, Ball MC, Nicotra AB (2003) Compensation

for herbivory by *Cucumis sativus* through increased photosynthetic capacity and efficiency. *Oecologia*. **134**: 167–175.

397. Timm CM, Carter KR, Carrell AA, Jun SR, Jawdy SS, Vélez JM, Lu TYS (2018) Abiotic stresses shift belowground populus-associated bacteria toward a core stress microbiome. Herr JR (ed.). *mSystems*. **3**

398. Tito R, Vasconcelos HL, Feeley KJ (2018) Global climate change increases risk of crop yield losses and food insecurity in the tropical Andes. *Glob Chang Biol*. **24**: e592–e602.

399. Tittoneill P, Vanlauwe B, Leffelaar PA (2005) Exploring diversity in soil fertility management of smallholder farms in western Kenya: Heterogeneity at region and farm scale. *Agric Ecosyst Environ*. **110**:149-165.

400. Tittoneil P, Muriuki A, Klapwijk CJ (2013) Soil heterogeneity and soil fertility gradients in smallholder farms of the East African Highlands. *Soil Sci Soc Am J*. **177**: 5

401. Tkemaladze GSh, Makhshvili KA (2016) Climate changes and photosynthesis. *Ann Agr Sci*. **14**: 119-126.

402. Tricker PJ, ElHabti A, Schmidt J, Fleury D (2018) The physiological and genetic basis of combined drought and heat tolerance in wheat. *J Exp Bot*. **69**: 3195–3210.

403. Tripathy JN, Zhang J, Robin S, Nguyen TT, Nguyen HT (2000) QTLs for cell-membrane stability mapped in rice (*Oryza sativa L.*) under drought stress. *Theor Appl Genet*. **100**: 1197–1202.

404. Tuba Z, Lichtenthaler HK, Csintalan Zs, Nagy Z, Sente K (1996) Loss of chlorophylls, cessation of photosynthetic CO<sub>2</sub> assimilation and respiration in the poikilochlorophyllous plant *Xerophyta scabrida* during desiccation. *Physiol Plant*. **96**: 383-388.

405. Turner MF, Heuberger AL, Kirkwood JS, Collins CC, Wolfrum EJ, Broeckling CD, Jahn CE (2016) Non-targeted metabolomics in diverse sorghum breeding lines indicates primary and secondary metabolite profiles are associated with plant biomass accumulation and photosynthesis. *Front Plant Sci*. **7**: 953.

406. Turner TR, James EK, Poole PS (2013) The plant microbiome. *Genome Biol*. **14**: 209.

407. Uga Y, Sugimoto K, Ogawa S (2013) Control of root system architecture by DEEPER ROOTING 1 increases rice yield under drought conditions. *Nat Genet.* **45**: 1097–1102.
408. Valladares F, Martinez-Ferri E, Balaguer L, Perez-Corona E, Manrique E (2000) Low leaf-level response to light and nutrients in Mediterranean evergreen oaks: a conservative resource-use strategy? *New Phytol.* **148**: 79–91.
409. Vandecar KL, Lawrence D, Clark D (2011) Phosphorus sorption dynamics of anion exchange resin membranes in tropical rain forest soils. *Soil Sci Soc Am J.* **75**: 1520.
410. Van den Dool H, Kratz PD (1963) A generalization of the retention index system including linear temperature programmed gas-liquid partition chromatography. *J Chromatogr.* **11**: 463–471.
411. van der Voort M, Kempenaar M, van Driel M, Raaijmakers JM, Mendes R (2016) Impact of soil heat on reassembly of bacterial communities in the rhizosphere microbiome and plant disease suppression. *Ecol Lett.* **19**: 375–82.
412. Van Vuuren MMI, Robinson D, Griffiths BS (1995) Nutrient inflow and root proliferation during the exploitation of a temporally and spatially discrete source of nitrogen in soil. *Plant Soil.* **178**: 185–192.
413. Vile D, Pervent, M, Belluau M, Vasseur F, Bresson J, Muller B, Granier C, Simonneau T (2012) *Arabidopsis* growth under prolonged high temperature and water deficit: Independent or interactive effects? *Plant Cell Environ.* **35**: 702–718.
414. Voothuluru P, Mäkelä P, Zhu J, Yamaguchi M, Cho IJ, Oliver MJ, Simmonds J, Sharp RE (2020) Apoplastic hydrogen peroxide in the growth zone of the maize primary root. Increased levels differentially modulate root elongation under well-watered and water-stressed conditions. *Front Plant Sci.* **11**: 392.
415. Vuylsteke M, Peleman JD, Van Eijk MJ (2007) AFLP-based transcript profiling (cDNA-AFLP) for genome-wide expression analysis. *Nature protocols.* **2**(6): 1399.
416. Wagner MR, Mitchell-Olds T (2018) Plasticity of plant defense and its evolutionary implications in wild populations of *Boechera stricta*. *Evolution.* **72**: 1034–1049.

417. Wahl S, Ryser P (2000) Root tissue structure is linked to ecological strategies of grasses. *New Phytol.* **148**: 459–471.
418. Waisel Y, Eshel A (2002) Functional diversity of various constituents of a single root system. *Plant Roots: the hidden half.* **3**: 157-174.
419. Wahid A, Gelani S, Ashraf M, Foolad M (2007) Heat tolerance in plants: an overview. *Environ Exp Bot.* 61(3):199–223.
420. Walker TS, Bais HP, Grotewold E, Vivanco JM (2003) Root exudation and rhizosphere biology. *Plant Physiol.* **132**: 44–51.
421. Walling LL (2000) The myriad plant responses to herbivores. *J Plant Growth Reg.* **19**(2): 195-216.
422. Wani SH, Sah SK, Hossain MA, Kumar V, Balachandran SM (2016) Transgenic approaches for abiotic stress tolerance in crop plants. In: Advances in plant breeding strategies: agronomic, abiotic and biotic stress traits, pp. 345-396. Springer, Cham.
423. Wasson AP, Richards RA, Chatrath R, Misra SC, Prasad SV, Rebetzke GJ, Kirkegaard JA, Christopher J, Watt M (2012) Traits and selection strategies to improve root systems and water uptake in water-limited wheat crops. *J Exp Bot.* **63**: 3485–3498.
424. Weldegergis BT, Zhu F, Poelman EH, Dicke M (2015) Drought stress affects plant metabolites and herbivore preference but not host location by its parasitoids. *Oecologia.* **177**: 701–713.
425. Westerband AC, Bialic-Murphy L, Weisenberger LA, Barton KE (2020) Intraspecific variation in seedling drought tolerance and associated traits in a critically endangered, endemic Hawaiian shrub. *Plant Ecol Divers.* 1-16
426. Wetzel WC, Kharouba HM, Robinson M, Holyoak M, Karban R (2016) Variability in plant nutrients reduces insect herbivore performance. *Nature.* **539**: 425–427.
427. Wetzel WC, Meek MH (2019) Physical defenses and herbivory vary more within plants than among plants in the tropical understory shrub *Piper polytrichum*. *Botany.* **97**: 113–121.
428. Wien HC (2020) Abiotic stress effects on vegetable crops. *The Physiology of Vegetable Crops.* 71.

429. Williams A, de Vries FT (2020) Plant root exudation under drought: implications for ecosystem functioning. *New Phytol.* **225**(5): 1899-1905.
430. Wingler A, Purdy S, MacLean JA, Pourtau N (2006) The role of sugars in integrating environmental signals during the regulation of leaf senescence. *J Expl Bot.* **57**: 391–399.
431. Winn AA (1996a) Adaptation to fine-grained environmental variation: an analysis of within-individual leaf variation in an annual plant. *Evolution*, **50**: 1111-1118.
432. Winn AA (1996b) The contributions of programmed developmental change and phenotypic plasticity to within-individual variation in leaf traits in *Dicerandra linearifolia*. *J Evol Biol.* **9**: 737-752.
433. Wu J, Baldwin IT (2009) Herbivory-induced signalling in plants: Perception and action. *Plant Cell Environ.* **32**: 1161–1174.
434. Xu L, Naylor D, Dong Z, Simmons T, Pierroz G, Hixson KK, Gao C (2018) Drought delays development of the sorghum root microbiome and enriches for monoderm bacteria. *Proc Natl Acad Sci.* **115**: E4284–93.
435. Yamada M, Hidaka T, Fukamachi H (1996) Heat tolerance in leaves of tropical fruit crops as measured by chlorophyll fluorescence. *Scientia Hort.* **67**: 39–48.
436. Yamaguchi M, Sharp RE (2010) Complexity and coordination of root growth at low water potentials: Recent advances from transcriptomic and proteomic analyses. *Plant Cell Environ.* **33**: 590–603.
437. Yang J, Duan G, Li C, Liu L, Han G, Zhang Y and Wang C (2019) The crosstalks between jasmonic acid and other plant hormone signaling highlight the involvement of Jasmonic Acid as a core component in plant response to biotic and abiotic stresses. *Front Plant Sci.* **10**: 1349.
438. Yang J, Ruegger PM, McKenry MV, Becker JO, Borneman J (2012) Correlations between root-associated microorganisms and peach replant disease symptoms in a California soil. *PLoS One.* **7**: e46420.
439. Ye ZP (2007) A new model for relationship between irradiance and the rate of photosynthesis in *Oryza sativa*. *Photosynthetica.* **45**: 637-640.
440. Yordanov I, Velikova V, Tsonev T (2003) Plant responses to drought and

- stress tolerance. *Bulg J Plant Physiol*. Special Issue: 187-206.
441. York LM, Nord EA, Lynch JP (2013) Integration of root phenes for soil resource acquisition. *Front Plant Sci*. **4**: 355.
442. Yu P, Hochholdinger F, Li C (2019) Plasticity of lateral root branching in maize. *Front. Plant Sci*. **10**: 363.
443. Zangerl AR, Hamilton JG, Miller TJ, Crofts AR, Oxborough K, Berenbaum MR, DeLucia EH (2002) Impact of folivory on photosynthesis is greater than the sum of its holes. *Proc Nat Acad Sci*. **99**: 1088–1091.
444. Zhan A, Schneider H, Lynch JP (2015) Reduced lateral root branching density improves drought tolerance in maize. *Plant Physiol*. **168**: 1603–1615.
445. Zhang H, Forde BG (1998) An *Arabidopsis* MADS box gene that controls nutrient-induced changes in root architecture. *Science*. **279**: 407– 409.
446. Zhang H, Jennings A, Barlow PW, Forde BG (1999) Dual pathways for regulation of root branching by nitrate. *Proceedings of the National Academy of Sciences, USA* **96**: 6529– 6534.
447. Zhang H, Forde BG (2000) Regulation of *Arabidopsis* root development by nitrate availability. *J Exp Bot*. **51**: 51– 59.
448. Zhang Q (2007) Strategies for developing Green Super Rice. Proceedings of the National Academy of Sciences, USA. **104**:16402–16409.
449. Zhang JL, Poorter L, Hao GY, Cao KF (2012) Photosynthetic thermotolerance of woody savanna species in China is correlated with leaf life span. *Ann Bot*. **110**: 1027–1033.
450. Zhang J, Kobert K, Flouri T, Stamatakis A (2014) PEAR: a fast and accurate Illumina Paired-End reAd mergeR. *Bioinformatics*. **30**: 614–20.
451. Zhao F, Zhang D, Zhao Y, Wang W, Yang H, Tai F, Li C, Hu X (2016) The difference of physiological and proteomic changes in maize leaves adaptation to drought, heat, and combined both stresses. *Front Plant Sci*. **7**: 1471.
452. Zhu S, Vivanco JM, Manter DK (2016) Nitrogen fertilizer rate affects root exudation, the rhizosphere microbiome and nitrogen-use-efficiency of maize. *Appl Soil Ecol*. **107**: 324–33.
453. Zingore S, Murwira HK, Delve RJ, Giller KE (2007) Soil type, management history and current resource allocation: three dimensions regulating variability in

- crop productivity on African smallholder farms. *Field Crop Res.* **102**: 296-305.
454. Zuffo AM, Steiner F, Aguilera JG, Teodoro PE, Teodoro LPR, Busch A (2020) Multi-trait stability index: A tool for simultaneous selection of soya bean genotypes in drought and saline stress. *J Agron Crop Sci.* **206**: 815–822.
455. Zywiec M, Delibes M, Fedriani JM (2012) Microgeographical, inter-individual, and intra-individual variation in the flower characters of Iberian pear *Pyrus bourgaeana* (Rosaceae). *Oecologia.* **169**: 713-722.

## LIST OF FIGURES

**Figure 1** Climate change impacts in Europe's regions (source: EEA Report No 01/2017 – Climate change, impacts and vulnerability in Europe 2016).

**Figure 2** Impact of climate change on agriculture (source : Ghatak et al, 2017).

**Figure 3** Proliferation of primary and secondary laterals by barley (*Hordeum vulgare*) grown in solution culture with the middle root section exposed to a 100-fold greater concentration of phosphate, nitrate, ammonium or potassium ions compared with roots above or below (LHL). Controls were supplied with high concentration of nutrients in all zones (HHH). Abbreviations: H, high; L, low, referring to nutrient concentrations experienced by the top, middle and bottom sections of the root system. (source: Drew, 1975)

**Figure 4** Hypothesized role of root exudates in the response of fast-growing and slow-growing plant species to drought and the potential consequences for ecosystem form and function. Arrows indicate exudation inputs into the soil, coloured dots indicate bacterial communities, thick grey lines represent decomposer fungi, and thin purple lines represent arbuscular mycorrhizal fungi. PGPR, plant growth-promoting rhizobacteria; SOM, soil organic matter. (source: Williams and de Vries, 2020 )

**Figure 5** Compound classes and roles exerted in response to abiotic stress.

**Figure 6** The stress matrix. Different combinations of potential environmental stresses that can affect crops in the field are shown in the form of a matrix. The matrix is color-coded to indicate stress combinations that were studied with a range of crops and their overall effect on plant growth and yield. [Adapted from Suzuki et al. (2014) and modified from Mittler (2006)]

**Figure 7** Photosynthetic activity and dark respiration, measured with a Li-Cor LI-6400 apparatus (A). Stomatal conductance (B), measured with a Li-Cor LI-6400 apparatus [source: Rizhsky et al (2002)].

**Figure 1.1** Leaf photosynthetic light-response curves measured on petiolate (●) and sessile leaves (○) of the *Salvia ceratophylloides* located at Mosorrofa (Mo) (A and C) Puzzi site (Pu) (B and D). The C and D panels showed the curves at lowest irradiance values. Data points represent means (N=4-9). Light curves were fitted by non-linear regression using the Ye et al. model (2007).



**Figure 1.2** Principal component analysis of untargeted metabolomics data from different leaves (sessile and petiolate) and sites (Mo and Pu) of *Salvia ceratophylloides* individuals: Mo-sessile (red), Mo-petiolate (green), Pu-sessile (blue) and Pu-petiolate (purple).

**Figure S1.1** Light saturation point ( $\mu\text{mol}(\text{photons}) \text{m}^{-2} \text{s}^{-1}$ ) (upper panel) and light compensation point ( $\mu\text{mol}(\text{photons}) \text{m}^{-2} \text{s}^{-1}$ ) (bottom panel) of different plant functional groups. The data [minimum (■) and maximum value (■)] are derived from Larcher. The dotted lines are drawn for a better comparison with the minimum and maximum value of *Salvia ceratophylloides*.

**Figure S1.2** Leaf mass per area ( $\text{g m}^{-2}$ ) of sun- and shade-species herbs, evergreen angiosperm and species, herbs and different *Salvia* species. The data of LMA of *Salvia* species, herbs, evergreen angiosperm and species are indicated by minimum (■) and maximum value (■) or by the average (black plot point and the standard deviation where reported)] and were derived from Martins et al. (2017) for *S. officinalis*, Mommer et al. (2007) for *S. pratensis*, Paz'-Dyderska et al. (2020) for *S. glutinosa*, Goergen et al. (2019) for *S. hispanica*, Knight and Ackerley (2002) for *S. mohavensis*, *S. leucophylla*, *S. dorrii var. dorrii* and *S. mellifera*, Poorter et al. (2009) for herbs, Duursma et al. (2016) for evergreen angiosperm and de la Riva et al. (2016) for evergreen species. Box plots point out the distribution of LMA values as observed for a wide range of sun- and shade-species herbs both annual and perennial, with the bottom and top part of the box indicating the 25<sup>th</sup> and 75<sup>th</sup> percentile, respectively, the two whiskers the 10<sup>th</sup> and the 90<sup>th</sup> percentile, respectively, and the horizontal line within the box the median value. The data for the box plot are derived by scientific literature as indicated in Table S1.1. The dotted lines were drawn for better comparisons and pointed out the range of LMA values of *Salvia ceratophylloides*.

**Figure 2.1** Protocol schedule including tomato growth and treatments (S: plant seeding; T1: Plant transfer to hydroponic system; T2: abiotic treatment start; T3: *Tuta absoluta* larvae infestation) and plant sampling events (H1-H4: samplings and analysis). Analysis: morphological analysis (leaf fresh and dry weight, leaf water content), physiological (photosynthetic rate, stomatal conductance, transpiration

rate and  $WUE_i$ ) and VOC profiling. The tomato responses were evaluated at temporal and spatial scales.

**Figure 2.2** Morphological traits. Leaf fresh (g), dry (g) and water content (%) of tomato plants treated with different stress (ABIO, BIO, COMB) or not treated (CTR) for different time of exposure (0, 1, 3 and 8 days). The data and error bars indicated the mean and the error standard, respectively (N=4).

**Figure 2.3** Gas exchange parameters. Photosynthetic rate ( $\mu\text{mol CO}_2 \text{ cm}^{-2} \text{ s}^{-1}$ ), Stomatal conductance ( $\text{mol H}_2\text{O cm}^{-2} \text{ s}^{-1}$ ), Transpiration rate ( $\text{mmol H}_2\text{O cm}^{-2} \text{ s}^{-1}$ ) and  $WUE_i$  ( $\mu\text{mol CO}_2 \text{ mol}^{-1} \text{ H}_2\text{O}$ ) of tomato plants treated with different stress (ABIO, BIO, COMB) or not treated (CTR) for different time of exposure (0, 1, 3 and 8 days). The data and error bars indicated the mean and the error standard, respectively (N=4).

**Figure 2.4** Principal component analysis applied to volatiles emission data obtained from tomato leaves treated with different stress (ABIO, BIO, COMB) or not treated (CTR) for 3 (A) and 8 days (B) of exposure.

**Figure 2.5A** sPLS-DA of volatile profiles obtained in tomato plants exposed to different stress (ABIO, BIO, COMB) or not stress (CTR) for 3 days of exposure. Choosing the number of components in sPLS-DA by performance test.

**Figure 2.5B** Mean classification by overall and balanced error rate (5 cross-validation averaged 50 times) for each sPLS-DA component. Choosing the number of volatiles for each sPLS-DA components by tuning test (B).

**Figure 2.5C** Estimated classification balanced error rates for volatile dataset (5 cross-validation averaged 50 times) with respect to the number of selected volatiles for the sparse exploratory approaches. sPLS-DA sample plot for the different components using 95% confidence ellipses. Component 1 vs. Component 2.

**Figure 2.5D** Estimated classification balanced error rates for volatile dataset (5 cross-validation averaged 50 times) with respect to the number of selected volatiles for the sparse exploratory approaches. sPLS-DA sample plot for the different components using 95% confidence ellipses. Component 1 vs Component 3.

**Figure 2.6A** sPLS-DA of volatile profiles obtained in tomato plants exposed to different stress (ABIO, BIO, COMB) or not stress (CTR) for 8 days of exposure. Choosing the number of components in sPLS-DA by performance test.

**Figure 2.6B** Mean classification by overall and balanced error rate (5 cross-validation averaged 50 times) for each sPLS-DA component. Choosing the number of volatiles for each sPLS-DA components by tuning test.

**Figure 2.6C** Estimated classification balanced error rates for volatile dataset (5 cross-validation averaged 50 times) with respect to the number of selected volatiles for the sparse exploratory approaches. sPLS-DA sample plot for the different components using 95% confidence ellipses. Component 1 vs. Component 2.

**Figure 2.6D** Estimated classification balanced error rates for volatile dataset (5 cross-validation averaged 50 times) with respect to the number of selected volatiles for the sparse exploratory approaches. sPLS-DA sample plot for the different components using 95% confidence ellipses. Component 1 vs Component 3.

**Figure 2.6E-F** Contribution plots by loading weights of the volatiles selected for the Component 2 (E) and Component 1 (F) of the sPLS-DA. The colour indicated the treatments for which the selected volatile has a maximal mean loading weight value.

**Figure 2.7** The combined impacts from abiotic (drought and N deficiency) and biotic stress (Infestation of *Tuta absoluta*) on morpho-physiological traits of tomato plants at 1, 3 and 8 days of treatment and VOC emission at 8 days of treatment. The combined impact of single stressors was estimated as synergist (red colour), additive (white colour) or antagonistic (blue colour) (greater than, equal to or less than expected effects, respectively, based on single stressor effect sizes). The vertical and error bars represent, respectively, the mean and the 95% confidence interval of the overall effect size difference between the observed and expected additive effects from combined abiotic and biotic stress on morpho-physiological and metabolic traits of tomato plants. The zero line represents the expected additive effects from combined stressors. When the means (and their 95% confidence limits) were higher than or less than the zero line, they were considered synergistic or antagonistic, respectively.

**Figure 2.8** Dissection of total variance components of the morpho-physiological traits and VOC responses at 8 days of treatments (control, abiotic stress, biotic stress, combined stress). Considering all treatments pooled, the contributions of treatment (blue color) and within-treatment (yellow color) level to the total variance

in mean of the morpho-physiological traits and VOC responses in the four treatments considered were estimated by Linear Mixed Models.

**Figure 2.9** Nested within-treatment variance partitions (% of the total) in the morpho-physiological responses of tomato plants to different abiotic and biotic stress. The between-plant variance comprise plant within treatment (red color) and the within-plant variance involved the leaves within plant within treatment (green color). The black color indicated the model error.

**Figure 2.10** Degree of vascular connectivity among different leaf positions of tomato plants by method of Orians et al.

**Figure 2.11** Tomato responses to the experimental conditions resembling the vascular pattern (red line) or architectural pattern (green line) or no pattern (blue line).

**Figure 2.12** Photosynthetic rate of three different leaves of tomato plants exposed for 8 days at diverse stresses [abiotic (ABIO); biotic (BIO); combined (COMB)]. No stresses (CTR). The box plot indicated the minimum, first quartile, median, third quartile, and maximum value. Different letters indicated significant difference among the mean groups (N=8;  $p < 0.05$  test of Tukey). The values within the figure indicated the F statistic with the p values (\*\*\*)  $p < 0.001$  derived from one-way ANOVA.

**Figure 2.13** Stomatal conductance of three different leaves of tomato plants exposed for 8 days at diverse stresses [abiotic (ABIO); biotic (BIO); combined (COMB)]. No stresses (CTR). The box plot indicated the minimum, first quartile, median, third quartile, and maximum value. Different letters indicated significant difference among the mean groups (N=8;  $p < 0.05$  test of Tukey). The values within the figure indicated the F statistic with the p values (\*  $0.05 < p < 0.01$ ;  $0.01 < p < 0.001$ ; ns not significant) derived from one-way ANOVA.

**Figure 2.14** Transpiration rate of three different leaves of tomato plants exposed for 8 days at diverse stresses [abiotic (ABIO); biotic (BIO); combined (COMB)]. No stresses (CTR). The box plot indicated the minimum, first quartile, median, third quartile, and maximum value. Different letters indicated significant difference among the mean groups (N=8;  $p < 0.05$  test of Tukey). The values within the figure

indicated the F statistic with the p values (\*  $0.05 < p < 0.01$ ;  $0.01 < p < 0.001$ ; ns not significant) derived from one-way ANOVA.

**Figure 2.15** WUEi of three different leaves of tomato plants exposed for 8 days at diverse stresses [abiotic (ABIO); biotic (BIO); combined (COMB)]. No stresses (CTR). The box plot indicated the minimum, first quartile, median, third quartile, and maximum value. Different letters indicated significant difference among the mean groups (N=8;  $p < 0.05$  test of Tukey). The values within the figure indicated the F statistic with the p values (\*  $0.05 < p < 0.01$ ; ns not significant) derived from one-way ANOVA.

**Figure 2.16** Leaf fresh weight of three different leaves of tomato plants exposed for 8 days at diverse stresses [abiotic (ABIO); biotic (BIO); combined (COMB)]. No stresses (CTR). The box plot indicated the minimum, first quartile, median, third quartile, and maximum value. Different letters indicated significant difference among the mean groups (N=8;  $p < 0.05$  test of Tukey). The values within the figure indicated the F statistic with the p values (\*  $0.05 < p < 0.01$ ; \*\*\*  $p < 0.001$ ; ns not significant) derived from one-way ANOVA.

**Figure 2.17** Leaf dry weight of three different leaves of tomato plants exposed for 8 days at diverse stresses [abiotic (ABIO); biotic (BIO); combined (COMB)]. No stresses (CTR). The box plot indicated the minimum, first quartile, median, third quartile, and maximum value. Different letters indicated significant difference among the mean groups (N=8;  $p < 0.05$  test of Tukey). The values within the figure indicated the F statistic with the p values (\*  $0.05 < p < 0.01$ ; \*\*\* $p < 0.001$ ; ns not significant) derived from one-way ANOVA.

**Figure 2.18** Leaf water content of three different leaves of tomato plants exposed for 8 days at diverse stresses [abiotic (ABIO); biotic (BIO); combined (COMB)]. No stresses (CTR). The box plot indicated the minimum, first quartile, median, third quartile, and maximum value. Different letters indicated significant difference among the mean groups (N=8;  $p < 0.05$  test of Tukey). The values within the figure indicated the F statistic with the p values (ns not significant) derived from one-way ANOVA.

**Figure 3.1** The maize growth in terms of fresh (A) and dry weight (B) in presence of single (drought and heat stress) and combined stress. The bars represented the error standard (N=4).

**Figure 3.2** Primary and seminal roots and their laterals of maize seedlings exposed to drought, heat and their combination (Combined).

**Figure 3.3** The combined impacts from drought and heat stress on selected traits of root primary (A), seminal (B), primary lateral (C) and seminal lateral (D) of maize plants. The combined impact of single stressors was estimated as synergist (red colour), additive (white colour) or antagonistic (blue colour) (greater than, equal to or less than expected effects, respectively, based on single stressor effect sizes). The vertical and error bars represent, respectively, the mean and the 95% confidence interval of the overall effect size difference between the observed and expected additive effects from combined drought and heat on root traits of maize plants. The zero line represents the expected additive effects from combined stressors. When the means (and their 95% confidence limits) were higher than or less than the zero line, they were considered synergistic or antagonistic, respectively.

**Figure 3.4** Choosing the number of components in sPLS-DA by performance test (A). Mean classification by overall and balanced error rate (5 cross-validation averaged 50 times) for each sPLS-DA component. Choosing the number of root traits for each sPLS-DA components by tuning test (B). Estimated classification balanced error rates for root morphology data set (5 cross-validation averaged 50 times) with respect to the number of selected root traits for the sparse exploratory approaches.

**Figure 3.5** sPLS-DA sample plot for the different components using 95% confidence ellipses. (A) Component 1 vs. Component 2, (B) Component 1 vs Component 2. Contribution plots by loading weights of the root traits selected for each sPLS-DA component. (C) Component 1, (D) Component 2, (E) Component 3.

**Figure 4.1** Comparison of Shannon diversity index between (A) treatments and (B) root classes within treatments. (C) CAP (Canonical Analysis of Principal coordinates) ordination using a Bray-Curtis distance matrix of samples. \*\*P=0.003

**Figure 4.2** Venn diagram representing the number of OTUs (Operational Taxonomic Units) differentially more abundant as response to specific stressors compared to the control group.

**Figure S4.1** – Photosynthetic rate ( $\mu\text{mol}(\text{CO}_2) \times \text{m}^{-2} \times \text{s}^{-1}$ ) and stomatal conductance ( $\text{gs}, \text{mol H}_2\text{O} \times \text{m}^{-2} \times \text{s}^{-1}$ ) of maize plants exposed for seven days to drought (D), heat (H) and their combination (C). The control (O) was obtained in presence of optimal water and temperature (see Materials and Methods). Different letters indicate significant differences between treatments (Fisher's LSD test).

## LIST OF TABLES

**Table 1.1** Leaf-level photosynthetic parameters of different leaf types (P: petiolate; S: sessile) of *Salvia ceratophylloides* individuals of two sites (Mosorrofa, Mo; Puzzi, Pu) estimated by nonlinear regression using the Ye et al. model. Different lower-case letters indicated significant differences at  $p < 0.05$  among the average within column (Tukey's test). Different capital case letters indicated statistical significant differences among the means along the rows ( $p < 0.05$ , Tukey's test).

**Table 1.2** Leaf-level stomatal conductance and transpiration rate of different leaf types (P: petiolate; S: sessile) of *Salvia ceratophylloides* individuals of two sites (Mosorrofa, Mo; Puzzi, Pu) measured at light intensity of  $200 \mu\text{mol m}^{-2} \text{s}^{-1}$ . Different lower-case letters indicated significant differences at  $p < 0.05$  among the average within column (Tukey's test). Different capital case letters indicated statistical significant differences among the means along the rows ( $p < 0.05$ , Tukey's test).

**Table 1.3** Leaf-level stomatal conductance and transpiration rate of different leaf types (P: petiolate; S: sessile) of *Salvia ceratophylloides* individuals of two sites (Mosorrofa, Mo; Puzzi, Pu) measured at light intensity of  $800 \mu\text{mol m}^{-2} \text{s}^{-1}$ . Different lower-case letters indicated significant differences at  $p < 0.05$  among the average within column (Tukey's test). Different capital case letters indicated statistical significant differences among the means along the rows ( $p < 0.05$ , Tukey's test).

**Table 1.4** Biometric and morphological parameters of different leaf types (P: petiolate; S: sessile) of *Salvia ceratophylloides* individuals of two sites (Mosorrofa, Mo; Puzzi, Pu). Different lower-case letters indicated significant differences at  $p < 0.05$  among the average within column (Tukey's test). Different capital case letters indicated statistical significant differences among the means along the rows ( $p < 0.05$ , Tukey's test).

**Table 1.5** Chemical characterization of volatile organic compounds in fresh sessile and petiolate leaves of two sites (Mosorrofa, Mo; Puzzi, Pu) of *Salvia ceratophylloides* plants.

**Table S1.1** Two-way ANOVA results and chemical characterization (average and error standard within brackets) of volatile organic compounds in fresh sessile and



petiolate leaves of *Salvia ceratophylloides* harvested in two different sites (Mosorrofa, Mo; Puzzi, Pu). Different lower-case letters indicated significant differences at  $p < 0.05$  among the average along the rows (Tukey's test) and they were only reported when the LTxSit interaction was significant. The bold identify the statistically significant factors and/or their interaction.

**Table 2.1** Results of two-way ANOVA [Treatment (Tr), Time (Ti), Block (Bl) TrxTi interaction (TrxTi)]. Statistics: F- and p-values. Within each root traits and time of exposure, the different letters indicated statistical differences among the means of the treatments ( $p < 0.05$ , test of Tukey).

**Table 2.2** Results of two-way ANOVA [Treatment (Tr), Time (Ti), Block (Bl) TrxTi interaction (TrxTi)]. Statistics: F- and p-values. Within each root traits and time of exposure, the different letters indicated statistical differences among the mean of the treatments ( $p < 0.05$ , test of Tukey).

**Table 2.3** Volatile organic compounds identified using gas chromatography/mass spectrometry (GC/MS) analysis by HS/SPME method in the leaves of the tomato plants treated with abiotic, biotic and combined stress. RT, retention time; KI, retention index.

**Table 2.4** Volatile organic compounds (Area %) from the leaves of tomato plants detected in at least two replicates out of three at each sampling time and treatments.

**Table 2.5** PERMANOVA results of the VOC emission of tomato plants exposed to different stress (Treatment) and Time of exposure (Ti).

**Table 2.6** PERMANOVA pairwise comparison between treatments within each time of exposure.

**Table 3.1** Morphology of primary root of maize plants exposed to single (drought and heat) and combined stress (drought + heat).

**Table 3.2** Morphology of seminal root of maize plants exposed to single (drought and heat) and combined stress (drought + heat).

**Table 3.3** Morphology of primary lateral root of maize plants exposed to single (drought and heat) and combined stress (drought + heat).

**Table 3.4** Morphology of seminal lateral roots of maize plants exposed to single (drought and heat) and combined stress (drought + heat).

**Table 3.5** Results of the PERMANOVA analysis testing the root morphology of maize plants against stress treatment.

**Table 4.1** Results from the mixed-effect linear model testing the Shannon diversity index against treatment, root class, root zone and their interactions.

**Table 4.2** Results from PERMANOVA analysis testing the effects of treatment, root class, root zone and their interactions on the structure of maize rhizosphere bacterial communities.

**Table S4.1** Soil physical and chemical characteristics.

**Table S4.2** PERMANOVA pairwise comparison between treatments in primary roots.

**Table S4.3** PERMANOVA pairwise comparison between treatments in crown roots.

**Table S4.4** PERMANOVA pairwise comparison between root classes (primary vs crown) within each treatment.